

MANGROLIDE A, A NOVEL MARINE DERIVED POLYKETIDE WITH SELECTIVE  
ANTIBIOTIC ACTIVITY

APPROVED BY SUPERVISORY COMMITTEE  
(14 spaces down)

NOTE: The top line is for the Supervising Professor's name. There should be as many lines as there are members of the committee. All signatures must be original and in ink. Adjust "Approved by Supervisory Committee" line upward if the committee list is very large.

John B. MacMillan, Ph.D., Mentor

---

Chou Chen, Ph.D., Chair

---

Jef De Brabander Ph.D.

---

Joseph Ready, Ph.D.

---

## DEDICATION

I would like to thank my mentor John MacMillan for the opportunity to develop as a scientist,  
my Committee for their guidance, and my family and friends for their support.

MANGROLIDE A, A NOVEL MARINE DERIVED POLYKETIDE WITH SELECTIVE  
ANTIBIOTIC ACTIVITY

by

MATTHEW THOMAS JAMISON, B.S.

DISSERTATION

Presented to the Faculty of the Graduate School of Biomedical Sciences

The University of Texas Southwestern Medical Center at Dallas

In Partial Fulfillment of the Requirements

For the Degree of

DOCTOR OF PHILOSOPHY

The University of Texas Southwestern Medical Center at Dallas

Dallas, Texas

May, 2013

Copyright

by

Matthew Thomas Jamison, 2013

All Rights Reserved

DISCOVERY OF BIOLOGICALLY ACTIVE NATURAL PRODUCTS FROM MARINE  
DERIVED BACTERIA

Publication No. \_\_\_\_\_

Matthew Thomas Jamison, Ph.D.

The University of Texas Southwestern Medical Center at Dallas, 2013

Supervising Professor: John B. MacMillan, Ph.D.

The ability of nature to produce complex, biologically active compounds has inspired researchers throughout history. The isolation of these molecules has been instrumental in the discovery of many medicinal compounds, especially to combat infections caused by pathogenic bacteria. Antibiotic resistance is a major challenge faced in hospitals today, and there is an urgent need for new antibiotics. The “Golden Age” of antibiotic development was spurred by compounds isolated from terrestrial bacteria. Unfortunately, the rate of discovery of new compounds has decreased and new techniques and sources are required. The marine environment contains novel

natural product-producing bacteria and has yielded new compounds with potent activity. This dissertation represents work towards new antibiotic discovery from marine natural products. Chapter 1 provides an introduction to marine natural product research with a focus on new developments in the field. Chapter 2 describes the isolation and characterization of a new macrolide, mangrolide A, which was discovered through a phenotypic screen against *Burkholderia cepacia*. Mangrolide A has selective activity against gram negative bacteria. The determination of the absolute stereochemistry of mangrolide A is described in chapter 3. In chapter 4, a new method to increase the production of mangrolide A and activate cryptic metabolite pathways in SNA-18 is applied and results in a new mangrolide analogue. Chapter 5 finishes with the results of a screen using an efflux deficient strain of *Pseudomonas aeruginosa*. This experiment led to the isolation of the known natural products alldimycin A-C and new ammosamide analogues.

## TABLE OF CONTENTS

CHAPTER ONE Marine Natural Products as a Source for New Antibiotics .....	1
1.1 Importance of Natural Product Research.....	1
1.2 Marine Natural Products .....	3
1.3 Marine Natural Products as a Source for Drug Development .....	5
1.3.1 $\omega$ -conotoxin MVIIA.....	6
1.3.2 Ecteinascidin-743.....	7
1.3.3 Halichondrin B.....	8
1.3.4 Dolastatin 10 .....	9
1.4 Marine Natural Products as a Source of Antibiotics.....	10
1.4.1 Ianthelliformisamines A-C.....	11
1.4.2 Marinopyrroles A and B .....	12
1.4.3 Sebastenoic acid.....	13
1.5 Culture Dependent Methods of Natural Product Discovery .....	14
1.5.1 Culturing New Strains in the Laboratory.....	16
1.5.2 Activating Cryptic Natural Product Pathways.....	18
1.6 Using Metagenomics in Natural Product Discovery .....	19
1.7 Antibiotics and Bacterial Resistance .....	24
1.8 New Antibiotic Development .....	25
1.9 Summary of Dissertation .....	26
CHAPTER TWO Isolation and Structure Determination of mangrolide A .....	28

2.1 Selection of the Marine-derived Bacteria SNA-18.....	28
2.2 Tiacumicin and mangrolide Natural Products .....	28
2.3 Extraction of SNA-18 .....	31
2.4 Purification of mangrolide A .....	32
2.5 UV and CD of mangrolide A.....	34
2.6 Biological Activity of mangrolide A .....	34
2.7 NMR Characterization of mangrolide A.....	35
2.8 Isolation and Characterization of mangrolide Analogs .....	39
2.9 Optimization of SNA-18 Culture Conditions .....	41
2.10 Effect of Polyketide Precursors on mangrolide A Production.....	42
2.10 SNA-18 Heat Shock and Oxidative Stress.....	46
2.11 Conclusion .....	47
CHAPTER THREE Stereochemistry of mangrolide A .....	48
3.1 Strategy for Determining Absolute Stereochemistry of mangrolide A .....	48
3.2 Relative Configuration of the mangrolide A Disaccharide.....	52
3.3 J-based Configuration Analysis of C-10 and C-11 .....	53
3.4 Olefin Configuration of mangrolide A .....	55
3.5 Mangrolide A Acid Catalyzed Hydrolysis.....	56
3.6 Mosher's Analysis on Methanolysis Product .....	58
3.7 Scandium Triflate Catalyzed Reduction of C-11 .....	59
3.8 Mosher's Analysis of C-7 .....	60



3.9 Strategy for Elucidating Mangrolide A C-17 Stereochemistry.....	63
3.10 Mangrolide A Protecting Group Strategies.....	63
3.11 Mangrolide A Hydrolysis Reactions.....	65
3.12 Nucleophilic Ring Opening Reactions.....	66
3.13 Mangrolide A Aglycon Hydrogenation .....	68
3.14 Mangrolide A Ester Reduction .....	69
3.15 Mosher's Ester Analysis on mangrolide A .....	71
3.16 Strategy for Determining Absolute Stereochemistry of C-10 and C-11 .....	72
3.17 Ozonolysis of mangrolide A .....	73
3.18 Strategy to Synthesize mangrolide Fragment 3.24 .....	73
3.18.1 Conjugate Addition of Diethyl Zinc to Furanone .....	74
3.18.2 Experiments to Form the Methyl Ketone from 3.20.....	75
3.18.3 Asymmetric Addition of Diethyl Zinc to Furanone.....	76
3.19 Oxidative Cleavage of mangrolide A .....	77
3.20 Epoxidation of C-8/9 Double Bond .....	78
3.21 Comparison with Synthetic mangrolide Aglycon.....	78
3.22 Comparison of mangrolide A Stereochemistry to lipiarmycin .....	79
3.23 Conclusion of Mangrolide Stereochemistry .....	80
CHAPTER FOUR SNA-18 Ribosome Engineering.....	81
4.1 Regulation of Antibiotic Production in Bacteria by ppGpp.....	81
4.2 Ribosome Engineering.....	83

4.2.1 Ribosome Engineering on SNA-18 .....	85
4.3 Engineering Streptomycin Resistant SNA-18 .....	86
4.4 Engineering Rifampicin Resistant SNA-18.....	86
4.5 Analysis of engineered SNA-18 .....	87
4.6 Scale up Fermentation of SNA-18 MP5 .....	90
4.7 Characterization of Engineered SNA-18 on Solid Media.....	91
4.8 Isolation of Monosaccharide Mangrolide Analogue.....	91
4.9 Progress towards Isolating Unknown UV 540 Compounds .....	93
4.10 Optimizing Culture Conditions of Engineered SNA-18 on Solid Media .....	96
4.11 Purification of Engineered SNA-18 Extracts.....	96
4.12 Conclusion .....	99
CHAPTER FIVE Isolation of Cytotoxic Natural Products from SNA-20 .....	100
5.1 Using Efflux Pumps to Screen for New Antibiotics.....	100
5.2 <i>Pseudomonas aeruginosa</i> and Cystic Fibrosis .....	101
5.3 <i>Pseudomonas aeruginosa</i> 96 Well Plate Bio-assay.....	103
5.4 SNA-20 Culture and Purification.....	105
5.5 Identification of alldymycin Natural Products.....	106
5.6 Identification of SNA-20-422 .....	108
5.7 Crystallization Attempts of SNA-20-422 .....	109
5.8 SNA-20 Media Experiments.....	111
5.8.1 Effect of Iron(III) vs Iron(II) on SNA-20 .....	112

5.8.2 Effect of pH on SNA-20 .....	113
5.8.3 Effect of Tryptophan and PM on SNA-20 .....	114
5.9 Conclusion .....	116
BIBLIOGRAPHY .....	193

## PRIOR PUBLICATIONS

1. Pan, E.; Jamison, M.; Yousufuddin, M.; MacMillan, J. B., Ammosamide D, an oxidatively ring opened ammosamide analog from a marine-derived *Streptomyces variabilis*. *Org Lett* **2012**, *14* (9), 2390-3.

## LIST OF FIGURES

FIGURE 1.1 .....	2
FIGURE 1.2 .....	4
FIGURE 1.3 .....	6
FIGURE 1.4 .....	7
FIGURE 1.5 .....	8
FIGURE 1.6 .....	9
FIGURE 1.7 .....	10
FIGURE 1.8 .....	12
FIGURE 1.9 .....	13
FIGURE 1.10 .....	14
FIGURE 1.11 .....	15
FIGURE 1.12 .....	17
FIGURE 1.13 .....	20
FIGURE 1.14 .....	22
FIGURE 1.15 .....	23
FIGURE 2.1 .....	30
FIGURE 2.2 .....	32
FIGURE 2.3 .....	34
FIGURE 2.4 .....	37
FIGURE 2.5 .....	39

FIGURE 2.6 .....	43
FIGURE 3.1 .....	50
FIGURE 3.2 .....	61
FIGURE 4.1 .....	82
FIGURE 4.2 .....	83
FIGURE 4.3 .....	85
FIGURE 4.4 .....	88
FIGURE 4.5 .....	93
FIGURE 4.6 .....	94
FIGURE 5.1 .....	104
FIGURE 5.2 .....	106
FIGURE 5.3 .....	107
FIGURE 5.4 .....	115

## LIST OF TABLES

TABLE 2.1.....	38
TABLE 2.2.....	40
TABLE 2.3.....	42
TABLE 3.1.....	53
TABLE 3.2.....	54
TABLE 3.3.....	56
TABLE 3.4.....	57
TABLE 3.5.....	59
TABLE 3.6.....	62
TABLE 3.7.....	64
TABLE 3.8.....	66
TABLE 3.9.....	67
TABLE 3.10.....	69
TABLE 3.11.....	70
TABLE 3.12.....	72
TABLE 3.13.....	79
TABLE 4.1.....	89
TABLE 4.2.....	95
TABLE 4.3.....	98

TABLE 5.1.....	102
TABLE 5.2.....	105
TABLE 5.3.....	108
TABLE 5.4.....	110
TABLE 5.5.....	111



## LIST OF CHARTS

CHART 2.1 .....	45
CHART 2.2 .....	46
CHART 5.1 .....	112
CHART 5.2 .....	113
CHART 5.3 .....	114

## LIST OF SCHEMES

SCHEME 3.1 .....	51
SCHEME 3.2 .....	60
SCHEME 3.3 .....	73
SCHEME 3.4 .....	74
SCHEME 3.5 .....	74
SCHEME 3.6 .....	75
SCHEME 3.7 .....	76
SCHEME 3.8 .....	77

## LIST OF APPENDICES

APPENDIX A NMR Spectra .....	117
------------------------------	-----

## LIST OF DEFINITIONS

4A MS – 4Å molecular sieve

CH<sub>3</sub>CN – Acetonitrile

CoA – Coenzyme A

COSY – Correlation spectroscopy

D-ala – D-alanine

D-lac – D-lactate

DCM – Dichloromethane

DEPT – Distortionless Enhancement by Polarization Transfer

DIBAL-H – Diisobutylaluminium hydride

DNA – Deoxyribonucleic acid

eDNA – Environmental DNA

GC – Gas chromatography

GDP – Guanosine 5'-diphosphate

GTP – Guanosine 5'-triphosphate

HETLOC – Hetero-(ω1)-half-filtered TOCSY

HMBC – Heteronuclear multiple-bond correlation spectroscopy

HPLC – High Performance Liquid Chromatography

HRMS – High Resolution Mass Spectroscopy

HSQC – Heteronuclear single-quantum correlation spectroscopy

kb – Kilobase

KMnO<sub>4</sub> – Potassium permanganate

KOH – Potassium hydroxide

LiOH – Lithium hydroxide

MDR – Multidrug resistance

MeOH – Methanol

Me(OMe)NH-HCl – N,O-dimethylhydroxylamine hydrochloride

MIC – Minimum inhibitory concentration

MRSA – Methicillin-resistant *Staphylococcus aureus*

MTPA-OH –  $\alpha$ -methoxy- $\alpha$ -trifluoromethylphenylacetic acid

NaOH – Sodium hydroxide

NaIO<sub>4</sub> – Sodium periodate

NMR – Nuclear Magnetic Resonance

NOE – Nuclear Overhauser Effect

NRPS – Non-ribosomal peptide synthesis

nM – Nanomolar

OSMAC – One strain many compounds

PKS – Polyketide synthases

PM – Polyketide precursor mixture

ppGpp – Guanosine 5'-diphosphate-3'-diphosphate

pppGpp – Guanosine 5'-triphosphate-3'-diphosphate

Red-Al – Sodium bis(2-methoxyethoxy)aluminum hydride

RNAP – RNA polymerase

ROESY – Rotating frame nuclear Overhauser effect spectroscopy

ROS – Reactive oxygen species

SAM – S-adenosyl methionine

TAR – Transformation-associated recombination

TES – Triethylsilyl

TFA – Trifluoroacetic acid

THF – Tetrahydrofuran

TMS – Trimethylsilyl

TOCSY – Total correlation spectroscopy

## CHAPTER ONE

### MARINE NATURAL PRODUCTS AS A SOURCE FOR NEW ANTIBIOTICS

#### 1.1 Importance of Natural Product Research

Throughout history mankind has recognized the medicinal properties of plants, fungi, and bacteria<sup>1</sup>. Advances in science have lead to the isolation and characterization of the biologically active small molecules found in nature. Beginning in the 1950's, the modern pharmaceutical industry has utilized these compounds as a source for new drug candidates. From the 1940's to the 1970's natural products were the key resource in the development of antibiotics (such as penicillin (**1.1**), tetracycline (**1.2**), and vancomycin (**1.3**)) as well as anti-cancer agents (such as Taxol (**1.4**), bleomycin (**1.5**), and vinblastine (**1.6**)). Natural products have remained important to drug development with seventy percent of small molecule drugs approved from 1981 to 2010 resulting from natural product research<sup>2</sup>. In addition to their pharmaceutical potential, natural products have contributed immensely as tools for studying biological processes, such as the mTOR inhibitor rapamycin<sup>3</sup>. Moreover, their complex structural architectures have challenged chemists to synthesize them and spurred the development of many new reactions<sup>3</sup>. Over the past thirty years a shift in paradigm to high throughput screening has led to a decline in natural product research in the industrial setting in favor of combinatorial small molecule libraries<sup>4</sup>. While million compound libraries would appear to guarantee success, recent studies of approved drugs showed that natural products occupy a more drug like chemical space and poses better

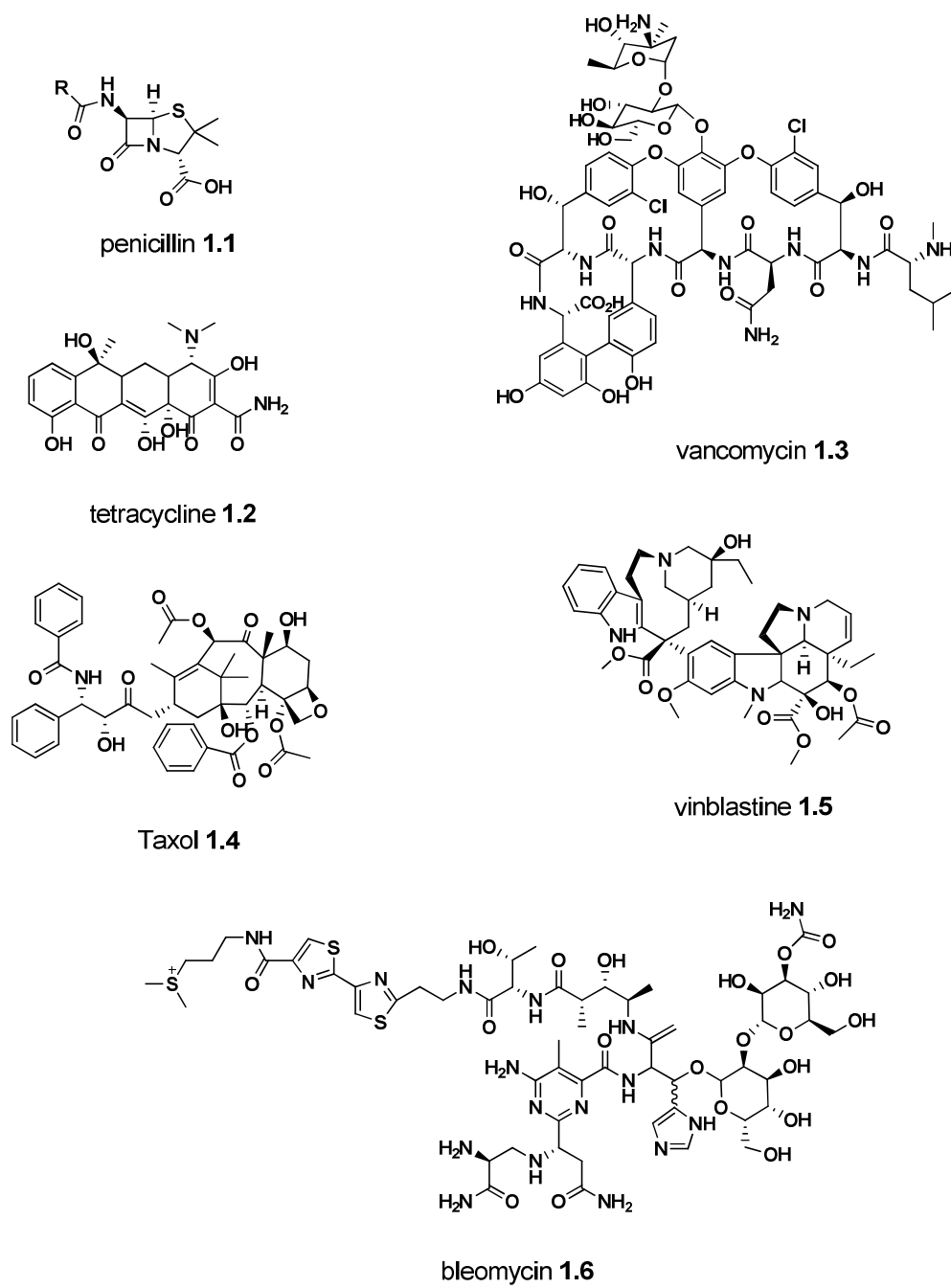


**Figure 1.1** Natural products with potent biological activity.



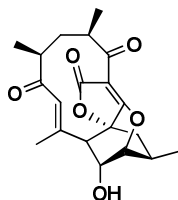
drug like properties than these synthetic libraries<sup>5</sup>. This is due in part to the evolution of highly specific molecules for a particular receptor and the adaptation of molecules to use active transport systems for crossing membranes. Natural product research will remain important as new technology improves our ability to access chemistry previously unreachable.

## 1.2 Marine Natural Products

Natural product research from terrestrial sources has yielded over 163,000 small molecules, while over 31,000 compounds have come from marine sources<sup>6</sup>. This is surprising considering that the ocean accounts for 70% of the earth's surface. The marine environment has double the biodiversity found on land with 15 phylum exclusive to the ocean<sup>7</sup>. These unique creatures include sponges, coral, ascidians, nudibranches, bryozoans, and tunicates, and they have evolved in a nutrient-limited environment with constant interaction between microbes and predators. In addition to the diversity of invertebrates, marine sediments contain around  $10^8$  bacteria per gram of wet mud and  $10^6$  cells per milliliter of seawater<sup>8</sup>. This is comparable to soil microbe levels which have been reported to be  $4 \times 10^7$  cells per gram<sup>9</sup>. Research by the Fenical lab has shown that natural product producing actinomycetes exist in the ocean and can be found worldwide<sup>10</sup>. Terrestrial actinomycetes have been a major source for antibiotic drug discovery but the high rediscovery rate of known compounds has increased the importance of finding new producing organisms<sup>10</sup>. The marine environment represents a great opportunity to discover new bacteria and thus new chemical structures. The discovery of abyssomicin C (**1.7**) is an excellent example (Figure 1.2). The abyssomicin producing strain was isolated from marine sediments

collected at a depth of 300 m and has been shown to be a new species of *Verrucosispora*<sup>11</sup>.

Abyssomicin C has low  $\mu\text{M}$  activity against gram positive bacteria and is the first inhibitor of *p*-aminobenzoate synthesis discovered from bacteria<sup>12</sup>.



abyssomicin 1.7

**Figure 1.2** Structure of abyssomicin

Symbiosis between marine bacteria and invertebrates is widespread and, in the case of sponges, bacteria can be up to forty percent of their biomass<sup>13</sup>. In fact, of the twenty marine natural compounds or drugs inspired by marine compounds that are in clinical use or in development, eighty percent are predicted to be produced by bacteria instead of the host organism from the original isolation<sup>14</sup>. This further highlights the importance of studying marine bacteria as a source of novel compounds.

Another unique aspect of the marine environment is the dilutive effect of a aqueous environment which selects for potent small molecules<sup>15</sup>. Evidence for this has been shown in a study from the National Cancer institute where 1% of marine samples had anti-cancer activity versus 0.1% for terrestrial sources<sup>16</sup>. While the marine environment has been underexplored,

recent data indicates a dramatic growth in marine natural product research with 1003 new metabolites published in 2010<sup>17</sup>.

### **1.3 Marine Natural Products as a Source for Drug Development**

Natural products in general have had a huge impact on commercial drug development, and marine natural products are beginning to be approved for use. Like their terrestrial counterparts, the path to approval for marine derived drugs can be difficult and the successes have been reviewed by Mayer *et al.* and Mollinski *et al.*<sup>18</sup>. The discovery of spongothymidine (**1.8**) and spongouridine (**1.9**) by Bergmann in the 1950's led to the first drugs developed from marine natural product research (Figure 1.3)<sup>19</sup>. These nucleosides contain arabinose instead of deoxyribose and represented the first discovery of nucleosides with unusual sugars. This compounds inspired the synthesis of the un-natural nucleosides Cytarabine (**1.10**) and Vidarabine (**1.11**) and were clinically used as anti-cancer and anti-viral medications respectively<sup>18a</sup>.

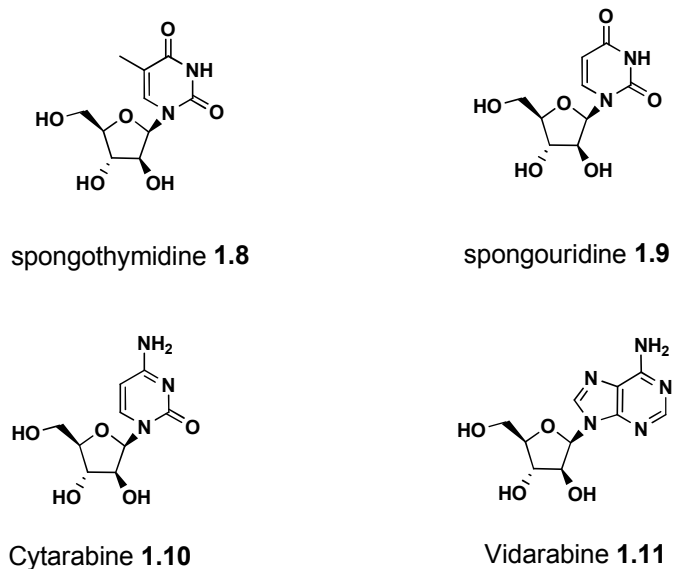
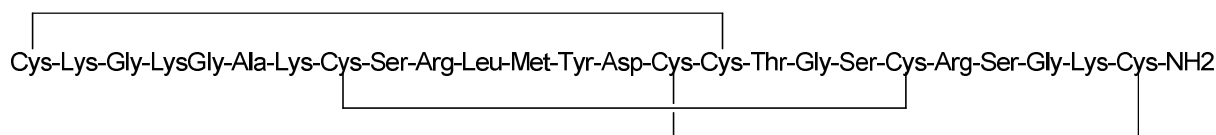


**Figure 1.3** Structures of the marine natural products spongothymidine and spongouridine and the drugs inspired by them.

### 1.3.1 $\omega$ -conotoxin MVIIA

The first FDA approved marine natural product was  $\omega$ -conotoxin MVIIA (Prialt™) for chronic pain (Figure 1.4)<sup>18b</sup>. The  $\omega$ -conotoxins are 25-29 amino acid peptides isolated from the fish hunting cone snail, *Conus magus*, in 1979<sup>20</sup>. MVIIA has a unique mechanism of action, selectively binding N-type calcium channels in the dorsal horn of the spinal cord<sup>18a</sup>. In addition, unlike opiate-based pain medications, no tolerance to the drug develops<sup>21</sup>. The  $\omega$ -conotoxins were one of five types of paralytic proteins present in the cone snail venom. Terrestrial organisms are known to use multiple toxins but not to the same degree found in the cone snails<sup>20</sup>.

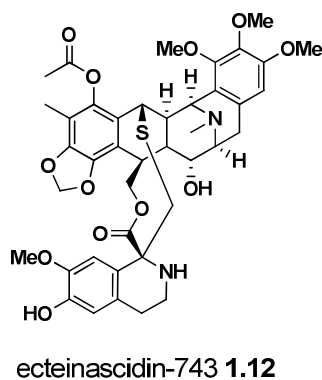
It was hypothesized that the ease of escape of prey in the marine environment led to the cone snails use of multiple toxins<sup>20</sup>.



**Figure 1.4** ω-conotoxin MVIIA.

### 1.3.2 Ecteinascidin-743

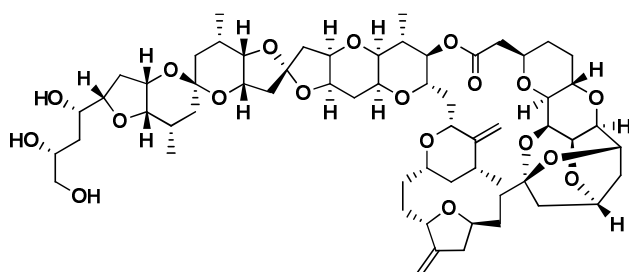
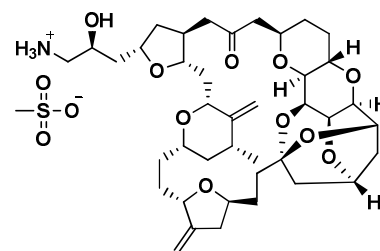
The development of ecteinascidin-743 (**1.12**) (trabectedin, Yondelis™) as an approved drug demonstrates some of the problems encountered in marine natural product research (Figure 1.5). In 1969 Sigel *et al.* reported anti-tumor activity from the extracts of marine tunicate *Ecteinascidia turbinata*<sup>18b</sup>. Due to a lack of material, the structure was not published until 1990 by both Reinhart and Wright<sup>22</sup>. **1.12** is a tetrahydroisoquinoline alkaloid and has been found to covalently modify the DNA minor groove as well as to affect nucleotide excision repair proteins<sup>18a</sup>. Total synthesis and aquafarming were used to obtain more **1.12**, but supply remained a problem until PharmaMar developed a semi-synthetic route from cyanosafracin<sup>18b</sup>. Nearly forty years after the initial discovery, **1.12** was approved for use in Europe for the treatment of soft tissue sarcomas<sup>18b</sup>.



**Figure 1.5** Structure of ecteinascidin-743

### 1.3.3 Halichondrin B

Halichondrin B (**1.13**) was first isolated from the sponge *Halichondria okadai* in 1986<sup>23</sup>. This polyether macrolide possesses potent, low nM activity against cell growth (Figure 1.6)<sup>23</sup>. **1.13** binds to tubulin causing mitotic arrest at the G2-M phase eventually leading to apoptosis<sup>24</sup>. Unlike other tubulin binding drugs such as paclitaxel, **1.13** causes irreversible mitotic arrest in cells<sup>25</sup>. The structure of **1.13** is complex, and the first total synthesis required ninety steps<sup>18b</sup>. Collaboration between academics and Eisai led to the discovery of a simplified halichondrin analogue, eribulin mesylate (**1.14**), with equal potency (Figure 1.6). In November 2010, **1.14** was approved by the FDA for treatment of metastatic breast cancer.

halichondrin B **1.13**Eribulin mesylate **1.14****Figure 1.6** Structures of halichondrin B and Eribulin mesylate

### 1.3.4 Dolastatin 10

Dolastatin 10 (**1.15**) was first detected in ethanol extracts of the sea hare *Dolabella auricularia*, collected by the Pettit group in 1972<sup>18b</sup>. These extracts had potent activity against murine p388 lymphocytic leukemia cells<sup>18b</sup>. Approximately 100 kg of *D. auricularia* were required to isolate 1 mg of each of the nine dolastatins initially detected<sup>26</sup>. A large scale collection of 1000 kg of *D. auricularia* was undertaken which led to the isolation of dolastatin 10<sup>26</sup>. **1.15** is the most active of the dolastatins and was found to inhibit microtubule and tubulin polymerization<sup>18b</sup>. Phase II trials were unsuccessful at demonstrating significant activity and **1.15** is no longer being pursued. A synthetic analogue of **1.15**, TZT-1027 (**1.16**), where the dolaphenine amino acid has been exchanged with phenethylamine is currently in phase III trials<sup>18a</sup>. **1.16** disrupts the vasculature inside tumors in addition to the antimitotic activity of the dolastatins<sup>18a</sup>. Clinical trials of **1.16** combined with monoclonal antibodies are in progress<sup>18a</sup>.

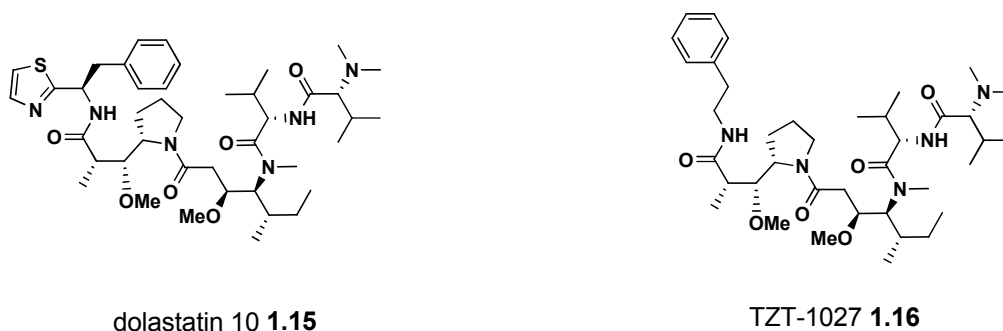


**Figure 1.7** Structures of dolastatin 10 and TZT-1027

These few examples of the marine natural products that are currently being evaluated in preclinical or clinical trials show the potential of the marine environment to produce chemically unique compounds with new biological mechanisms. Numerous reviews have been written on the topic and the references are included<sup>15, 18b, 27</sup>.

#### 1.4 Marine Natural Products as a Source of Antibiotics

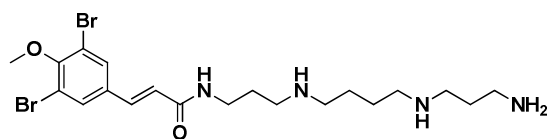
The “Golden Age” of antibiotic discovery resulted in 20 classes of antibiotics<sup>15</sup>. These drugs and their derivatives have been successfully used for 50 years, but the spread of antibiotic resistance has rendered many drugs ineffective. This has led to the 10 x 20 initiative which calls for the development of 10 new classes of antibiotics by 2020<sup>28</sup>. The marine environment has the potential to be an important source for new antibiotic discovery. Bacteria are the main producers of antibiotic compounds and are ubiquitous in the ocean<sup>10</sup>. In addition, antibiotic metabolites have been purified from a variety of organisms such as sponges, marine derived fungi, algae, coral, and tunicates. These natural products have been well reviewed by both Mayer and Hughes



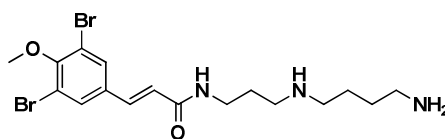
and some recent publications of novel antibacterial marine natural products have been highlighted below<sup>15, 29</sup>.

#### 1.4.1 Ianthelliformisamines A-C

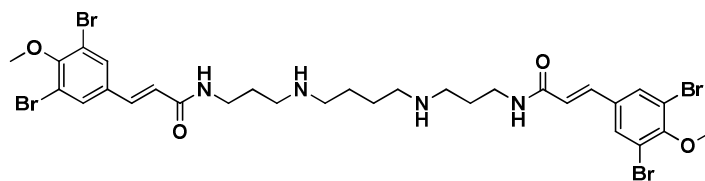
A recent publication detailing the isolation of ianthelliformisamines A-C is an excellent example of antibiotic compounds from marine sources with interesting biological activity. Xu *et al.* began with a high throughput screening of a marine natural products library that had been fractionated based on LogP values<sup>30</sup>. This library had been created aiming to select for metabolites with better physicochemical properties<sup>31</sup>. Initial screening of this library was done against a MexAB-OprM knockout strain of the Gram negative pathogen *Pseudomonas aeruginosa*. MexAB-OprM is a multidrug efflux pump, and removing it can sensitize *P. aeruginosa* to antibiotics<sup>32</sup>. Active fractions were then retested against wild-type *P. aeruginosa* and MRSA. This was done to determine which fractions displayed Gram selectivity. Extracts from the sponge *Suberea ianthelliformis* were selected and purification led to three new bromotryrosine derived natural products, ianthelliformisamines A-C (Figure 1.8). Ianthelliformisamine A (**1.17**) was selective for gram negatives with an IC<sub>50</sub> of 6.8 µM against *P. aeruginosa* versus 77% inhibition of *S. aureus* at 175 µM. Changing the spermine in A to spermidine in B (**1.18**) reduced activity to 80% inhibition at 87.5 µM. Ianthelliformisamine C (**1.19**) has an additional cinnamyl attached to the spermine in A and has potent activity against both *P. aeruginosa* 8.9 µM and *S. aureus* 4.1 µM.



ianthelliformisamines A **1.17**



ianthelliformisamines B **1.18**



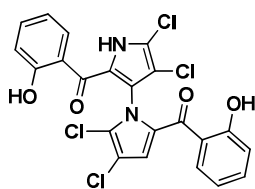
ianthelliformisamines C **1.19**

**Figure 1.8** Structures of ianthelliformisamines A-C

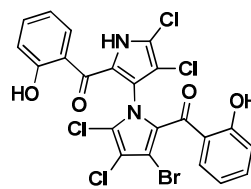
### 1.4.2 Marinopyrroles A and B

The discovery of marinopyrrole A (**1.20**) and B (**1.21**) by the Fenical group is a good example of the potential for new chemical structures from marine bacteria<sup>33</sup>. Isolated from an actinomycetes cultured from a deep sea sediment sample, **1.20** and **1.21** are the first natural products that have a N,C2-linked bispyrrole (Figure 1.9). Interestingly, these molecules were purified as single atropo-enantiomers indicating that the bispyrrole formation is a selective, enzyme catalyzed reaction. **1.20** and **1.21** have potent antibacterial activity against MRSA

(MIC<sub>90</sub> of 0.61  $\mu$ M and 1.1  $\mu$ M) and some cytotoxic activity against human cancer cell line HCT-116 (IC<sub>50</sub> of 8.8  $\mu$ M and 9.0  $\mu$ M). Research has shown that **1.20** binds to the anti-apoptotic protein Mcl-1 and targets it for degradation<sup>34</sup>. Mcl-1 is over expressed in some cancer cell lines and is a target in cancer treatment research.



marinopyrrole A **1.20**



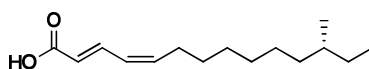
marinopyrrole B **1.21**

**Figure 1.9** Structures of marinopyrrole A and B

### 1.4.3 Sebastenoic acid

Investigating environmental niches can lead to the discovery of new bacteria and new natural products<sup>3</sup>. Studies of the microbiome present in soil, ocean, and human gut showed that each source contained distinct populations of bacteria including natural product-producing actinomycetes<sup>35</sup>. This lead Sanchez *et al.* to investigate the microbiome present in the stomach and intestines of marine fish<sup>35</sup>. Twenty-nine bacteria were cultured using techniques designed to select for actinomycetes. Taxonomic analysis identified Actinobacteria, Proteobacteria, and Firmicutes as the major phyla isolated and some of the strains were related to previously uncultured bacteria. Extracts from twenty-one of the strains isolated were tested for antibacterial activity against a variety of Gram positive pathogens and Gram negative *vibrio* species known to

infect fish. Nine of the extracts displayed antibiotic activity with eight possessing activity against at least one *vibrio* species. One strain was selected for further investigation based on low sequence identity to previously isolated bacteria. Purification of the sole active metabolite lead to sebastenoic acid (**1.22**), a new branched chain fatty acid (Figure 1.10). **1.22** was reported to have low  $\mu\text{M}$  activity (10-23.8  $\mu\text{M}$ ) against Gram positive bacteria and an MIC of 110.6  $\mu\text{M}$  against *Vibrio mimicus*. This research was the first publication of a natural product from the fish microbiome and demonstrated the potential of the fish microbiome as a new source of antibiotic natural products.



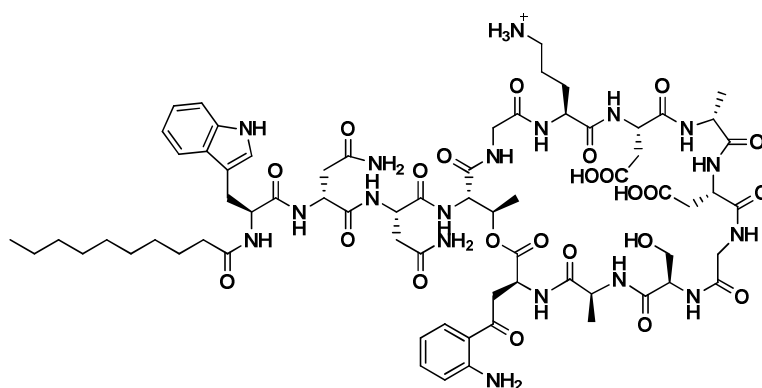
sebastenoic acid **1.22**

**Figure 1.10** Structure of sebastenoic acid

## 1.5 Culture Dependent Methods of Natural Product Discovery

Bacteria have been an important source of antibiotic compounds<sup>36</sup>. They have evolved biosynthetic pathways which allow them to produce compounds which give them an advantage in their environment<sup>37</sup>. Traditionally they have to be isolated and cultured in the laboratory in order to obtain an extract which can be tested for biological activity. Not all bacteria possess the ability to produce natural products and this has been linked to genome size<sup>38</sup>. Bacteria with less than 3Mb rarely contain PKS and NRPS genes. Actinomycetes are unique in that 5-10% of their genomes are predicted to produce secondary metabolites. Due to sharing of genetic information,

many actinomycetes produce the same compounds. The aminoglycoside streptomycin is produced by 1% of soil actinomycetes isolated<sup>8</sup>. With over 2000 antibiotic compounds discovered from bacteria, dereplication of known compounds is a challenge for natural product isolation<sup>39</sup>. When the total isolated organisms from an environmental sample is compared to the genetic data of predicted organisms, it is apparent that only a small percentage of bacteria are cultivated in the lab<sup>40</sup>. New antibiotics can still be discovered through traditional laboratory culture methods. The recently approved lipopeptide antibiotic daptomycin (**1.23**) is an excellent example (Figure 1.11). Daptomycin was isolated from *Streptomyces roseosporus* by Eli Lilly and is a potent Gram positive antibiotic<sup>41</sup>. It possesses a unique bactericidal activity that targets multiple membrane proteins and is effective against multi drug resistant pathogens. Due to its unique mechanism of action, daptomycin has a low rate of resistance development.

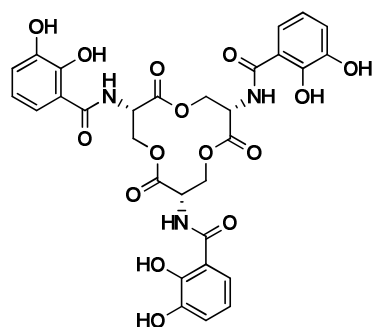
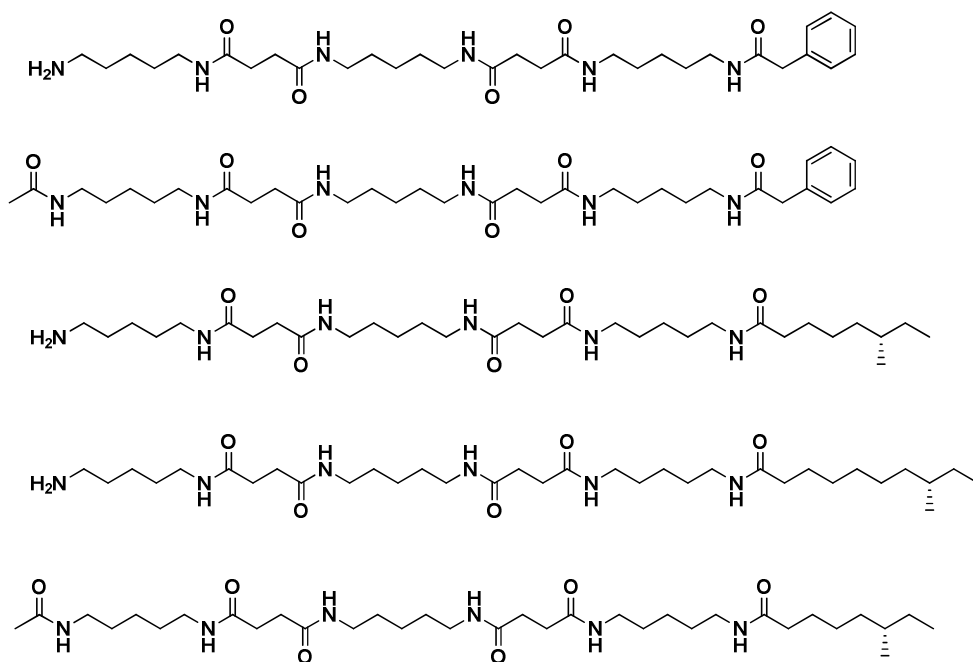


daptomycin **1.23**

**Figure 1.11** Structure of daptomycin.

### 1.5.1 Culturing New Strains in the Laboratory

New approaches for culturing bacteria have been successful at isolating uncultured bacteria. Due to the variety of bacteria that exist in nature, no single method will be able to grow every strain present in a sample. For example, the SAR11 clade of *Alphaproteobacteria* which are ubiquitous in the marine environment are unculturable under typical laboratory conditions<sup>42</sup>. Using sterile sea water as media, Rappé *et al.* diluted fresh sea water samples until approximately twenty-two bacteria were present in 1ml wells of a microtiter plate<sup>43</sup>. The use of small scale cultivation allowed for a variety of culture conditions to be tested and they successfully obtained cultures containing only SAR11 bacteria. This method termed “dilution to extinction” has been used to isolate many new bacteria<sup>42</sup>. The success of culturing the SAR11 bacteria was due to mimicking the natural environment through the use of natural sea water. An extension of this has been the use of diffusion chambers to culture bacteria directly in their environment. Developed by the Lewis and Epstein labs, diffusion chambers use semipermeable membranes which allow nutrients and small molecules to exchange between the environment and a suspension of soil in agar<sup>44</sup>. This technique can culture up to 40% of the bacteria present in a soil sample including rare phyla such as *Acidobacteria* and *Verrucomicrobia*<sup>45</sup>. By modifying the pore size, these chambers can be used to trap filamentous bacteria allowing for the isolation of rare actinomycetes<sup>46</sup>. A major advantage of diffusion chambers is that successive rounds of culturing can adapt some of the bacteria to growth on petri dishes allowing for traditional culture methods to be applied<sup>45</sup>. A better understanding of the various growth factors

enterobactin **1.24**acyl-desferrioxamine siderophores **1.25****Figure 1.12** Structures of marine derived siderophores.

present in the environment is necessary in order to increase the diversity of bacteria cultivable in the lab.

A clever approach was used by D'Onofrio *et al* to uncover small molecules required for growth by uncultured bacteria<sup>47</sup>. Using a series of co-culture experiments they isolated a strain (KLE1104) that only grew in co-culture with a helper strain (KLE1011) or with the addition of spent *E. coli* media. The signaling molecules produced by *E. coli* are known, and a collection of deletion strains was used to determine the required metabolite. The siderophore enterobactin (**1.24**) was found to be the sole requirement for growth (Figure 1.12). The helper strain, KLE1011 was regrown in low iron media to stimulate siderophore production and five new acyl-desferrioxamine siderophores (**1.25**) were isolated. Next, six KLE1011 dependent strains were tested for growth in the presence of these five siderophores and 21 commercially derived siderophores. Each strain was found to have a unique set of siderophores capable of stimulating growth.

### 1.5.2 Activating Cryptic Natural Product Pathways

The environmental signals which are required for growth are also important signals regulating the production of secondary metabolites. Whole genome sequencing of actinomycetes has revealed that most secondary metabolites remain undiscovered<sup>48</sup>. This is not surprising as laboratory fermentation does not recreate the complex chemical environment found in nature. The practice of varying culture conditions to influence secondary metabolite production is referred to as OSMAC, and techniques can include changing the available nutrients, mimicking



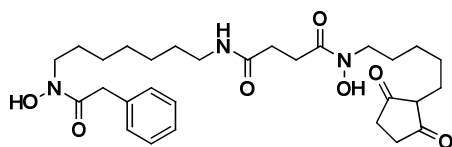
environmental stress, and co-culture experiments<sup>49</sup>. For example, *Streptomyces venezuelae* produces the antimicrobial jadomycin A and can be induced to produce a new glycosylated form, jadomycin B, when exposed to high temperatures or a low concentration of ethanol<sup>50</sup>. OSMAC has drawbacks as it can be labor intensive and difficult to detect compounds that are produced in low abundance. Improvements in mass spectrometry and automation have helped streamline the process. Berrue *et al.* demonstrated this using a 96 well plate format and ultra high performance chromatography to optimize media conditions for coral associated bacteria and were able to dereplicate metabolite production even in wells containing a mixed culture of bacteria<sup>51</sup>.

## 1.6 Using Metagenomics in Natural Product Discovery

Another limitation to culture dependent methods is that they only capture a small sample of bacteria that exist in the environment. Metagenomic analysis indicates that less than ninety-five percent of bacteria can be cultured in the laboratory<sup>40</sup>. Additionally, as mentioned, the products of most biosynthetic gene clusters are not detectable in culture extracts<sup>48</sup>. These factors could be biasing natural product isolation towards the same chemical entities. This could also explain the high rate of rediscovery of natural products. In the advent of the “-omics” era, it has become possible to explore the wealth of natural product pathways that exist in uncultured bacteria.

The basis of natural product metagenomics is in the creation of libraries of clones from fragments of environmental DNA. Due to the tight clustering of biosynthetic genes it is possible to obtain all the genes responsible for the expression of a secondary metabolite, including genes

for precursor production, tailoring enzymes, and host resistance. Once the eDNA library has been created, it can be analyzed for biosynthetic pathways through phenotypic screening and direct sequence analysis<sup>52</sup>. Phenotypic screening requires transforming each clone into a heterologous host and new compounds are identified by changes in appearance or development of new biological activity. The first successful isolation of a new small molecule was identified through a phenotypic screen of 1020 clones in *Streptomyces lividans* by the Anderson and Davies laboratories<sup>53</sup>. They found five new compounds, terragine A-E (**1.26**), through HPLC-MS analysis of extracts from the cultured recombinants (Figure 1.13). Because only a fraction of clones will contain entire gene clusters, phenotypic screening is limited to smaller eDNA libraries and has only resulted in the isolation of relatively simple natural products such as siderophores, tryptophan derivatives, and fatty acid like molecules.



terragine A **1.26**

**Figure 1.13** Structure terragine A

The use of DNA sequencing for identifying biosynthetic genes has yielded better results. Current technology can create a 10,000,000 clone library which provides complete coverage of all organisms present in an environmental sample<sup>54</sup>. To identify clones containing putative

natural product pathways, primers are designed which target conserved sequences in biosynthetic pathways. Natural product gene clusters are usually very large and the random nature of clone generation does not guarantee that the entire sequence will be captured. King *et al.* hypothesized that targeting type II polyketide synthases would be more successful<sup>55</sup>. Type II PKS are smaller due to the use of an iterative K<sub>α</sub> and K<sub>β</sub> subunits. Using primers based on the K<sub>β</sub> sequence, they were able to identify and heterologously express a new natural product erdacin A (**1.27**) (Figure 1.14). This represents a significant milestone in metagenomic research due to the complex structure of **1.27**. This molecule was found to have significant anti-oxidative properties (twice that of vitamin C). Further analysis of the eDNA<sup>56</sup> library has led to more natural products with unusual carbon skeletons. Notably, the fasamycins (**1.28**) containing a mono- or di-chlorinated polyphenol system (Figure 1.14). These compounds displayed potent anti-bacterial activity against gram positive bacteria, including methicillin resistant *Staphylococcus aureus* and vancomycin resistant *Enterococcus faecalis*. It has been determined that these molecules bind and inhibit type II fatty acid biosynthesis in bacteria<sup>57</sup>. Interestingly, the same core structure was identified in a culture dependent screen of natural products targeting bacterial fatty acid biosynthesis by Merck<sup>57</sup>.

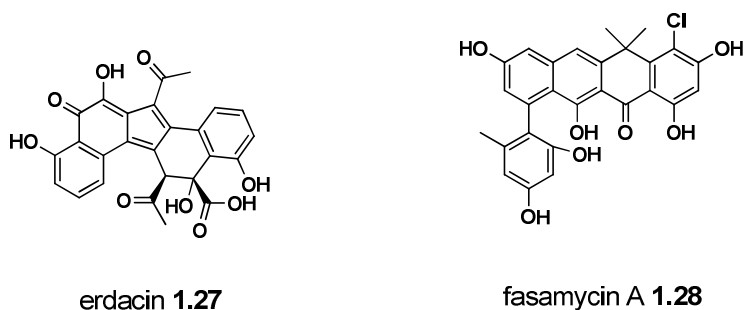


**Figure 1.14** Structure erdacin and fasamycin A

Not every biosynthetic pathway will fit on one cosmid, and overcoming this limitation will be important to the success of this technique. Work done by Kim *et al.* on applying transformation-associated recombination to bacterial metagenomics could be a solution to this problem<sup>58</sup>. TAR is a technique developed for creating large DNA cosmids using *Saccharomyces cerevisiae*. Vectors containing complimentary sequences to DNA of interest are transformed in *S.cerevisiae* with fragmented genomic DNA. Colonies successfully transformed with both the vector and its complimentary sequence are combined into one cosmid up to 600kb in size<sup>59</sup>. Brady *et al.* successfully used this technique to combine the sequence data of two plasmids that they identified to contain a complete natural product pathway. Expression of the new clone led to the isolation of the fluostatins (**1.29**)<sup>60</sup> (Figure 1.15). Application of TAR to metagenomic research could lead to the discovery of more complex natural products.

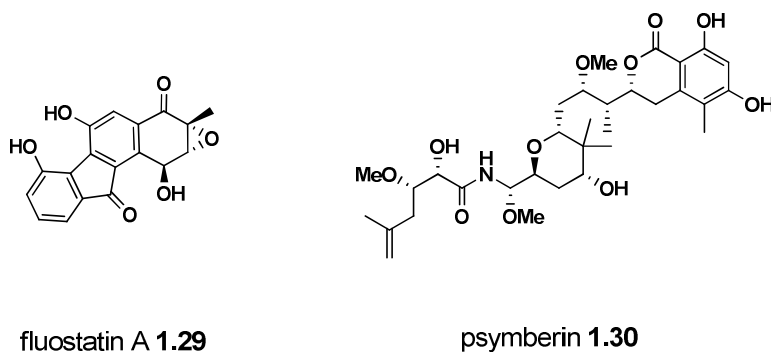


**Figure 1.15** Structure fluostatin A and psymberin

Metagenomics has the greatest potential in isolating the biosynthetic genes of symbiotic bacteria which are often unculturable separate from the host organism. Many marine natural products isolated from marine organisms are predicted to be produced by bacteria and are often produced in low concentrations<sup>14</sup>. This was the case for the polyketide psymberin (**1.30**) which was detected in fractions in of *Psammocinia* aff. *bulbosa* that displayed potent cytotoxic activity<sup>61</sup> (Figure 1.15). The structure of psymberin remained unsolved until ten years of *Psammocinia* sp. fractions were combined and purified using bioactivity as a guide. Pure psymberin was found to have less than 2.5 nM activity against leukemia, breast cancer, melanoma, and colon cancer cell lines. Structurally it is related to the pederin polyketides which were discovered from a beetle bacterial symbiote, so it was hypothesized that psymberin is produced by bacteria living in the sponge. Using metagenomics in organisms such as sponges is challenging due to the amount of bacteria that are present. Total DNA isolated from *Psammocinia* aff. *bulbosa* was probed using primers targeting ketosynthase domains and

eighty-one gene fragments were amplified<sup>62</sup>. All of these genes were predicted to produce methyl-branched fatty acids commonly found in sponge symbionts. To overcome this, a nested PCR approach was used where initial amplification of all polyketide ketosynthase genes was followed by a second amplification using primers designed to target a unique ketosynthase predicted from psymberin's structure. This method was successful resulting in a single 62kb polyketide gene cluster predicted to produce psymberin.

### 1.7 Antibiotics and Bacterial Resistance

The discovery of the sulfonamide drugs in 1935 was a turning point in human history. The mortality rate for meningitis fell from 70-90% to 10%, greatly improving survival chances for children<sup>4</sup>. The serendipitous discovery of penicillin by Alexander Fleming started an era of rapid discovery of new antibiotics (mostly from natural products). Unfortunately, clinical use of antibiotics quickly selected for the resistant strains that naturally exist. A lack of understanding of resistance mechanisms led scientists to believe that chemical modification of existing compounds could outpace bacterial resistance. Since the development of the antifolate synthesis inhibitor trimethoprim in 1968, only three new classes of antibiotics have been approved. The result has been the overuse of available antibiotics in clinical and agricultural settings, leading to the appearance of multidrug resistant strains<sup>63</sup>. Referred to as the ESKAPE pathogens, *Enterococcus faecium*, *Staphylococcus aureus*, *Klebsiella pneumoniae*, *Acinetobacter baumannii*, *Pseudomonas aeruginosa*, and *Enterobacter species* are responsible for 40% of hospital acquired infections and are resistant to at least one commonly used antibiotic<sup>63b, 64</sup>.

Antibiotics are ubiquitous in nature, and bacteria have developed a diverse array of mechanisms to limit their effects. The main resistance mechanisms are over expression of the target, chemically inactivation of the drug, or increased efflux of the drug from the bacteria. Once bacteria develop a resistant trait, they can transfer the gene or genes between species. Evolutionary pressures leads to clustering of resistance genes together and the spread of multidrug resistance. In the case of MDR strain of *A. baumannii*, a 86 kb resistance island was discovered to posses 45 genes promoting resistance to a broad spectrum of antibiotics<sup>65</sup>.

Combined with difficulty in finding new classes of antibiotics through chemical screening or natural product isolation, we are now facing a serious lack of new drugs and increasing multidrug resistant bacteria.

### **1.8 New Antibiotic Development**

Further research of the bacterial response to antibiotics could lead to novel drug targets, but there is a huge investment of time and money required to bring a new drug to market. Modifying the structures of approved drugs can overcome resistance. Vancomycin is a potent glycopeptide antibiotic that is key in treating gram positive infections and is the drug of last resort for methicillin-resistant *Staphylococcus aureus*. Vancomycin inhibits cell wall biosynthesis by binding to the D-Ala-D-Ala terminus of peptidoglycan through five hydrogen bonds. Resistance to vancomycin arises from a chemical modification of D-Ala-D-Ala to D-Ala-D-Lac late in the synthesis of peptidoglycan resulting in a 1000-fold reduction in binding<sup>66</sup>. The Boger lab hypothesized that they could design a vancomycin analog which could bind both

substrates. Molecular modeling indicated that D-Ala-D-Lac causes repulsive lone pair interactions with the residue 4 carbonyl<sup>67</sup>. Through an impressive late stage derivitization, Xie et al. selectively converted the residue 4 carbonyl to an amidine<sup>68</sup>. This amidine analogue was found to bind to D-Ala-D-Lac 600-fold greater than the vancomycin aglycon while only reducing the binding affinity of D-Ala-D-Ala by 2-fold. Bioassay data showed that the modification restored activity of vancomycin against resistant strains.

Altering known antibiotics has been successful in extending their usefulness. From 2000 to 2011, twenty new antibiotics were approved of which seventeen were derived from existing chemical scaffolds<sup>27</sup>. None of the three new classes of antibiotics are effective against gram negative bacteria. Overall, advances in molecular biology and chemistry have not kept pace with bacterial resistance. Target based drug discovery has not been effective for antibiotics because of the limited permeability of bacterial membranes and active efflux prevent access to the target *in vivo*<sup>69</sup>. This is especially true for gram negative bacteria which possess a second protective membrane. In order to find new gram negative antibiotics, whole cell-phenotypic screens will remain useful.

## **1.10 Summary of Dissertation**

This dissertation represents work towards new antibiotic discovery from marine natural products. Chapter 2 describes the isolation and characterization of a new macrolide antibiotic, mangrolide A, which was discovered through a phenotypic screen against *Burkholderia cepacia*. The determination of the absolute stereochemistry of mangrolide A is described in Chapter 3. In



Chapter 4, I describe my work to increase the production of mangrolide A and activate cryptic metabolite pathways in SNA-18. Chapter 5 finishes with the results of a screen I conducted using an efflux deficient strain of *Pseudomonas aeruginosa* which lead to the isolation of the known natural product alldimycin and new ammosamide analogues.

## CHAPTER 2

### ISOLATION AND STRUCTURE DETERMINATION OF MANGROLIDE A

#### 2.1 Selection of Marine-derived Bacteria SNA-18

The goal of this work was to discover new compounds with antibiotic activity against gram negative pathogens. To accomplish this, a phenotypic screen of a library of 1000 natural product fractions was conducted against the gram negative pathogen *B. cenocepacia*. These fractions were created from extracts of marine-derived bacteria which included Actinomycetes, Firmicutes, and  $\alpha$ -proteobacteria. Typically, 5 L of the isolated strain were incubated and extracted by XAD-7 resin. The crude extract was purified by reversed phase chromatography on C18 silica gel with a water/MeOH step gradient. Ten fractions were collected and adjusted to 10 mg/mL in DMSO for use in 96 well plate and disk diffusion assays. One of the active fractions, from strain SNA-18, displayed gram negative selectivity when it was found to be inactive against the gram positive bacteria, *Bacillus subtilis*. SNA-18 was isolated from a mangrove sediment sample from Sweetings Cay Bahamas, and 16S sequencing identified it as an Actinomycete, *Actinoallotecihius spitensis* (97% similarity). Antibiotics that are selective for gram negative bacteria are unusual so work was begun to determine the active component(s) produced by SNA-18.

#### 2.2 Tiacumicin and mangrolide Natural Products

Bacteria possess the ability to pass the genetic information encoding antibiotic synthesis and resistance mechanisms between species. Because of this, re-isolation of known natural

products is a common occurrence in natural product research. Natural product biosynthesis produces a core structure that is then modified by mechanisms such as glycosylation, methylation, and halogenation to produce a variety of analogues. These analogues can possess different biological activities, and in some cases the difference can be dramatic. For example, the pederin family of natural products are potent cytotoxins originally isolated from the *Paederus* beetle in 1953<sup>70</sup> (Figure 2.1). A structurally related molecule, psymberin (**2.2**), was discovered in 2004 from sponge extracts and contains a dihydroisocoumarin extension and lacks the acetal unit. Psymberin (**2.1**) was found to have a significantly different cytotoxic profile when tested against the NCI 60 human cancer cell line panel. This demonstrates the potential of marine sources to produce molecules with biological activities from that are unique from their terrestrial counterparts.

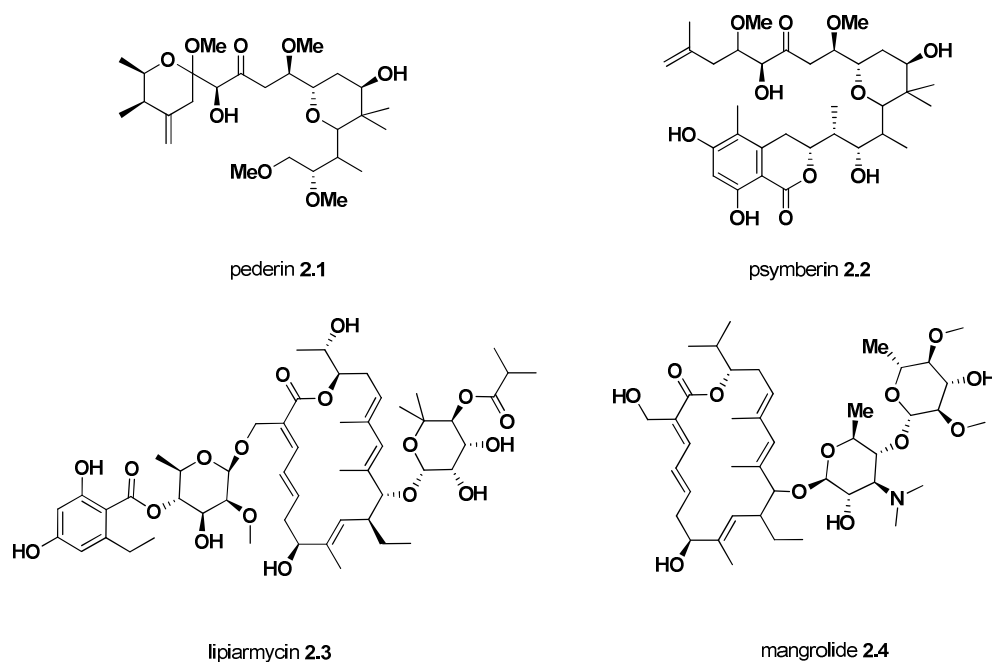


**Figure 2.1** Structures of similar natural products with different molecular targets

The high resolution mass spectrometry data and distinct proton NMR shifts of mangrolide A indicated that it was a new natural product. Only after solving the planar structure was it apparent that mangrolide A (**2.4**) contained an almost identical 18-member polyketide ring structure found in lipiarmycin (**2.3**) which was first isolated in 1975 from *Actinoplanes deccanensis* (figure 2.1)<sup>71</sup>. Lipiarmycin A3 has been isolated from three other terrestrial sources (*Dactylosporangium aurantiacum*, *Micromonospora echinospora*, and *Catellatospora* sp. Bp3323-81) and is also referred to as tiacumicin B<sup>72</sup>. It is a broad spectrum gram positive antibiotic including activity against drug resistant strains, but lipiarmycin is not active against gram negative bacteria<sup>72a, 73</sup>. This is an important difference between mangrolide A and lipiarmycin as mangrolide A is selective for gram negative bacteria.

Structurally, the main difference between the two molecules is in the moieties appended to the macrolide ring. Lipiarmycin has a modified D-rhamnose and dichlorinated homo-orsellinic acid extension from the allylic primary alcohol and a monosaccharide at C-11. Mangrolide lacks any modification on the primary alcohol and has a disaccharide attached at C-11. A recent paper has established the biosynthetic pathway for lipiarmycin<sup>74</sup>. In addition, Xiao *et al.* created mutant strains by deleting the lipiarmycin tailoring genes and isolated eighteen analogues<sup>74</sup>. The structure activity relationship of these compounds revealed that the dichlorinated homo-orsellinic acid moiety is critical for the antibacterial activity<sup>74</sup>. Lipiarmycin is a transcription inhibitor and has been shown to target the 3.2 region of the  $\sigma^{70}$  subunit and the RNAP  $\beta'$  subunit switch-2 element<sup>75</sup>. In collaboration with the McKnight lab, we have uncovered the mechanism of action of mangrolide A and have found that it causes mistranslation during transcription. While similar in structure, mangrolide A has a different and important antibacterial activity than lipiarmycin A3 demonstrating the usefulness of marine natural products as new sources of bioactive molecules. Herein, I will report the isolation, structural elucidation, and biological activity of mangrolide A.

### 2.3 Extraction of SNA-18

SNA-18 can be grown on both solid and liquid culture (figure 2.2). Standard A1+C (10g starch, 4g peptone, 2g yeast extract, and 1g calcium carbonate per liter) at 75% artificial seawater was used to prepare media. SNA-18 grows quickly in liquid media with a short lag phase and reaches stationary phase in approximately seven days and produces a distinct green phenotype. Sometimes a blue ring is observed on the flask at the edge of the media. SNA-18 can grow at

lower concentrations of seawater, although growth was significantly inhibited in media lacking seawater. Growth on solid media was slower with SNA-18, forming wrinkled secondary structures. Large scale (20L) fermentations were started by adding 25mL of SNA-18 culture to a Fernbach flask containing 1 liter of A1+C media. These flasks were incubated for 7-9 days before activated XAD-7 resin was added. The resin was left for a minimum of three hours before filtering and extraction with acetone overnight. The crude extract was dried and then resuspended in methanol and filtered by centrifugation to remove insoluble material. The methanol solution was generally dried after adding C18 silica gel to create a powder for dry loading of a C18 silica gel flash column.

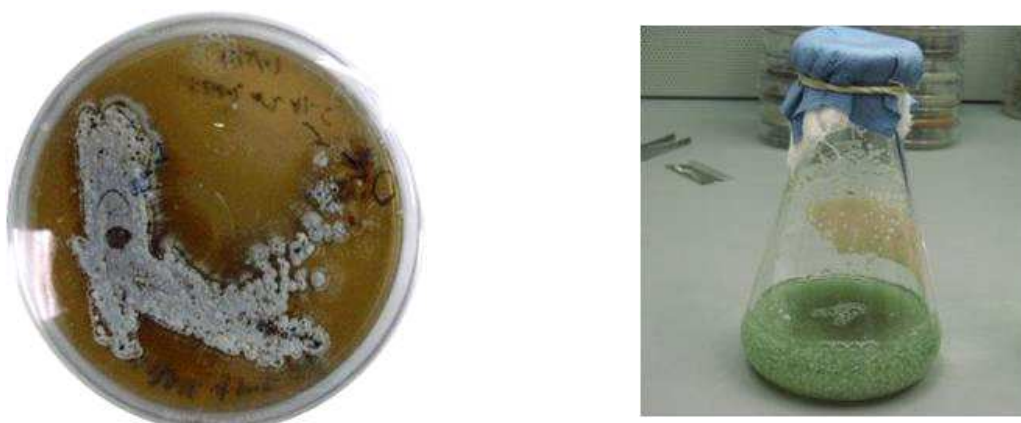


**Figure 2.2** Left image is SNA-18 streaked on solid media. Right image is SNA-18 grown in liquid culture, 125 mL flask, with the typical greenish phenotype observed.

## 2.4 Purification of mangrolide A

The initial purification of mangrolide A was performed on fractions received from a post-doc, Ana Paula Ph.D, from a reversed phase C18 separation of SNA-18 crude extract using water/MeOH. The 90% and 100% methanol fractions were combined (SNA-18-90, 303 mg) and

separated on a normal phase column using silica gel and a DCM/MeOH step gradient starting at 98% DCM. The concentration of MeOH was increased by 2% every 100ml of mobile phase added until 20% MeOH was reached. Methanol concentration was then increased to 25%, 30%, 30%/.05% H<sub>2</sub>O, and 30%/.01% TFA. Thin layer chromatography was used to analyze fractions and similar fractions were combined. <sup>1</sup>H NMR of these fractions revealed an interesting fraction (SNA-18-90-10, 28.2 mg) containing polyketide-like signals. SNA-18-90-10 was further separated by HPLC using a water/acetonitrile gradient on an Agilent 1200 series HPLC with a Phenomenex Luna 5 micron, 100 Å, 250x10.00 mm column. The method began at 60% water until 5min, decreased to 20% by 8min, stayed at 20% till 11min, and then was returned to 60% by 19min. Five fractions were collected and the third fraction (SNA-18-90-10c, 4.95 mg) contained a pure compound with a HRMS (ESI-TOF) [M + H]<sup>+</sup> *m/z* of 780.4890. This material was used to generate a 2D NMR data set for structure determination.

The optimized strategy was as follows: The crude extract from 20 liters of SNA-18 was dissolved with MeOH and filtered by centrifugation to remove any MeOH insoluble material. This methanol soluble extract was then purified using reversed phased C18 flash chromatography using a water/MeOH gradient starting at 30% MeOH then 50% MeOH followed by increasing the concentration by 10% steps until 100% MeOH was reached. A final wash of 100% MeOH with 0.1% TFA was collected as well. This method was repeated with another 20 liters SNA-18 crude extract and the mangrolide containing fractions from both separations were combined for another round of C18 flash chromatography. An identical gradient was used with mobile phase adjusted to 0.1% formic acid. This mimics the HPLC conditions used in the lab

and improved the separation of mangrolide from the other compounds present. Pure fractions of mangrolide A can be obtained from this purification and an additional HPLC step was used to purify any mixed fractions.

## 2.5 UV and CD of mangrolide A

Optical rotation measured  $[\alpha]_D^{25} = +100$  (c, 0.001g/ml, MeOH). UV was measured at a concentration of  $2.567 \times 10^{-7}$  M; 265.60nm(log  $\epsilon$  6.33), 234.60(log  $\epsilon$  6.48), and 201.60nm(log  $\epsilon$  6.57). CD spectrum in figure 2.3.

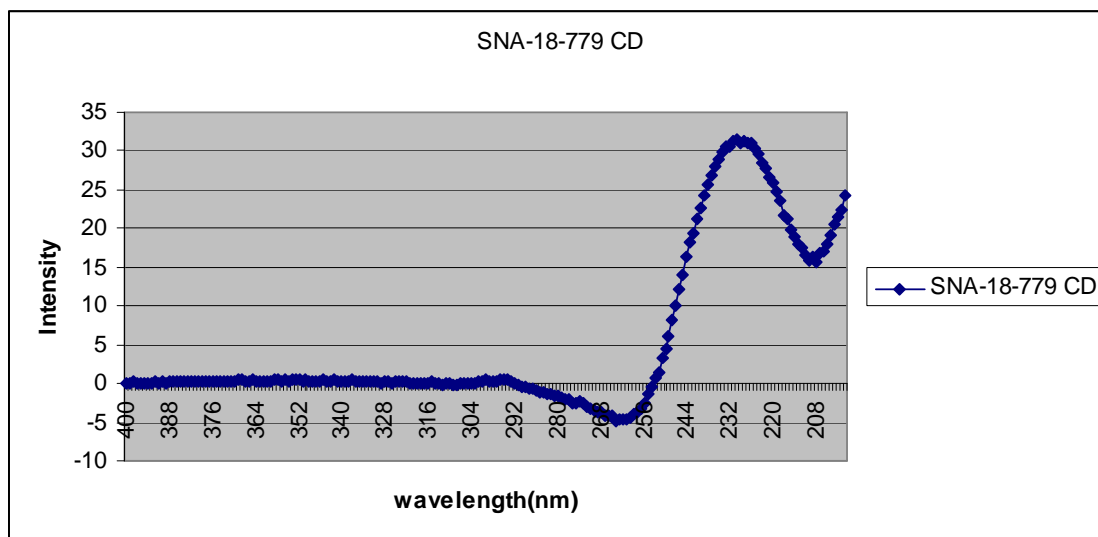


Figure 2.3 CD spectra of mangrolide A

## 2.6 Biological activity of mangrolide A

Mangrolide A was originally detected due to its activity against *Burkholderia cenocepacia*. Activity against a variety of bacteria was tested by others and showed that mangrolide A was active against *B. cenocepacia* (MIC<sub>50</sub> 0.34  $\mu$ M), *Acinetobacter baumannii* (MIC<sub>50</sub> 0.78  $\mu$ M), *Escherichia coli* (MIC<sub>50</sub> 1.2  $\mu$ M), and *Staphylococcus aureus* (MIC<sub>50</sub> 18  $\mu$ M).



When tested in disk diffusion assay against *P. aeruginosa* strain PA046 no activity was observed. A 96 well plate assay against *Bacillus subtilis* showed an MIC<sub>50</sub> 260  $\mu$ M. Further research was conducted by the McKnight group. Their results are not detailed in this dissertation, but they were able to determine that mangrolide A was causing misincorporation of amino acids during translation.

## 2.7 NMR Characterization of mangrolide A

The primary data set of  $^1\text{H}$ ,  $^{13}\text{C}$ , DEPT, COSY, HMQC, HMBC 4Hz, HMBC 8Hz, TOCSY, and ROESY experiments were collected using deuterated methanol as the solvent. A second data set of  $^1\text{H}$ ,  $^{13}\text{C}$ , COSY, HMQC, and HMBC experiments were collected with deuterated dimethyl sulfoxide. Data was collected on Varian 500 and 600 Mhz NMR using 5mm tubes (Table 2.1). A molecular formula of  $\text{C}_{42}\text{H}_{69}\text{NO}_{12}$  was derived from the HRMS-ESI-TOF  $[(\text{M}+\text{H})^+ m/z 780.4890]$ . Analysis of the proton and carbon chemical shifts indicated a polyketide structure with five double bonds, three vinyl methyls, a di-methyl amine, and two sugar moieties (Figure 2.4). COSY correlations were used to construct three spin systems (figure 2.4). Three olefinic protons H-3 ( $\delta_{\text{H}}$  7.17), H-4 ( $\delta_{\text{H}}$  6.6), and H-5 ( $\delta_{\text{H}}$  5.93) form a conjugated double bond system with H-5 being further correlated the H-6 diastereotopic methylene pair at ( $\delta_{\text{H}}$  2.5, 2.69). An oxygen bearing H-7 ( $\delta_{\text{H}}$  4.23) completed partial structure 1. The second spin system established started between two methyl doublets, H-19( $\delta_{\text{H}}$  1.03) and H-20( $\delta_{\text{H}}$  0.99) linked a methine at H-18( $\delta_{\text{H}}$  2.11), which was further correlated to the H-17 oxymethine ( $\delta_{\text{H}}$  4.71). Next a correlation to a diastereotopic methylene H-16 ( $\delta_{\text{H}}$  2.45, 2.52), followed by a vinyl H-15( $\delta_{\text{H}}$  5.5) completed partial structure 3. The third spin system started with a methyl triplet, H-

23( $\delta_{\text{H}}$  0.92), which led to a pair of methylene protons at H-24( $\delta_{\text{H}}$  1.35, 2.13). Next was a methine, H-10( $\delta_{\text{H}}$  2.71) which had correlations to vinyl proton H-9( $\delta_{\text{H}}$  5.19) and oxymethine H-11( $\delta_{\text{H}}$  3.78) to complete partial structure 2. Analysis of HMBC correlations was used to connect the three fragments together (figure 2.4). Correlations from the vinyl proton at H-3 to the carbonyl at C-1 established the  $\alpha$ ,  $\beta$ ,  $\gamma$ ,  $\delta$  unsaturated ester. A key signal from C-17 to the C-1 carbonyl allowed for the connection of the two fragments. The third fragment was connected through correlations from the hydroxyl containing C-7 to C-9 and established the substituted double bond between them. C-11 provided the key signal across the glycosidic bond to establish the location of the sugars and to the vinyl singlet at C-13. The data from C-11 and C-15 allowed the construction of the conjugated double bond system and completed the planar structure of the macrolide.

Structure elucidation of the two sugars was straightforward. COSY correlations were observed between the anomeric position C-1' ( $\delta_{\text{H}}$  4.41,  $\delta_{\text{C}}$  104.19), an oxymethine C-2' ( $\delta_{\text{H}}$  3.67), an amine methine C-3' ( $\delta_{\text{H}}$  3.47), oxymethine C-4' ( $\delta_{\text{H}}$  3.7), oxymethine C-5' ( $\delta_{\text{H}}$  3.46), and the methyl C-6' ( $\delta_{\text{H}}$  1.29). HMBC correlations established the dimethyl amine at C-3' to complete the structure of the known sugar, mycaminose (figure 2.5).

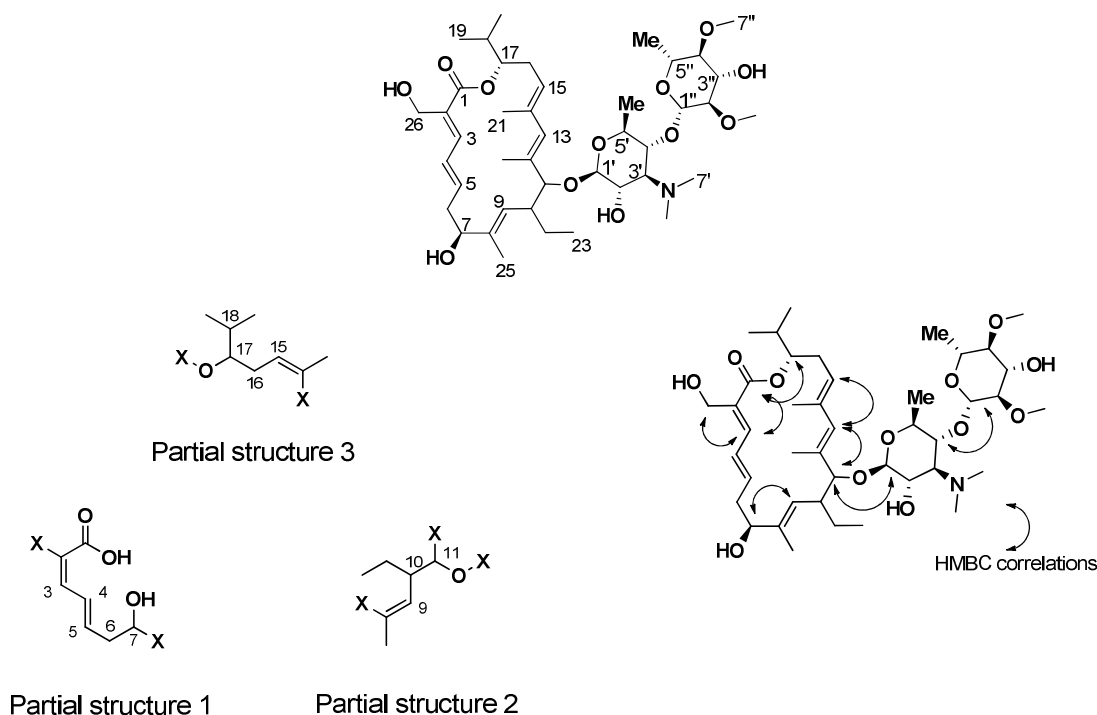


**Figure 2.4** Top, numbered structure of mangrolide A. Bottom left are the three partial structures of the macrolide ring assembled from COSY data. Bottom right are the key HMBC correlations used to assemble the macrolide ring.

The second sugar was assembled in a similar fashion, with COSY correlations observed between the anomeric proton at C-1'', four oxymethines (C-2'', C-3'', C-4'', and C-5''), and the methyl at C-6''. The upfield shifts of C-3'' and C-4'' ( $\delta_{\text{H}}$  2.94 and 2.81) and HMBC correlations from methyl singlets ( $\delta_{\text{H}}$  3.55 and 3.57) indicated the presence of two O-methyls to give 6-deoxy-2,4-dimethyl-glucose as the second sugar. The disaccharide was connected with an HMBC correlation from C-1'' across the glycosidic bond to C-4' (figure 2.5). The relative configuration of the sugars was determined through coupling constant analysis and will be discussed further in chapter 3.2.

mangrolide A				
position	<sup>13</sup> C	<sup>1</sup> H, mult (J in Hz)	COSY	HMBC
1	169.4			
2	129.0			
3	144.5	7.14, d (11.6)	4	1, 2, 5, 26
4	128.3	6.57, t (13.5)	3, 5	2, 3, 6
5	142.6	5.89, ddd (4.7, 9.3, 15.2)	4, 6	3, 6, 7,
6	37.0	2.5, 2.69 m	5, 7	4, 5, 7, 8, 9
7	73.5	4.25, m	6, 9, 25	5, 6, 8, 9, 15
8	137.0			
9	124.2	5.17, dt (1.2, 10.5)	10, 25	7, 8, 10, 11, 25
10	42.8	2.71, m	9, 11	9, 11, 12, 23, 24
11	95.1	3.77, d (9.7)	10	10, 13, 22, 24, 1'
12	136.9			
13	134.5	5.82, s	21, 22	11, 12, 15, 21, 22
14	136.4			
15	125.3	5.46, t (8.0)	16	13, 16, 21,
16	29.7	2.42, 2.52, m	15, 17	13, 15, 17, 18
17	79.8	4.69, ddd (4.2, 4.4, 8.5)	16, 18	1, 15, 18, 19, 20
18	31.7	2.06, m	17, 19, 20	16, 17, 19, 20
19	18.8	1.01, d (6.8)	18	17, 18, 20
20	19.9	0.97, d (6.8)	18	17, 18, 19
21	17.4	1.65, s	13	13, 14, 15
22	13.8	1.78, s	13	11, 12, 13
23	11.2	0.89, t (7.5)	24	10, 24,
24	26.8	1.34, 2.09 m	10, 23	9, 10, 11, 23
25	15.2	1.64, s	7, 9	7, 8, 9
26	56.6	4.36, 4.31, d (12.0)		1, 2, 3
1'	104.19	4.41, d (7.4)	2'	11, 2', 3'
2'	69.4	3.67, dd (9.8, 7.4)	1', 3'	1', 3'
3'	71.3	3.47, t (10.4)	2', 4'	2', 4',
4'	77.8	3.7, t (9.4)	3', 5'	1', 3', 5', 6'
5'	73.0*	3.46, dd (8.4, 6.2)	4', 6'	
6'	18.0*	1.34 d (6.2)	5'	4', 5'
7'	49.9*	3.12, s		3'
8'	49.6*	3.12, s		3'
1''	104.23	4.47, d (7.9)	2''	4'
2''	84.9	2.94, dd (9.4, 7.9)	1'', 3''	1'', 3'', 7''
3''	77.1	3.44, t (9.1)	2'', 4''	2'', 4''
4''	86.1	2.81, t (9.2)	3'', 5''	3'', 5'', 8''
5''	73.0*	3.42, dd (9.6, 6.2)	4'', 6''	
6''	17.8*	1.35 d (6.2)	5''	4'', 5''
7''	61.1	3.55, s		2''
8''	61.4	3.57, s		4''

**Table 2.1** NMR data table for mangrolide A. \* marks positions that overlap in the HSQC.

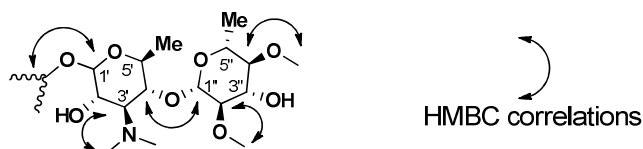


**Figure 2.5** Key HMBC correlations used to assemble the mycaminose, 6-deoxy-2,4-dimethyl-glucose disaccharide.

## 2.8 Isolation and Characterization of mangrolide Analogs

Crude extract from thirty liters of SNA-18 was combined and separated by flash chromatography on C18 using a water/methanol step gradient. The 100% methanol fraction was further purified by two rounds of C18 HPLC to yield 1.6 mg of mangrolide B and 1.1 mg of mangrolide C.  $^1\text{H}$ , COSY, HSQC, and HMBC NMR experiments were collected and the data was used to propose the planar structures (Table 2). Mangrolide B and C have a  $m/z$   $M+H$  of 794 and 808 respectively an increase of 14 ( $\text{CH}_2$ ) and 28 ( $\text{C}_2\text{H}_4$ ) mass units over mangrolide A. Comparison with mangrolide A's chemical shifts indicated that the difference was in the ethyl substituent. A propyl substituent was proposed for mangrolide B based on COSY correlations from the methyl at 0.96 to a methylene at 1.34 which was coupled to a new methylene signal at 2.04. Mangrolide C has very similar chemical shifts as mangrolide B and the assignment is not conclusive but it is likely that a butyl or iso-butyl substituent has replaced the propyl group. More material is needed to verify these structures.

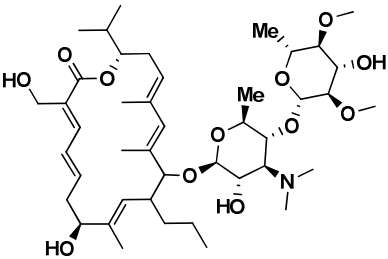
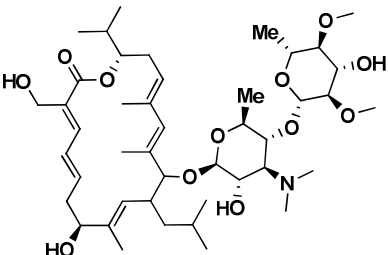
	position	mangrolide B		mangrolide C	
		<sup>13</sup> C	<sup>1</sup> H	<sup>13</sup> C	<sup>1</sup> H
 <p>mangrolide B 2.5</p>	1	*	*	*	*
	2	*	*	*	*
	3	144.2	7.14	144.2	7.14
	4	128.1	6.57	127.9	6.56
	5	142.4	5.9	142.3	5.98
	6	37	2.5, 2.72	36.9	2.5, 2.72
	7	73.3	4.24	73.1	4.25
	8	*	*	*	*
	9	124.1	5.16	124	5.17
	10	42.7	2.7	42.6	2.7
	11	94.7	3.77	94.6	3.76
 <p>mangrolide C 2.6</p>	12	*	*	*	*
	13	134.3	5.83	134.2	5.82
	14	*	*	*	*
	15	125.2	5.46	125	5.46
	16	37	2.50	29.6	2.5, 2.42
	17	79.6	4.69	79.6	4.69
	18		2.08	31.6	2.08
	19	20.14	0.96	19.9	0.96
	20	18.8	1.02	18.7	1.02
	21	*	*	*	*
	22	*	*	*	*
	23	20.14	0.96	11.4	0.92
	24	30.5	1.34	14.3	1.01
	25	28	2.09	18.0	1.29
	26	*	*	26.8	1.64
	27	56.4	4.35	*	*
	28	-	-	56.3	4.36

Table 2.2 NMR data for mangrolide B and C

## 2.9 Optimization of SNA-18 Culture Conditions

One challenge with this project, as will be detailed in chapter 3 and 4, was obtaining enough material for experiments and bioassays. While the initial yield of 1 mg/L is good compared to most natural products, any increase would reduce the time spent on purification. In order to better understand mangrolide A production, a time course experiment was conducted in which SNA-18 was cultured in different nutrient sources. One liter of five different media recipes were inoculated with SNA-18 and incubated on a rotary shaker for 10 days (Table 2.3).

Samples were collected after 2, 3, 4, 6, 7, 8, and 10 days. Analysis by LC/MS revealed A1BFe+C to be the best media for mangrolide A production and it could be detected after a few days and the production of mangrolide A peaked after 7 days. No mangrolide A was detected in Acidic Gauze 1, Basic Gauze 1, and Calicheamicin medium.

Media	Ingredients
A1BFe+C	10 g starch, 4 g yeast extract, 2 g peptone, 1 g calcium carbonate, 0.4 g FeSO <sub>4</sub> ·4H <sub>2</sub> O, 0.1 g KBr
TCG	5 g casitone, 4 g glucose, and 3 g tryptone
Acidic Gauze 1	20 g starch, 1 g NaNO <sub>3</sub> , 0.5 g K <sub>2</sub> HPO <sub>4</sub> , 0.5 g MgSO <sub>4</sub> ·7H <sub>2</sub> O, 0.5 g NaCl, 0.01 g FeSO <sub>4</sub> , and adjust to pH 5.4 with phosphate buffer
Basic Gauze 1	10 g glucose, 5 g peptone, 5 g yeast extract, 1 g K <sub>2</sub> HPO <sub>4</sub> , 0.2 g MgSO <sub>4</sub> ·7H <sub>2</sub> O, 10 g Na <sub>2</sub> CO <sub>3</sub> , and adjust to pH 10-10.5 with NaHCO <sub>3</sub> -Na <sub>2</sub> CO <sub>3</sub> buffer
Calicheamicin	20 g sucrose, 5 g molasses, 2 g peptone, 2.5 g calcium carbonate, 0.1 g FeSO <sub>4</sub> ·7H <sub>2</sub> O, 0.2 g MgSO <sub>4</sub> ·7H <sub>2</sub> O, and 0.1 g potassium iodide

**Table 2.3.** Recipes for medium used to improve mangrolide production. All amounts are in g/L.

## 2.10 Effect of Polyketide Precursors on mangrolide A Production

The biosynthesis of polyketide natural products is well understood and has been reviewed in detail<sup>76</sup>. Similar to fatty acid synthesis, the process begins with acetyl-CoA and successive additions of malonyl-CoA extend the chain in two carbons increments. Other precursors, such as methyl malonyl-CoA, and starter units, such as isobutyl-CoA, can be incorporated by the PKS complex<sup>77</sup>. The structure of mangrolide A is very interesting in that it possess both an isobutyl starter unit as well as propionate and butyrate extensions (figure 2.6). It is possible that the biosynthetic pathway for mangrolide A requires four polyketide precursors (propionate positions could be formed from SAM methyltransferase). Interestingly, the mangrolide analogs isolated appear to only differ in the substitution at the C10 position indicating that the analogs were a result of a promiscuous acyltransferase. The hypothesis was that the addition of polyketide



precursors to the media could improve mangrolide production and potentially increase the ratio of **2.5** and **2.6** to **2.4**.

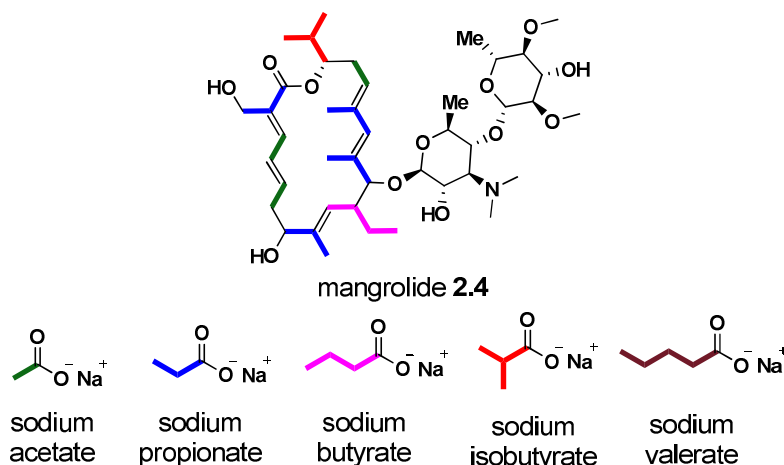


**Figure 2.6** Structure of mangrolide A with polyketide subunits highlighted. Colors are coordinated with the precursors purchased for the feeding experiments. Sodium valerate was included to determine if a new mangrolide analog could be produced.

To test the hypothesis, five polyketide precursors were purchased in their sodium salt form (figure 2.6). Initial experiments were conducted to establish standard conditions for SNA-18 growth and analysis. All experiments were conducted in 250 mL flasks containing 50 mL of media. Three flasks were cultured simultaneously for each condition tested and combined for extraction with an equal part of ethyl acetate. The organic layer was dried, suspended in methanol, and centrifuged to remove insoluble material. The supernatant was dried and resuspended in methanol at a concentration of 10 mg/mL for analysis by LC/MS. Mangrolide A production was monitored by measuring the UV absorbance and calculating the area under the curve. Each experiment contained SNA-18 untreated as a control and the data was normalized to this sample, so mangrolide production was reported as a relative measurement in each

experiment. A modified recipe of A1+C, referred to as A1+C-2, was used in which the starch was reduced to 5 g/L. This was done to encourage the uptake of the precursors added. No change in growth was observed at 5 g/L of starch but 2 g/L clearly inhibited growth. The effect of sodium acetate on SNA-18 was measured at two concentrations, 1 g/L and 3 g/L. At 3 g/L, sodium acetate appeared to inhibit growth of SNA-18 while 1 g/L did not. No change was detected if the sodium acetate was added at day one or split into multiple additions. All experiments were conducted with a single addition of 1 g/L of precursors when the SNA-18 cultures were started.

Following the above protocol, the effect of sodium acetate, sodium propionate, and sodium butyrate on mangrolide production in SNA-18 was measured (Chart 2.1). In all three conditions, production of **2.4** increased relative to the control. Unfortunately, no dramatic change in production of the mangrolide analogues was observed. Also, the flasks containing propionate and butyrate appeared much greener in color than the control flasks. The individual effects of valeric acid and isobutyric acid were tested, but no change was detected possibly due to poor solubility of the acids. Valeric acid and isobutyric acid were converted to the sodium salt with sodium hydroxide in later experiments.

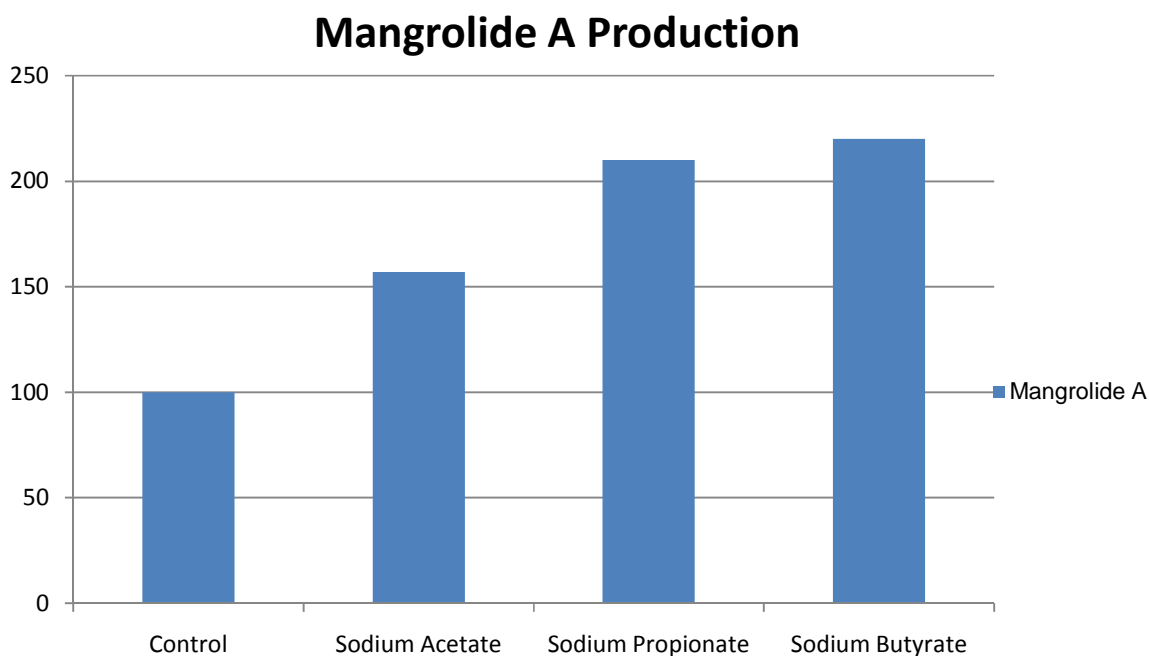


**Chart 2.1** UV absorbance of mangrolide A was measured. SNA-18 with no precursors added was the control and the data was normalized to this. Each bar represents the combined extract of three cultures.

Since the precursors were increasing the total amount of mangrolide production, a mixture of all the precursors was made. The polyketide precursor mixture consists of the following ratio: 30% sodium butyrate, 30% sodium propionate, 10% sodium isobutyrate, 10% sodium valerate, and 20% sodium acetate. It was added to cultures at 1g/L. The initial experiment testing the PM showed the same green phenotype, but after extraction a decrease in mangrolide production was observed. This appeared to be an error so the experiment was repeated comparing A1+C-2, A1+C, and A1+C with PM (Chart 2.2). This confirmed that the PM was increasing production of **2.4** and that the reduced starch media had a negative effect as well.

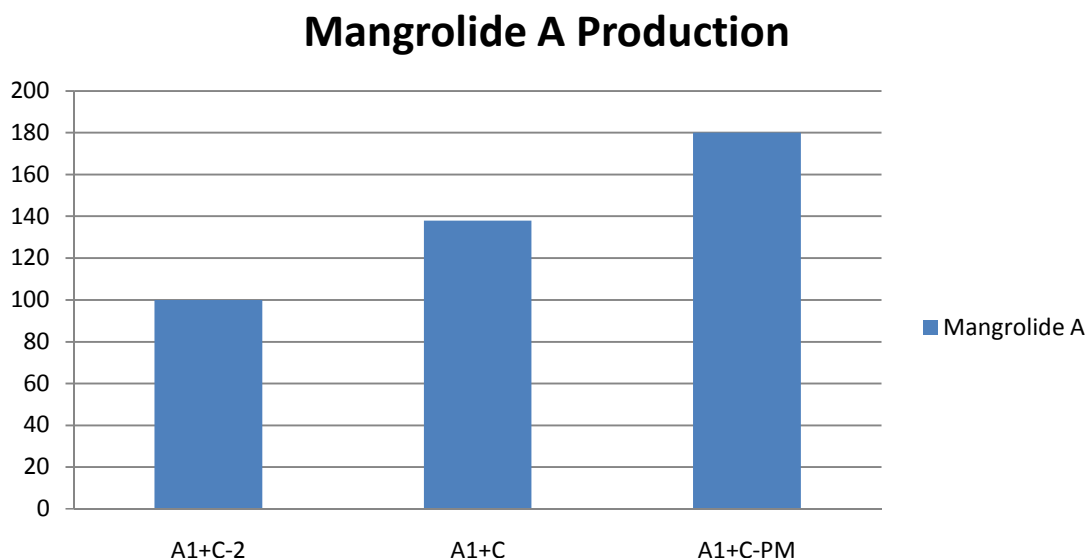


**Chart 2.2** UV absorbance of mangrolide A was measured. SNA-18 grown in reduced starch medium, A1+C-2 with no PM was the control and the data was normalized to this. A1+C-PM is A1+C media with PM added. Each bar represents the combined extract of three cultures.

## 2.10 SNA-18 Heat Shock and Oxidative Stress

The goal of this experiment was to try and stimulate the production of secondary metabolites from SNA-18 by stressing the bacteria during culture. Ethanol was used to simulate heat shock and hydrogen peroxide was used to cause oxidative stress<sup>50, 78</sup>. SNA-18 were inoculated into three Fernbach flasks containing A1+BFe+C media and after six days one liter of each was challenged with either 6% v/v of ethanol or 0.5% v/v of H<sub>2</sub>O<sub>2</sub> with the third left unchanged as a control. After two days the cultures were extracted using standard XAD-7 resin method. The crude extracts were purified on an ISCO using reversed phase conditions with a C-18 column. The fractions collected were analyzed by LC/MS and tested for antibacterial properties. No change in UV profile or antibiotic activity was observed for following ethanol or H<sub>2</sub>O<sub>2</sub> treatment.

## 2.11 Conclusion

From a phenotypic screen of a marine natural product library, an extract from a marine derived bacterium was detected with selective, gram negative activity. Bio assay and spectroscopy guided fractionation of the active component led to **2.4**. NMR elucidation of the planar structure of mangrolide A revealed an interesting polyketide natural product. The structure of **2.4** is complex with multiple unsaturated systems that isolate the stereocenters on the macrolide. In order to complete the project, it was critical to determine the absolute stereochemistry of **2.4**.

## CHAPTER THREE

### STEREOCHEMISTRY OF MANGROLIDE A

#### 3.1 Strategy for Determining Absolute Stereochemistry of mangrolide A

The stereochemistry of a molecule is a fundamental property and is required to establish the 3-D orientation of the molecule. Small changes in stereochemistry can significantly alter the biological properties. For example, (R)- and (S)-carvone have different odors, peppermint and caraway, respectively<sup>79</sup>. For medicinal compounds the wrong stereochemistry can cause harmful side effects as was seen with thalidomide, a drug which was prescribed to treat morning sickness but racemized in vivo and the enantiomer caused birth defects<sup>80</sup>. Mangrolide A contains 14 stereocenters which corresponds to 16,384 possible conformations, making the total synthesis of mangrolide A impossible without knowledge of the stereochemistry. This is crucial information to enable the synthesis of mangrolide analogs that have improved efficacies and pharmacokinetic properties.

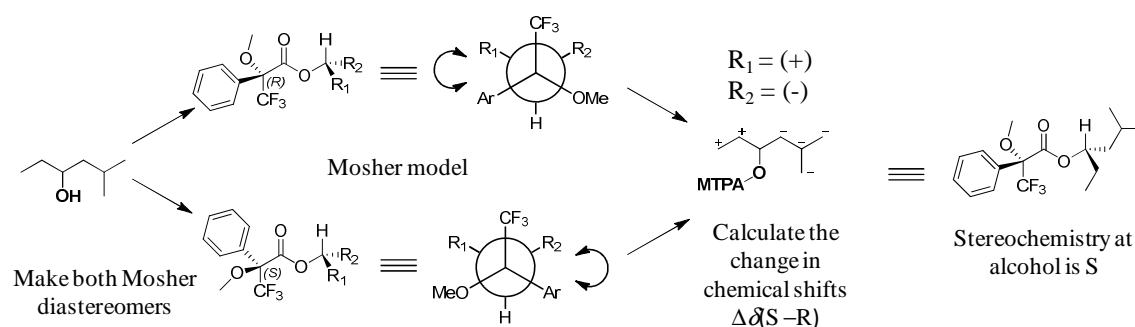


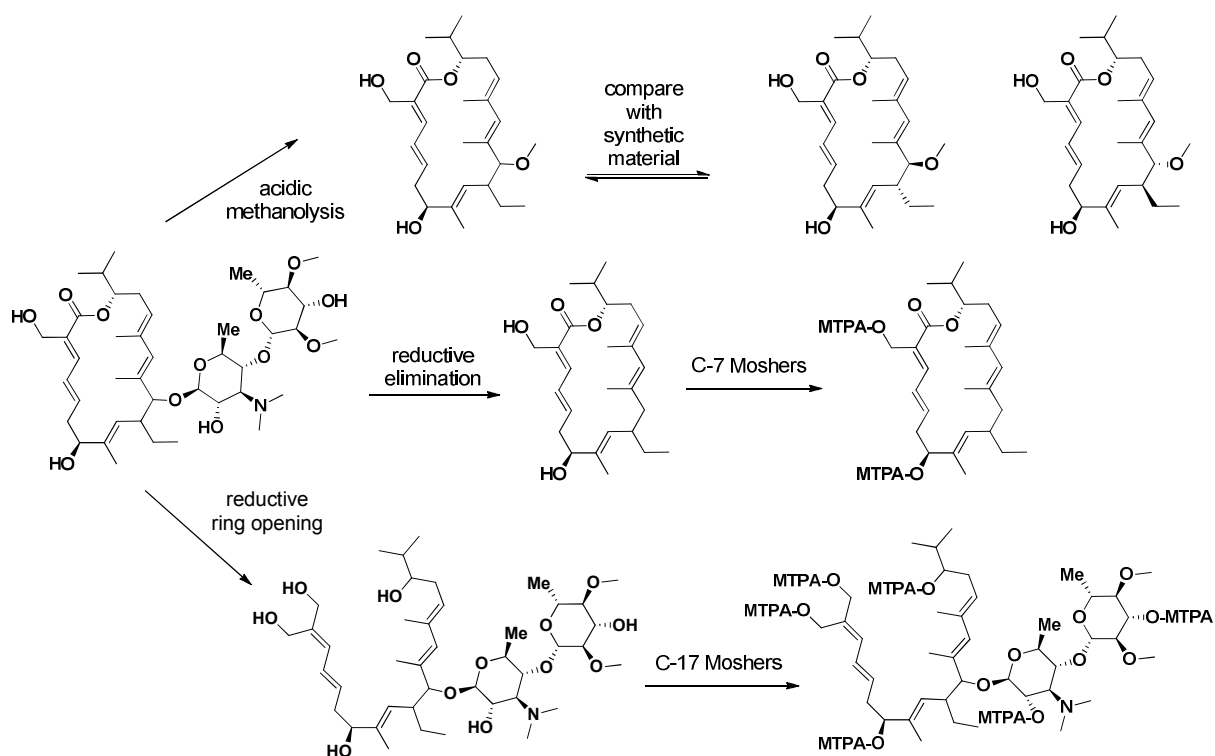
**Figure 3.1** Example of the Mosher's ester on a hypothetical compound where  $R_1 \neq R_2$ . The Newman Projection shows the standard conformation with the arrow highlighting the anisotropic effect between the aryl and  $R_1$ .

Elucidation of the absolute stereochemistry is a major challenge in natural product research. Techniques used include optical rotation, CD, x-ray crystallography, and NMR based techniques. Obtaining suitable crystals of small molecule natural products is difficult and is limited by the small amounts of compound typically isolated. As such, considerable effort was placed on crystallization of mangrolide A with no success. Although methods utilizing CD to obtain the stereochemistry was considered, ultimately none of the existing, non-destructive techniques could be used reliably. Elucidation the stereochemistry of mangrolide A relied heavily on NMR based techniques. Of these, the most commonly used is Mosher's analysis. First published in 1973 by Dale and Mosher, it is an empirical method to determine the absolute configuration of a position containing a secondary alcohol or amine. This is accomplished by acetylating the alcohol with a chiral reagent, MTPA-OH. The newly formed ester can adopt different configurations but the one that best explains the method is shown in (figure 3.1). The key to this technique is how the aryl group is positioned relative to the substituent  $R_1$  and  $R_2$ .

Anisotropic shielding from the aryl group affects  $R_1$  and  $R_2$  differently and causes an upfield shift in the positions on the aryl side. By forming both the R- and S-MTPA esters and subtracting the R-MTPA chemical shifts from the S-MTPA shifts, a change in chemical shifts  $\Delta\delta(S-R)$  can be determined for each position. These values can either be positive or negative and each substituent should be entirely negative or positive. The substituent with positive  $\Delta\delta(S-R)$  values is assigned to  $R_1$  and the substituent with negative  $\Delta\delta(S-R)$  values is assigned to  $R_2$  to give the absolute configuration at that position. This method has been extensively verified by experimentation, but there are some limitations. All of the values must be consistently positive or negative for  $R_1$  or  $R_2$ , and any discrepancy prevents the confident assignment of the stereocenter. The presence of additional secondary alcohols can cause misassignment as well depending on proximity.

The strategy for solving the stereochemistry of mangrolide A involved separating the molecule in two parts, the macrolide ring and disaccharide. The relative stereochemistry of the disaccharide can be determined through  $^3J_{HH}$  coupling constants. The macrolide ring presented a challenge since it contained four stereocenters isolated in three systems thus requiring separate approaches (Figure 3.2). The approach for C-7 and C-17 was to selectively degrade mangrolide in order to access secondary alcohols amenable to Mosher's ester analysis. The relative stereochemistry between C-10 and C-11 was determined through  $J$ -based analysis. This information will be used to create synthetic standards for comparison.

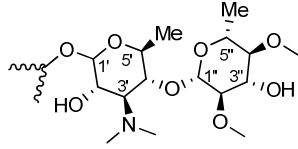




**Scheme 3.1** Strategy to determine the absolute stereochemistry of the macrolide ring.

### 3.2 Relative Configuration of the mangrolide A Disaccharide

Mangrolide A (**3.1**) contains a disaccharide consisting of mycaminose and 6-deoxy-2,4-dimethyl-glucose appended to the macrolide ring at the C-10 position. The constrained nature of the six member ring of sugars allows for a straightforward determination of the relative stereochemistry using  $^1\text{H}$ - $^1\text{H}$  coupling constants. The Karplus correlation can relate the dihedral angle to the coupling constant for vicinal protons. Protons with a large coupling constant (8-14 Hz) are predicted to be axial to each other while a small coupling constant (1-7 Hz) indicates an equatorial relationship<sup>81</sup>. In order to accurately determine the coupling constants of the sugars, 1D-TOCSY data was collected irradiating the anomeric proton signals (Table 3.1). This clarified the overlapping  $^1\text{H}$  spectrum of the sugars. Large coupling constants were observed between positions on mycaminose (7.4, 9.8, 10.4, 9.4, and 8.4 Hz) and 6-deoxy-2,4-dimethyl-glucose (7.9, 9.4, 9.1, 9.2, and 9.6 Hz) indicating that the protons were arranged in the trans-axial configuration. The absolute stereochemistry can be inferred from the fact that the laevo-rotatory isomer of sugars is rarely observed in nature.

	No.	$J$ in Hz
	$^3J_{H1'}$	d, 7.4
	$^3J_{H2'}$	dd, 9.8, 7.4
	$^3J_{H3'}$	t, 10.4
	$^3J_{H4'}$	t, 9.4
	$^3J_{H5'}$	dd, 8.4, 6.2
	$^3J_{H6'}$	d, 6.2
	$^3J_{H1''}$	d, 7.9
	$^3J_{H2''}$	dd, 9.4, 7.9
	$^3J_{H3''}$	t, 9.1
	$^3J_{H4''}$	t, 9.2
	$^3J_{H5''}$	dd, 9.6, 6.2
	$^3J_{H6''}$	d, 6.2

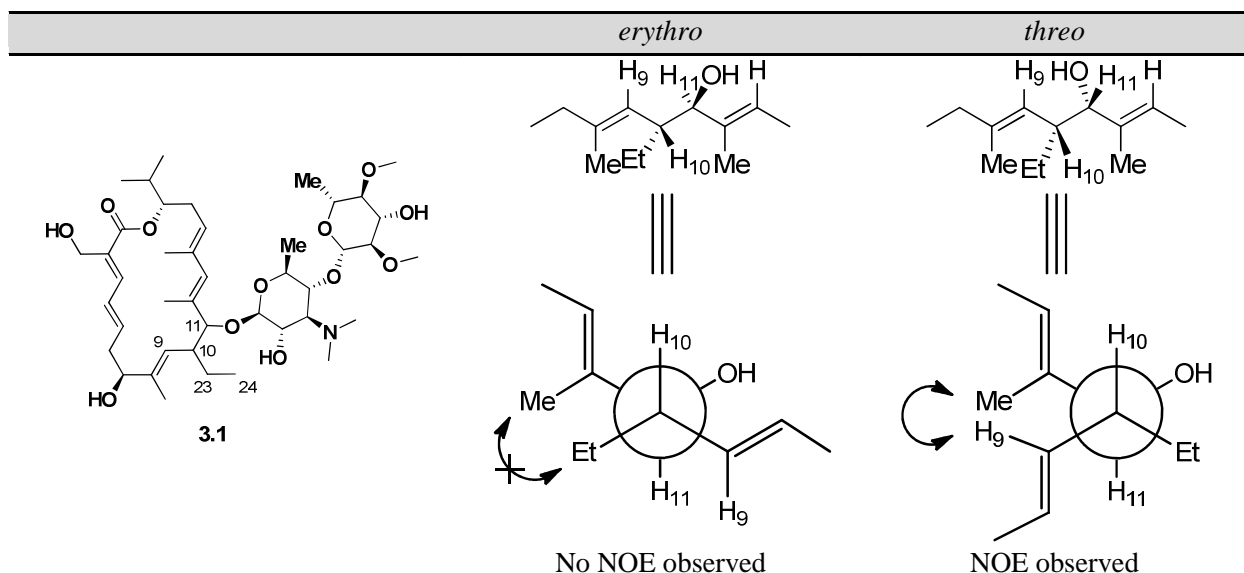
**Table 3.1** Coupling constant data used to determine disaccharide configuration.

### 3.3 J-based Configuration Analysis of C-10 and C-11

The high degree of unsaturation of the macrolide ring isolates the four stereocenters in the macrolide ring. Only at positions C-10 and C-11 can information be gained about the relative stereochemistry. To do this,  $^1J_{CH}$  and  $^{2,3}J_{CH}$  coupling constants were analyzed using the HETLOC NMR experiment. This data was combined with  $^3J_{HH}$  coupling constants and compared to the predicted values for the *threo* and *erythro* configurations<sup>82</sup> (Table 3.2). This method is referred to as *J*-based configuration analysis and was developed to determine the relative configuration of natural products<sup>82</sup>.

To gather the necessary data, approximately 9 milligrams of compound was purified by HPLC. HETLOC and  $^1H$  data was collected on a 600 MHz Varian NMR (Table 3.2). The HETLOC experiment is a modified TOSCY, and is limited to carbons containing protons thus preventing the analysis of the quaternary carbon at C-12. Based on the large  $^3J_{HH}$  between H-10 and H-11, two Newman projections were possible for the anti-orientation of the protons (*erythro*

and threo). The  $^{2,3}J_{\text{CH}}$  coupling constants measured by the HETLOC were compared to the theoretical values for the Newman projections and a good match was observed. Unfortunately, it was not possible to distinguish between the two configurations. A key NOE correlation between the C12 methyl and H-9 provided evidence for the threo configuration. However, while the data available suggests the threo configuration, it is not conclusive.



<u>Actual</u>		<u>estimated</u>		<u>estimated</u>	
$^3J_{\text{H10-H11}}$	9.5 Hz	$^3J_{\text{H10-H11}}$	Large	$^3J_{\text{H10-H11}}$	Large
$^3J_{\text{C11-H9}}$	1.4 Hz	$^3J_{\text{C11-H9}}$	Small	$^3J_{\text{C11-H9}}$	Small
$^3J_{\text{C10-H12}}$	-	$^3J_{\text{C10-H12}}$	-	$^3J_{\text{C10-H12}}$	-
$^3J_{\text{H23-H12}}$	2.4 Hz	$^3J_{\text{H23-H12}}$	Small	$^3J_{\text{H23-H12}}$	Small
$^2J_{\text{C11-H10}}$	5.8 Hz	$^2J_{\text{C11-H10}}$	Large	$^2J_{\text{C11-H10}}$	Large

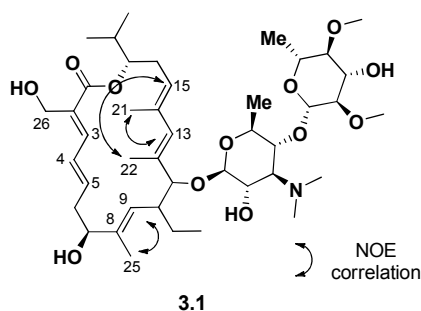
**Table 3.2** Standard and Newman projections between C-10 and C-11 for both the *erythro* and *threo* conformations. Arrows mark key NOE correlations.

### 3.4 Olefin Configuration of mangrolide A

Mangrolide A (3.1) contains an alpha, beta, gamma, delta-unsaturated ester, a conjugated diene, and a trisubstituted alkene. Determination of the cis/trans configurations of these olefins was accomplished through  $^3J_{HH}$  and  $^3J_{CH}$  coupling constants as well as NOE correlations (Table 3.3). For the unsaturated ketone system, H-4 showed a triplet with a coupling of 12.5 Hz indicating that it is trans to both H-3 and H-5. This was supported by a  $^3J_{CH}$  coupling of 6.8 Hz between C-26 and H-3 which points to a trans configuration.

The alkene at C-8 and C-9 was predicted to be cis based on a small  $^3J_{CH}$  coupling of 3.1 Hz between the methyl C-25 and H-9 and a large coupling of 11.3 between H-9 and C-7. A NOE correlation between C-25 and H-9 further supported this assignment. The chemical shifts of H-9 and C-25 in mangrolide matched the chemical shifts of lipiarmycin A which contained a trans olefin at this position. The configuration of this double bond was confirmed to be trans after the De Brabander group completed the synthesis of the macrolide ring. This is an unusual situation in that the coupling constants predict the wrong configuration.

The two methyl substituents on the conjugated diene prevented the use of  $^3J_{HH}$  coupling constants. Large  $^3J_{CH}$  coupling of 7.8 and 7.2 was observed for C21/H15 and C22/H13 respectively indicating a cis diene. NOE correlations remain inconsistent between C-22/H-15 and C-21/H13 indicating that the ring conformation of this molecule is unusual.

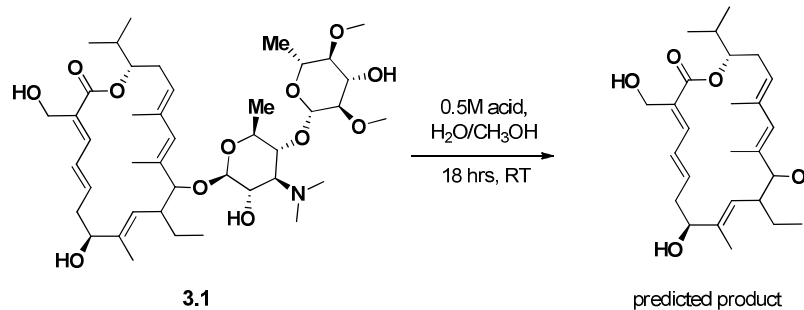


No.	<i>J</i> in Hz
$^3J_{H4}$	triplet, 12.5 Hz
$^3J_{C26-H3}$	6.8 Hz
$^3J_{C25-H9}$	3.1 Hz
$^3J_{C21-H15}$	7.8 Hz
$^3J_{C22-H13}$	7.2 Hz

**Table 3.3** Coupling constant data used to determine olefin configuration. NOE correlations are indicated by arrows.

### 3.5 Mangrolide A Acid Catalyzed Hydrolysis

In order to remove the sugars from the macrolide ring, mangrolide A (**3.1**) was subjected to acidic methanolysis (Table 3.4). It was expected that HCl (0.5M) in methanol could catalyze a nucleophilic addition of methanol to C-10 to form a methyl ether and remove the disaccharide. To accomplish this, 6-7 mg of **3.1** was dissolved in dry methanol (1mL) and 1M methanolic HCl (1mL) was added dropwise while stirring at room temperature. The reaction proceeded for approximately eighteen hours before the majority of the starting material was consumed. Three products were detected by LC/MS with a *m/z* of 469 in positive ion mode which corresponds to the  $[M+Na]^+$  of the expected product. The reaction was neutralized with NaOH, dried under reduced pressure, and separated with DCM and water. The organic layer contained the products which were separated by C18 reversed phase HPLC using a standard gradient of water/CH<sub>3</sub>CN plus 0.1% formic acid. When this material was purified by normal phase HPLC a forth product with the same mass was detected. The aqueous layer appeared to contain the sugar residues



Substrate	Acid	Temperature (°C)	Solvent	Products
<b>3.1</b>	0.5M HCl	23°C	50/50 H <sub>2</sub> O/CH <sub>3</sub> OH	<b>3.2, 3.3, 3.4,</b> and <b>3.5</b>
<b>3.1</b>	0.5M HCl	-72°C	50/50 H <sub>2</sub> O/CH <sub>3</sub> OH	No reaction
<b>3.1</b>	0.5M H <sub>2</sub> SO <sub>4</sub>	-72°C	50/50 H <sub>2</sub> O/CH <sub>3</sub> OH	<b>3.2, 3.3, 3.4,</b> and <b>3.5</b>

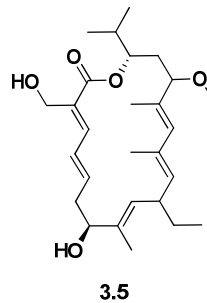
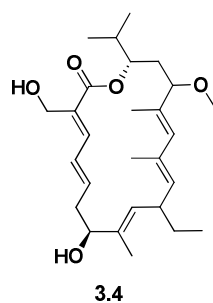
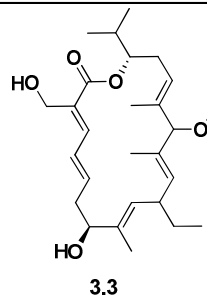
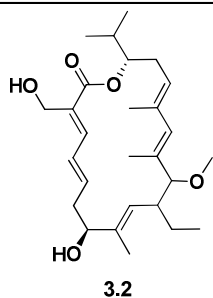


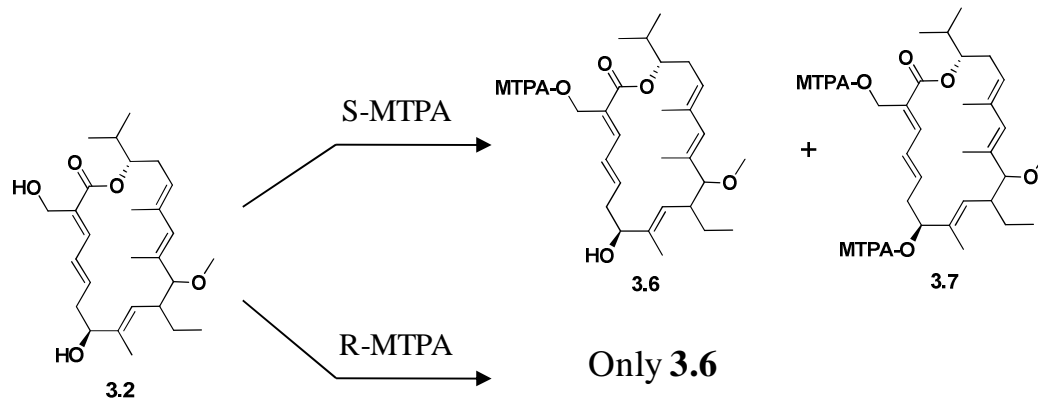
**Table 3.4** Conditions tested for acidic methanolysis of **3.1**. Four products were purified and structures were solved by 2-D NMR.

based on proton NMR data. Two dimensional NMR data sets were collected for the four products. From this it was determined that the mixture of products consisted of the macrolide ring with a methyl ether at either C-11, C-13, or C-15. The allylic nature of C-10 was able to stabilize the cation charge and cause the nucleophilic addition of methoxide to occur at different positions on the conjugated diene. The reaction was very consistent in producing the same products. When the reaction was cooled to  $-72^{\circ}\text{C}$ , no products were observed. When a stronger acid,  $\text{H}_2\text{SO}_4$ , was used the same result was observed.

### **3.6 Mosher's Analysis on Methanolysis Product 3.2**

The aglycon **3.2** produced by the methanolysis reaction was suitable for use in Mosher's analysis for solving the stereochemistry at the secondary alcohol at C-7. Approximately, 0.8 mg of **3.2** was split evenly and the reaction was conducted using equal parts pyridine- $\text{d}_5$  and  $\text{CDCl}_3$  and twenty equivalents of S-MTPA-Cl (Table 3.5). The reaction proceeded overnight at room temperature and the starting material was undetectable by LC/MS with one major product present. The use of deuterated solvents allowed the mixture to be dried and directly analyzed by NMR. The reaction was repeated with R-MTPA-Cl but despite multiple attempts the C-7(S) diastereomer could not be produced. It was possible that the conformation of the aglycon was preventing the formation of this Mosher diastereomer. Due to the fact that the methanolysis reaction produced multiple products other methods to remove the sugars were investigated.





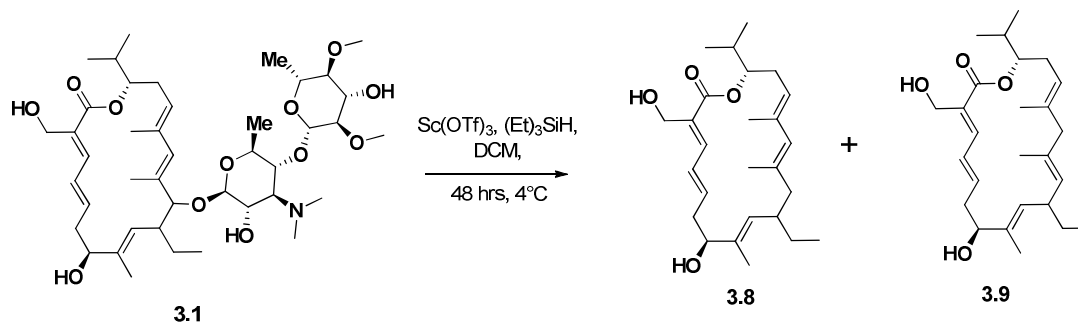
Substrate	Mosher reagent (Equivalents)	Solvent	Temperature, (°C)	Product
<b>3.2</b>	S-MTPA-Cl, 20 equiv	pyridine-d <sub>5</sub> , CDCl <sub>3</sub>	23°C	<b>3.7</b>
<b>3.2</b>	R-MTPA-Cl, 25 equiv	pyridine-d <sub>5</sub> , CDCl <sub>3</sub>	23°C	<b>3.6</b>
<b>3.2</b>	R-MTPA-Cl, 25 equiv	pyridine-d <sub>5</sub> , CDCl <sub>3</sub>	50°C	Could not be determined

**Table 3.5** Experiments towards producing di-MTPA aglycon.

### 3.7 Scandium Triflate Catalyzed Reduction of C-11

In order to avoid the allylic nature of the C-11 ether, a Lewis acid catalyzed reaction was attempted with the goal of cleaving the sugars through the sugar acetal. Following a published protocol, mangrolide A (6mg) was reacted with scandium triflate and triethylsilane in DCM at -72°C (Scheme 3.1)<sup>83</sup>. The reaction was allowed to warm to 4°C and remained at this temperature for 48 hours. Work up was accomplished by evaporating the DCM and resuspending in MeOH with 0.1% formic acid. The MeOH was evaporated under nitrogen and the material was separated with water/DCM. The water layer contained the sugars and

remaining starting material and the products were present completely in the organic layer. One major and two minor products were isolated by reversed phase C-18 HPLC. 2D NMR data revealed the structure of the major product **3.8**, to be the aglycon ring with the sugar linked carbon reduced to a methylene at C-11, a deoxygenation of the aglycon. One of the minor products **3.9** was determined to be the aglycon with a methylene at C-13 and an olefin between C-11/C-12. These products were unexpected but not unprecedented as Qin *et al.* has demonstrated that scandium triflate can reduce aryl pyranosides<sup>83</sup>. Like the acidic methanolysis, the electronics of the conjugated diene allylic to C-11 was influencing the reaction and producing a mixture of products.



**Scheme 3.2** Scandium triflate catalyzed reduction of **3.1**

### 3.8 Mosher's Analysis of C-7

The product of the scandium triflate reaction was carried forward for Mosher's ester analysis. A different protocol for the MTPA acetylation was followed (Table 3.6)<sup>84</sup>. Distilled pyridine, DMAP, and **3.8** (0.8mg) were combined and stirred at room temperature. After which, either S or R-MTPA-Cl was added and stirred overnight. Work up was accomplished by drying the reaction and extraction with water/ether. The organic layer was dried under nitrogen and

NMR data was collected in  $\text{CDCl}_3$ . The proton at C-7 had shifted upfield to 5.507 and 5.524 ppm in the S and R-Moshers respectively indicating that both were successfully made. The downfield region of the proton spectrum was well resolved but significant overlap in the upfield region was preventing the identification of some key signals. In order to overcome this, 1-D TOCSYs were collected by irradiating the C-5 and C-9 protons (Figure 3.2). The change in chemical shift between the two derivatives was calculated and fit to the established Mosher model to determine the stereochemistry of position 7 as S (Table 3.6).

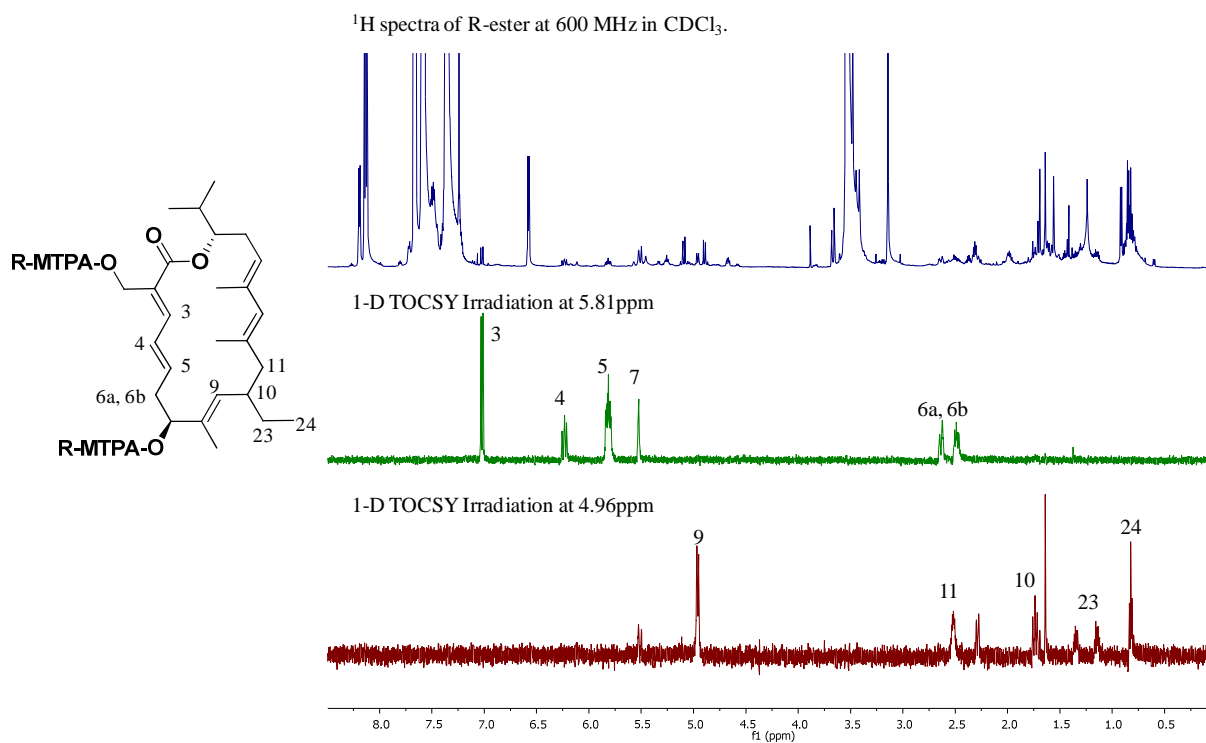
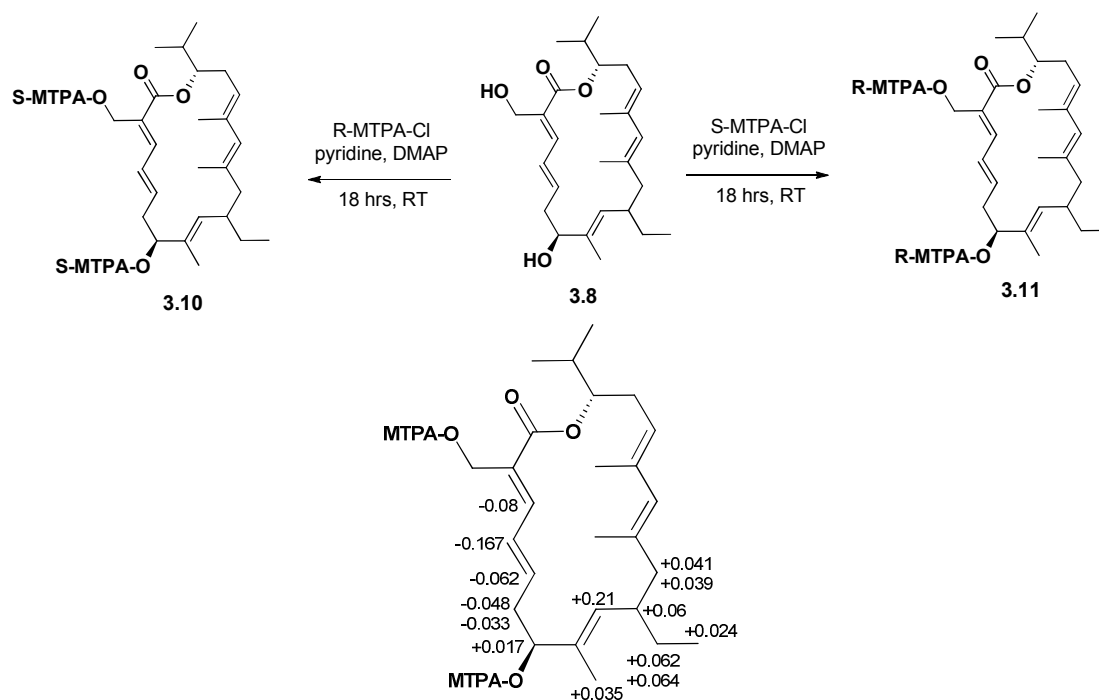


**Figure 3.2**  $^1\text{H}$  spectrum of 7R-3.8 is shown on top. The 1D-TOCSY experiments removed overlap and allowed for the accurate measurement of the chemical shifts around C-7.



No.	$\delta$ 7S-ester $^1\text{H}$ , mult ( $J$ in Hz)	$\delta$ 7R-ester $^1\text{H}$ , mult ( $J$ in Hz)	$\Delta\delta^{SR}$ (ppm)
3	7.022, d (11.6)	7.102, d (11.5)	-0.08
4	6.233, t (13.8)	6.4, t (13.2)	-0.167
5	5.815, ddd (4.9, 9.4, 15)	5.877, ddd (4.7, 9.4, 14.8)	-0.062
6a	2.637, m	2.685, m	-0.048
6b	2.489, m	2.522, m	-0.033
7	5.524, m	5.507, m	+0.017
9	4.96, d (9.6)	4.75, d (9.4)	+0.21
10	2.526, m	2.466, m	+0.06
11a	2.289, m	2.248, m	+0.041
11b	1.738, m	1.699, m	+0.039
23a	1.352, m	1.29, m	+0.062
23b	1.153, m	1.107, m	+0.046
24	0.824, t (7.3)	0.8, t (7.4)	+0.024
25	1.64, s	1.605, s	+0.035

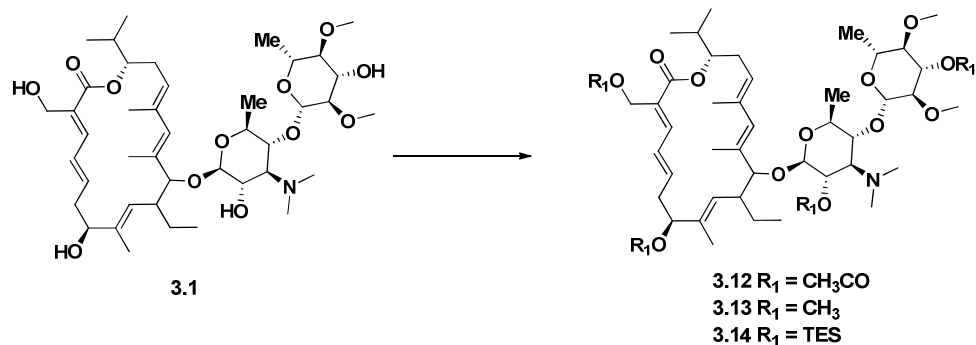
**Table 3.6** Mosher's analysis of **3.8**.

### 3.9 Strategy for Elucidating Mangrolide A C-17 Stereochemistry

The strategy to solving the stereocenter at C-17 would be similar to the approach used for the C-7 hydroxyl. Hydrolysis of the macrolide ester would reveal a secondary alcohol at C-17 amenable to Mosher's analysis. In order to simplify the Mosher's analysis the macrolide ring would be separated from the disaccharide and the remaining alcohols would be protected. Esters are susceptible to a variety of reaction conditions and it was expected to be straightforward to determine successful reaction conditions.

### 3.10 Mangrolide A Protecting Group Strategies

Mosher's analysis works best when only one secondary alcohol is present, so different protecting group strategies for mangrolide A were considered (Table 3.7). These experiments were challenging as mangrolide A has three secondary alcohols and one primary alcohol. Global protection of **3.1** with acetic anhydride was straightforward but the protecting group was not stable to acid catalyzed hydrolysis of the ester. Methylation of **3.1** was attempted with methyl iodide and silver nitrate but the reaction resulted in a mixture of mangrolide plus two, three, and four methyl additions which could not be separated. Other methylating reagents, TMS-diazomethane and methyl triflate, were tested but no reaction with mangrolide A was observed. Finally, a triethylsilyl group was successfully added to all four alcohols to produce **3.14** and this substrate was tested under a variety hydrolysis conditions. Using (0.5N) KOH in methanol at 55°C for approximately eighteen hours, the only product observed was the loss of a TES protecting group. This was observed for other bases including LiOH and NaOH.



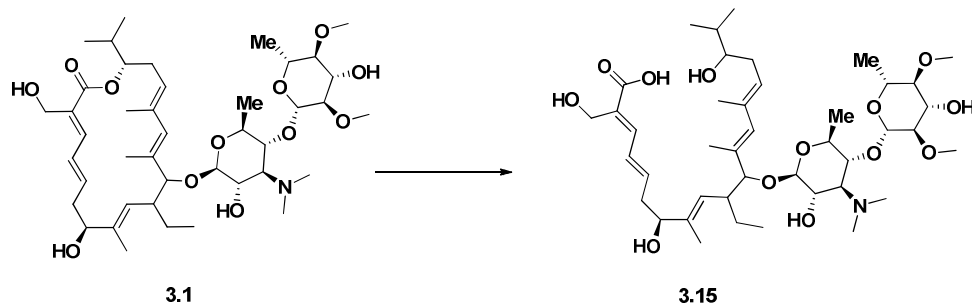
Substrate	Conditions	Results
3.1	Acetic anhydride (24 equiv), pyridine, 48hr, 23°C	Successful addition of all acetate groups
3.1	4A MS, ether, methyl iodide, AgO <sub>2</sub> , 18hr, 50°C	multiple products
3.1	Methyl triflate, lutidine, DCM, 3hr, -72°C to 50°C	No reaction
3.1	Methyl triflate, lutidine, pyridine, 18hr, -72°C to 80°C	No reaction
3.1	TES triflate, lutidine, DCM, 3hr, -72°C	<b>3.14</b>
3.14	0.5N KOH in methanol, 18hr, 55°C	Loss of one TES group
3.14	0.5N LiOH, THF, 18hr, 23°C to 60°C	No reaction
3.14	0.5N NaOH, 1,4 dioxane, 4hr, 23°C to 60°C	Loss of 1, 2, and 3 TES groups
3.14	0.5N NaOH, 1,4 dioxane, 18hr, 90°C	Degradation of starting material and no products detected

**Table 3.7** Mangrolide A global protection experiments and base catalyzed ester hydrolysis reactions on TES protected mangrolide.

When 0.5N NaOH and **3.14** were heated to 90°C overnight, no products and little starting material was detected indicating that the material was degrading. In light of these results, the strategy of adding protecting groups to mangrolide A before opening the ring was abandoned.

### **3.11 Mangrolide A Hydrolysis Reactions**

While removal of the secondary alcohols either by protecting groups or loss of the disaccharide would have been the optimal approach for Mosher's analysis on C-17, none of the previous experiments to open the ring had been successful. Mangrolide A had good ionization and solubility but these qualities were lost as mangrolide is made more non-polar. Material limitations were a problem throughout these experiments so the previous conditions were repeated using unmodified mangrolide A as the substrate (Table 3.8). The goal was to determine if any method could open the ester and a successful reaction should be easier to detect by LC/MS on **3.1**. Starting with 1N LiOH in THF/MeOH at room temperature no change in **3.1** was observed. Increasing the concentration of the LiOH to 2N had no effect and when the reaction was refluxed at 80°C the starting material disappeared with no identifiable products present. Changing the base to 2N NaOH had the same results. In addition, acid hydrolysis conditions were tested with 6N HCl in methanol at room temperature, but only the macrolide aglycon products previously described were observed.



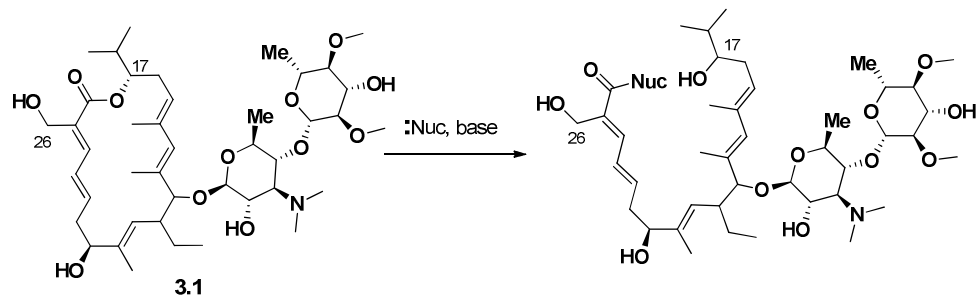
Substrate	Conditions	Results
<b>3.1</b>	1N LiOH, THF, MeOH, 0°C to r.t.	no reaction
<b>3.1</b>	2N LiOH, THF, MeOH, r.t.	no reaction
<b>3.1</b>	2N LiOH, THF, MeOH, 80°C	degraded
<b>3.1</b>	2N NaOH, r.t.	no reaction
<b>3.1</b>	2N NaOH, 80°C	degraded
<b>3.1</b>	6N HCl	de-glycosylation products

**Table 3.8** Acid or base catalyzed hydrolysis of **3.1**

### 3.12 Nucleophilic Ring Opening Reactions

Nucleophilic addition to the ester was tested as an alternative approach to opening the ring (Table 3.9). Butane thiol was chosen as the nucleophile and sodium hydroxide was the base used. After 18 hours at 75°C, no reaction was detected. The same result was observed when triethylamine was substituted as the base. After increasing the concentration of both reagents and increasing the time of the reaction a product was detected with an unexpected mass. This product was purified by HPLC and the proton NMR showed that the  $\alpha$ ,  $\beta$ ,  $\gamma$ ,  $\delta$  unsaturated ester was intact and that the butane thiol had attacked at the C-26 position to replace the alcohol.





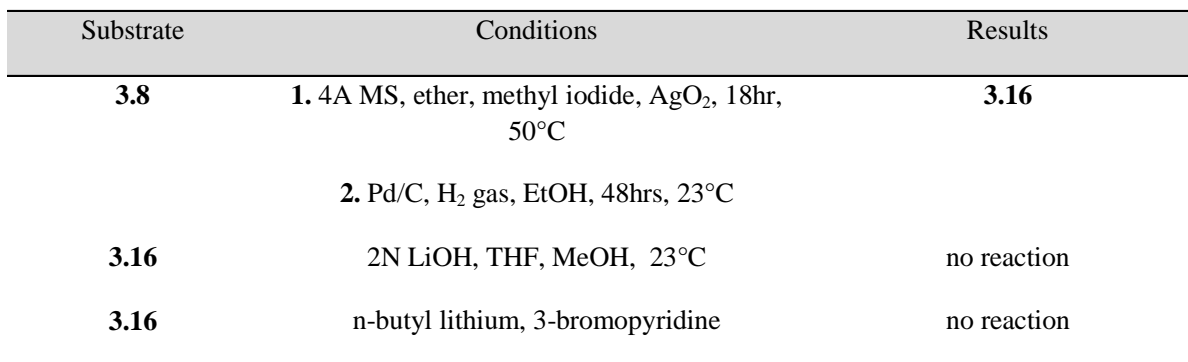
Substrate	Conditions	Results
<b>3.1</b>	NaOH (1.5 equiv), butane thiol (5 equiv), CH <sub>3</sub> CN, 8hrs, 75°C	no reaction
<b>3.1</b>	Triethylamine (2 equiv), butane thiol (10 equiv), CH <sub>3</sub> CN, 18hrs, 75°C	No reaction
<b>3.1</b>	Triethylamine (10 equiv), butane thiol (40 equiv), CH <sub>3</sub> CN, 72hrs, 75°C	Unidentified products
<b>3.1</b>	Sodium hydride (0.5M), dry methanol, 4A MS, 18hrs	m/z 798, 762, and 815 [M+H]
<b>3.1</b>	Sodium hydride (0.5M), dry methanol, 4A MS, 18hrs, 55°C	degredation
<b>3.1</b>	Sodium hydride (6 equiv), dry methanol, 4A MS, 48hrs,	m/z 794 [M+H], C-26 O-methylated product
Methyl protected <b>3.3</b>	Sodium hydride (1M), dry methanol, 4A MS, 72hrs,	No products could be identified
Methyl protected <b>3.4</b>	Triethylamine (10 equiv), butane thiol (20 equiv), DCM, 72hrs, 45°C	No products could be identified

**Table 3.9** Nucleophilic additions to mangrolide ester.

Next, sodium methoxide was considered as it is a smaller nucleophile and would be impacted less by steric interactions. This reagent was more reactive and would generate many products that were unable to be identified. After optimizing conditions one product was purified but the same nucleophilic addition to C-26 was observed. To try and reduce the reactivity of the C-26 hydroxyl, a methyl protected analogue was made from the macrolide products of the acid catalyzed deglycosylation. Both methods, sodium hydride and butane thiol, were tested but neither method produced identifiable products.

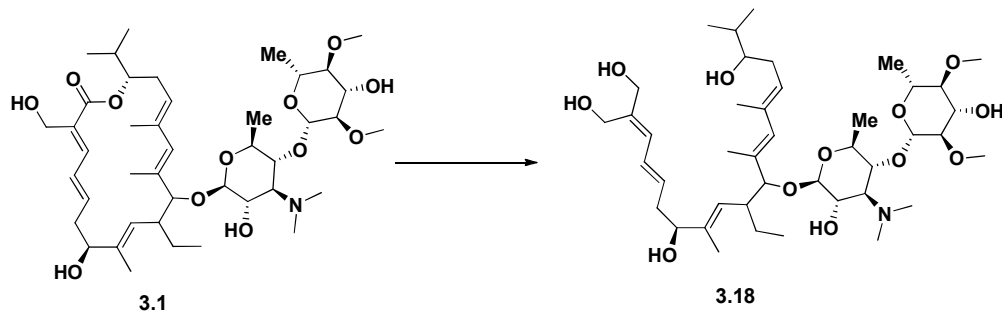
### 3.13 Mangrolide A Aglycon Hydrogenation

The electronics of the  $\alpha$ ,  $\beta$ ,  $\gamma$ ,  $\delta$  unsaturated ester appeared to be hindering attempts to open the ring. Removing this unsaturated system could allow the hydrolysis or nucleophilic reactions to work. To accomplish this, a methyl protected version of **3.8** was stirred under hydrogen with palladium on carbon to yield the hydrogenated macrolide **3.17** (Table 3.10). One advantage of using the reduced macrolide was that hydrogenation would convert both **3.8** and **3.9** to the same product. Reduction of the ester with sodium borohydride on **3.16** was attempted but no reaction was detected. Loss of the double bonds increased the overlap in the proton NMR spectra but the C-17 proton has a distinct shift at 4.76 which would change significantly if released from the ester. Next, the LiOH catalyzed hydrolysis was run at room temperature for 48hrs with no change in starting material detected. Finally, a nucleophilic addition with n-butyl lithium and 3-bromopyridine was tried. The loss of the double bonds in the hydrogenation product **3.16** prevented the detection of products by UV and **3.16** did not ionize by MS, and the



### 3.14 Mangrolide A Ester Reduction

Reduction of the ester to a primary alcohol was the final method attempted to open the macrolide ring (Table 3.11). Initially, DIBAL-H was chosen as the reducing agent. The methyl protected version of **3.3** was dissolved in ether and cooled to -72°C before adding DIBAL-H (1.2 equiv). After thirty minutes the reaction was warmed to room temperature and stirred overnight. Only starting material was detected after extraction. The solubility of **3.3** was better in DCM so the reaction was repeated using DCM as a solvent but no change in starting material was detected.



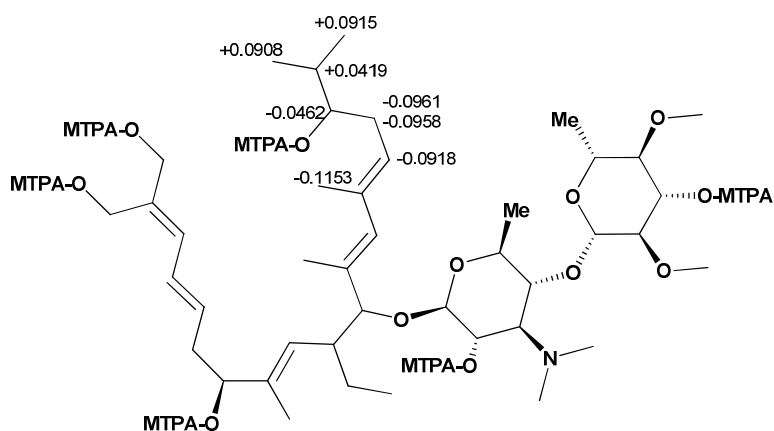
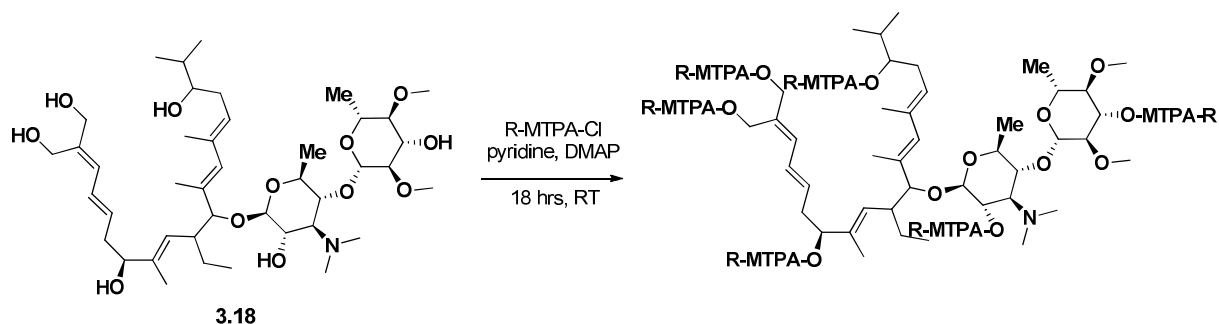
Substrate	Conditions	Results
<b>3.3</b>	1. 4A MS, ether, methyl iodide, AgO <sub>2</sub> , 18hr, 50°C 2. DIBAL-H, toluene -78 °C to r.t.	no reaction
<b>3.3</b>	1. 4A MS, ether, methyl iodide, AgO <sub>2</sub> , 18hr, 50°C 2. DIBAL-H, DCM -78°C to r.t.	no reaction
<b>3.6</b>	Red-Al, pyridine, 0°C	Ring opened
<b>3.1</b>	Red-Al, pyridine, 0°C	<b>3.18</b>

**Table 3.11** Experiments to reduce the mangrolide ester.

After trying DIBAL-H, a different reducing reagent, Red-Al, was tested. Unprotected methanolysis product **3.6** was dissolved in distilled pyridine and cooled to 0°C before Red-Al (10 equiv) was added. After workup the correct mass was detected by LC/MS but many other products were present. Approximately 0.2 mg of **3.18** was obtained by reversed phase HPLC and the proton NMR confirmed that the ester had been reduced. Due to the lack of material only the C-17 R-Mosher derivative was formed. A modified Mosher's method using barium perchlorate to induce shifts was to be used but the solubility of the macrolide with four MTPA additions was poor in the polar solvents necessary to dissolve the barium perchlorate. A new approach was attempted using unprotected mangrolide A as the substrate for the Red-Al reduction. The same procedure was followed and the reaction produced few products and enough material was obtained to make both Mosher derivatives.

### 3.15 Mosher's Ester Analysis on mangrolide A

The unprotected mangrolide analogue has six positions that can be acetylated by MTPA-Cl and could potentially create significant overlap in the proton spectrum. The C-17 position is distant from the other secondary alcohols and the other MTPA groups should not interfere with the analysis. Following the same protocol used in section 3.8, **3.18** was converted into both S-MTPA and R-MTPA derivatives (Table 3.12). Proton NMR had significant overlap in both the upfield and downfield regions but the C-17 shift was distinct enough to collect 1-D TOSCY data. The  $\Delta\delta^{SR}$  was calculated and applied to the Mosher model to determine the stereochemistry of C-17 as S.



No.	$\delta$ 17S-ester $^1\text{H}$ , mult ( <i>J</i> in Hz)	$\delta$ 17R-ester $^1\text{H}$ , mult ( <i>J</i> in Hz)	$\Delta\delta^{SR}$ (ppm)
20	0.9196, d (6.4)	0.8288, d (4.5)	0.0908
19	0.9095, d (6.0)	0.818, d (4.5)	0.0915
18	1.9028, m	1.8609, m	0.0419
17	4.952, m	4.9982, m	-0.0462
16a	2.39, m	2.4861, m	-0.0961
16b	2.2674, m	2.3632, m	-0.0958
15	5.1605, m	5.2523, t (6.2)	-0.0918
21	1.5612, s	1.6765, s	-0.1153

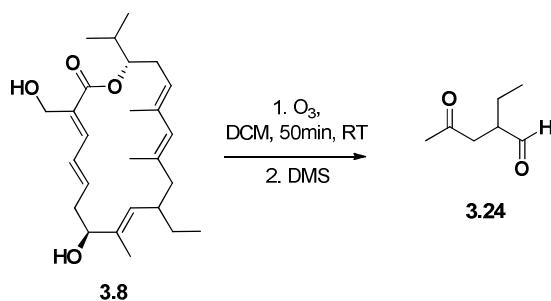
**Table 3.12** Mosher's analysis on hex-MTPA ring opened mangrolide.

### 3.16 Strategy for Determining Absolute Stereochemistry of C-10 and C-11

The remaining stereocenters on mangrolide A, the C-10 ethyl and C-11 ether, represented a difficult challenge for solving the absolute stereochemistry. Previous experiments had revealed the relative configuration between them but there was no definitive way to relay this information with the known stereocenters. Also, the chemistry of the allylic ether prevented a simple

hydrolysis to create a secondary alcohol for Mosher's analysis. The approach chosen for these centers was based on isolating a fragment of the macrolide containing C-10/11 and comparison to a synthetic standard of known stereochemistry. This method would have its own challenges since mangrolide A contains five double bonds and any method to cleave them would produce many fragments.

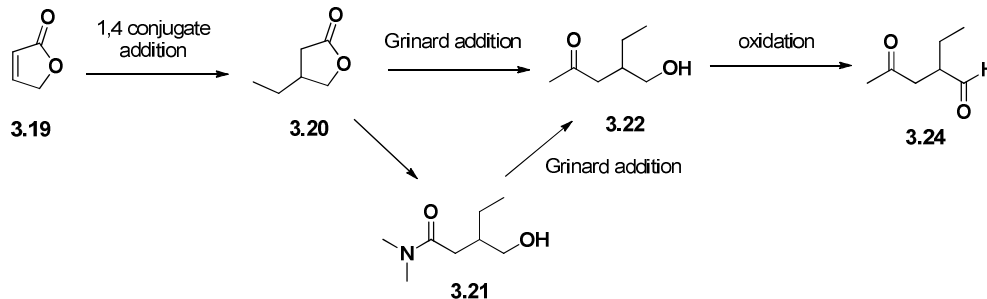
### 3.17 Ozonolysis of mangrolide A



**Scheme 3.3** Route to synthesize **3.24** for comparison to mangrolide ozonolysis products.

Ozonolysis is a common method of cleaving double bonds. Oxygen is converted to ozone and reacts with  $sp^2$  carbons resulting in the formation of peroxides. The choice of workup can be either reductive or oxidative and can allow for control of the end product. The mangrolide A aglycon **3.8** (0.6mg) was dried in a small vial to which 1mL of DCM saturated with ozone was added<sup>85</sup> (Scheme 3.2). After 50 minutes the starting material had disappeared and DMS was added for a reductive workup. The material was dried, resuspended in MeOH, and analyzed by GC. Many products were present from this reaction and while the desired fragment could not be identified by GC/MS, its presence was considered likely.

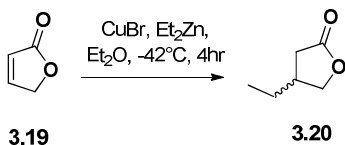
### 3.18 – Strategy to Synthesize mangrolide Fragment 3.24



**Scheme 3.4** Route to synthesize **3.24** for comparison to mangrolide ozonolysis products.

In order to create the synthetic fragment, a route was devised that would begin with 2(5H)-furanone (**3.19**) (Scheme 3.3). A 1, 4 conjugate addition would install the ethyl substituent and **3.20** would be opened with a Grignard addition with methyl magnesium bromide to create the methyl ketone. The Grignard addition to the lactone will result in the over addition of two methyls. This problem can be overcome by forming Weinreb amide **3.21** before the Grignard reaction. Oxidation of the secondary alcohol to an aldehyde would complete the synthesis of **3.23**.

### 3.18.1 Conjugate Addition of Diethyl Zinc to Furanone



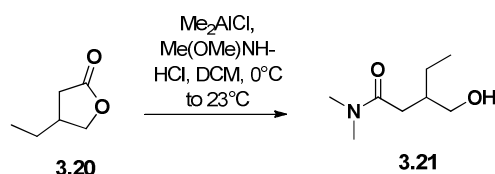
**Scheme 3.5** Conditions used in 1, 4 addition of ethyl substituent to furanone.

Initially a non-stereoselective 1, 4 addition was used in order to easily create material to optimize the later reactions (Scheme 3.4). The ethyl lactone **3.20** was successfully formed using diethyl zinc and copper bromide from previous literature<sup>86</sup>. Furanone (1 equiv) was added to



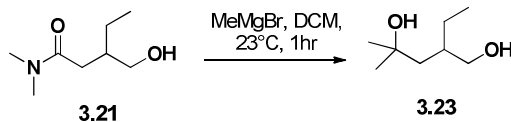
copper bromide (0.5 equiv) in ether and the mixture was cooled to  $-42^{\circ}\text{C}$  for five minutes. To this a 1M solution of diethyl zinc in hexanes (1.5 equiv) was added and stirred for two hours. Workup was accomplished by adding saturated ammonia chloride and filtering. The organic layer was extracted with ether three times, washed with sodium chloride, and dried with magnesium sulfate. The boiling point of **3.20** is predicted to be approximately  $105\text{--}108^{\circ}\text{C}$  so the product was purified by Kugelrohr distillation.

### 3.18.2 Experiments to Form the Methyl Ketone from **3.20**



**Scheme 3.6** Conditions used to form Weinreb amide.

The next step was to convert the lactone to the methyl ketone via the Grignard addition of methyl magnesium bromide (Scheme 3.5). The ketone of **3.22** was more reactive to Grignard reagents than **3.20** and the straight addition of  $\text{MeMgBr}$  would result in a dimethylated product. A method to limit the reaction to one Grignard addition was found in the literature<sup>87</sup>. It involved a two step process where the Weinreb amide is formed prior to Grignard addition<sup>87</sup>. A solution of  $\text{Me}(\text{OMe})\text{NH-HCl}$  in  $\text{DCM}$  was cooled to  $0^{\circ}\text{C}$  before  $\text{Me}_2\text{AlCl}$  was added and stirred for 1 hr at  $23^{\circ}\text{C}$ . To this **3.20** was added and stirred for 30 minutes. The reaction was quenched with phosphate buffer (8 pH), diluted with  $\text{DCM}$ , and filtered through celite. The organic layer was dried with  $\text{MgSO}_4$  and evaporated to yield **3.21** as a yellow oil.



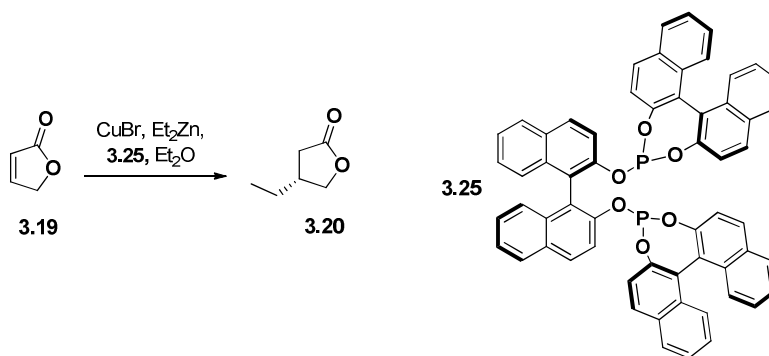
**Scheme 3.7** Grignard reaction with MeMgBr.

Next, **3.21** was dissolved in DCM and methyl magnesium bromide was added at 23°C and stirred for one hour (Scheme 3.6). The reaction was quenched with water, filtered through celite, and extracted with ether. Proton NMR showed the undesired dimethylated product **3.23**. A one pot protocol for formation of methyl ketones from lactones was found and tested on the 2(5H)-furanone<sup>88</sup> but was unsuccessful in forming the methyl ketone.

### 3.18.3 Asymmetric Addition of Diethyl Zinc to Furanone

The asymmetric addition of the ethyl to 2(5H)-furanone was accomplished by adding a chiral aryl diphosphate ligand **3.25** to the previous method (Scheme 3.7). The ligand had to be prepared in advance of the reaction in two steps. First, S-BINOL was refluxed in phosphorus trichloride (PCl<sub>3</sub>) overnight under nitrogen. The excess PCl<sub>3</sub> was removed under reduced pressure and washed with toluene three times. The mixture was suspended in benzene, frozen, and evaporated under high vacuum to a white powder. Phosphorus NMR was used to confirm the formation of the product <sup>31</sup>P NMR (CDCl<sub>3</sub>) δ 179.4 (s). This material was then dissolved in toluene and excess S-BINOL and cooled to 0°C. Triethylamine was added and the solution was stirred for three hours at 0°C before warming to 23°C and stirred overnight. The mixture was filtered through alkaline alumina and dried under reduced pressure. Comparison to published proton spectra indicated that **3.25** was the product. Unfortunately, when the ligand was used in

the asymmetric addition of diethyl zinc very little product **3.20** was recovered. At this point in the project the difficulties in both the methyl ketone reaction and the asymmetric 1,4 conjugate addition indicated that this was not a good approach. In addition, concerns were raised that the carbonyl in **3.24** could epimerize the stereochemistry at the ethyl during the ozonolysis and would prevent the determination of the correct stereochemistry.



**Scheme 3.8** Asymmetric 1,4 addition of ethyl to **3.19**

### 3.19 Oxidative Cleavage of mangrolide A

Oxidative cleavage of mangrolide was investigated using  $\text{KMnO}_4$  and  $\text{NaIO}_4$ <sup>89</sup>. Mangrolide A (2.5mg) was dissolved into a 2:1 mixture of acetone/water and 100  $\mu\text{L}$  of a solution of  $\text{KMnO}_4$ ,  $\text{NaIO}_4$ , and  $\text{NaHCO}_3$  (0.4 equvi, 1 equiv, and 2 equiv) was added to the vial. The reaction turned brown from purple and after 30 minutes the acetone was evaporated and the material was extracted with DCM. LC/MS revealed that the majority was still starting material with three product peaks. The  $m/z$  for the products indicated some degradation and possible loss of the sugars. The reaction was purified by HPLC and a proton was collected for each of the products but all the double bonds appeared intact.

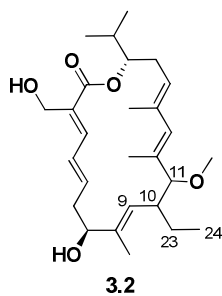
### 3.20 Epoxidation of C-8/9 Double Bond

Mangrolide A has one isolated olefin at C-8/9 with an allylic hydroxyl that could be selectively modified using Sharpless asymmetric epoxidation. This would create a new stereocenter at C-9 with stereochemistry that could be relayed to C-10/11. Following the standard protocol solutions of (-) diethyl tartrate (15mol%, DCM), titanium(IV) isoperoxide (12mol%, DCM), and tert-butyl hydroperoxide (1M, DCM) were made and cooled to -20°C in an water/EtOH/powdered dry ice bath<sup>90</sup>. The catalyst was prepared by mixing diethyl tartrate and titanium(IV) isoperoxide at -20°C for 30 minutes after which the tert-butyl hydroperoxide (3 equiv) was added and stirred for an additional 30 minutes. To this solution mangrolide A (4mg) was dissolved in DCM and added in two, 100µL additions. After stirring for 2 hours at -20°C the reaction was quenched with 100µL of a 30% NaOH solution in brine, warmed to room temperature, and extracted with DCM. Analysis of the organic layer by LC/MS indicated that a small amount of product 16 mass units higher was produced. This material was purified by HPLC and a proton NMR revealed that the product still had all of the olefins intact and the new oxygenation could not be determined. This reaction was repeated a number of times and the catalyst was changed to vanadium (IV)(acac)<sub>2</sub> but the same product was produced.

### 3.21 Comparison with Synthetic mangrolide Aglycon

The Dr. Jef DeBrabander group began a total synthesis of mangrolide A and completed the mangrolide aglycon with a methyl ether at the C-11 position. Their synthesis was designed to access either of the possible C-10/11 configurations. This material can be compared to the methyl ether aglycon **3.2** generated by the methanolysis reaction. Comparison of the <sup>1</sup>H-<sup>1</sup>H

coupling constants should be enough to identify the correct stereochemistry for the C-10/11 position (Table 3.13).

	No.	$\delta_{\text{H}}$ , mult, ( $J$ in Hz)
 <p style="text-align: center;"><b>3.2</b></p>	9	5.15, d, (10.6)
	10	2.58, dddd, (3, 9.6, 10.2, 10.3)
	11	3.29, d, (9.6)
	23a	1.9, m
	23b	1.25, dddd, (7.3, 7.3, 7.3, 13.3)
	24	0.87, t, (7.3)

**Table 3.13** Coupling constant data for mangrolide aglycon **3.2** obtained from 1D-TOCSY irradiating at C-9.

### 3.22 Comparison of mangrolide A Stereochemistry to lipiarmycin

Mangrolide A possesses a similar core macrolide as the known natural product lipiarmycin. Two major differences have been determined so far. First, the methyl substituted double bond between C-8/C-9 is Z in mangrolide A. This configuration is supported by an NOE data and  $^3J_{\text{CH}}$  coupling constants discussed in section 3.4. Unfortunately the assignment remains in question as the  $^1\text{H}$  and  $^{13}\text{C}$  chemical shifts are almost identical between mangrolide A and lipiarmycin indicating that C-8/C-9 could be E. The DeBrabander group will be synthesizing the mangrolide aglycon with both configurations in order to confirm the assignment. The other difference between these two molecules is the stereochemistry at the C-17 starting unit. Since the precursor is different between the two molecules, the stereochemistry cannot be assumed to be the same.

### 3.23 Conclusion of Mangrolide Stereochemistry

The complexity of natural products can create unexpected challenges to elucidating the absolute stereochemistry. In the case of mangrolide A, a strategy of selective degradation was attempted in order to create substrates amenable to Mosher's ester analysis. This was accomplished to determine the absolute stereochemistry of C-7 and C-17 as C-7S and C-17S. Experiments in collaboration with the De Brabander lab are ongoing to solve the C10/C11 stereocenters. In all these experiments an important factor which limited success was the amount of mangrolide A available. While SNA-18 can be cultured, the time required to culture and purify is not trivial. Improving the production of secondary metabolites is difficult, but recent research has lead to a method referred to as ribosome engineering, which can increase the production of antibiotic compounds<sup>91</sup>. SNA-18 was a good test case since mangrolide A had been characterized and was easily detected, even in crude extracts. Chapter 4 details the results of ribosome engineering on SNA-18.

## CHAPTER FOUR

### SNA-18 RIBOSOME ENGINEERING

#### 4.1 Regulation of Antibiotic Production in Bacteria by ppGpp

As mentioned in chapter 2, optimizing the production of mangrolide A was an important step for the success of this project. Improvements were accomplished utilizing changes in the media conditions; however a higher yield was still desired. Also, Actinomycetes like SNA-18 have the ability to produce other secondary metabolites that are not expressed in laboratory conditions. For these two reasons, a recently reported methodology from the Ochi lab where they used ribosomal engineering to alter bacterial secondary metabolite production seemed promising. Antibiotic metabolites are typically produced when bacteria switch from exponential growth to the stationary phase. This switch has been attributed to nutrient limitation and is referred to as the stringent response<sup>92</sup>. A key discovery was made in 1969 when Cashel and Gallant observed the rapid production of two phosphorylated compounds in amino acid starved *E. coli*<sup>93</sup>. Termed “magic spots”, these compounds were revealed to be ppGpp and pppGpp and are synthesized from GDP and GTP respectively (figure 4.1).

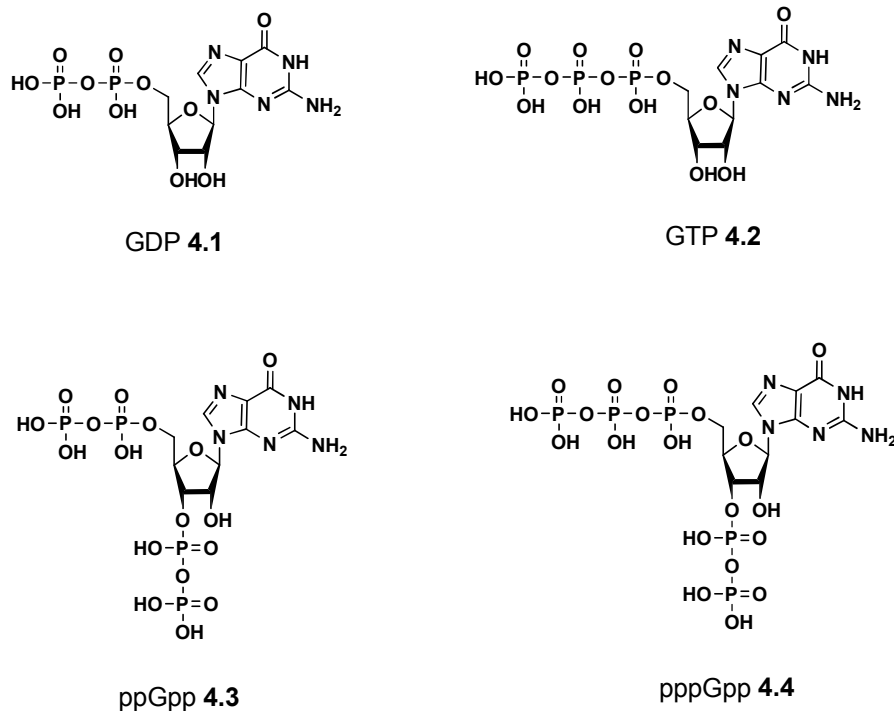


**Figure 4.1** Structures of GDP, GTP, ppGpp, and pppGpp

Two enzymes are responsible for ppGpp production in *E. coli*, RelA and SpoT<sup>94</sup>. RelA is activated by amino acid starvation and SpoT responds to a variety of conditions such as phosphate starvation and fatty acid metabolism<sup>94</sup>. Unlike RelA, SpoT is a bifunctional enzyme that can hydrolyze ppGpp back to GDP. Interestingly, these enzymes and their homologues have only been found in bacteria and plants. A complete understanding of how ppGpp influences bacterial physiology remains to be revealed, but ppGpp can alter transcription both directly and indirectly. It has been shown that ppGpp binds to RNAP near the active site<sup>95</sup>. Another protein DksA, is required for the stringent response and interacts with the RNAP secondary channel<sup>96</sup>. Together, this complex will initiate transcription of genes possessing an AT rich sequence near the transcriptional start site and down regulate genes with a corresponding GC rich sequence.



The indirect effect of ppGpp is through inhibition of sigma-70 dependent promoters which increases the availability of RNAP to interact with alternative sigma factors<sup>96</sup>. In addition, synthesis of ppGpp decreases the intracellular concentration of GTP which triggers the morphological changes and sporulation observed during the stringent response.

A recent paper by Wexselblatt et al. demonstrated the potential of small molecule inhibitors of ppGpp synthesis as therapeutic agents<sup>97</sup>. They designed a non-hydrolyzable ppGpp mimic that was capable of inhibiting ppGpp synthesis. This mimic prevented *B. subtilis* from entering stationary phase and inhibited biofilm formation. As secondary metabolite production is a highly regulated process in the growth cycle of bacteria, there is growing evidence that ppGpp plays a role in secondary metabolite production.

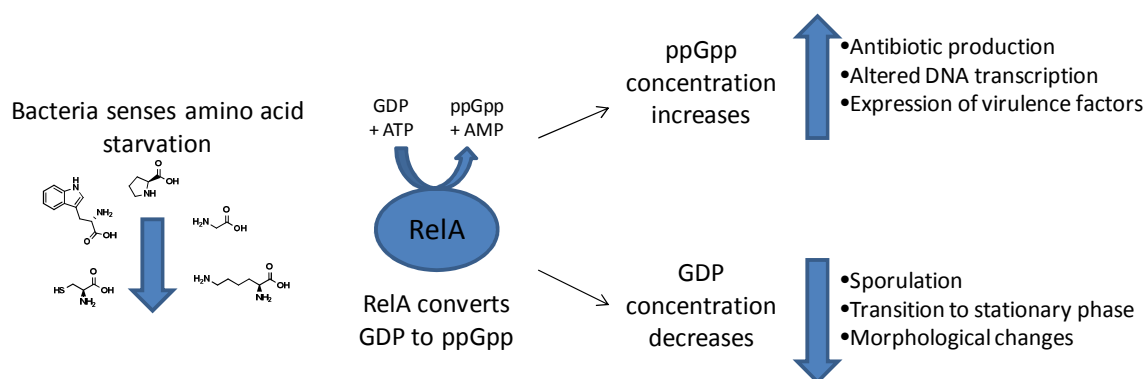


**Figure 4.2** GDP and GTP are converted to ppGpp and pppGpp by RelA.

## 4.2 Ribosome Engineering

Through mutations that inhibit ppGpp synthesis a direct link between antibiotic production and the stringent response has been observed. The Ochi lab observed that mutations conferring streptomycin resistance could induce the production of the antibiotic pigment

actinorhodin (4.5) in *Streptomyces lividans*<sup>98</sup> (Figure 4.3). Actinorhodin production was not seen in the wild type strain under normal fermentation conditions. A point mutation, Lys-88 to Glu, in the *rpsL* gene encoding the ribosomal protein S12 was found to be responsible for the gain in streptomycin resistance and actinorhodin production. This changed ppGpp synthesis in *S. lividans* reducing it by half under nutrient limiting conditions which activate ppGpp synthesis. Furthermore, this mutation could restore actinorhodin production in ppGpp deficient strains (RelA null) of *S. coelicolor*. This effect is not limited to streptomycin. Other antibiotics which target the ribosome can create point mutations (different from Lys-88 to G) that activate antibiotic production in the same manner. Successive exposure of *S. coelicolor* to eight different antibiotics had a cumulative effect resulting in an 180-fold increase in actinorhodin production<sup>99</sup>. The mechanism behind this remains unclear, but the *rpsL* mutations have been found to stabilize the 70S subunit and increase protein synthesis<sup>100</sup>. The Ochi lab has named this method ribosome engineering and it is a useful technique for both industry and academic labs<sup>101</sup>.

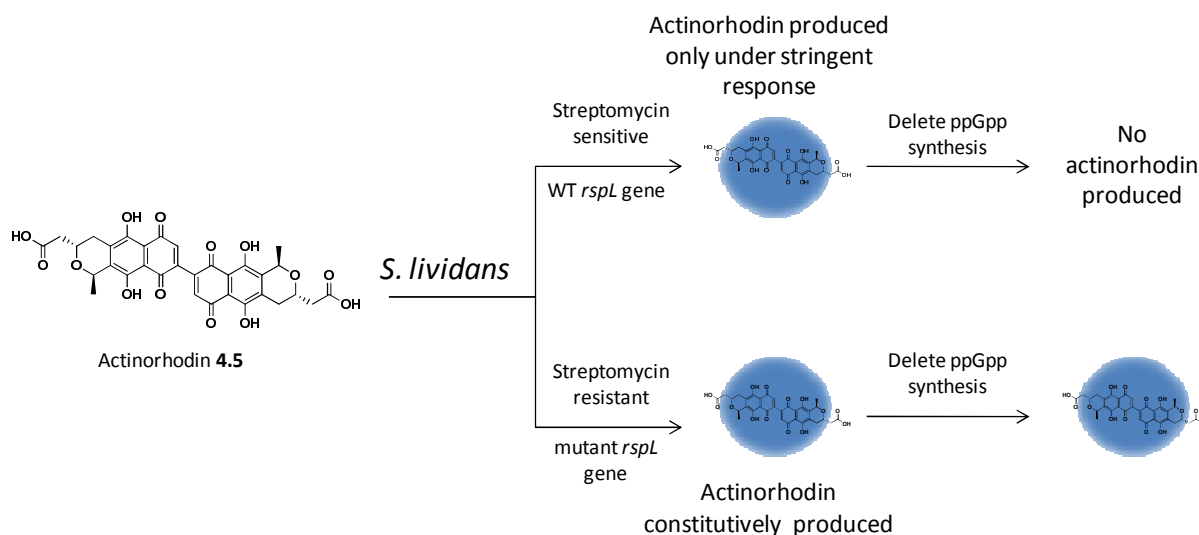


**Figure 4.3** Ochi *et al* studied a strain of *S. lividans* which produced actinorhodin under nutrient limiting conditions. Streptomycin resistance trigger antibiotic production even when ppGpp synthesis was inhibited.

The Ochi group applied this method to a collection of soil isolated actinomycetes that did not produce any detectable antibiotic activity. They found that 43% of previously non-antibiotic producing strains now possessed antibiotic activity<sup>91</sup>. Purification of one of these engineered strains lead to eight new cyclic depsipeptides, piperidamycins A-H, active against gram positive bacteria (1.56 µg/ml against *S. aureus*).

#### 4.2.1 Ribosome Engineering on SNA-18

For this thesis, ribosome engineering of SNA-18 offered the possibility of increasing the yield of mangrolide A and activating the expression of cryptic secondary metabolites. More mangrolide A was needed for the stereochemistry and pharmacology experiments. My hypothesis was that ribosome engineering could be used to increase the production of mangrolide A and potentially discover new secondary metabolites from SNA-18.

### 4.3 Engineering Streptomycin Resistant SNA-18

In order to generate streptomycin resistant SNA-18, the MIC of streptomycin against SNA-18 had to be determined. Using a disk diffusion assay on A1+C agar plates, a range of streptomycin concentrations were tested for growth inhibition. SNA-18 showed no growth inhibition up to 400  $\mu$ M streptomycin indicating that it already possesses a streptomycin resistance mechanism. Streptomycin is an aminoglycoside and resistance can occur through multiple pathways (notably through phosphorylation/acetylation of the hydroxyl groups on the glycosides) and it is likely that one or more phosphotransferase are expressed by SNA-18<sup>102</sup>.

### 4.4 Engineering Rifampicin Resistant SNA-18

Rifampicin can be used as an alternative to streptomycin for ribosome engineering. Similar to streptomycin, rifampicin resistance results from a point mutation in a ribosomal protein except the mutation associated with rifampicin resistance is found in the  $\beta$ -subunit of RNAP<sup>91</sup>. Rifampicin was investigated for activity against SNA-18. Initial disk diffusion assays showed a high level of inhibition and the MIC was determined to be less than 0.5  $\mu$ M. A1+C agar plates with 0.2  $\mu$ M or 0.4  $\mu$ M rifampicin were made and a 50 ml liquid culture of SNA-18 was grown until densely populated in the growth phase. 200  $\mu$ L of this culture was added to plates and spread using a sterile glass rod. After a month, small colonies approximately 50-80 per plate appeared on the 0.4  $\mu$ M plates. Seven colonies were isolated and grown in 50 mL cultures. Little change was detected in mangrolide production and no change in rifampicin resistance was observed. Since rifampicin is sensitive to light it is possible that these colonies were spores that survived until conditions allowed them to grow.

An alternative approach was investigated in which rifampicin was added to liquid cultures of SNA-18. Rifampicin was added to three, 50 mL cultures of growth phase SNA-18 to create a final concentration of 0.5, 1, and 2  $\mu$ M. At days 2, 4, and 6, 200  $\mu$ L culture aliquots were spread on A1+C agar plate containing a matching concentration of rifampicin. Colonies were detected from day 4 and 6 and one colony from each concentration was picked (MP5, M1, and M2) and grown in liquid culture for further analysis. All three strains had a dramatic change in resistance to rifampicin (Table 4.1). Resistance was determined by highest concentration which showed no inhibition by disk diffusion assay. Resistant colonies were observed at the highest concentration tested (12 mM) and one colony was picked for testing (M5).

#### **4.5 Analysis of engineered SNA-18**

Characterization of the engineered strains was accomplished through LC/MS analysis and PCR sequencing of the *rpoB* gene which encodes the RNAP  $\beta$ -subunit and the rifampicin resistance mutation. Two 50 mL liquid cultures of MP5, M1, and M2 were grown for seven days then extracted with 50 mL of ethyl acetate. A SNA-18 culture was used as control and grown and extracted in the same manner for comparison. UV absorbance was measured by LC/MS and the area under the peak was used to compare mangrolide A production (Table 4.1). A standard curve of pure mangrolide A was made but comparison with the crude extracts was inconsistent. This was likely due to the presence of other UV active compounds with the same elution time as mangrolide A.

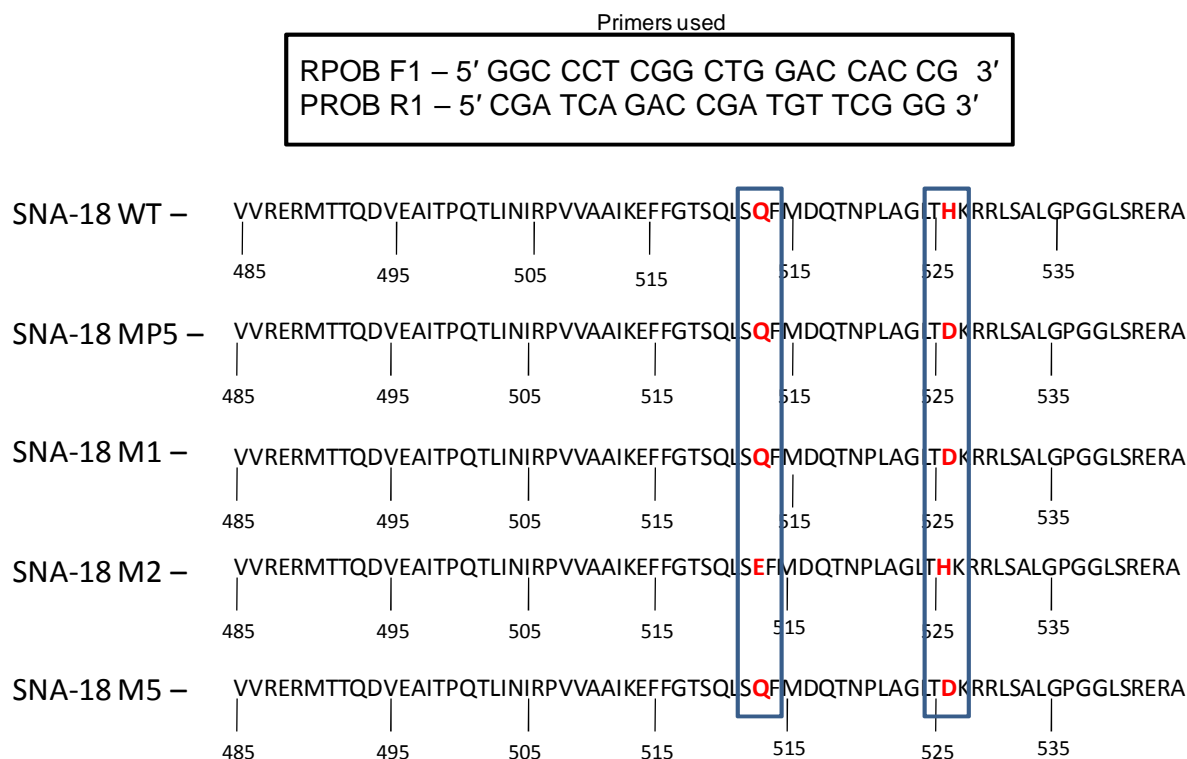


**Figure 4.4** Primers from the literature were used to sequence part of the RPOB gene in SNA-18 and engineered SNA-18. Sequences were translated to the amino acid sequence and the mutations observed are highlighted.

Characterization of the engineered strains was accomplished through LC/MS analysis and PCR sequencing of the *rpoB* gene which encodes the RNAP  $\beta$ -subunit and the rifampicin resistance mutation. Two 50 mL liquid cultures of MP5, M1, and M2 were grown for seven days then extracted with 50 mL of ethyl acetate. A SNA-18 was used as a control, UV absorbance was measured by LC/MS, and the area under the peak was used to compare mangrolide A production (Table 4.1). A standard curve of pure mangrolide A was made but comparison with the crude extracts was inconsistent. This was likely due to the presence of other UV active compounds with the same elution time as mangrolide A. So the total UV

absorbance was recorded to determine the relative amount of mangrolide produced in each experiment.

In order to determine if resistance was due to the *rpoB* mutation, primers designed by the Ochi lab were used to amplify a section of *rpoB* in SNA-18<sup>91</sup> (Figure 4.4). Analysis of the sequences obtained confirmed that in three of the strains isolated (MP5, M2, and M5) contained a point mutation changing a histidine 526 residue to aspartic acid. The M1 strain was found to have a mutation causing a glutamine 513 to glutamic acid which had not been reported in the Ochi research. Rifampicin is used to treat tuberculosis and the mutations causing resistance in clinical isolates have been well documented. Over seventy mutations conferring rifampicin resistance have been documented and 95% of these occur in an 81 nucleotide region known as the rifampicin resistance-determining region<sup>103</sup>. The histidine 526 to aspartic acid is the most common and is found in 43% of clinical isolates while the glutamine 513 to glutamic acid is rare, only found in 3% of isolates<sup>103</sup>. This confirmed the presence of the desired mutations in the engineered SNA-18 strains.

Strain	Mutation	Mangrolide A production (mAU*s)	Rifampicin Resistance ( $\mu$ M)
SNA-18	none	1773	<0.5
SNA-18-MP5	His537 to Asp	9018	>500
SNA-18-M1	Gln513 to Glu	9047	1500
SNA-18-M2	His537 to Asp	8636	1500
SNA-18-M5	His537 to Asp	Not measured	1500

**Table 4.1** Data for SNA-18 and the four rifampicin resistant strains isolated.

#### **4.6 Scale up Fermentation of SNA-18 MP5**

The majority of mangrolide A was purified from extracts of twenty liter fermentations. Since mangrolide production appeared enhanced in the engineered strains, a twenty liter fermentation of SNA-18-MP5 was initiated using A1+C media in Fernbach flasks. Mangrolide production was monitored after SNA-18-MP5 was transferred to the Fernbach flasks. Due to space limitations nine of the flasks were on a shaker outside of the laboratory culture room. After four days, a dramatic difference in mangrolide production was observed between the two rooms with the flasks inside the lab containing an estimated 0.92 mg/L and the outside flasks 0.1 mg/L. These flasks were moved to the lab culture room and mangrolide production appeared to increase. The difference in temperature between the two rooms was thought to be the cause, since the culture room was noticeably warmer. After seven days, the flasks started in the culture room were extracted and the other nine were extracted four days later. The extraction followed a standard protocol using XAD-7 resin to yield 7.6 grams of crude extract which was then separated into methanol soluble and insoluble fractions. Initial purification of the methanol soluble material was accomplished through reversed phase C-18 flash chromatography using a water/MeOH gradient beginning at 30% water. Thirteen fractions were collected and the mangrolide containing fractions were identified by LC/MS and combined. A second round of C-18 flash chromatography was conducted on this material using a step gradient of water/MeOH with 0.1% formic acid starting at 50% water. Twenty one fractions were collected and LC/MS



and NMR was used to combine them into seven fractions. This yielded 133mg (dry, white/yellow powder) of very pure mangrolide A and 73.9 mg (oil) of a mixture of mangrolide A and analogues. Further purification of the mixture was not performed, but this represents the highest yield of mangrolide purified to date at 6.6 mg/L of mangrolide A, roughly a threefold increase from previous experiments.

#### **4.7 Characterization of Engineered SNA-18 on Solid Media**

During the experiments conducted in 4.4, it was observed that the engineered strains of SNA-18 had a different growth phenotype when grown on solid media compared to SNA-18. Specifically, the new strains appeared very dark almost black. This color change was not uniform and the presence of sub-inhibitory concentrations of rifampicin seemed to enhance it. Furthermore, when the agar and bacteria were extracted with ethyl acetate, a red/pink color was observed in the organic layer. LC/MS analysis of the solid media extract revealed a new UV chromophore with absorbance at 540/560. Mass data was inconclusive due to poor ionization. To investigate this, large 200 mL agar plates were used to grow SNA-18 -M5 on solid media. Previous research has shown that growing *Streptomyces* on solid media can activate secondary metabolite pathways that are not expressed in liquid culture<sup>104</sup>.

#### **4.8 Isolation of Monosaccharide Mangrolide Analogue**

Ten, A1+C agar plates of SNA-18-M5 were extracted by ethyl acetate and analyzed by LC/MS. In addition to the unknown colored compound, a new UV signal with the same profile as mangrolide was observed. This predicted mangrolide analogue was less polar than the mangrolide analogs previously identified and appeared to have a mass of 822 m/z  $[M+H]^+$ .

Purification of this compound by Sep-Pak followed by reversed phase, C18 HPLC yielded 1.54 mg of pure mangrolide D. 1-D and 2-D NMR experiments (proton, gCOSY, gHSQC, and gHMBC) were collected in CD<sub>3</sub>OD and used to solve the planar structure (Figure 4.1 and Table 4.2). Comparison to mangrolide A showed that all the vinyl protons were unchanged indicating that the aglycon portion was practically intact except for C-26 which lacks the primary alcohol found on mangrolide A. The presence of only one anomeric proton in the HSQC revealed that the new analogue possessed only one sugar residue at C-11. COSY correlations were used to construct two new spin systems: a two carbon system starting from the anomeric proton at C-1' and a three carbon system starting from the methyl protons at C-6'. HMBC correlations from C-7' linked the two fragments. Carbon chemical shifts were used to finish the assignment of the sugar. A shift of 56.5 at C-3' implied that an amine was attached and the carbon shift of 76.6 at C-4' indicated a hydroxyl. The predicted structure was found to match the known sugar vancosamine, originally isolated from vancomycin. The [M+Na] ion (582 m/z) was detected by MS further confirming the proposed structure. Mangrolide D has not been tested for biological activity due to the lack of purified material. Re-examination of SNA-18 grown on solid media revealed small amounts of mangrolide D present, but it was not detected in liquid culture extracts. The level of mangrolide D production has not been reproducible across extractions and has limited further experiments with this analogue.

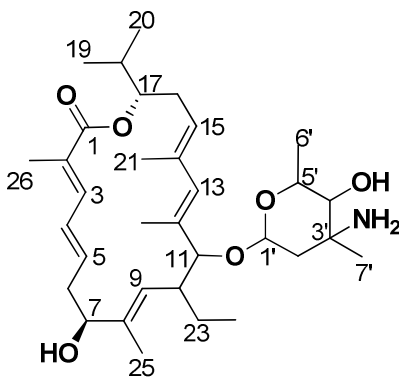


**Figure 4.5** Numbered structure of mangrolide D

#### 4.9 Progress towards Isolating Unknown UV 540 Compounds

The appearance of color in extracts of engineered SNA-18 was a clear indication that new secondary metabolites were being produced. LC/MS analysis revealed a new UV absorption at 540 nm. SNA-18 wild type was grown on solid media and compared to the new strains (figure 4.6). This UV absorbance is unusual and was barely detected in wild type SNA-18 indicating that the difference observed was due to the *rpoB* mutation. Unfortunately, even in the engineered strains this compound was present at very low titers. Two challenges were encountered in this project: obtaining consistent yields and purifying the unknown compounds.

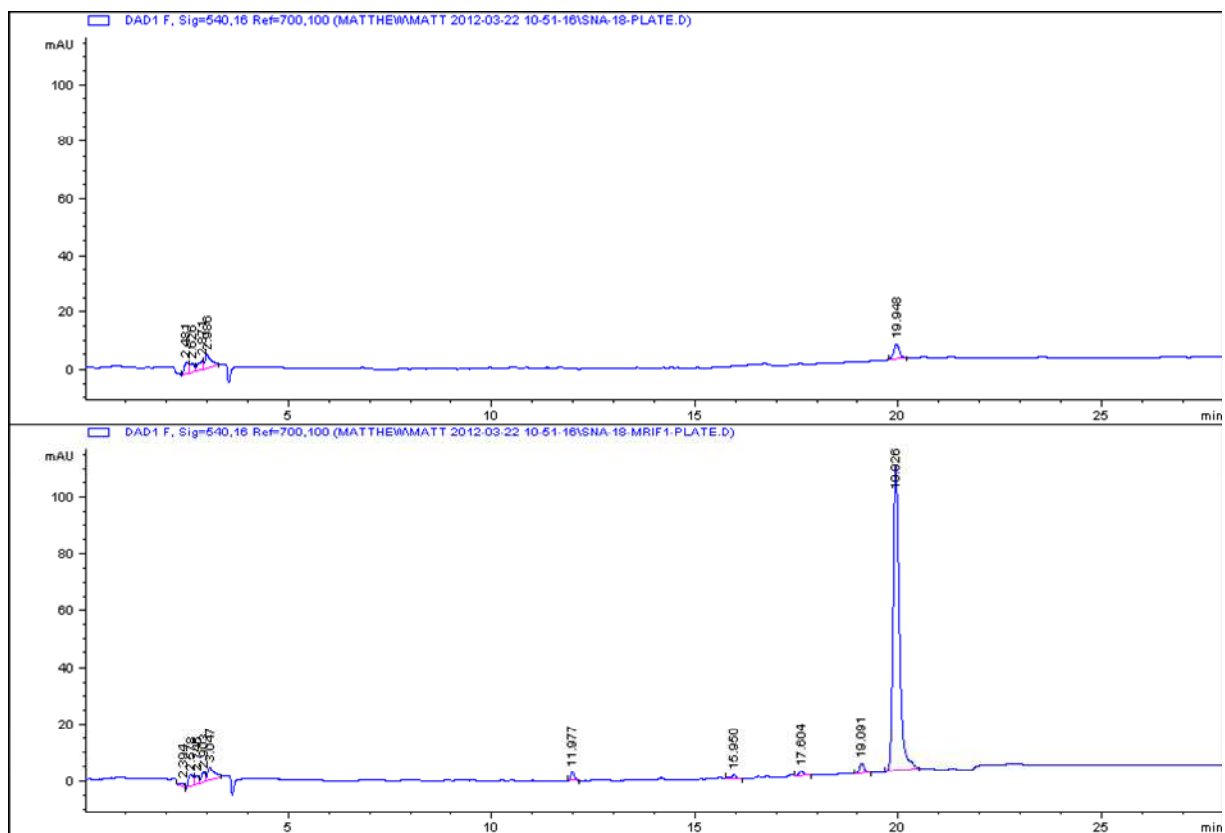


**Figure 4.6.** LC/MS trace at 540 nm of SNA-18 (top) and SNA-18-M1 (bottom). Both were grown on solid media and extracted following the same protocol. Extract was dissolved to a concentration of 10mg/mL before injecting on LC/MS. Scale of the top spectra was matched to the bottom.

mangrolide D				
position	<sup>13</sup> C	<sup>1</sup> H, mult ( <i>J</i> in Hz)	COSY	HMBC
1	170.7			
2	125.4			
3	141.8	7.0, d (11.1)	4	1, 2, 4, 5, 26
4	128.9	6.4, t (12.3)	3, 5	2, 3, 6
5	140	5.77, ddd (4.5, 9.3, 15.0)	4, 6	
6	37.1	2.70, 2.48, m	5, 7	
7	73.5	4.22, m	6	
8	137.3			
9	124	5.13, d (10.5)	10	7, 11, 25
10	43.4	2.65, dddd (3.45, 9.9, 9.9, 10.5)	9, 11	
11	92.6	3.67, d (9.8)	10	
12	135.6			
13	134.6	5.84, s		
14	136.8			
15	125.9	5.43, t (8.2)	16	13, 16, 21
16	29.7	2.44, m	15, 17	
17	79.8	4.64, ddd (4.5, 4.7, 8.1)	16, 18	1, 15, 19, 20
18	31.9	2.1, m	17, 19, 20	17, 19, 20
19	18.5	1.0, d (6.8)	18	17, 18, 20
20	19.4	0.94, d (6.6)	18	17, 18, 19
21	17.4	1.68, s		13, 14, 15
22	13.8	1.82, s		11, 12, 13
23	30.2	1.34, m	10, 24	
24	11.4	0.89, t (7.4)	23	10, 23
25	15.3	1.65, s		7, 8, 9
26	12.3	1.85, s		1, 2, 3
1'	99.1	4.97, d (4.1)	2'	11, 3', 5'
2'	41.2	1.95, 2.11, m	1'	1', 3', 4'
3'	56.8			
4'	76.7	3.21, d (9.5)	5'	3', 5', 6', 7'
5'	67.5	3.69, m	4', 6'	
6'	18.1	1.15, d (6.3)	5'	4', 5'
7'	19.8	1.53, s		2', 3', 4'

**Table 4.2** NMR data table for mangrolide D.

#### **4.10 Optimizing Culture Conditions of Engineered SNA-18 on Solid Media**

Liquid cultures of both SNA-18 and the modified strains were consistent in their growth and expression of secondary metabolites. The dark phenotype of SNA-18 mutants grown on solid media has not been as consistent. Best results were observed when plates were streaked with sterile cotton to obtain a uniform lawn versus using a stamp which produces discrete colonies. Contamination of the large 200 mL plates is difficult to avoid, so streptomycin was added to the media as SNA-18 was already resistant to it. In addition, streptomycin is poorly soluble in organic solvents so very little would be extracted from the agar using ethyl acetate. Plates were made with 100  $\mu$ M streptomycin and this significantly diminished contamination. Streptomycin also improved the consistency of the desired phenotype and increased yields of the unknown compounds. This was expected since it has been reported that sub-lethal concentrations of antibiotic can also activate secondary metabolite pathways<sup>98</sup>. The concentration of streptomycin was increased to 250  $\mu$ M with no negative effects observed.

#### **4.11 Purification of Engineered SNA-18 Extracts**

Since the desired compounds were only detected when SNA-18 mutants were grown on solid media, the purification of them was different than normal and required optimization. The method began with sectioning the agar of four 200 mL plates into approximately one inch squares and extracting them in Fernbach flask containing ethyl acetate. The flasks were shaken for 12 to 16 hours and the solvent was filtered and dried under reduced pressure. A second round of ethyl acetate extraction was repeated to improve recovery. These compounds are very soluble in methanol, DCM, and DMSO. Initially, reversed C18 Sep-Pak was used to separate the

crude extract and the compound co-eluted with mangrolide with significant tailing. From the LC/MS, it was observed that the material was only eluting at 100% acetonitrile so normal phase conditions were considered. Separation on TLC was successful with either 92.5/7.5% DCM/methanol or 25/70/5% hexane/ethyl-acetate/IPA. Normal phase HPLC was not very effective due to tailing of the compound. The poor compound separation by affinity chromatography lead to the use of LH-20 size exclusion chromatography. In order to separate the desired compounds from the polar media components and insoluble agar, the dried crude extract was suspended in a water/DCM partition. The organic layer was collected and dried to yield a cleaner extract. This material was dissolved in methanol, centrifuged, and loaded on a column of LH-20. Methanol was used as the mobile phase and an automated fraction collector was set to collect fractions every fifteen minutes. Fifty-three fractions were collected and combined to make 24 fractions which were analyzed by LC/MS (Table 4.3). In addition, these fractions were tested for antibiotic activity against *B. subtilis* and proton NMR data was collected on select fractions. Activity was observed from fraction 25-26 onwards. Not every fraction was tested as the same compounds were observed in multiple fractions and some of the fractions contained very little material. Separation between peaks was very good so reversed phase HPLC was used to purify two of the fractions. Fraction 25-26 was separated using water/methanol gradient starting at 20% methanol and continuing to 100 in 25 minutes. No formic acid was added and the semi-prep C18 column was acid free and three peaks were collected. Fraction 27-28 was purified in the same manner with the gradient starting at 30% methanol and five fractions were collected. Little material remained in these fractions so activity

Fraction	Weight	<i>B. subtilis</i> inhibition	NMR collected
1-3			
4-5			
6-7			
8-9			
10-11			
12-13			
14-15	26.5mg	Not active	
16-17	25mg	Not active	<sup>1</sup> H
18-20	8.8mg	Very faint activity	
21-24	18mg	Not active	<sup>1</sup> H
25-26	4mg	7mm clear	<sup>1</sup> H
27-28	2.2mg	11mm clear	<sup>1</sup> H
29	1mg	11mm clear	<sup>1</sup> H
30-32	2mg	10mm clear	<sup>1</sup> H
33	0.4mg		
34	0.7mg		
35-36	0.8mg	9mm clear	
37-39	0.5mg		<sup>1</sup> H
40-41	1mg		<sup>1</sup> H
42-43	1.3mg	8mm clear	<sup>1</sup> H
44-46	1.5mg		
47-49	1mg		
50-52	1mg		
Wash	1.5mg	Very faint activity	

**Table 4.3** Data from LH-20 separation of SNA-18-mutant crude extract. Fractions 8-11 contained mangrolide compounds and starting with 14 the colored compounds were observed. *B. subtilis* inhibition was measured by diameter of inhibition by disk diffusion on agar. Not every fraction was tested to conserve limited material and overlap of identical compounds in adjacent fractions. Proton NMR was collected on selected fractions.



was tested by spotting onto a TLC plate and covering it with an overlay of top agar and bacteria. Fraction 3 from 25-26 and 2, 3, and 5 from 27-28 showed activity through this method. Work is continuing on the characterization of these compounds, but a large scale up will be necessary to solve the structures.

#### **4.12 Conclusion**

There are few techniques that can be applied to aid in drug discovery. Ribosome engineering is a straightforward method which can improve antibiotic production and discovery of new compounds. This was achieved when applied to SNA-18. Mangrolide A production was increased three-fold along with previously undetected molecules which also had antibiotic activity. Generating the SNA-18 rifampicin mutants showed potential as a new tool for obtaining novel compounds and experiments are underway to determine if this method can be used on other marine derived bacteria. It is possible that this method could lead to the discovery of compounds with different biological activity. Identifying new compounds which are not antibiotics will be a key challenge in applying this method to natural product discovery. Bacteria can produce a wide variety of medically relevant compounds and chapter five describes a screen for antibiotic compounds which led to the discovery of new analogs of a marine natural product with cytotoxic activity.

## CHAPTER FIVE

### ISOLATION OF CYTOTOXIC NATURAL PRODUCTS FROM SNA-20

#### 5.1 Using Efflux Pumps to Screen for New Antibiotics

An important part of natural product discovery is the assay used to probe for medically relevant compounds. This thesis has focused on isolating new antibiotic compounds, particularly ones active against gram negative bacteria. There is a serious need for new antibiotics in order to overcome the rise in drug resistant strains, as was introduced in chapters 1 and 2<sup>63b</sup>. Gram negative bacteria are more difficult to treat due to three features. First is the outer membrane wall, which is unique to gram negatives and protects the bacterium from large and hydrophobic molecules<sup>105</sup>. The outer membrane encloses a periplasmic space that contains enzymes such as  $\beta$ -lactamases which can chemically inactivate antibiotics<sup>105</sup>. Finally, efflux pumps actively remove antibiotics thus lowering their concentration in the cytosol<sup>105</sup>. These defense mechanisms also make screening a natural product fraction library challenging. The fractions in a natural product library are typically mixtures of compounds and the concentration of the individual compounds is unknown. Active compounds may not be present in a high concentration and could be overlooked in a screen against gram negative bacteria. While further purification of the library can improve results, this is often prohibitive due to time and equipment limitations. A better approach would be to inhibit or knockout the efflux pumps in order to increase the sensitivity of the bacteria to antibiotic compounds, thus allowing the potential to discover new therapeutic targets. It has been shown that a strain of *Staphylococcus aureus*

lacking the NorA multidrug resistance pump was 5-30 fold more sensitive to antibiotics<sup>32b</sup>. The goal of this project was to test the MacMillan lab natural product fraction library against efflux deficient strains of *Pseudomonas aeruginosa* in order to find new gram negative natural products and therapeutic targets.

## 5.2 *Pseudomonas aeruginosa* and Cystic Fibrosis

*Pseudomonas aeruginosa* is a ubiquitous, gram negative bacterium that naturally exists in aquatic environments. While it does not typically infect healthy individuals, *P. aeruginosa* causes chronic infections in burn victims, immune compromised individuals, cystic fibrosis patients, and is the sixth most occurring pathogen in hospital acquired infections<sup>106</sup>. The adaptability of *P. aeruginosa* is likely due to its complex genome. At 6.1 Mb and 5570 open reading frames, it is one of the largest prokaryote genomes sequenced<sup>107</sup>. *P. aeruginosa* contains a variety of virulence factors that enhance its ability to colonize and resist treatment. It has a type three secretion system and four known exozymes (ExoS, ExoT, ExoU and ExoY) which alter immune response in the cell<sup>32a, 108</sup>. Biofilm formation enhances resistance to antibiotics and allows *P. aeruginosa* to colonize patients with cystic fibrosis<sup>109</sup>. Cystic fibrosis is a genetic disorder and is characterized by a mutation in the cystic fibrosis transmembrane regulator which disrupts a chloride channel in the lung and causes a sticky mucus to build up in the lungs<sup>110</sup>. This creates an environment that *P. aeruginosa* and other opportunistic bacteria such as *Burkholderia cepacia* and *Achromobacter xylosoxidans*, can infect and aid in biofilm formation<sup>111</sup>. Eighty percent of patients with cystic fibrosis will be infected with *P. aeruginosa* and there are 30,000 people in the US with cystic fibrosis<sup>111</sup>. Infection is chronic and *P.*

*aeruginosa* undergoes a series of mutations that increase its virulence and drug resistance<sup>112</sup>. *P. aeruginosa* is innately resistant to some antibiotics due to its many efflux pumps (the four key multidrug resistance pumps are MexAB-OprM, MexCD-OprJ, MexEF-OprN, and MexXY-OprM) and antibiotic inactivating enzymes such as  $\beta$ -lactamases and aminoglycoside modifiers<sup>113</sup>. Resistance to antibiotics can develop during treatment and MDR *P. aeruginosa* is defined by resistance to at least three members of the following classes of antibiotics: penicillins, cephalosporins, carbapenems, and aminoglycosides<sup>114</sup>. Pan-resistant *P. aeruginosa* has been observed with resistance to the drug of last resort, colistin<sup>115</sup>. By using a efflux knockout strain of *P. aeruginosa* in a phenotypic screen, I hoped to find new natural products with new antibiotic activity against it.

Stain Name	Description
CB 046	WT PA01
CB 462	$\Delta$ (MexH1-OprD)
CB 480	$\Delta$ (OprH)
CB 494	$\Delta$ (MexJK)
CB 536	$\Delta$ (MexCD-OprJ)
CB 540	
CB 602	$\Delta$ (MexXY)
CB 603	$\Delta$ (MexEF-OprN)
CB 614	$\Delta$ (PA2811-PA2812)
CB 1101	

**Table 5.1.** *Pseudomonas aeruginosa* strains used in 96 well plate bioassay and the corresponding efflux knocks.

### 5.3 *Pseudomonas aeruginosa* 96 Well Plate Bio-assay

The MacMillan lab natural product extract library consisted of bacteria extracts fractionated by reversed phase C18 chromatography into ten fractions in DMSO at a concentration of 5mg/mL. These fractions were held in 96 well plates, referred to as JM-1 through JM-8, with eight fractionated extracts per plate. In order to test the library for compounds with gram negative antibiotic activity, a 96 well plate liquid plate assay was developed. Strains of *Pseudomonas aeruginosa* were obtained from Cumbre Pharmaceuticals which had different efflux pumps knocked out (Table 5.1). The bacteria were prepared for the assay through by inoculating 50 mL of LB broth in a 125 mL flask with a single colony of a strain grown on LB plates. The culture was incubated on a rotary shaker for approximately 18hr at 200rpm and 27°C. 500µL of this culture was transferred to a fresh 50 mL of LB and shaken at 200 rpm and 27°C for four hours. The 96 well plates are prepared in advance with 230µL LB and 10µL of the extract. A positive control (10mg/mL gentamycin in DMSO, 1 well), negative control (10mg/mL penicillin in DMSO, 1 well), DMSO only (4 wells), and bacteria only (1 well) were included in the plate for data analysis. Some of the natural product extracts contained compounds with UV absorbance so the UV absorbance (580nm) was measured prior to the addition of the bacteria. Then 10µL of the bacteria culture was added to every well and the plates were gently shaken for 16 hours after which the absorbance is measured. The initial absorbance was subtracted from the final absorbance and graphed (Figure 5.1). Fractions with UV absorbance less than the DMSO control were retested on a disk diffusion assay to confirm the biological activity.

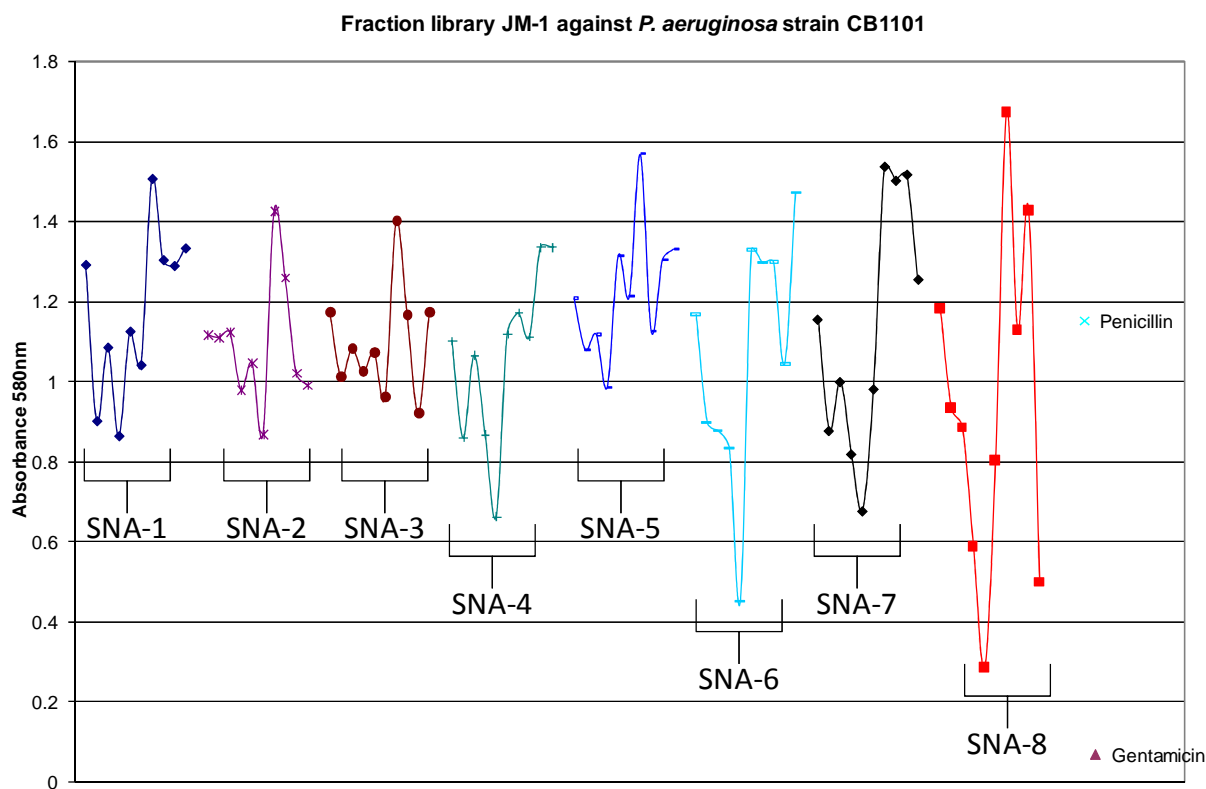


**Figure 5.1.** Example of data for JM-1 against CB1101.

Data was fairly consistent across the different efflux knockout strains but CB1101 was the most sensitive and was capable of revealing active fractions (**Table 5.2**). LC/MS data was collected for these fractions and this led to the observation that one of the extracts from SNA-20 contained the known natural products ammosamide A and B<sup>116</sup>. This strain was chosen for further investigation as the ammosamide compounds were not reported to possess antibiotic activity.

96 WP	Active Fractions
JM-1	F5, H5, A5, D6, and H1
JM-2	F6
JM-3	A2
JM-4	A5 and F5
JM-5	None active
JM-6	H8 and G8
JM-7	Not tested
JM-8	A6, B6, and D6
JM-9	None active

**Table 5.2.** 96 well plates from natural product library and the fractions confirmed to be active.

#### 5.4 SNA-20 Culture and Purification

The method of culturing and extraction of SNA-20 was similar to method for SNA-18. One significant difference was the addition of iron sulfate and potassium bromide to the A1+C media (A1BFe+C) used in SNA-20 fermentation. SNA-20 has an orange/yellow phenotype and changes to a dark black color after 7-9 days. Similar growth is observed on solid media with significant sporulation. Fermentation began by adding 25 mL of SNA-20 starter culture to a Fernbach flask containing 1 L of A1BFe+C media. These flasks were shaken for 7-9 days at 200 rpm and 27°C before activated XAD-7 resin was added. The resin and media was shaken at 200 rpm for a minimum of three hours before filtration and extraction with acetone overnight. The acetone was filtered and evaporated under reduced pressure to yield the crude extract. Crude extract was generally dried after adding C18 silica gel to create a powder for dry loading on a C18 flash column.

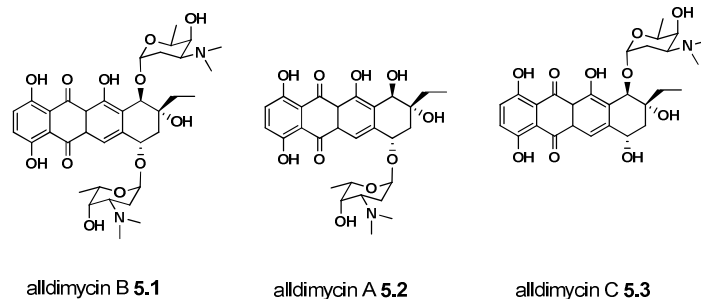


**Figure 5.2** Structures of alldimycin natural products purified from SNA-20

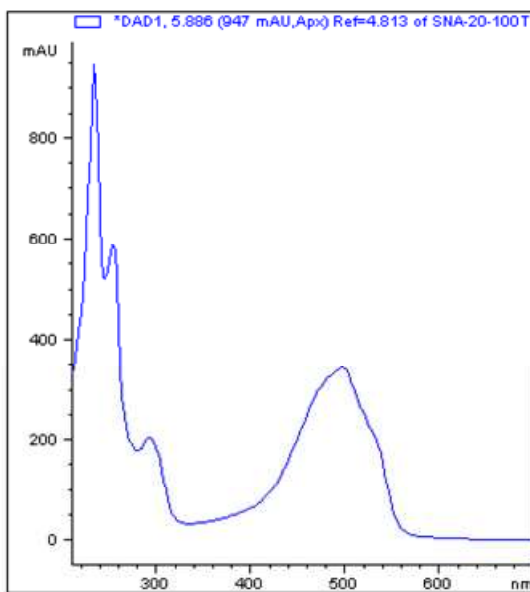
The crude extract was fractionated by flash column chromatography on reversed phase C18 bonded silica gel with a H<sub>2</sub>O/MeOH step gradient (90:10-0:100 with a 0:100+0.1TFA wash). 11 fractions were collected and fraction 11 contained the antibiotic activity. Fraction 11 was further purified by an additional round flash column chromatography on C18 bonded silica gel with a H<sub>2</sub>O/MeOH step gradient (50:50-0:100) with 0.05% TFA added in every step. 17 fractions were collected and fraction 10 had activity and was fairly pure. This material was purified by reversed phase C18 HPLC (Vydac C18 250 × 10mm, 5μ, 2.5mL/min, UV 254 nm) using a gradient with H<sub>2</sub>O/CH<sub>3</sub>CN to yield 10 fractions. Fraction 2 contained alldimycin B (**5.1**, 2.97 mg,  $t_R = 9.1$  min), fractions 8 and 9 contained trace amounts of alldimycin A (**5.2**) and C (**5.3**).

### 5.5 Identification of alldimycin Natural Products

LC/MS analysis of **5.1** revealed  $m/z$  of 701(M+H)<sup>+</sup> and a distinct UV pattern (figure 5.3). <sup>1</sup>H and 2-D NMR data was collected on a 600 MHz Varian spectrometer in CD<sub>3</sub>OD, but the lack of material prevented a complete carbon spectrum (Table 5.3). Based on the proton NMR spectra **5.1** had fewer proton signals than expected for a 700 MW compound. The presence of



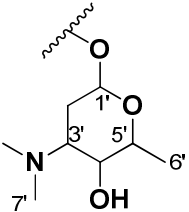
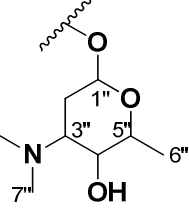
three (7.90, 7.81, and 7.36 ppm) aromatic signals indicated that **5.1** could be a type 2 polyketide with multiple quaternary carbons. No HMBC data for the aromatic region was obtained and prevented complete assignment of the structure. Analysis of the HSQC data revealed two anomeric positions, ( $\delta_{\text{H}}$  5.53,  $\delta_{\text{C}}$  102.1) and ( $\delta_{\text{H}}$  5.45,  $\delta_{\text{C}}$  97.6) and COSY correlations were used to assemble two rhodosamine sugars. An antibase search of known natural products with a mass of 700 and two rhodosamines allowed for the identification of **5.1** as alldimycin B. NMR data could not be obtained for fractions 8 and 9 but their  $m/z$  of 544( $\text{M}+\text{H}$ )<sup>+</sup>, antibiotic activity, and longer retention time ( $t_{\text{R}}$  = 13.6 min) is consistent with the mono-rhodosamine alldimycins (**5.2**) and (**5.3**).



**Figure 5.3** UV absorption spectrum of alldimycin B.

The alldimycins are structurally similar to the anthracycline antibiotics and were shown to inhibit DNA and RNA synthesis in murine leukemia L1210 cells<sup>117</sup>. The anthracycline

antibiotics were first discovered in 1939 and have been used clinically to treat cancer, particularly adult myelogenous leukemia<sup>118</sup>. Anthracyclines have multiple cytotoxic effects including: DNA and RNA inhibition, free radical formation, and a variety of DNA damaging mechanisms<sup>119</sup>. Cardiac toxicity is the main side effect to these drugs and research to understand and limit cardiac stress is ongoing<sup>120</sup>.

	No.	$\delta_C$	$\delta_H$ , mult, ( <i>J</i> in Hz)	COSY
	1'	102.1	5.53, d ( <i>J</i> = 2.4)	2'
	2'	28	2, 2.14, m	1', 3'
	3'	63.1	3.28, m	2', 4'
	4'	66.04	3.91, s	3', 5'
	5'	68	4.22, dd ( <i>J</i> = 6.6, 7.2)	4', 6'
	6'	16.9	1.31, d ( <i>J</i> = 6.6)	5'
	7'	41.3	2.72, s	
	8'	41.3	2.72, s	
	1''	97.6	5.45, d ( <i>J</i> = 2.3)	2''
	2''	28.6	1.89, 1.78, m	1'', 3''
	3''	62.8	3.17, d ( <i>J</i> = 10.6)	2'', 4''
	4''	66.1	3.87, s	3'', 5''
	5''	68.4	4.03, dd ( <i>J</i> = 6.5, 7.2)	4'', 6''
	6''	16.9	1.3, d, ( <i>J</i> = 6.5)	5''
	7''	41.2	2.67, s	
	8''	41.2	2.67, s	

**Table 5.3.** Partial structures assembled from 5.1 NMR data.

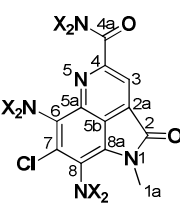
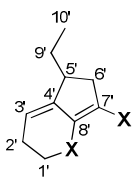
## 5.6 Identification of SNA-20-422

From the previous isolation of the alldimycins a dark green band was observed (fraction 17). This material was purified using the same reversed phase C18 HPLC conditions (Vydac C18 250 × 10mm, 5 $\mu$ , 2.5mL/min, UV 254 nm) and a H<sub>2</sub>O/CH<sub>3</sub>CN gradient to yield SNA-20-422 (**5.4**). No antibiotic activity was detected from **5.4**. Two proton chemical shifts, 3.92 and 8.29, indicated that **5.4** was an ammosamide analog. 2-D and <sup>13</sup>C NMR experiments were

collected and the data was used to assemble two partial structures (Table 5.4). The ammosamide core contains 10 quaternary carbons with only two hydrogen containing positions capable of HMBC correlations. Another challenge with the ammosamide compounds is that C-2 can be a C=O, C=S, or a C=N. An HMBC from C-1a to a  $\delta_C$  of 150.1 suggests that C-2 in **5.4** is an amidine consistent with the data published in Pan *et al*<sup>121</sup>. COSY correlations were used to construct two partial fragments and HMBC correlations were used to link the two fragments together. No HMBC correlations between the fragment and the ammosamide core are present and it has not been determined how to fit the NMR data to a plausible structure.

### 5.7 Crystallization Attempts of SNA-20-422

With the difficulties in solving the structure of **5.4** with NMR methods alone, attempts were made to obtain a crystal. Twenty liter fermentation of SNA-20 only yielded 2-3 mg of **5.4**. Furthermore, **5.4** would degrade rapidly (less than an hour) in pyridine and slowly in DMSO (a few hours) which limits useful solvents for NMR and crystallization. While **5.4** is soluble in methanol and H<sub>2</sub>O, it is not soluble in CHCl<sub>3</sub> and non-polar solvents such as hexane. Initially **5.4** was dissolved in MeOH and allowed to evaporate in a small section of a 5mm NMR tube. This resulted in small crystals that did not refract. Repeated attempts using methanol did not produce crystals again. Ethanol and acetone were tested separately without success. Over time, it appeared that the material was slowly decomposing into unidentifiable products.

	No.	$\delta_c$	$\delta_H$ , mult, ( <i>J</i> in Hz)	COSY	HMBC
 <p>5.4</p>	1				
	1a	39.1	3.92, s		2, 8a
	2	150.1			
	2a				
	3	118.8	8.29, s		
	4				
	4a				
	5				
	5a				
	5b				
	6				
	7				
	8				
	8a	113.1			
	1'	40.8	3.59, m	2'	2', 3', 8'
	2'	24.7	2.54, m	1', 3'	1', 3', 4'
	3'	125.1	6.22, m	2'	1', 2', 5', 8'
	4'	144.4			
	5'	42.6	2.90, m	6', 9'	
	6'	38.6	3.2, 2.68, m	5'	4', 5', 7', 8', 9'
	7'	99.1			
	8'	153.6			
	9'	28.9	1.57, 1.84, m	5', 10'	10', 4', 5', 6'
	10'	11.2	1.06, t (7.4)	9'	5', 9'

**Table 5.4.** NMR data for **5.4** NMR data. Quaternary carbons on the ammosamide core could not be confidently assigned

Media	Ingredients
A1+BFe+C	10g starch, 4g yeast extract, 2g peptone, 1g calcium carbonate, 0.4g $\text{FeSO}_4 \cdot 4\text{H}_2\text{O}$ , 0.1g KBr
TCG	5g castitone, 4g glucose, and 3g tryptone
A1+C	10g starch, 4g yeast extract, 2g peptone, and 1g calcium carbonate
A1+C-P	10g starch, 4g yeast extract, 2g castitone, and 1g calcium carbonate
CA1	10g cellulose, 2g yeast extract, and 1g peptone,
CGS	4g castitone, 10mL glycerol, and 5g soy media

**Table 5.5** Recipes for medium used to improve ammosiamide analog production. All amounts are in g/L.

## 5.8 SNA-20 Media Experiments

Similar to the experiments with SNA-18, media optimization was investigated in order to increase production of ammosamide analog **5.4** and possibly alter the metabolite profile of SNA-20. Experiments were conducted in three, 50mL flasks per condition tested. Production of **5.4** was monitored by ESI-MS ion extraction as the UV was not usually seen due to the abundance of ammosamide A and B produced. Media was inoculated with 1.5mL of SNA-20 after it had reached stationary phase. The three cultures were incubated for eight days on a rotary shaker (200rpm, 27°C), combined, and extracted with an equal part of ethyl acetate. The crude extract was filtered and adjusted to 10 mg/mL before analysis by LC/MS. Six different media recipes were tested with varying carbon and nitrogen sources (Table 5.5). In addition, A1+C and A1+C with iron sulfate added were tested to see if the extra iron was necessary. SNA-20 did not show

any growth in CA1 and CGS conditions and TCG appeared normal but was lacking production of ammosamide compounds (Chart 5.1). A1BFe+C had the highest production of **5.4** by LC/MS and appeared black before extraction.

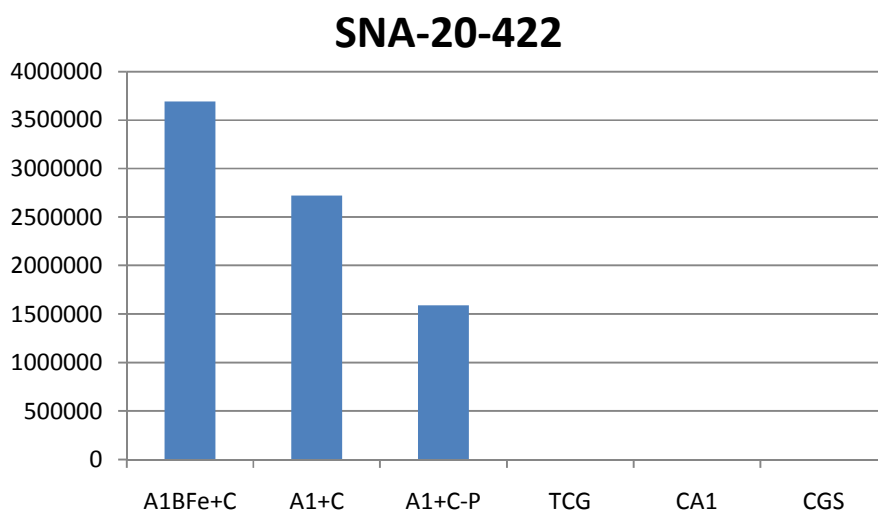


**Chart 5.1** MS ionization of **5.4** measured from extracts of SNA-20 grown in different medias.

### 5.8.1 Effect of Iron(III) vs Iron(II) on SNA-20

After it was observed that the addition of iron sulfate to the media enhanced production, a follow up experiment was conducted to test whether the use of iron(II) would be better absorbed by the bacteria. The iron sulfate typically added in the recipe is iron(III) which requires the use of siderophores by bacteria in order for them to absorb it. An iron(II) solution was prepared and filter sterilized before adding to the A1+C media. The iron(III) was performed best and both conditions with iron had higher production than the A1+C media, consistent with the previous experiment (Chart 5.2).

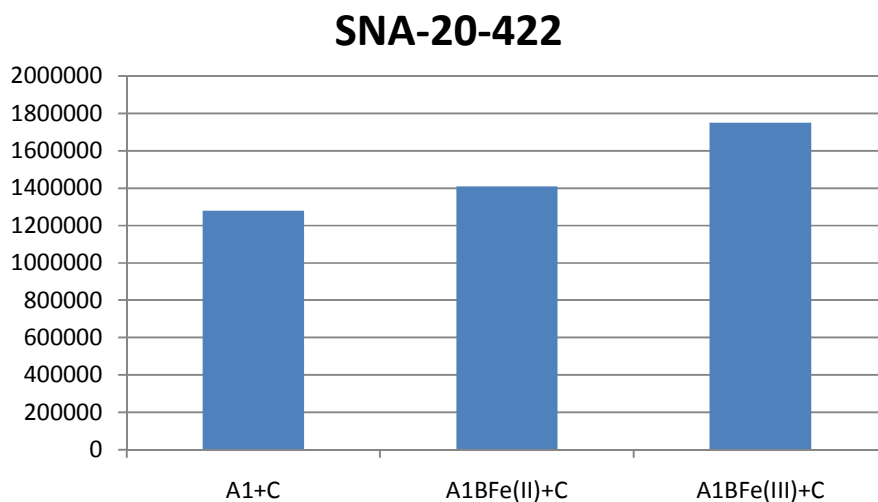


**Chart 5.2** MS ionization of **5.4** measured from extracts of SNA-20 grown in A1+C with different iron sources.

### 5.8.2 Effect of pH on SNA-20

The effect of pH on SNA-20 was tested as well. The standard A1BFe+C is around 7.0-7.5pH. To accomplish this, 300  $\mu$ L of 1N HCl was added to 50mL of A1BFe+C to bring the pH to 6.0-6.5 and 300  $\mu$ L of 1N NaOH to increase the pH to 8.0-8.5. After six days the flasks were combined and extracted. Unfortunately, either change in the pH resulted in less production of **5.4** (Chart 5.3).

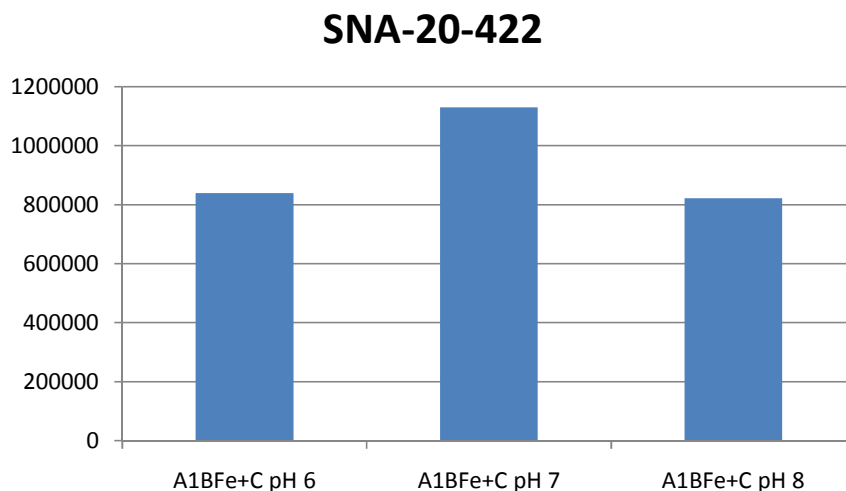


**Chart 5.3** MS ionization of **5.4** measured from extracts of SNA-20 grown in A1BFe+C at different pH.

### 5.8.3 Effect of Tryptophan and PM on SNA-20

Finally the effect of additional precursors on SNA-20 was tested. The biosynthesis of the ammosamide compounds probably uses tryptophan so 1g/L of tryptophan was added to A1BFe+C media. The polyketide precursor mixture developed for SNA-18 was also tested along with combination of tryptophan and precursor mixture. Interestingly, the addition of the precursor mixture dramatically reduced the production of **5.4** (Figure 5.4). Little change was detected with the addition of tryptophan but the UV profile of the extract showed a number of new peaks compared the control.



## SNA-20-422

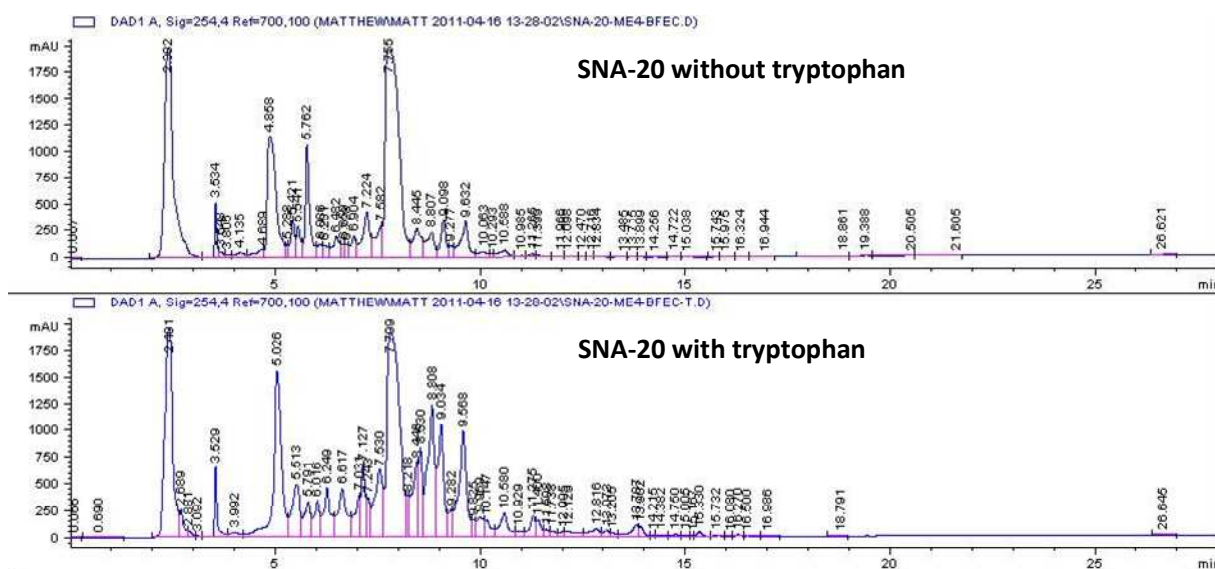
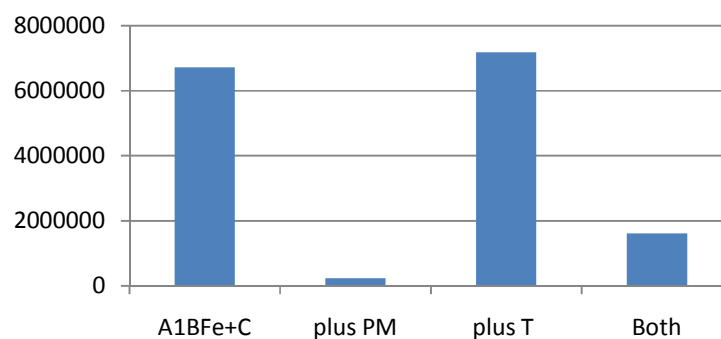


**Figure 5.4** Chart with MS ionization of 5.4 measured from extracts of SNA-20 grown in A1BFe+C with tryptophan or PM added. The LC/MS trace of SNA-20 with and without tryptophan is shown below

## 5.9 Conclusion

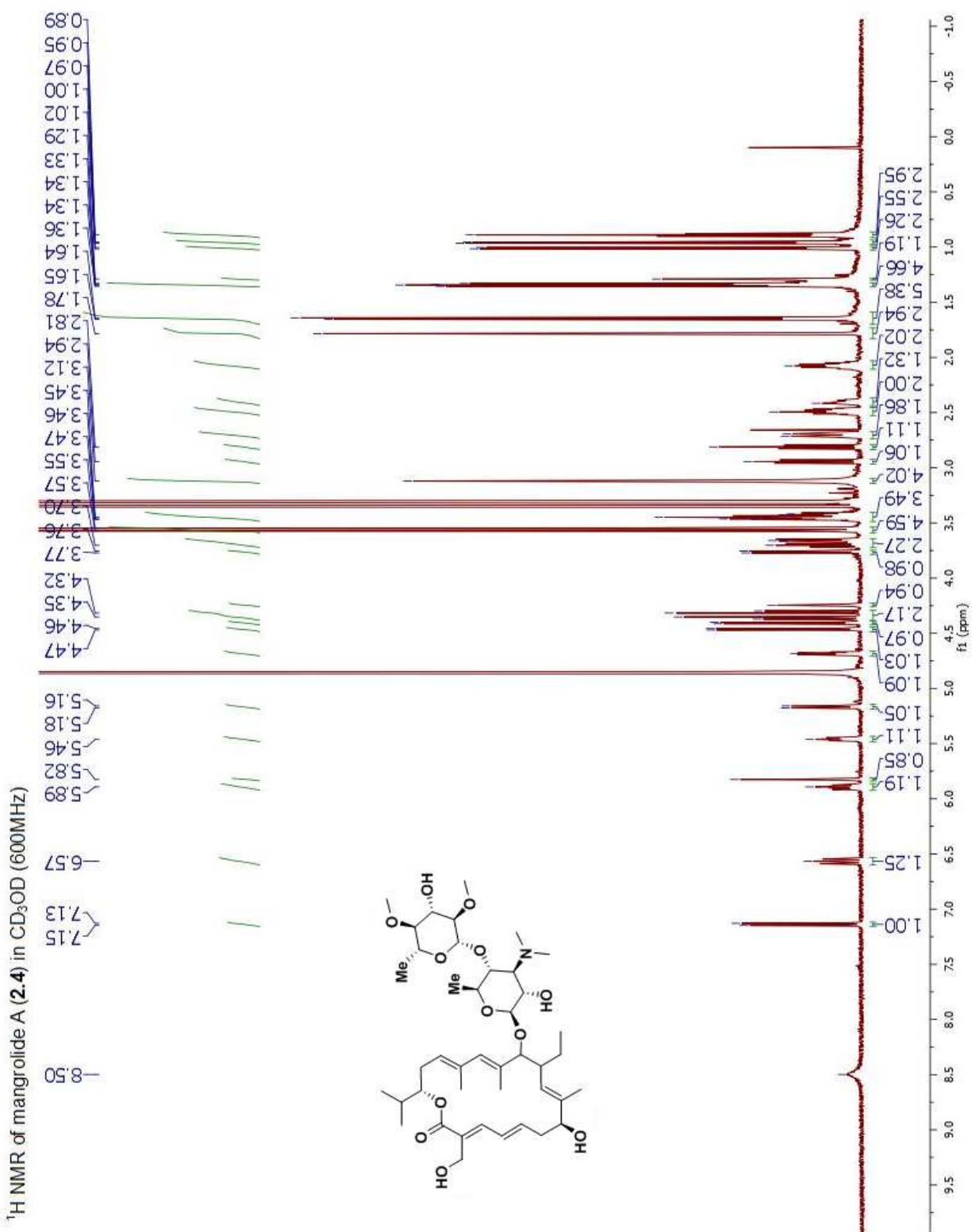
The discovery of natural products with therapeutic potential is dependent on the method used to detect a desired activity. Gram negative bacteria are a serious health concern and new drugs are needed. In order to find new compounds that target gram negative bacteria, a screen employing a sensitized strain of *P. aeruginosa* was tested against a marine natural product library. Investigation into one the active fractions led to the isolation of the known cytotoxic natural products alldimycin A-C and ammosamide A-B. Careful observation of the extracts from the producing strain SNA-20 revealed that a new ammosamide analogue was present. While the structure was not confirmed, research into the compounds was continued by Ende Pan Ph.D and resulted in new insights into the biosynthesis of the ammosamide natural products<sup>121-122</sup>.

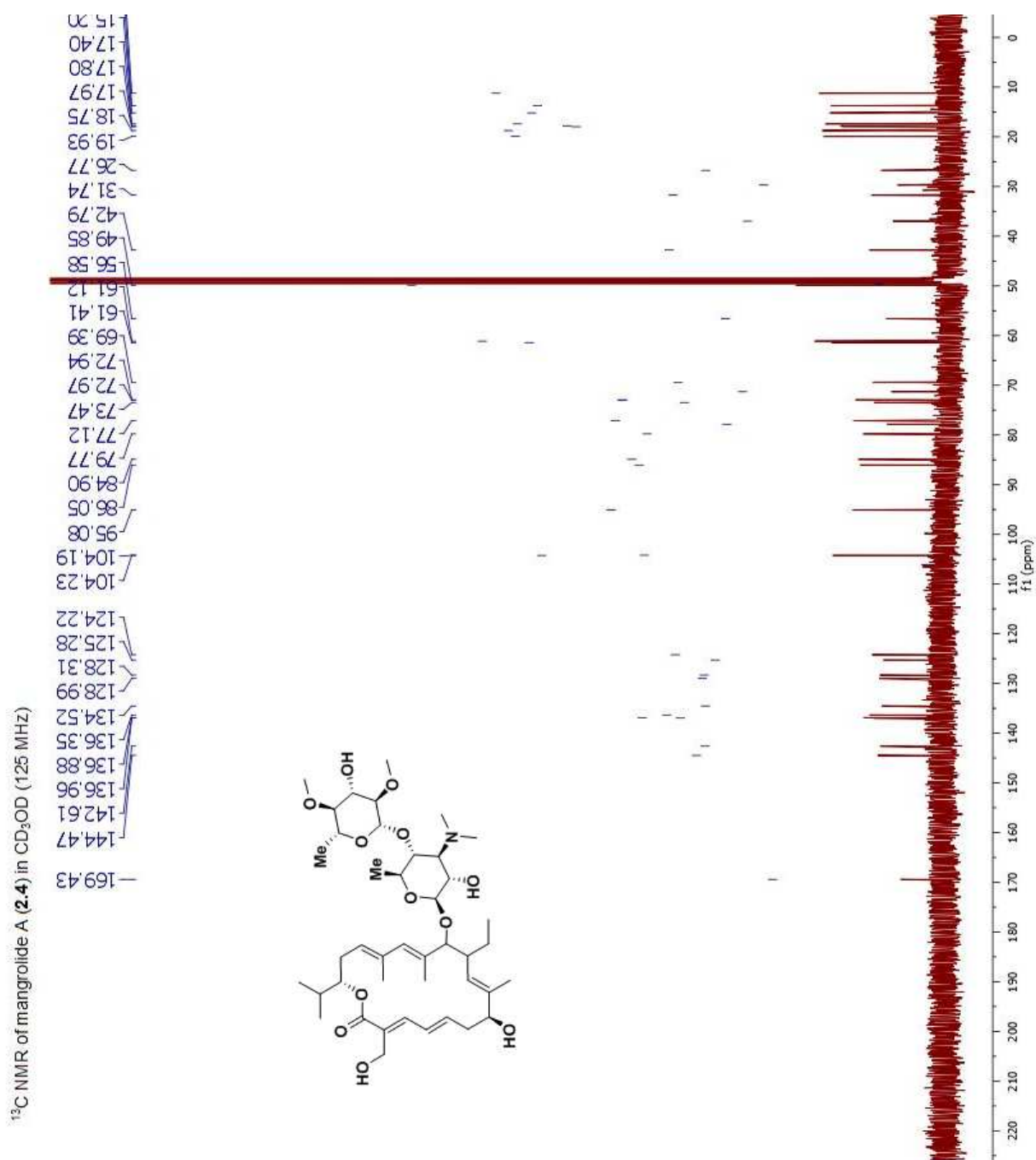
Investigation into the other active fractions is currently ongoing.

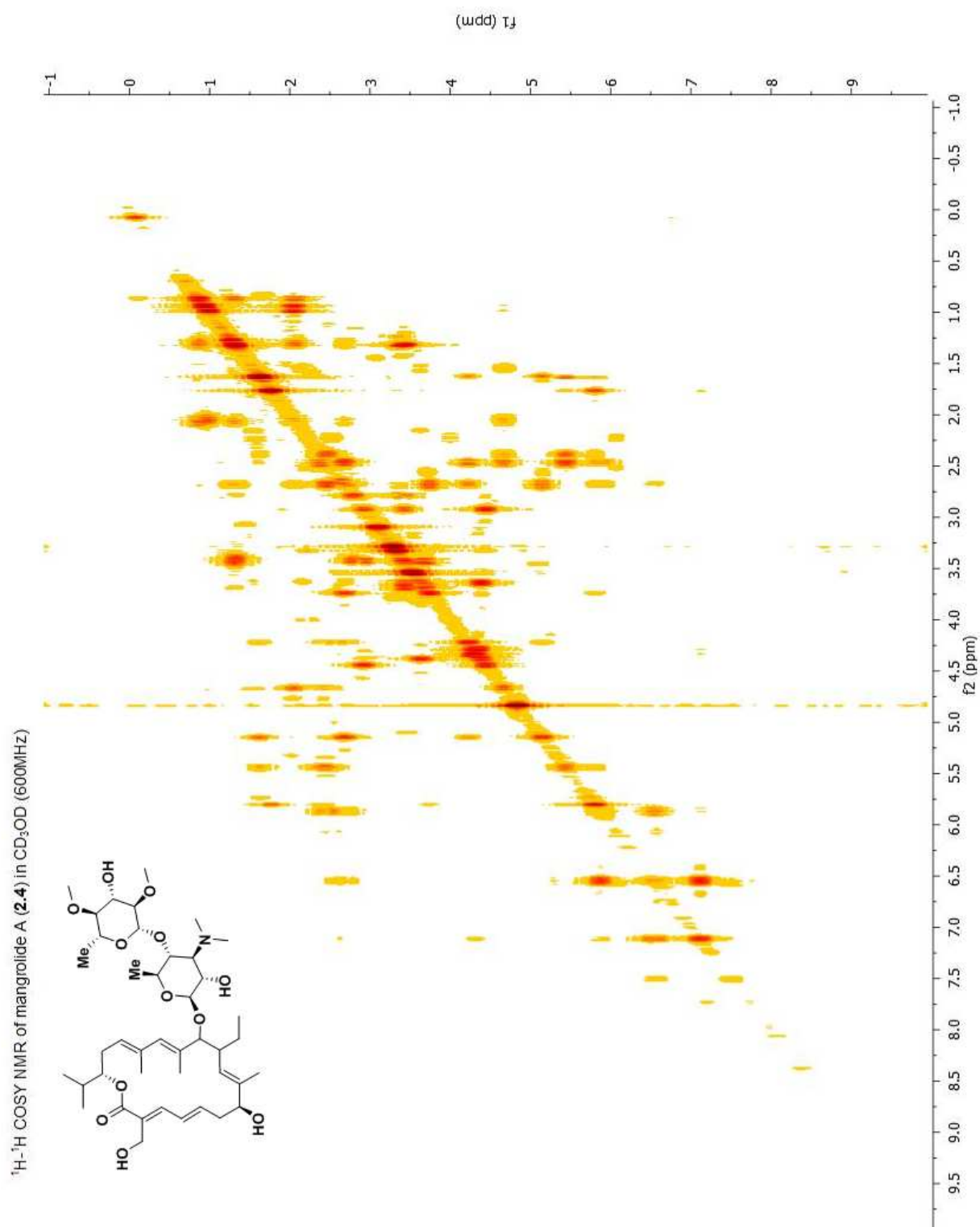
## **APPENDIX A**

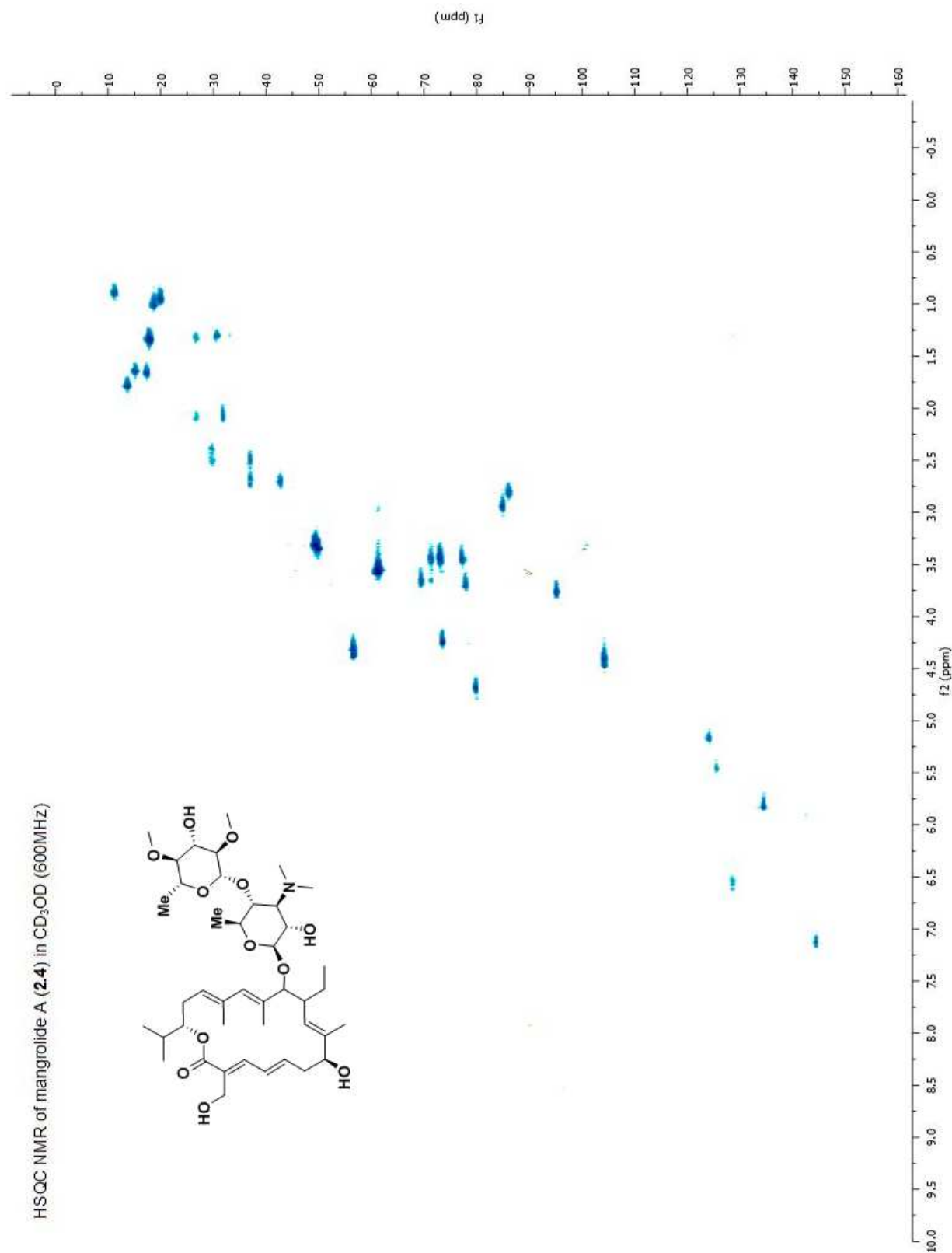
### **NMR SPECTRA**

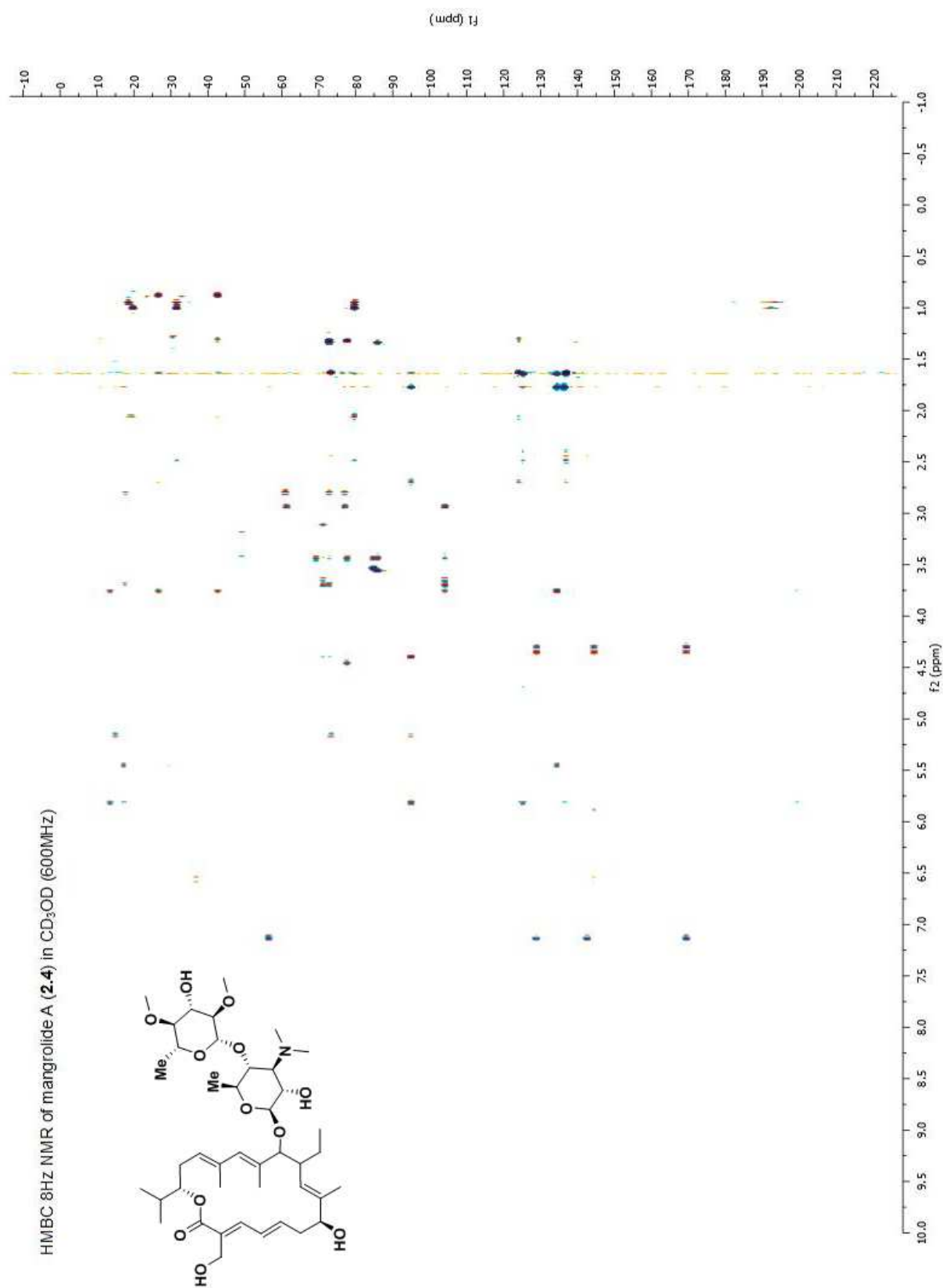
## NMR data for mangrolide A (2.4)



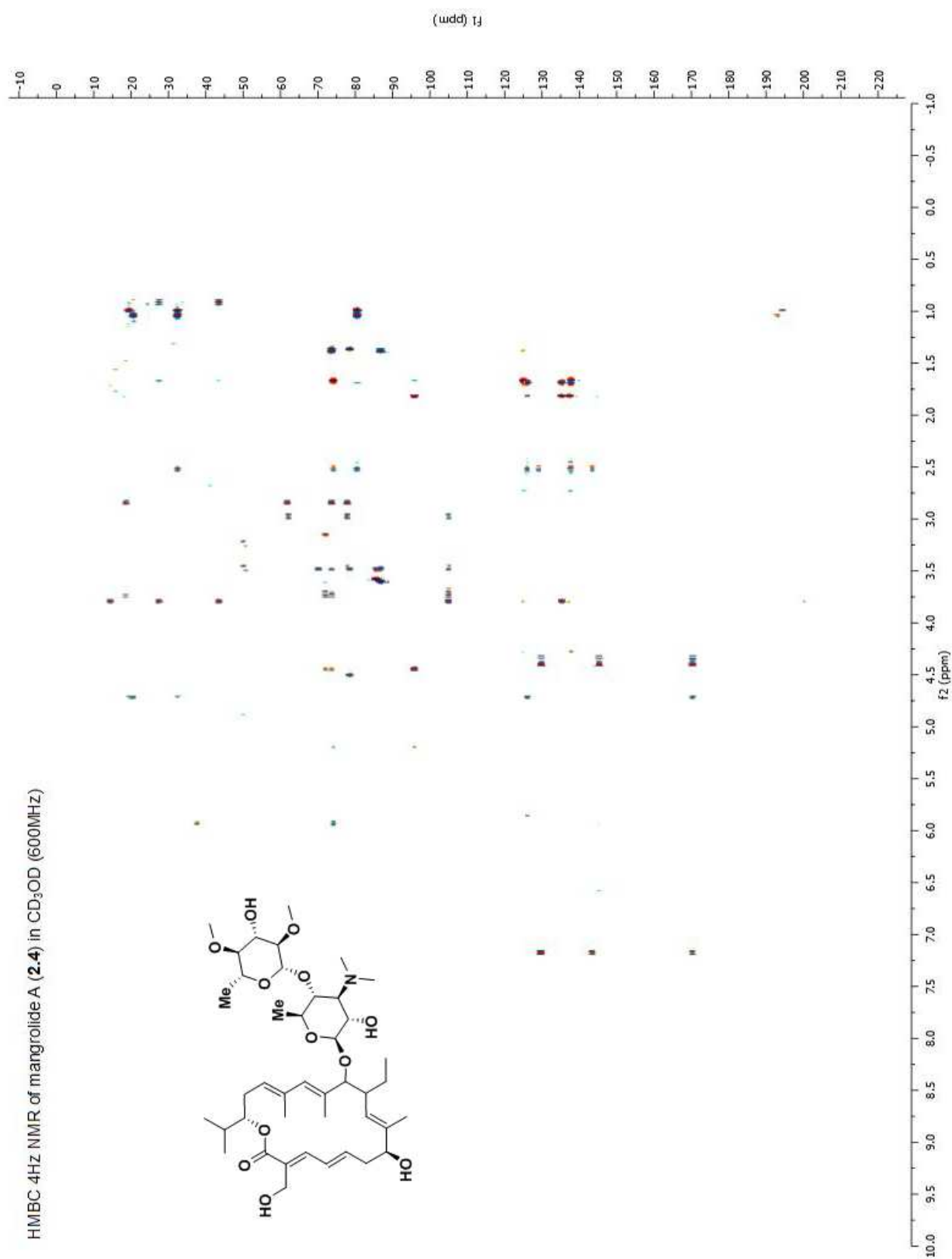


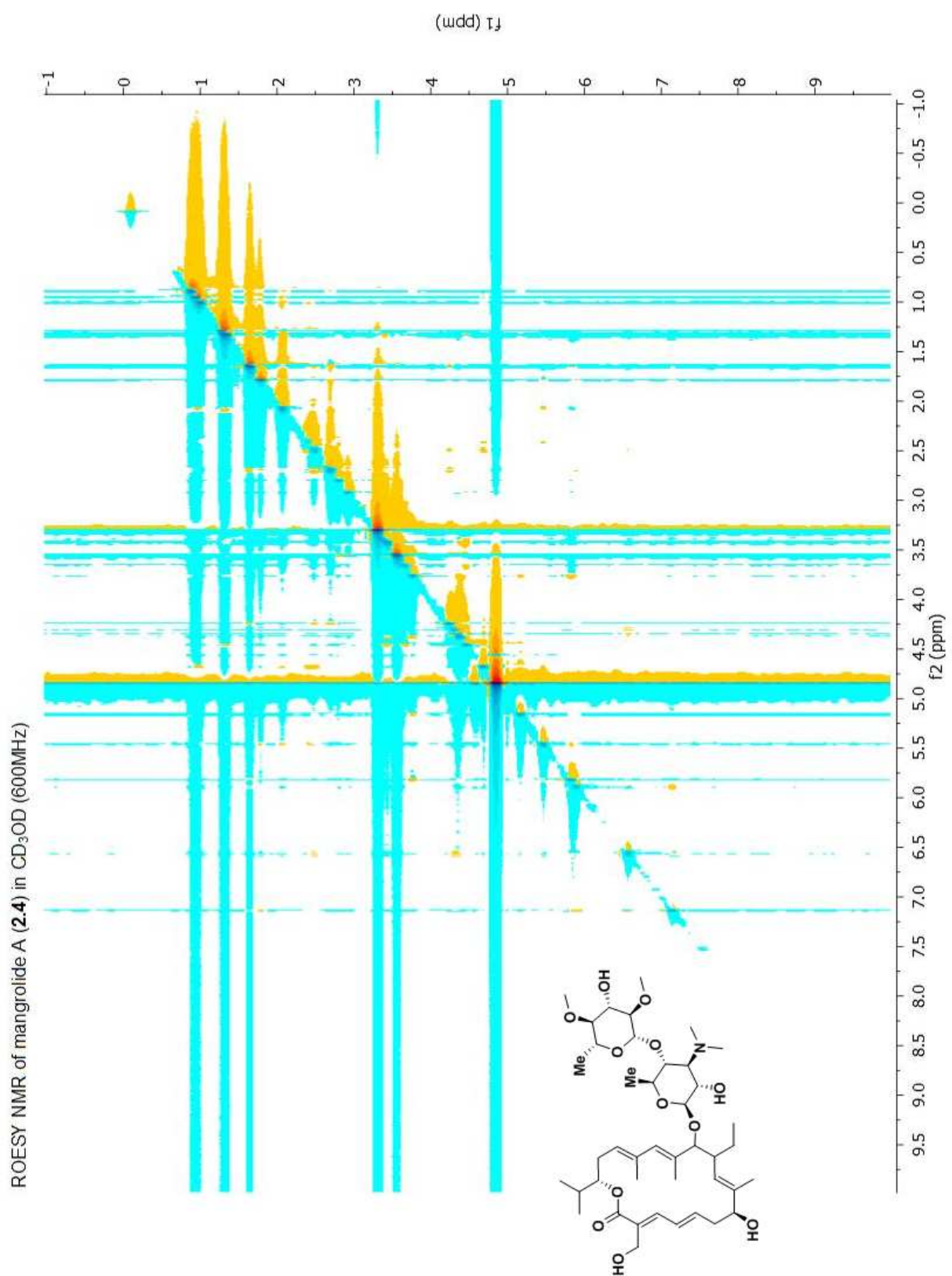


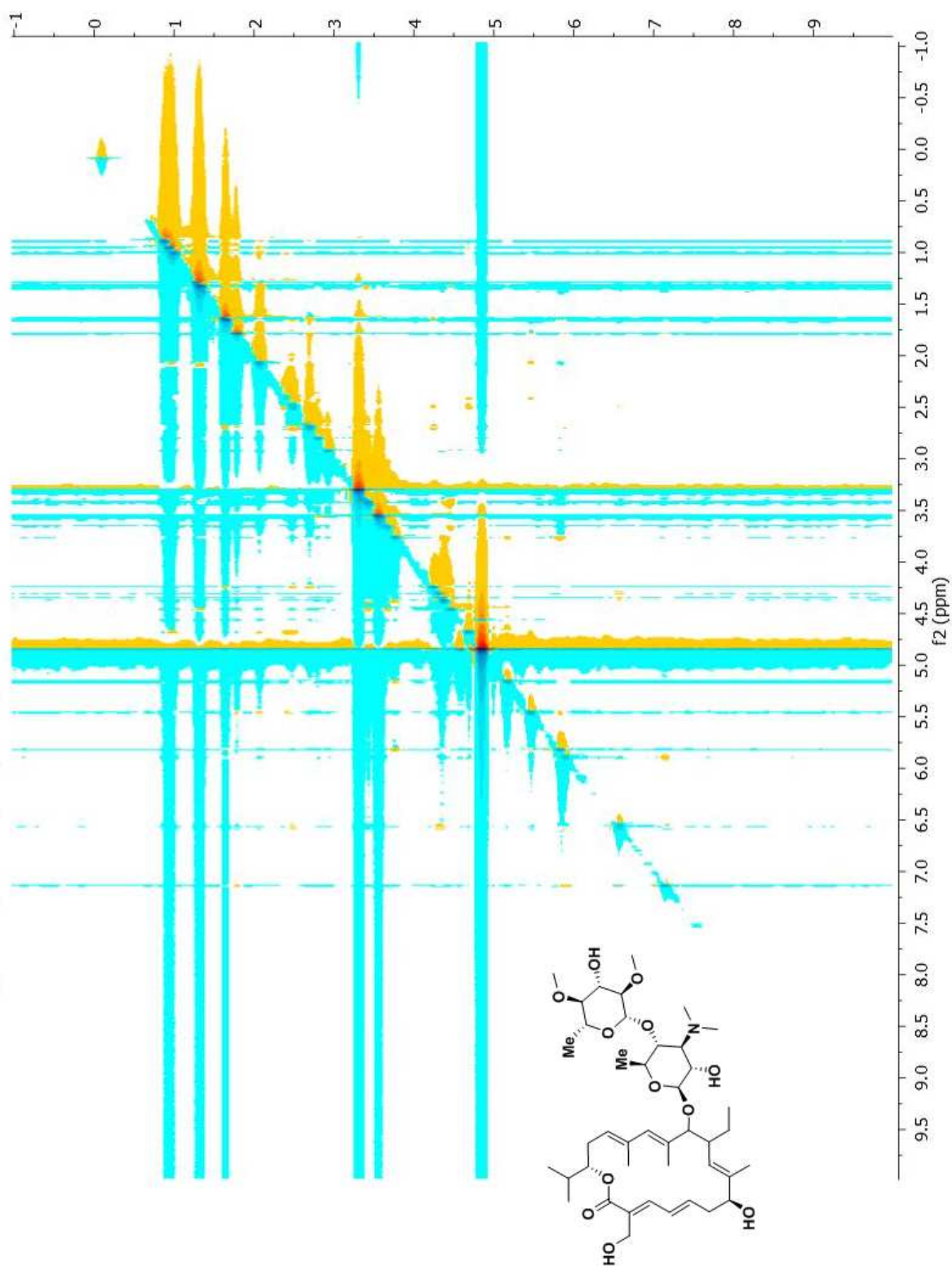




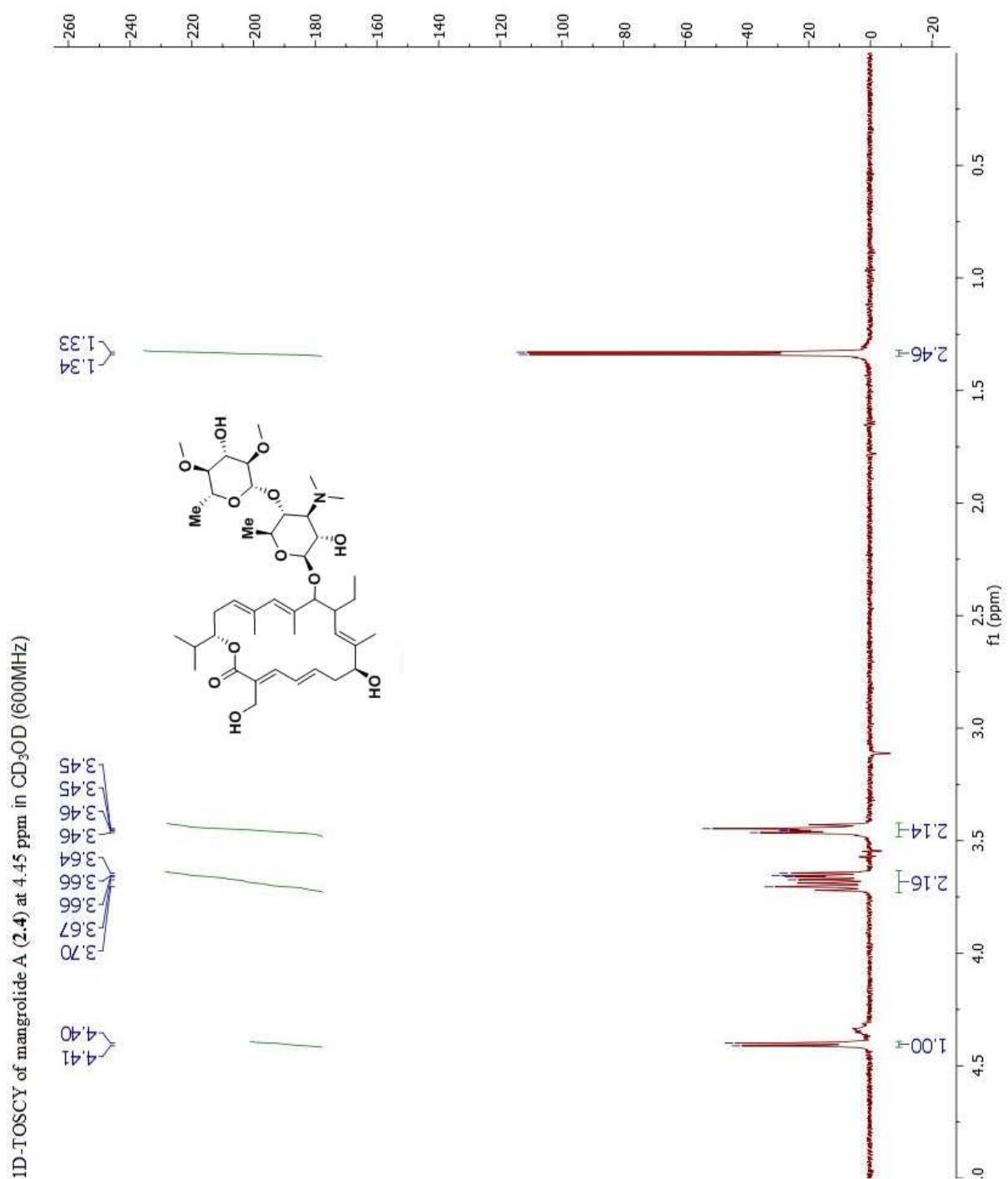


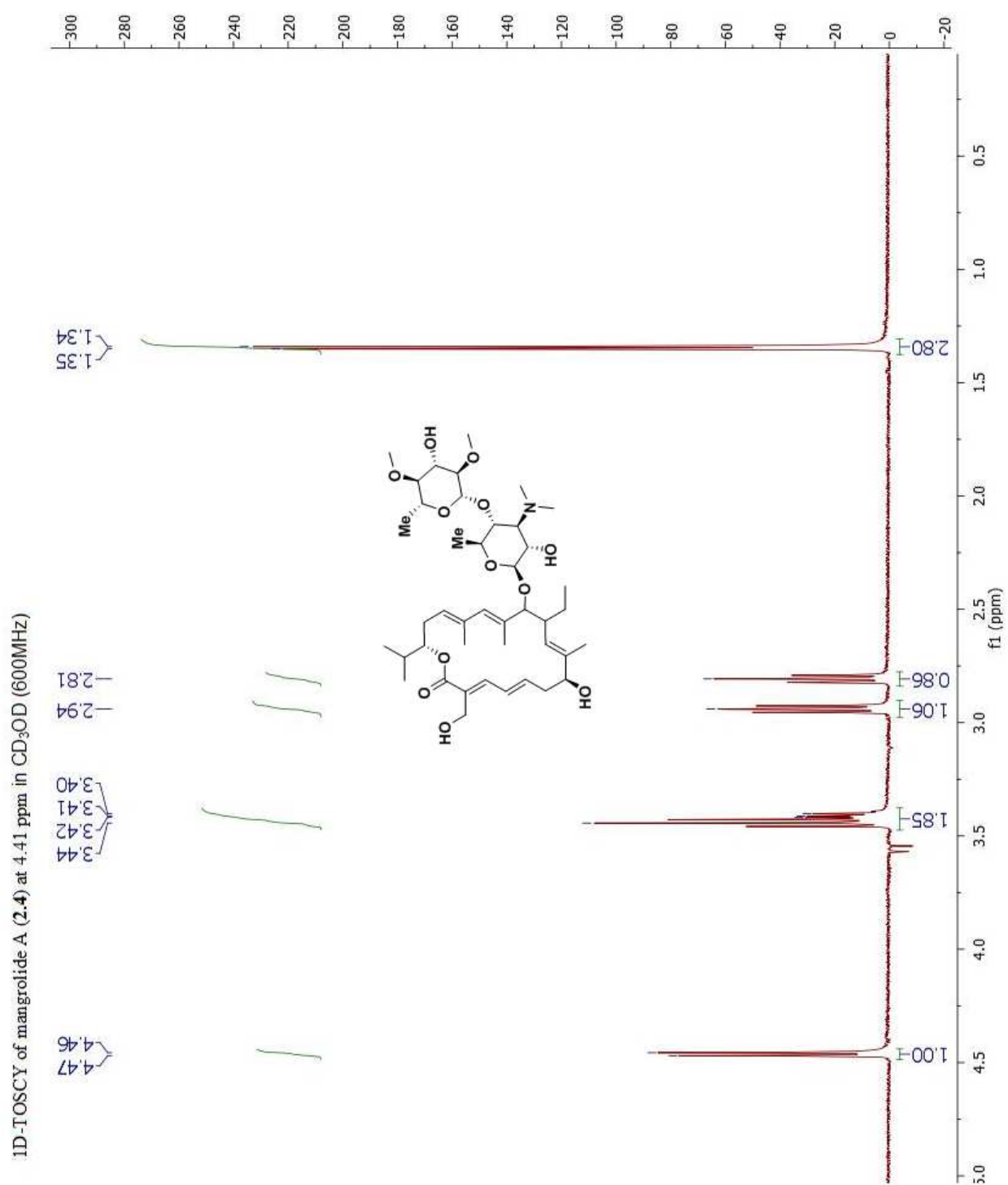
HMBC 4Hz NMR of mangrolide A (**2.4**) in CD<sub>3</sub>OD (600MHz)



ROESY NMR of mangrolide A (2.4) in CD<sub>3</sub>OD (600MHz)

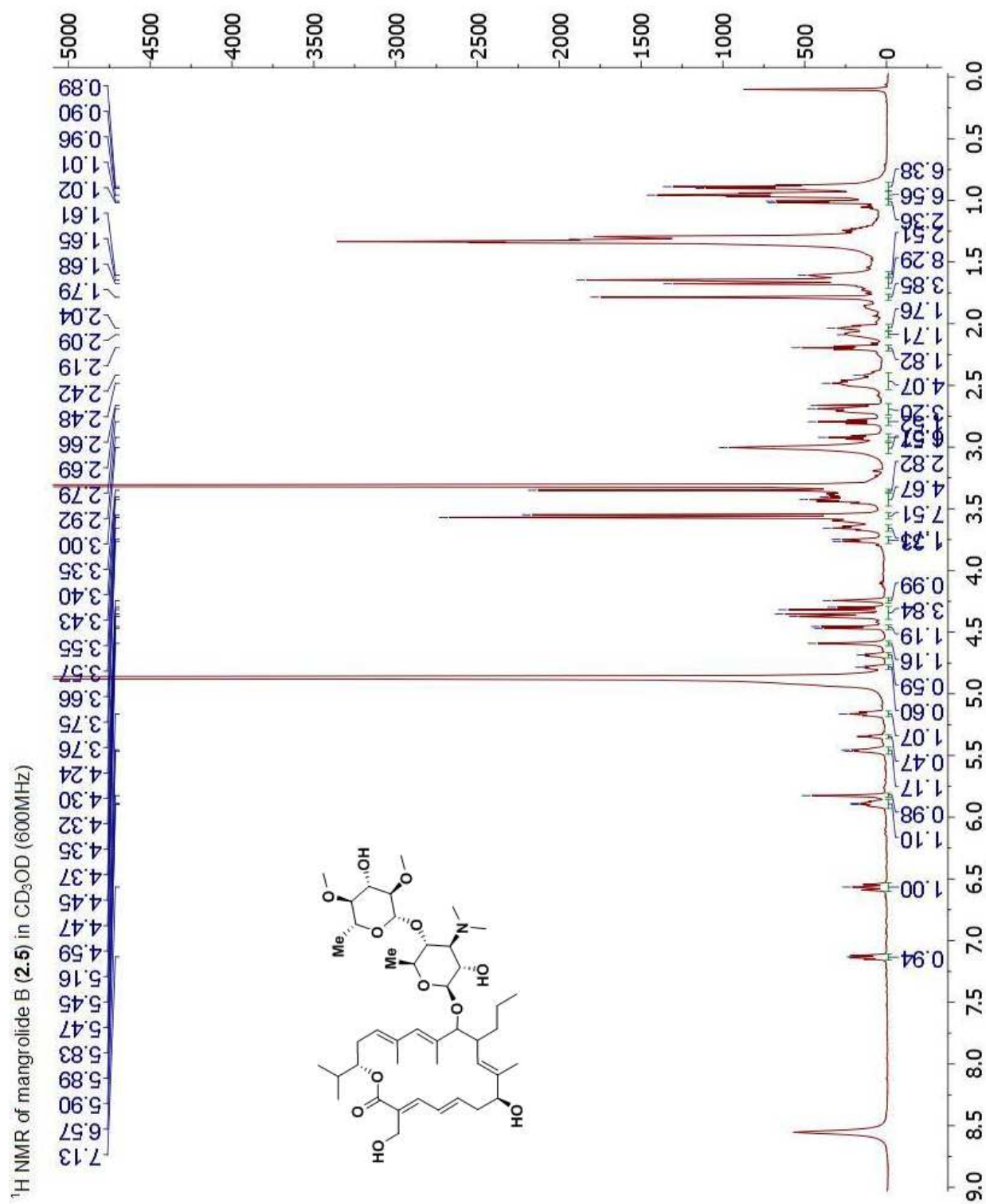




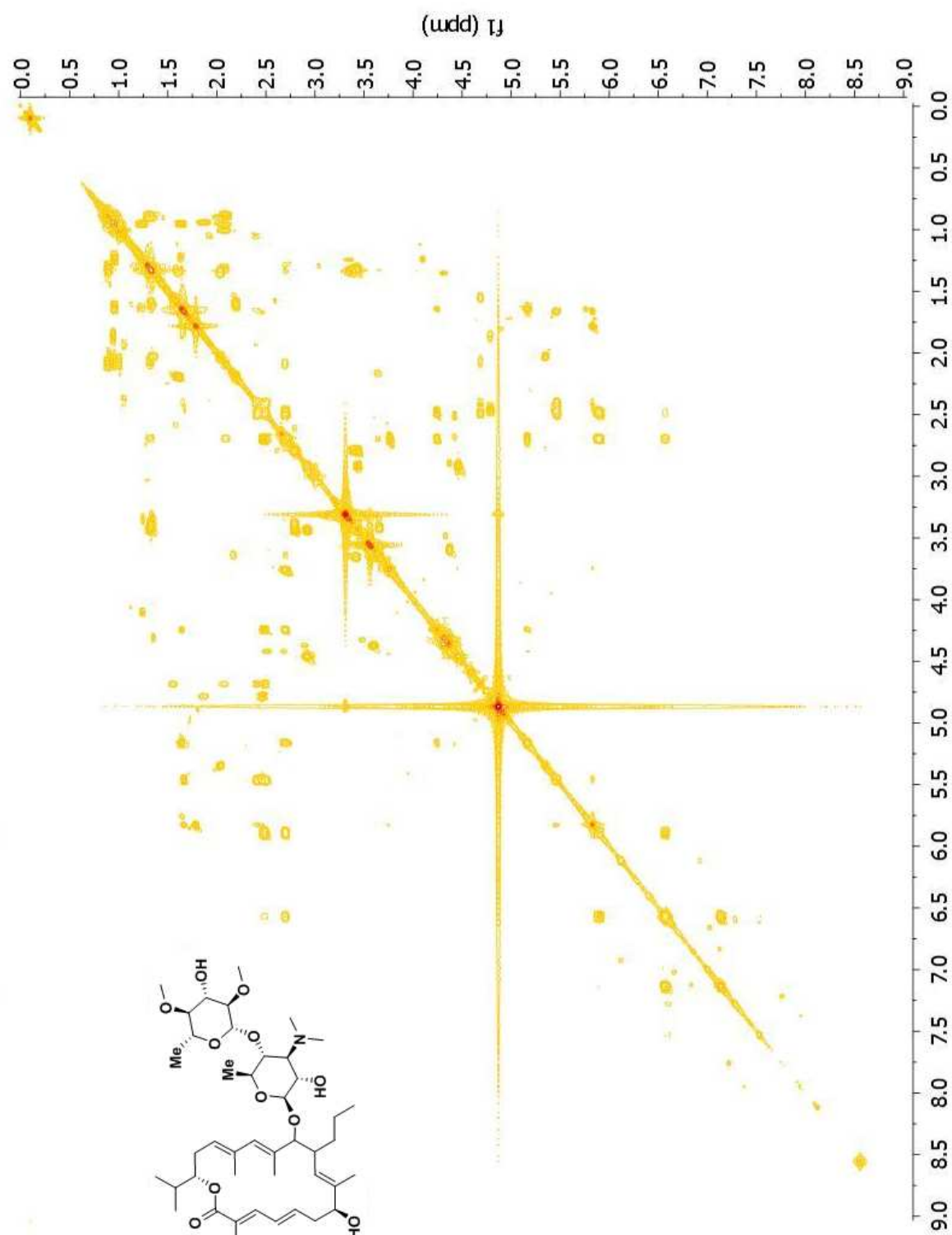




## Mangrolide B NMR Data



$^1\text{H}$ - $^1\text{H}$  COSY NMR of mangrolide B (**2.5**) in  $\text{CD}_3\text{OD}$  (600MHz)

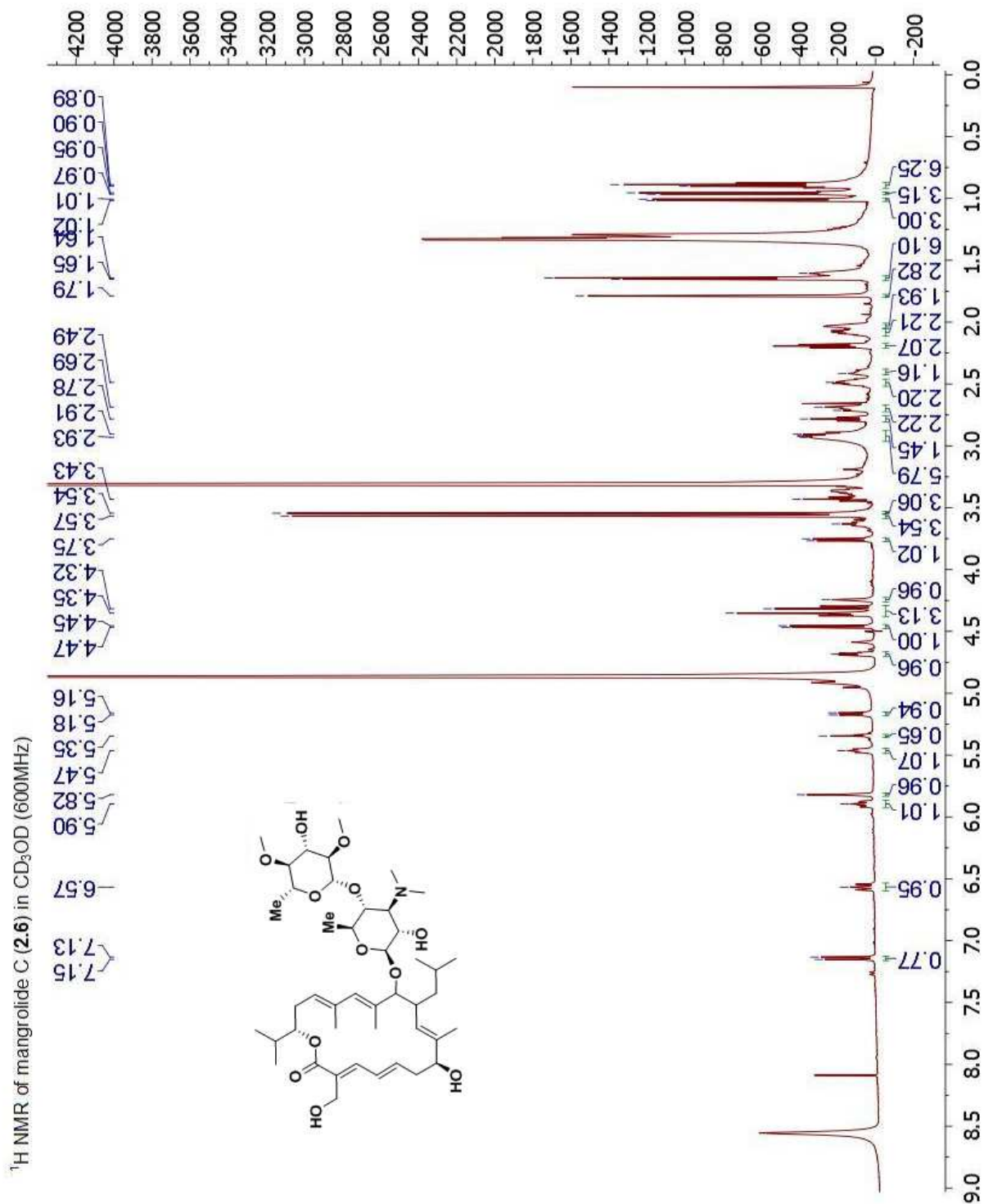


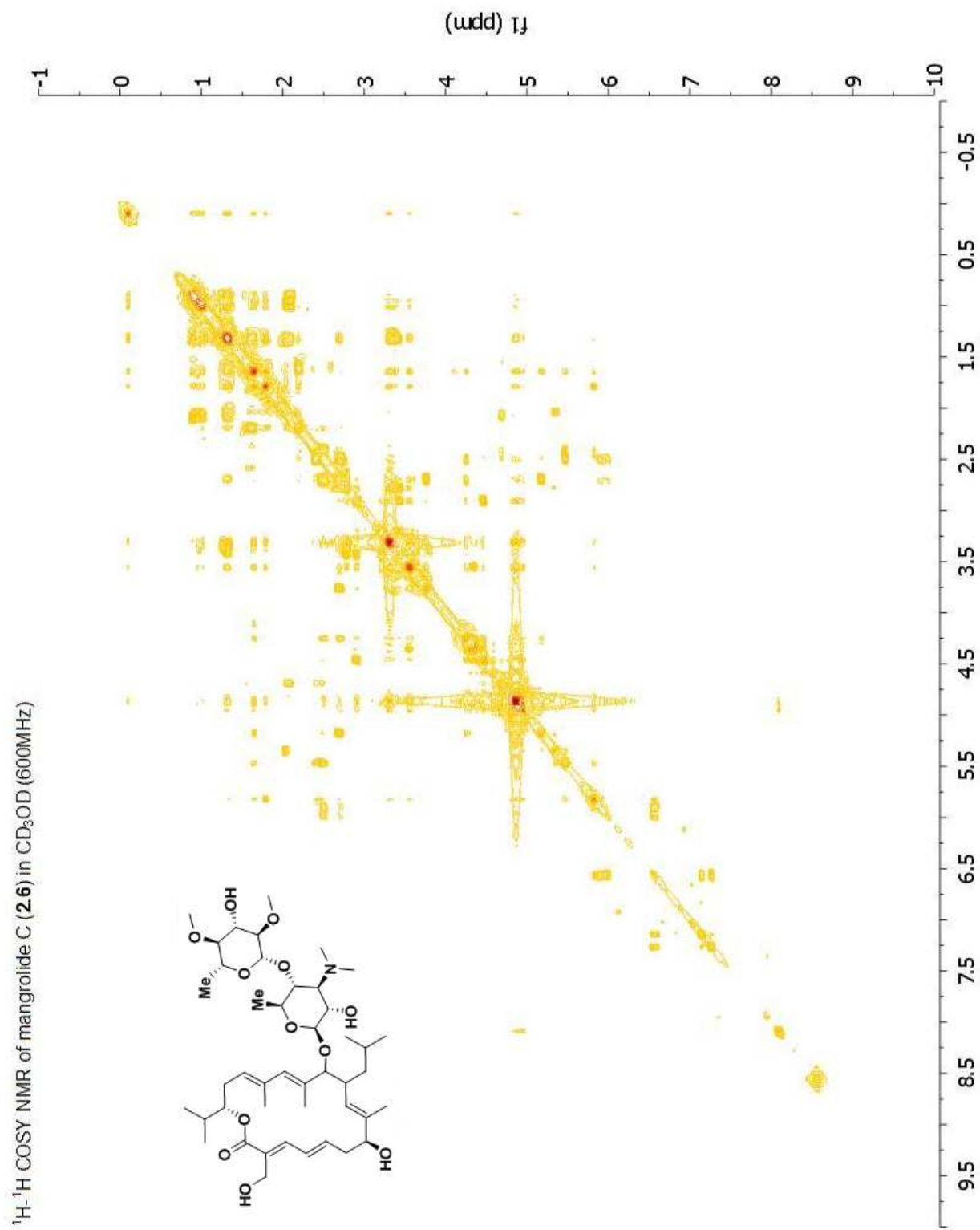


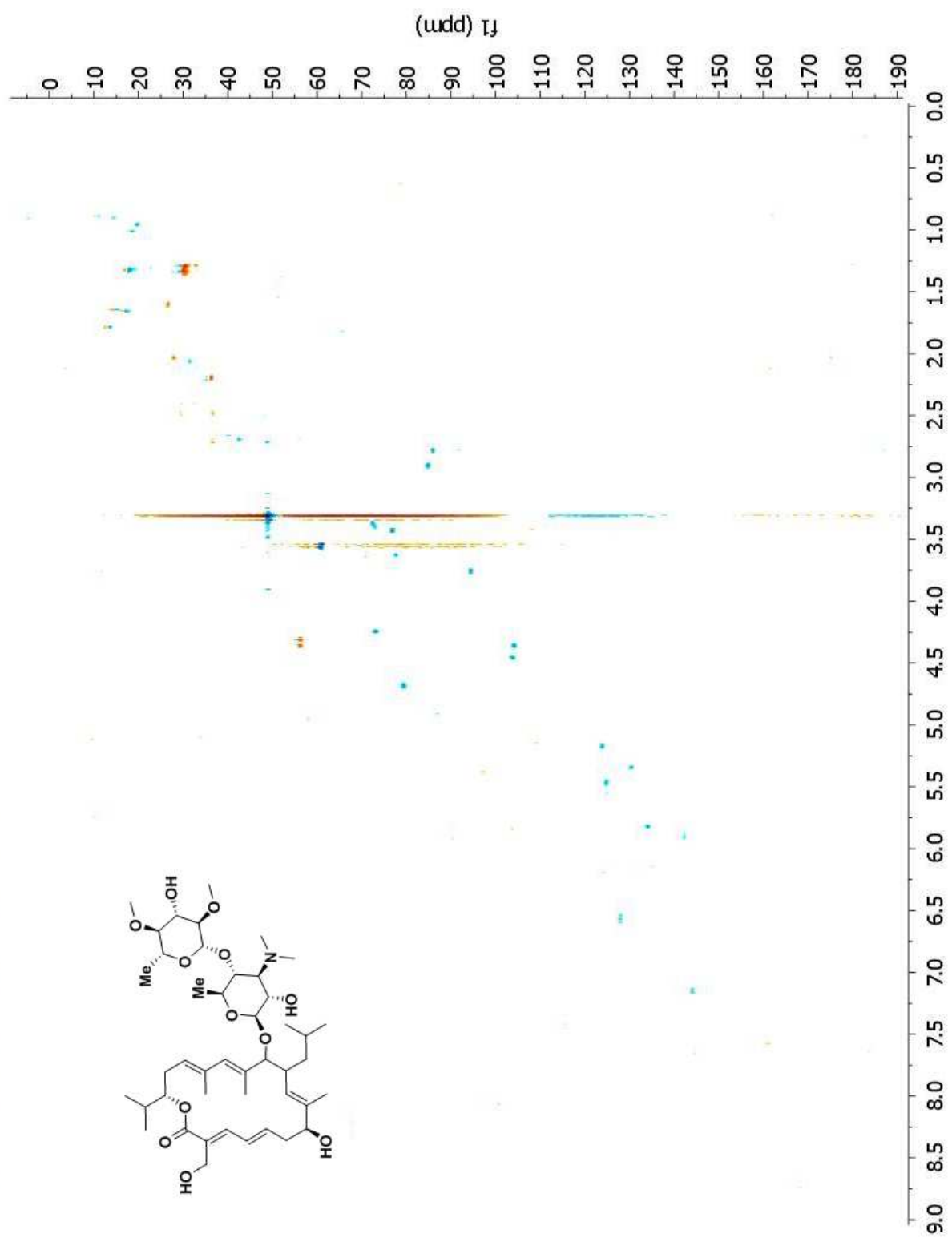






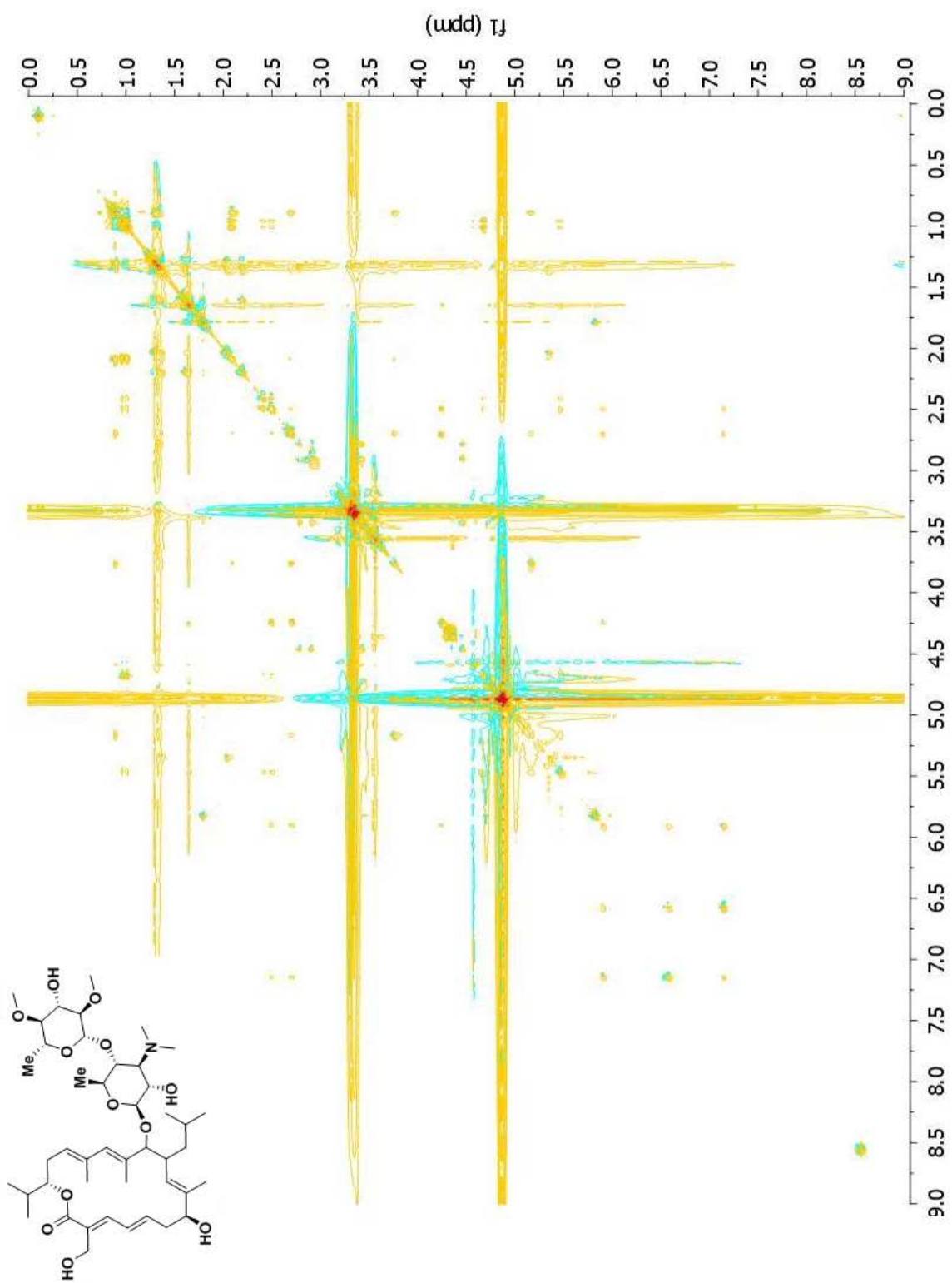




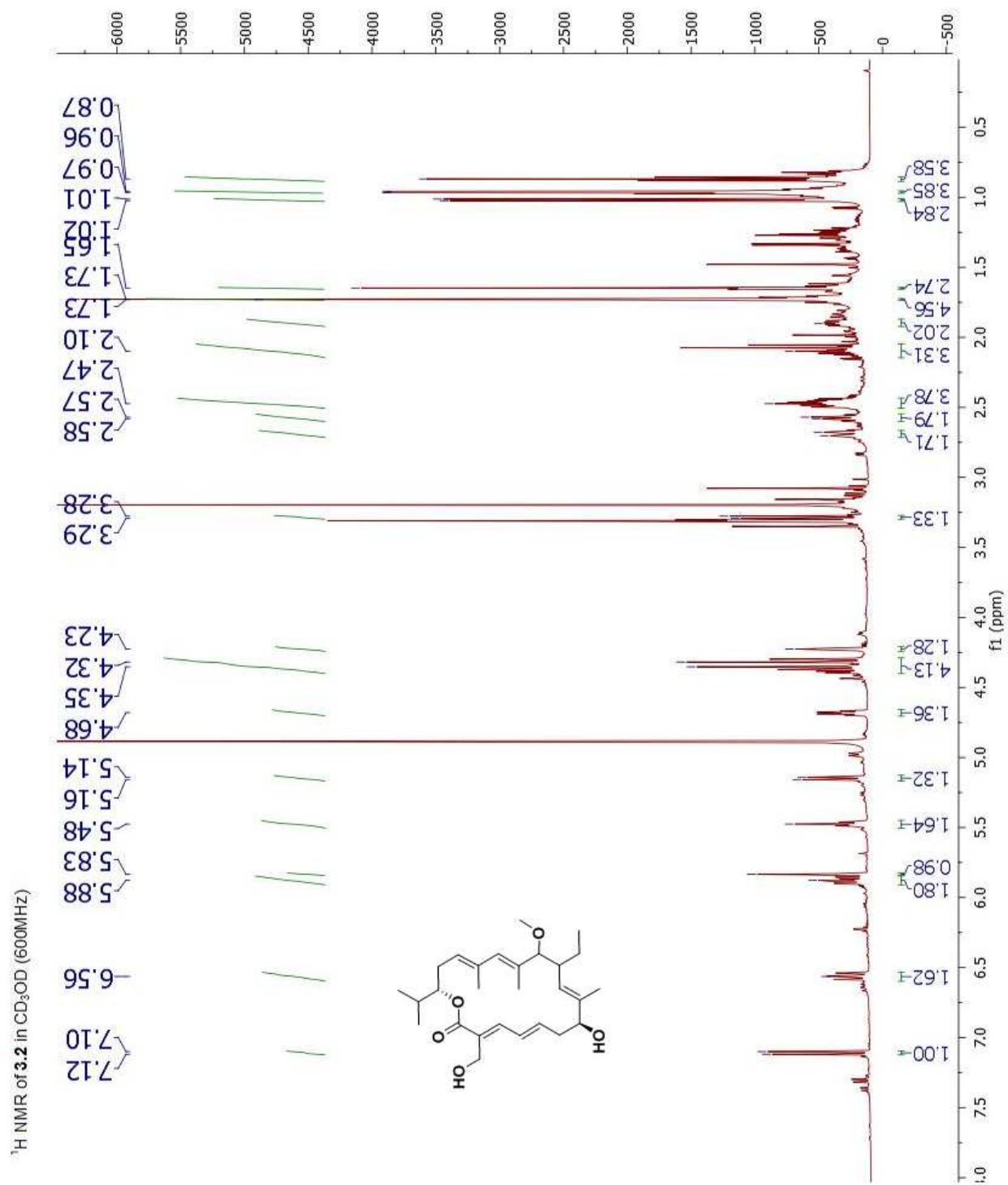
HSQC NMR of mangrolide C (**2.6**) in CD<sub>3</sub>OD (600MHz)



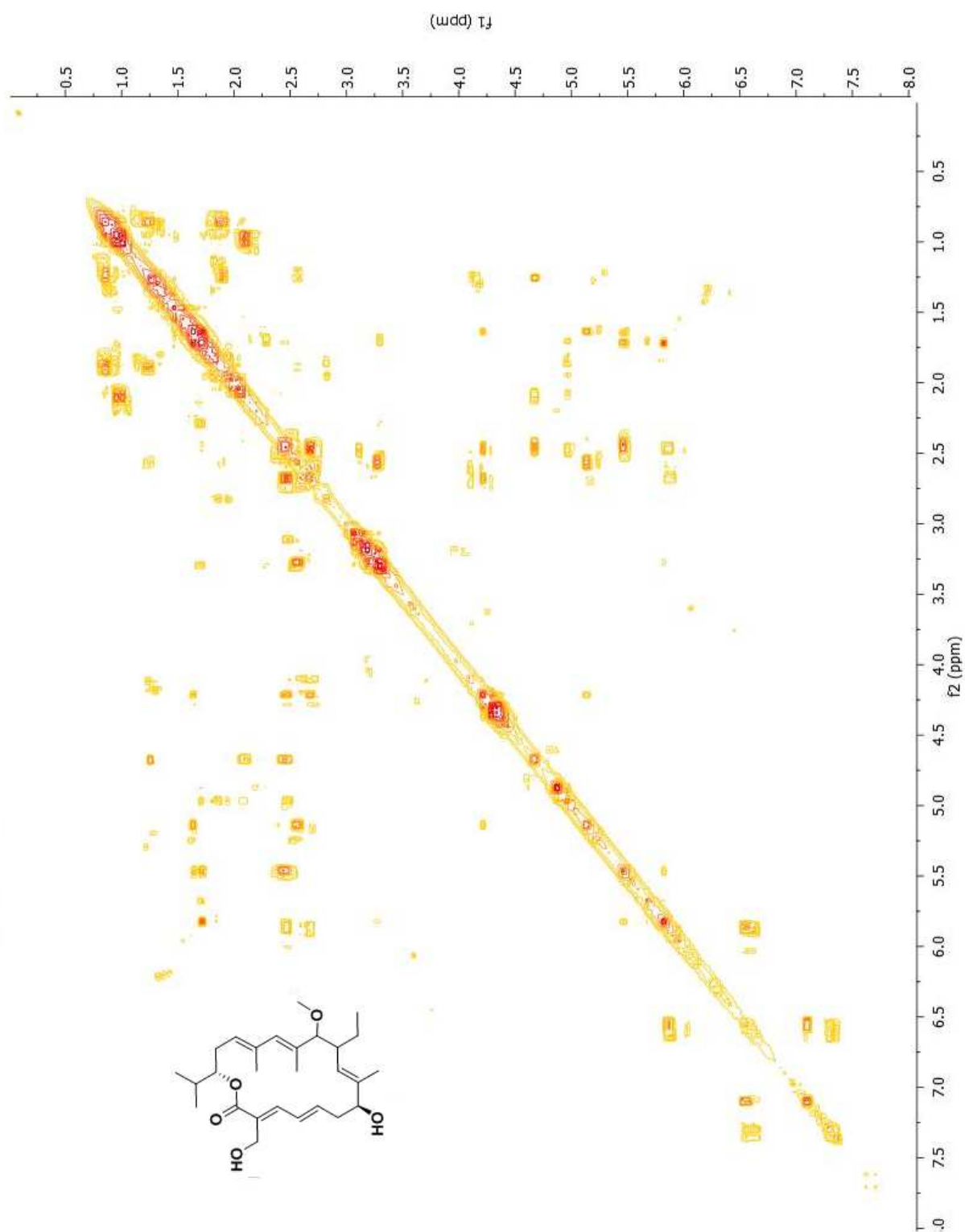


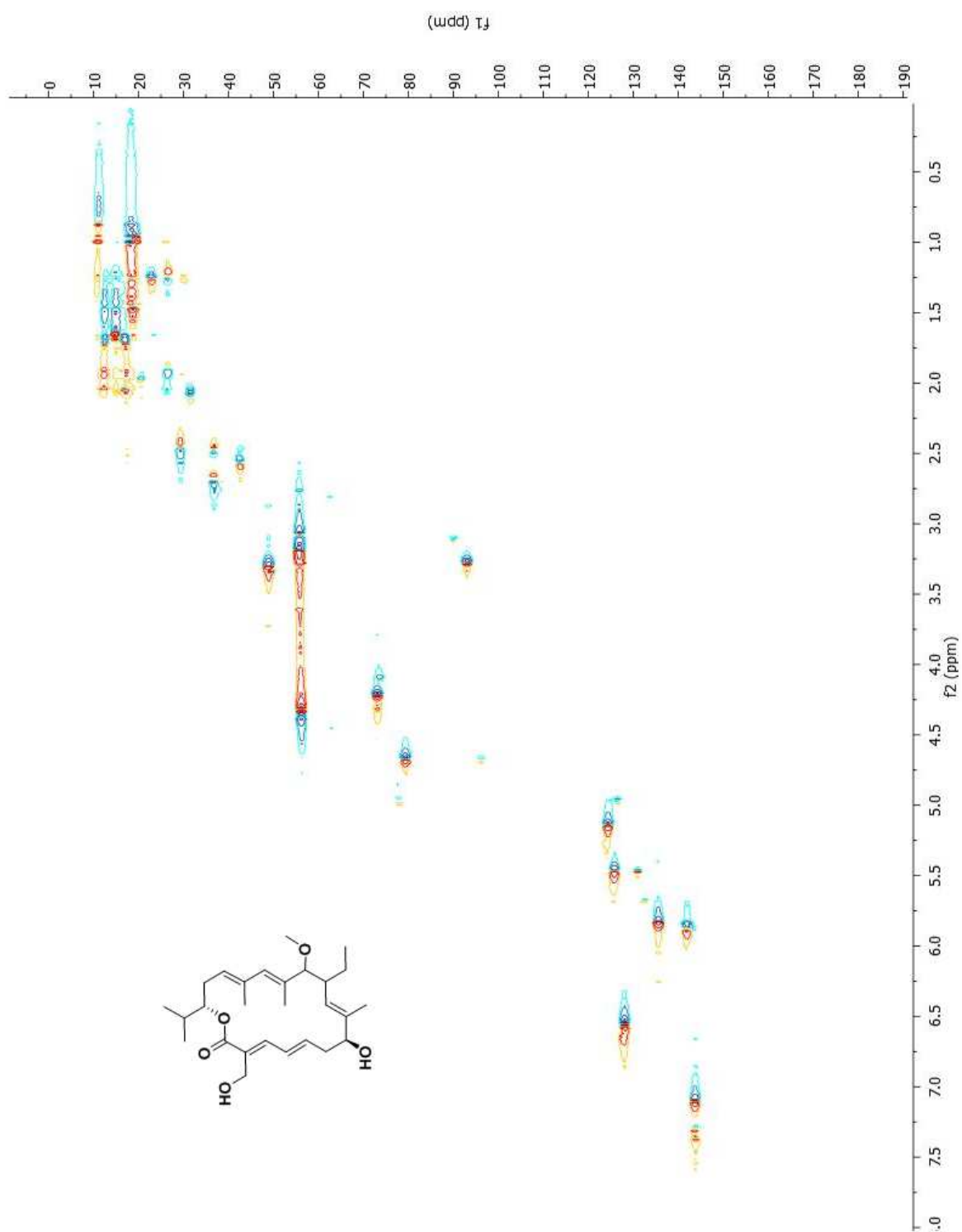
TOCSY NMR of mangrolide C (**2.6**) in CD<sub>3</sub>OD (600MHz)

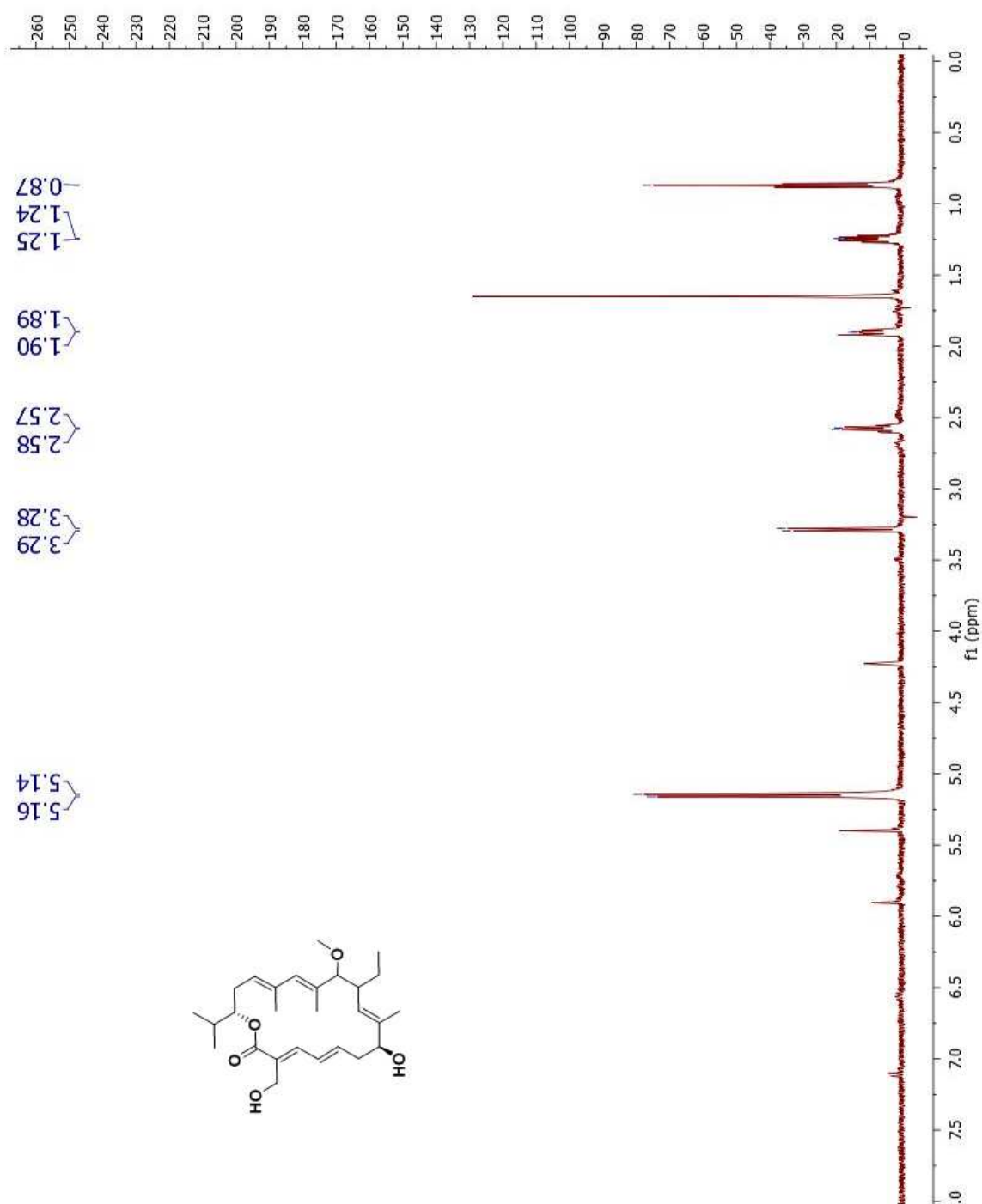


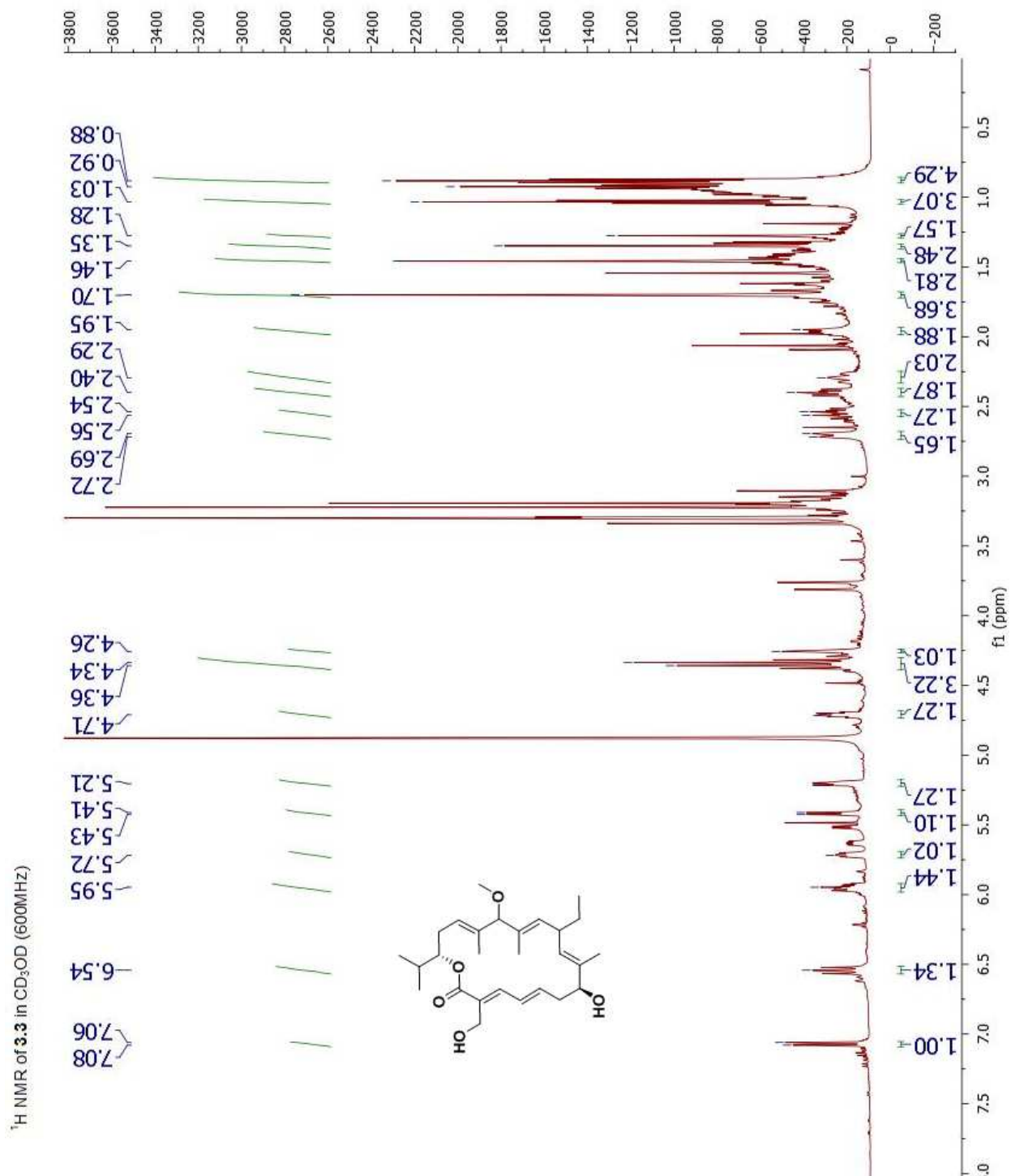
NMR data for **3.2**

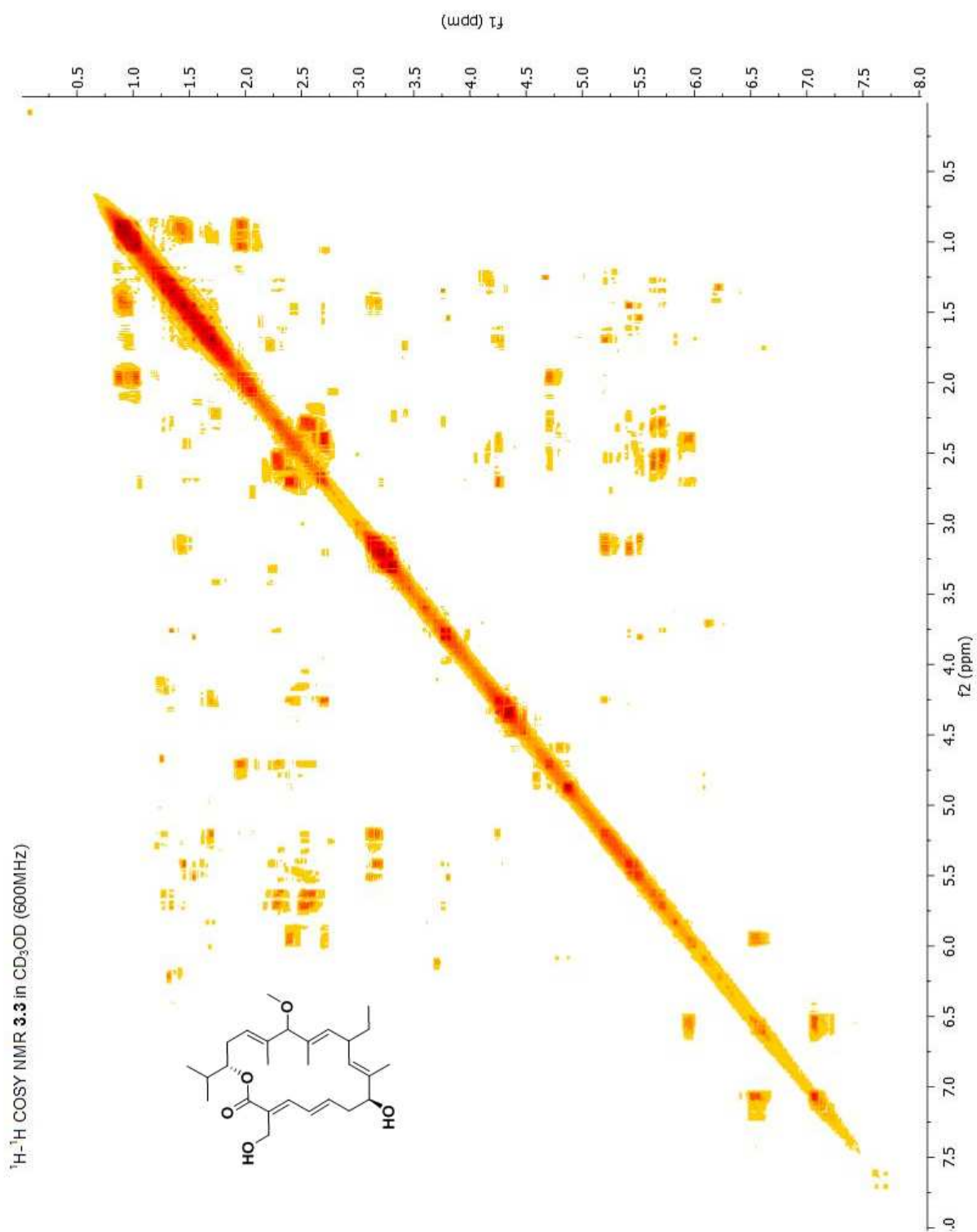
$^1\text{H}$ - $^1\text{H}$  COSY NMR **3.2** in  $\text{CD}_3\text{OD}$  (600MHz)

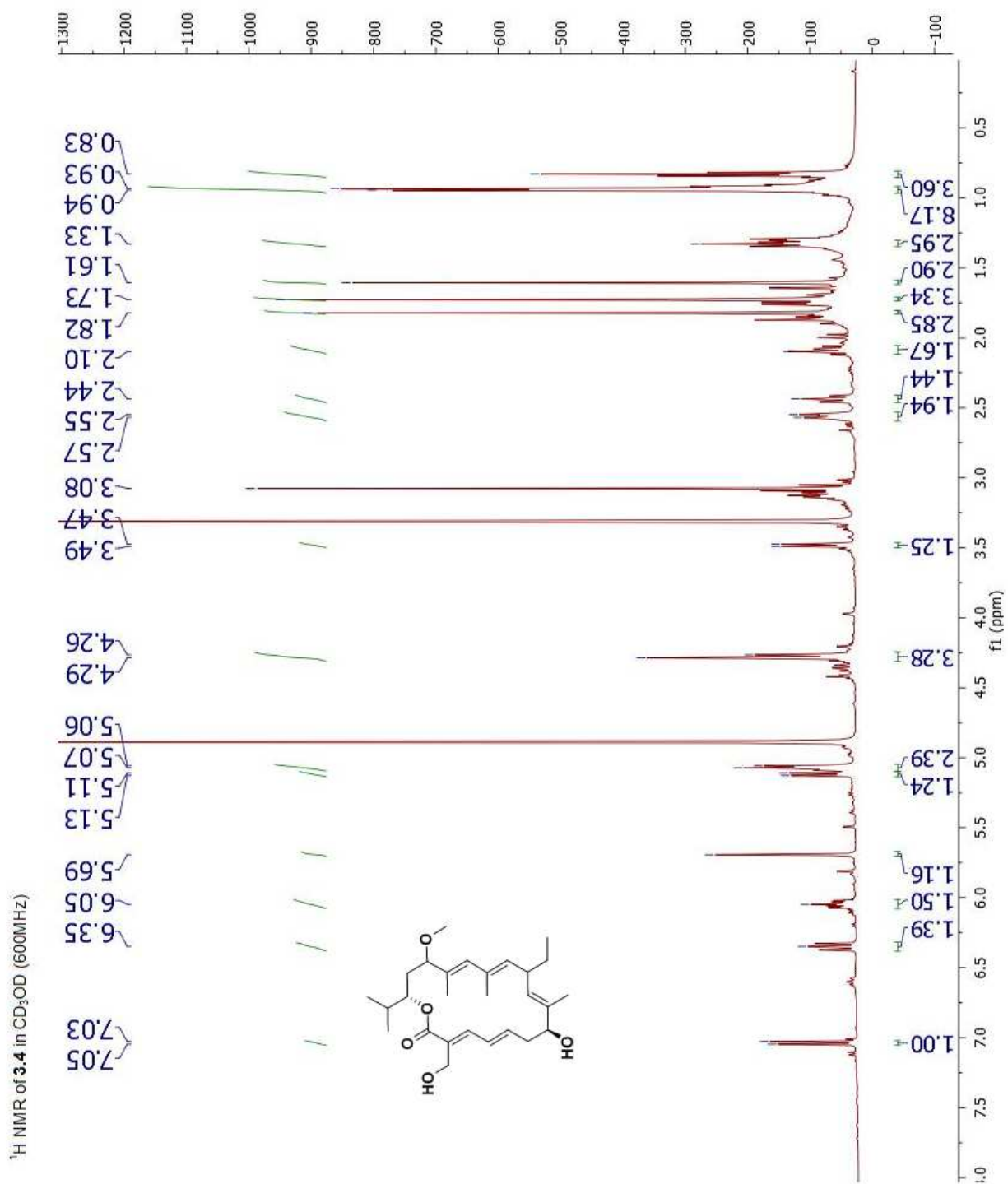


HSQC NMR **3.2** in CD<sub>3</sub>OD (600MHz)

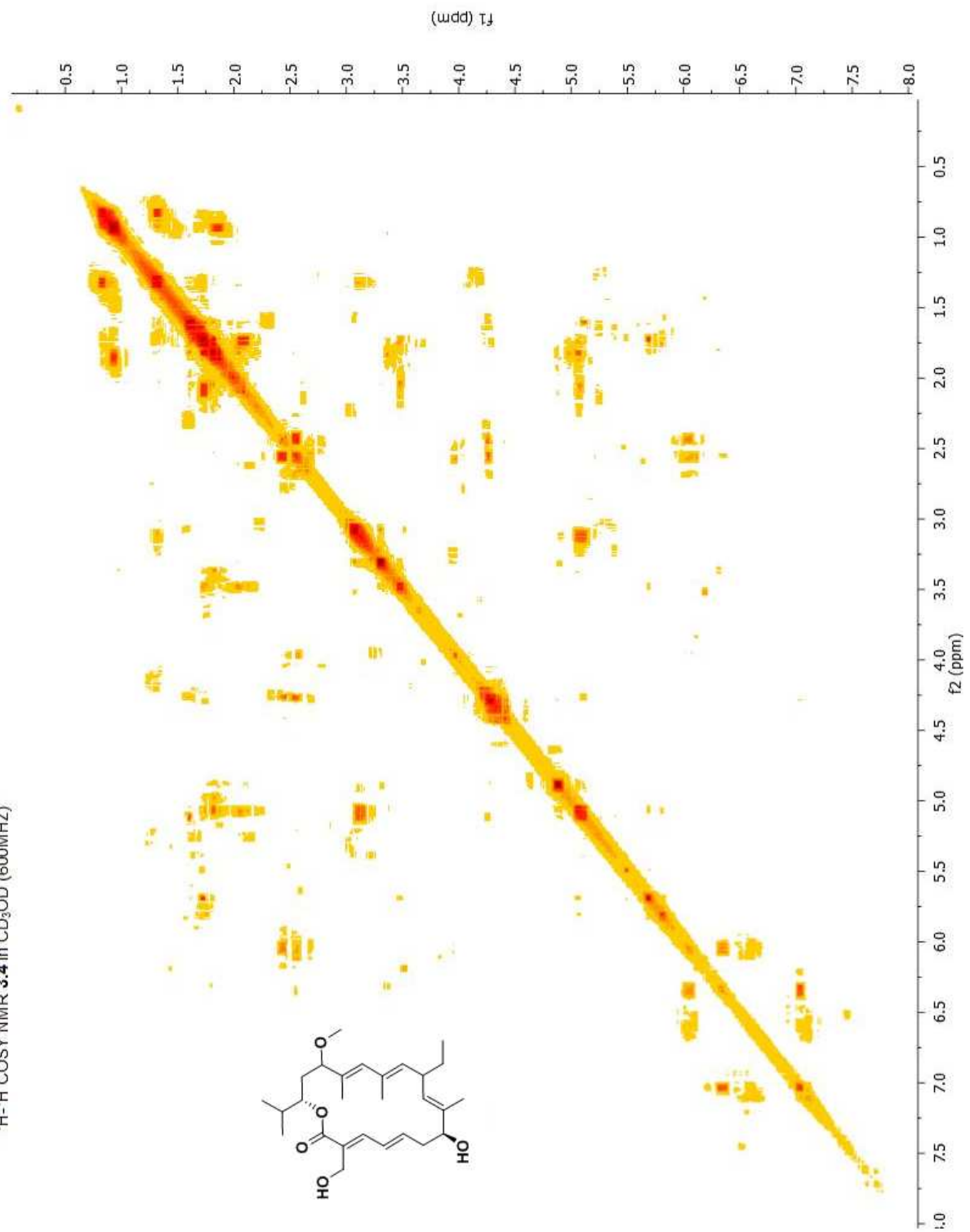


NMR data for **3.3**

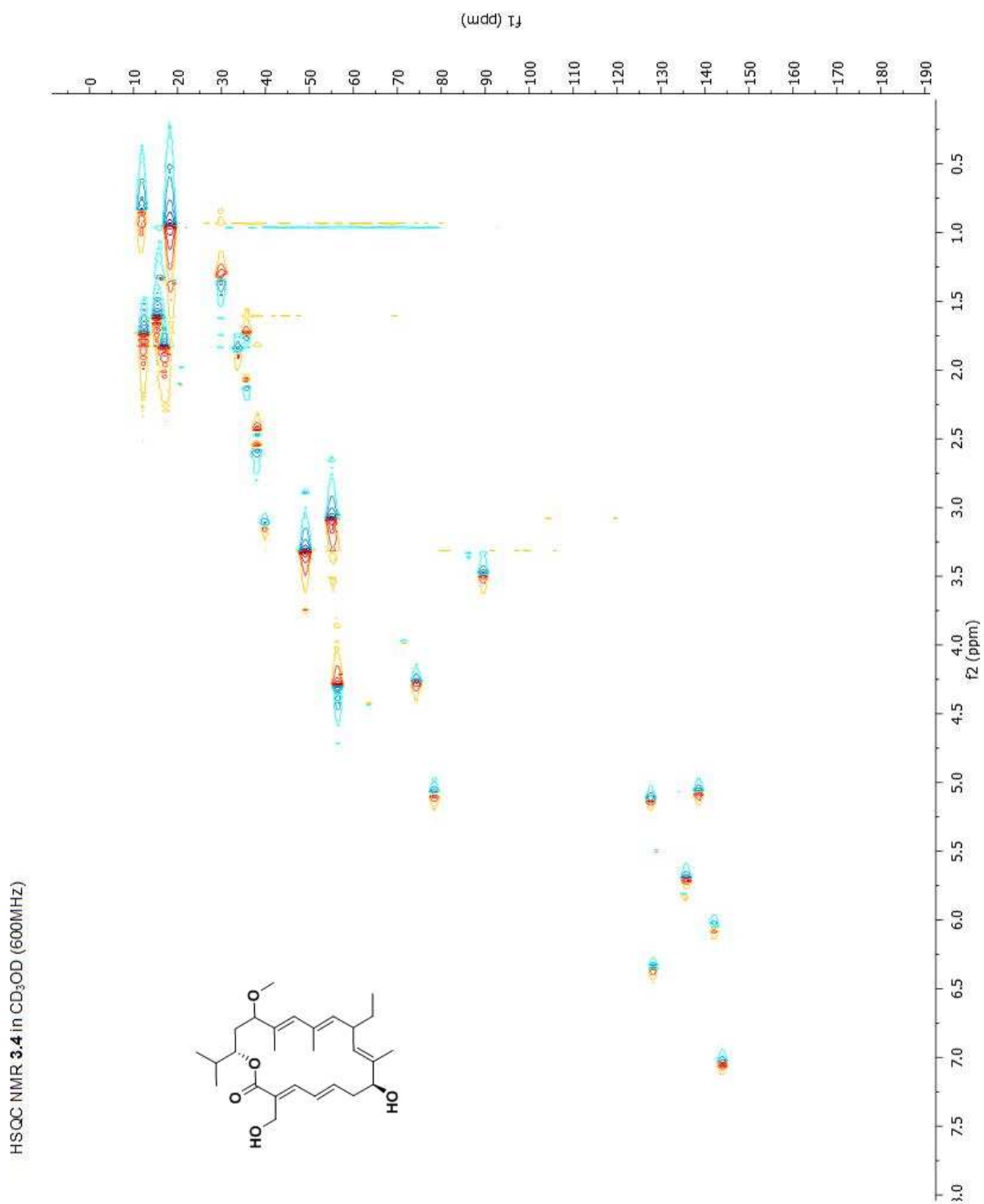


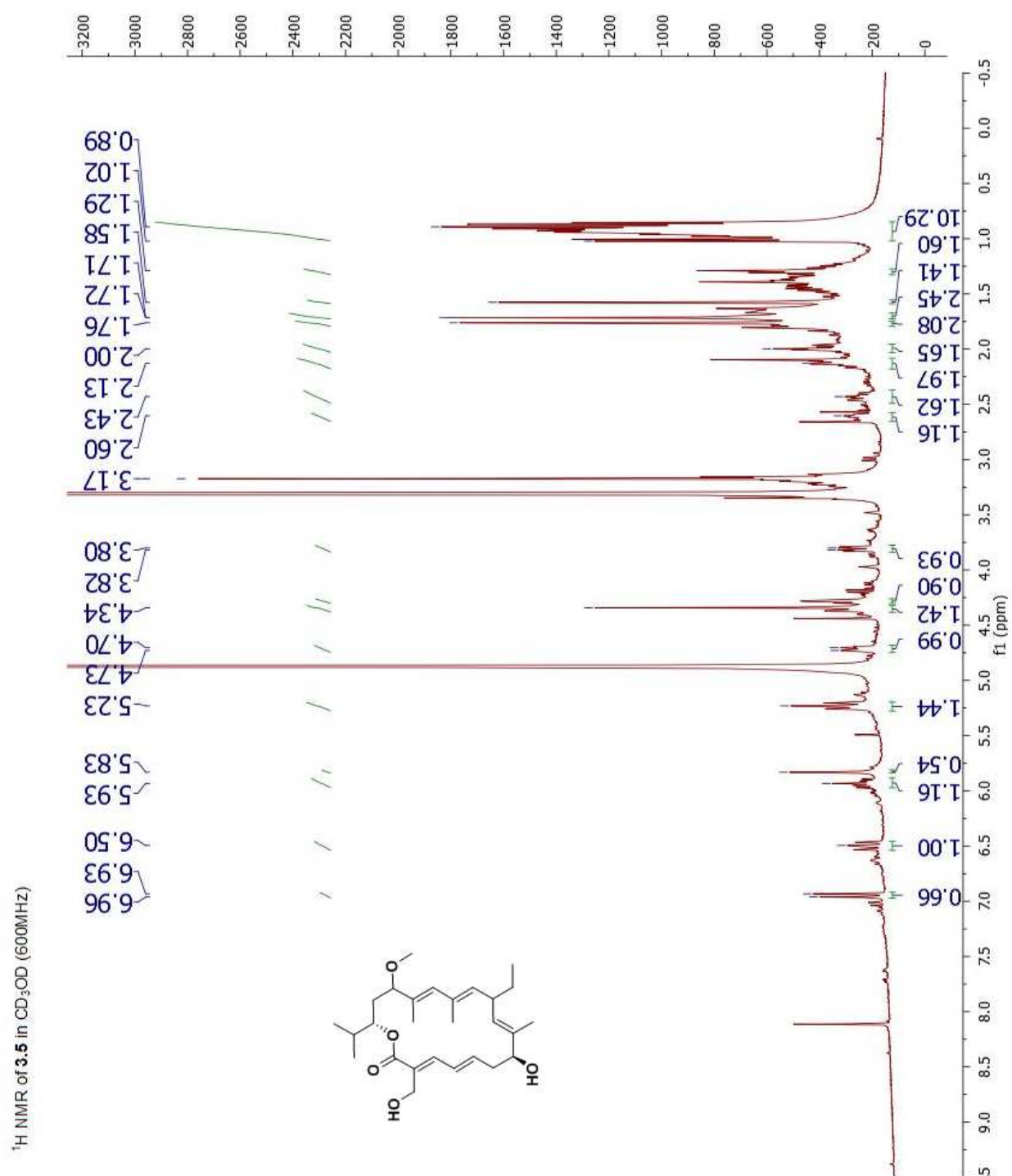
NMR data for **3.4**

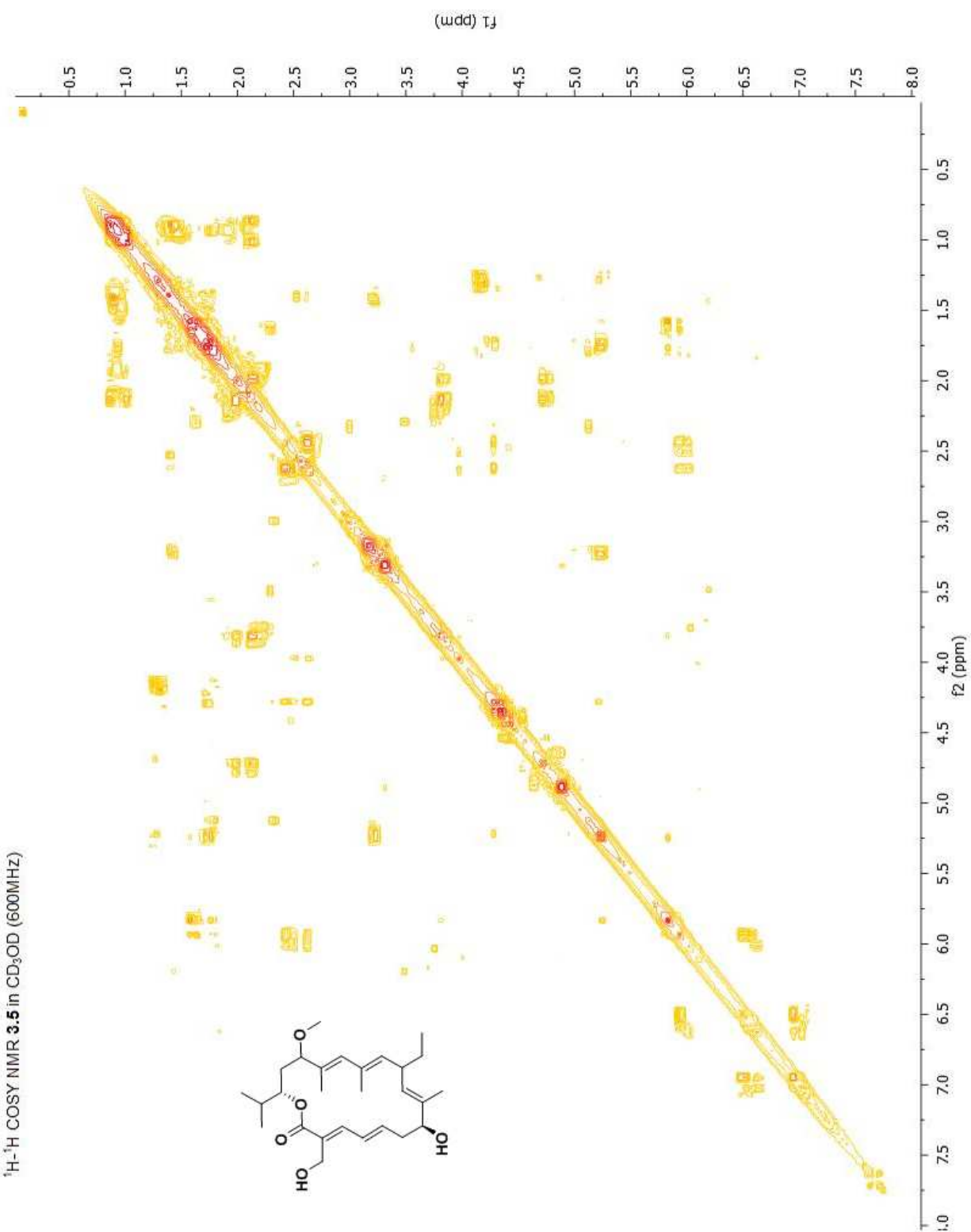


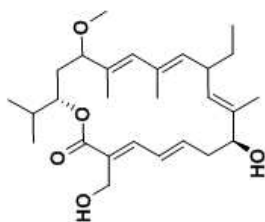
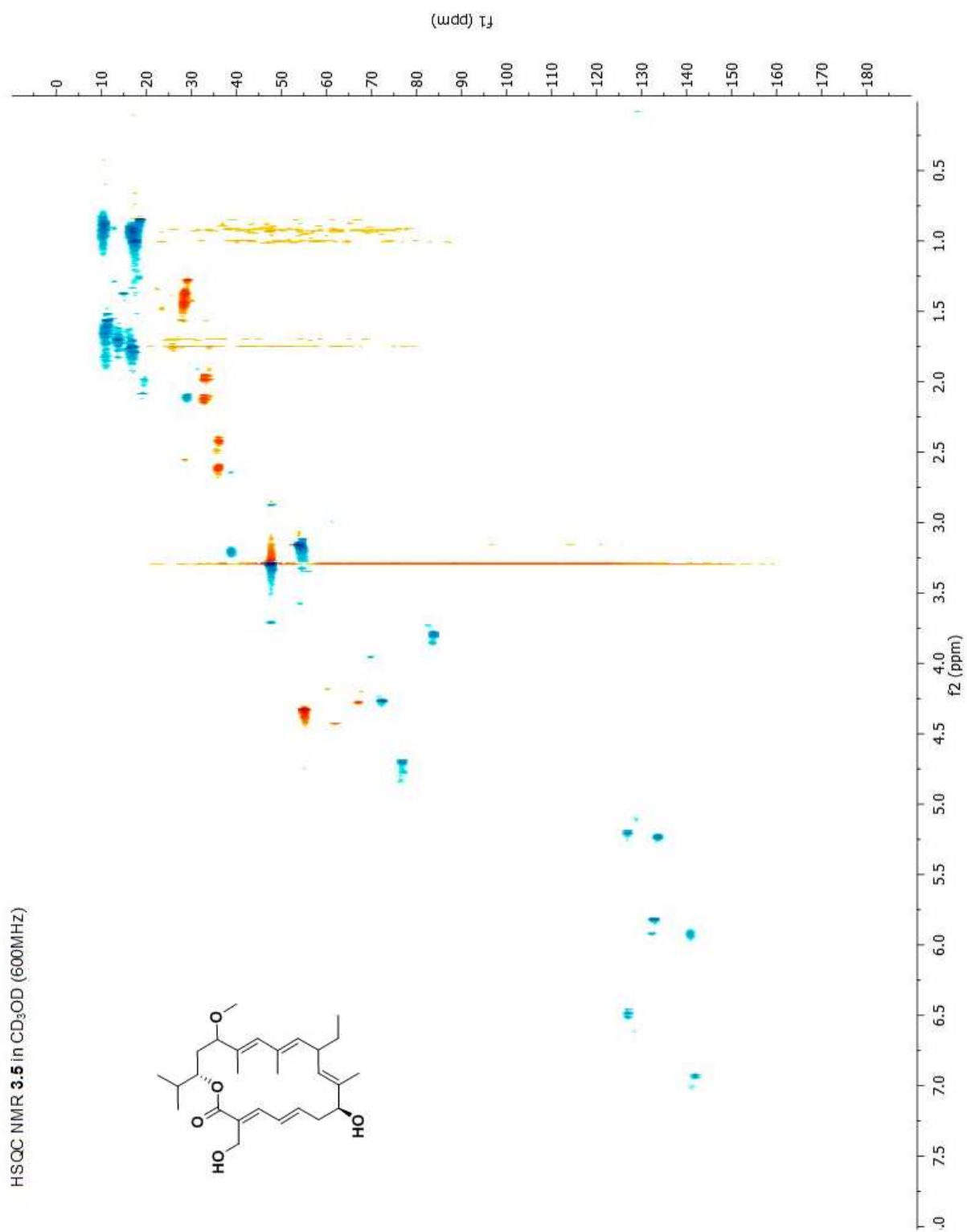


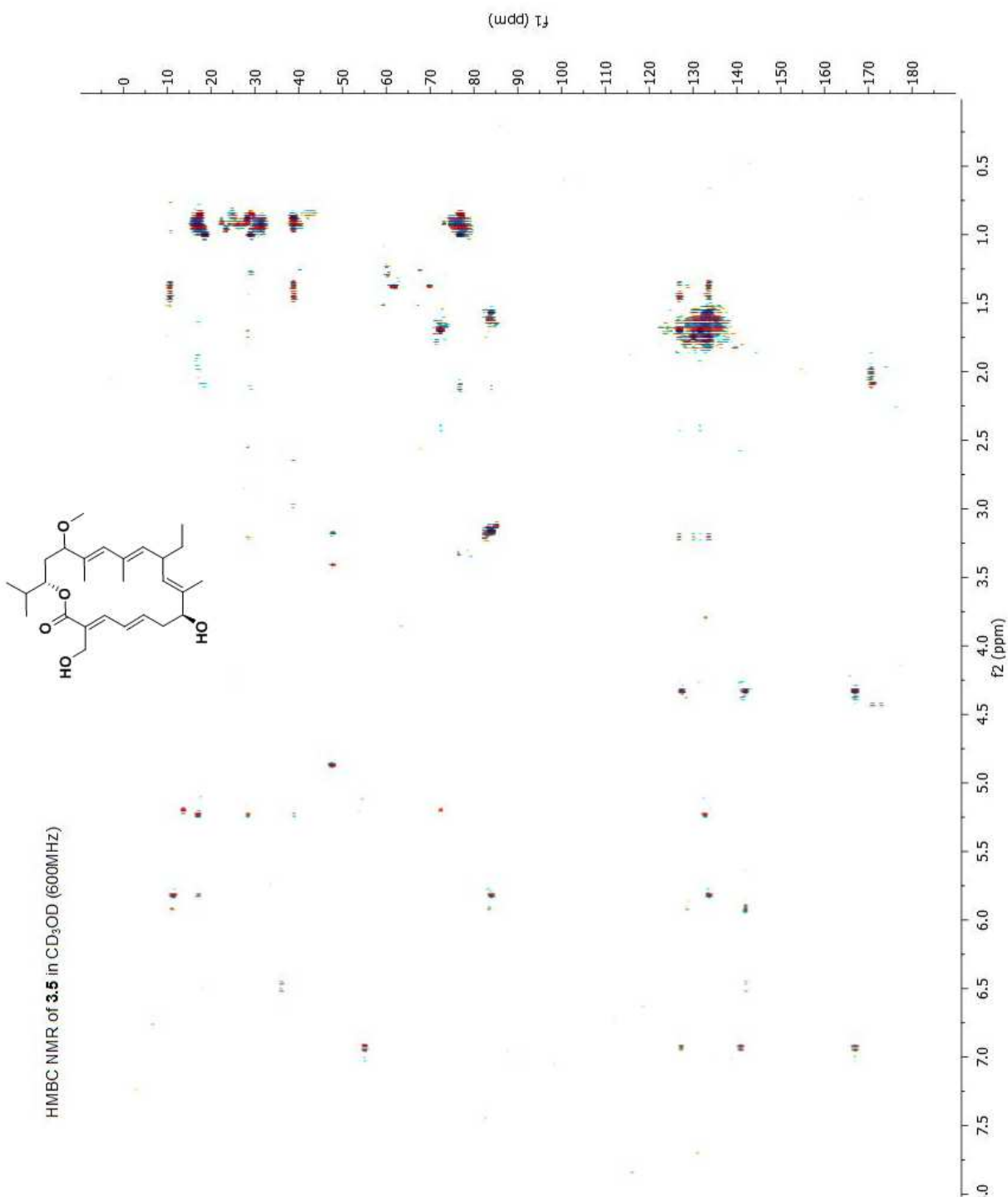


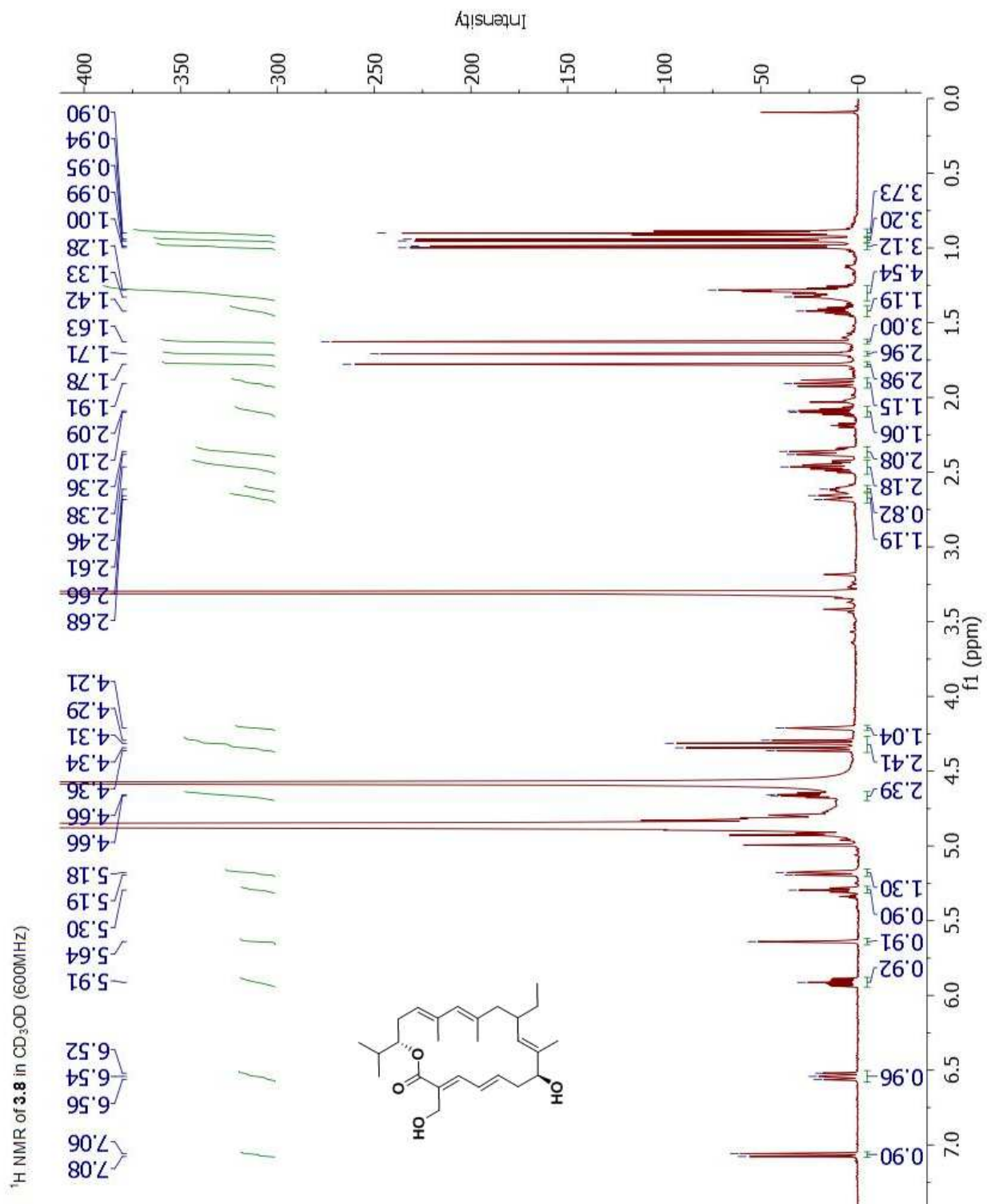


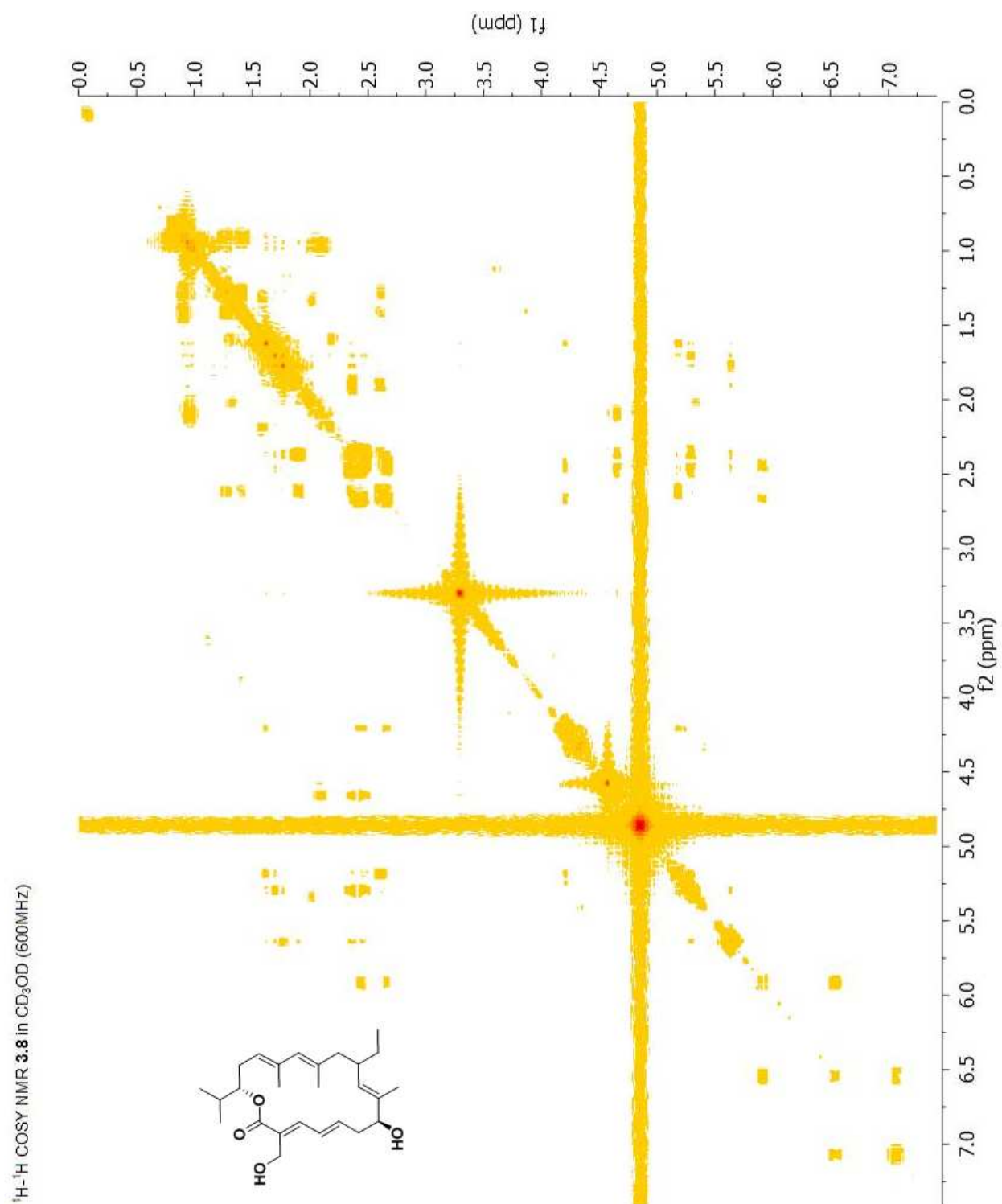
NMR data for **3.5**

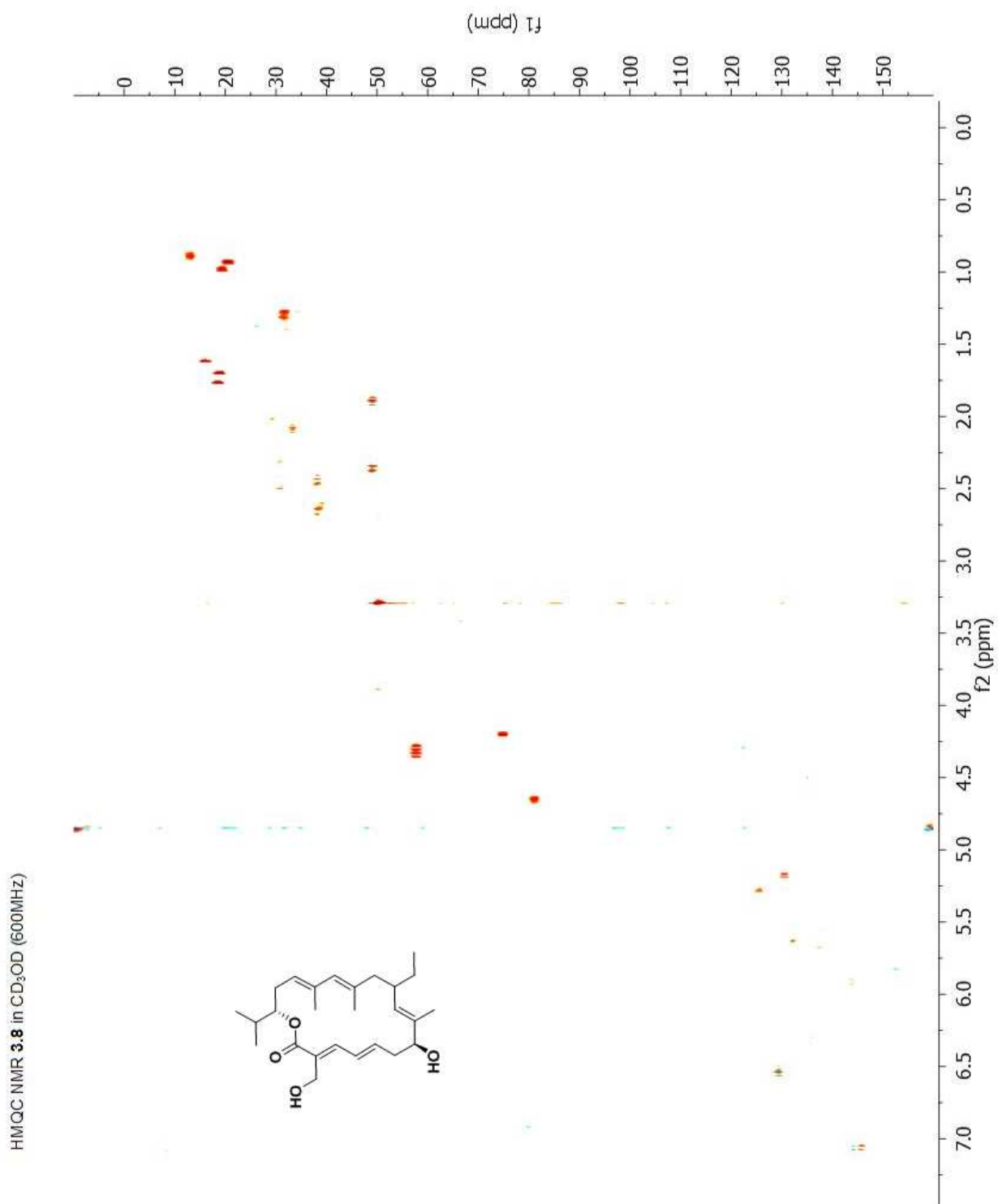




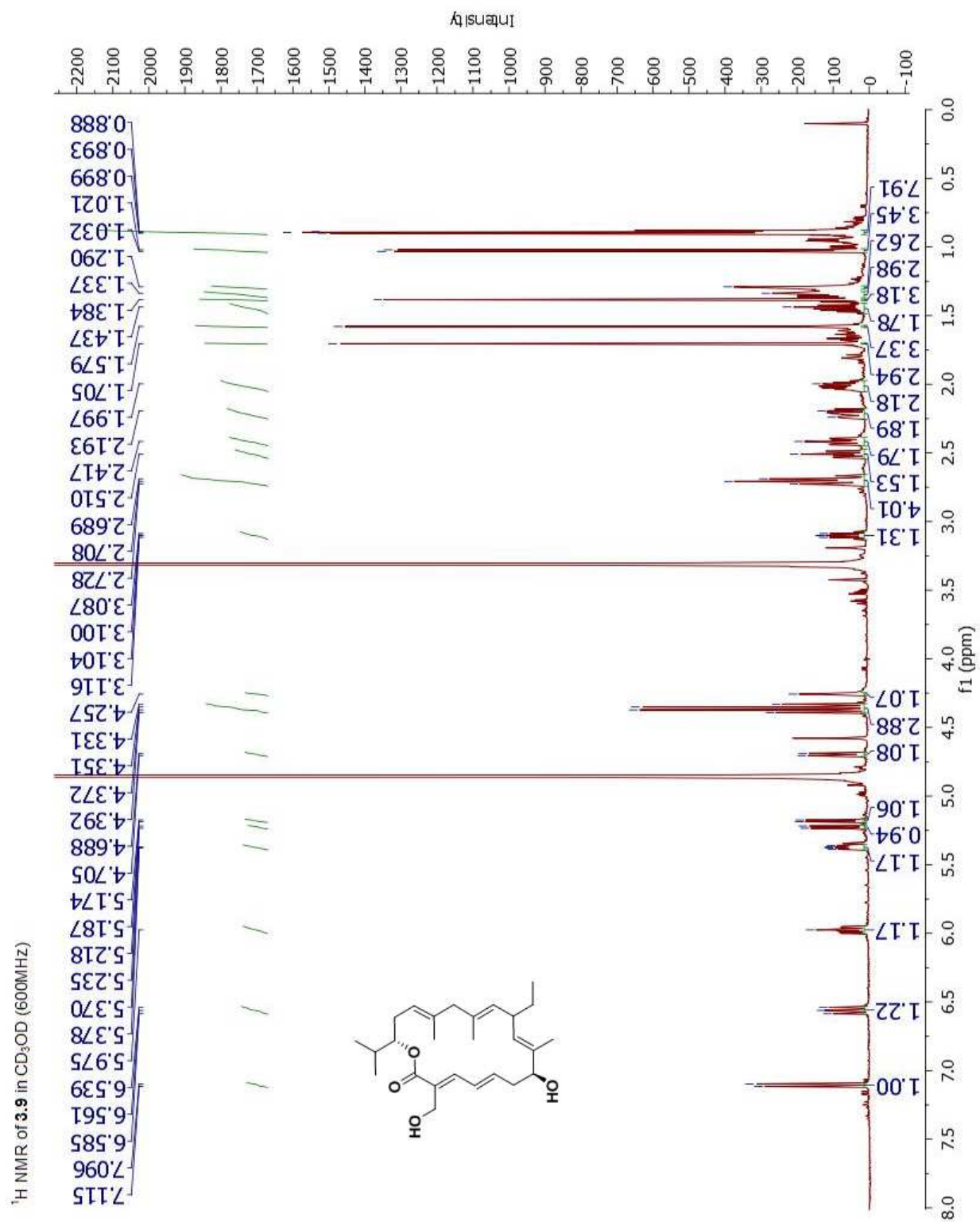


NMR data for **3.8**

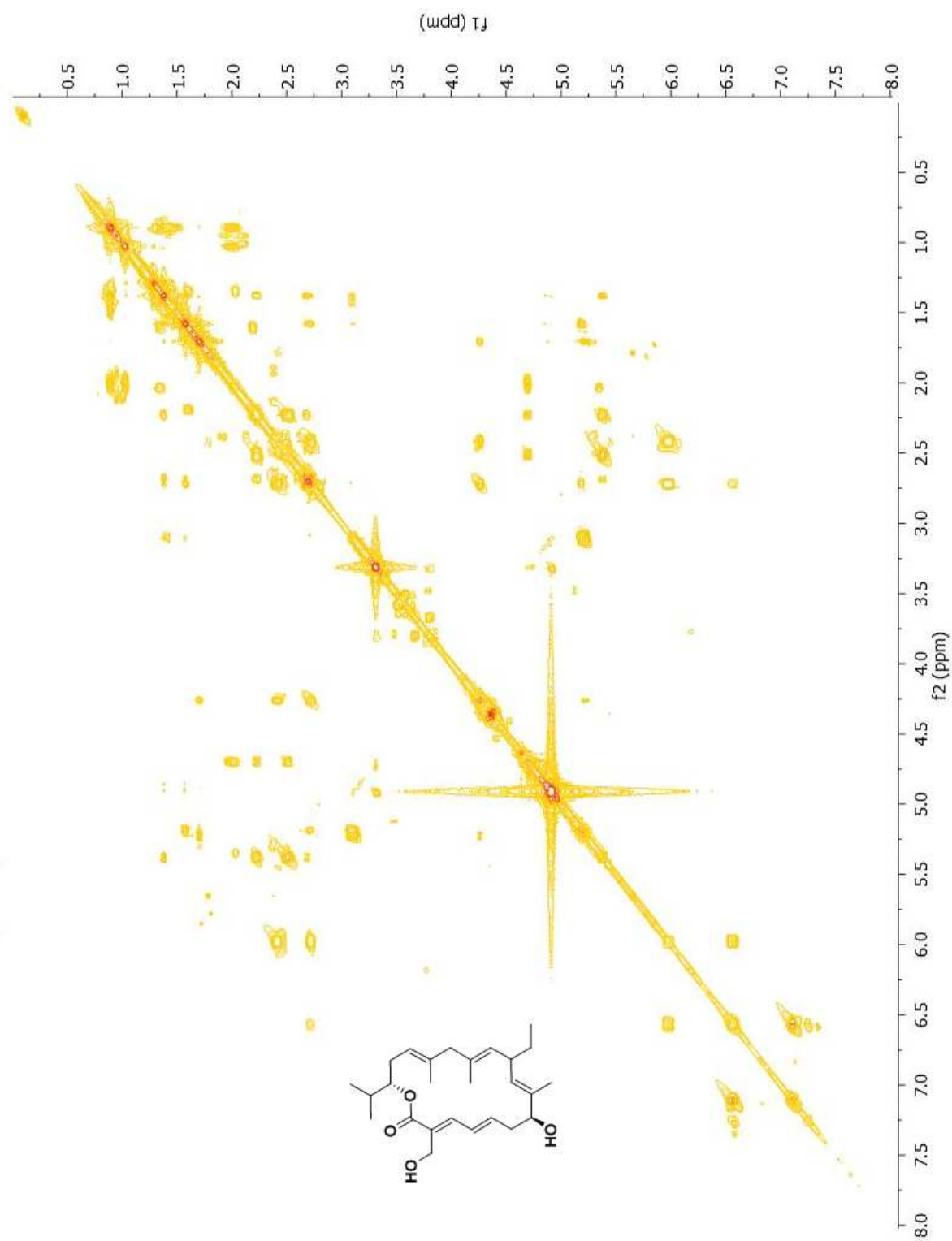


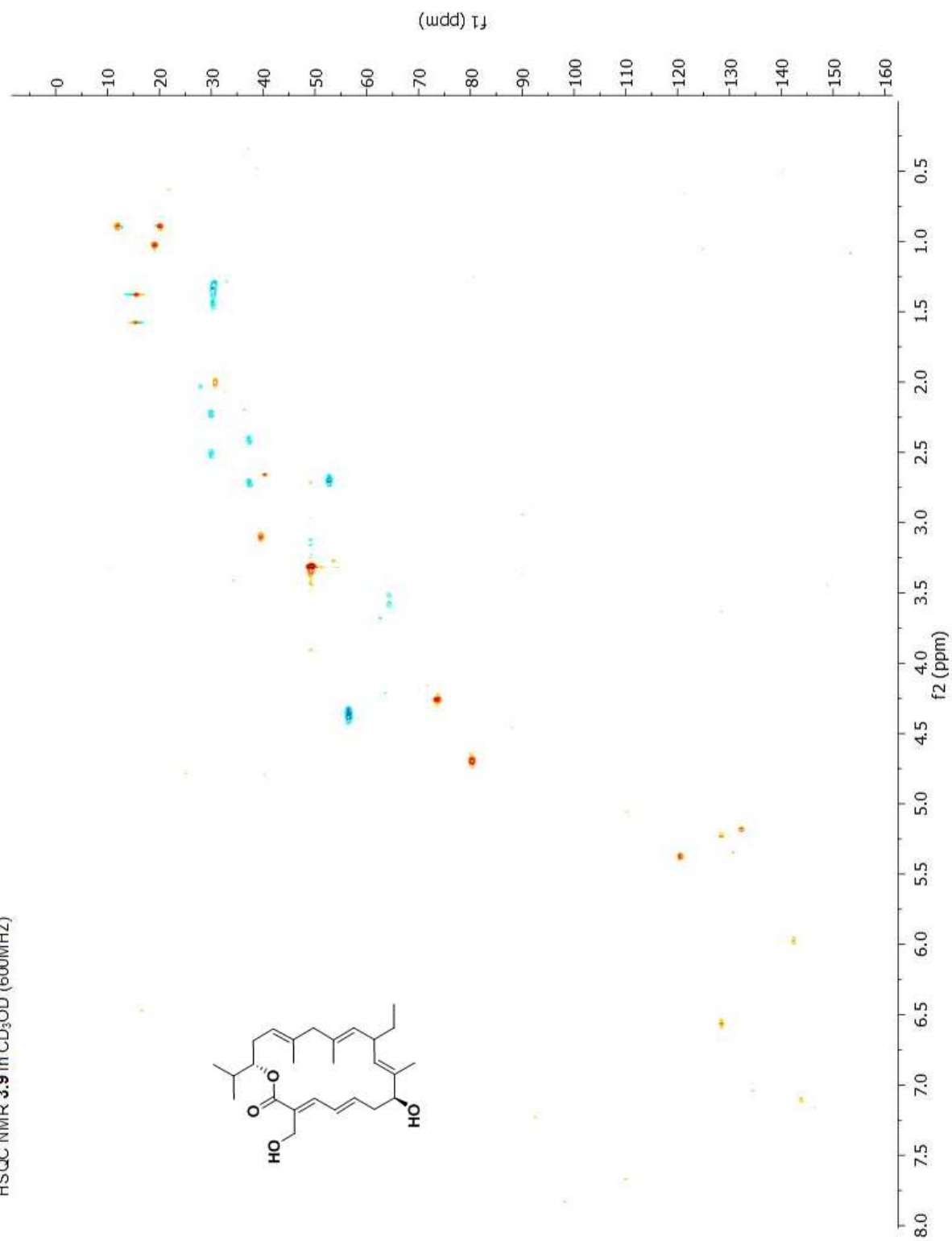


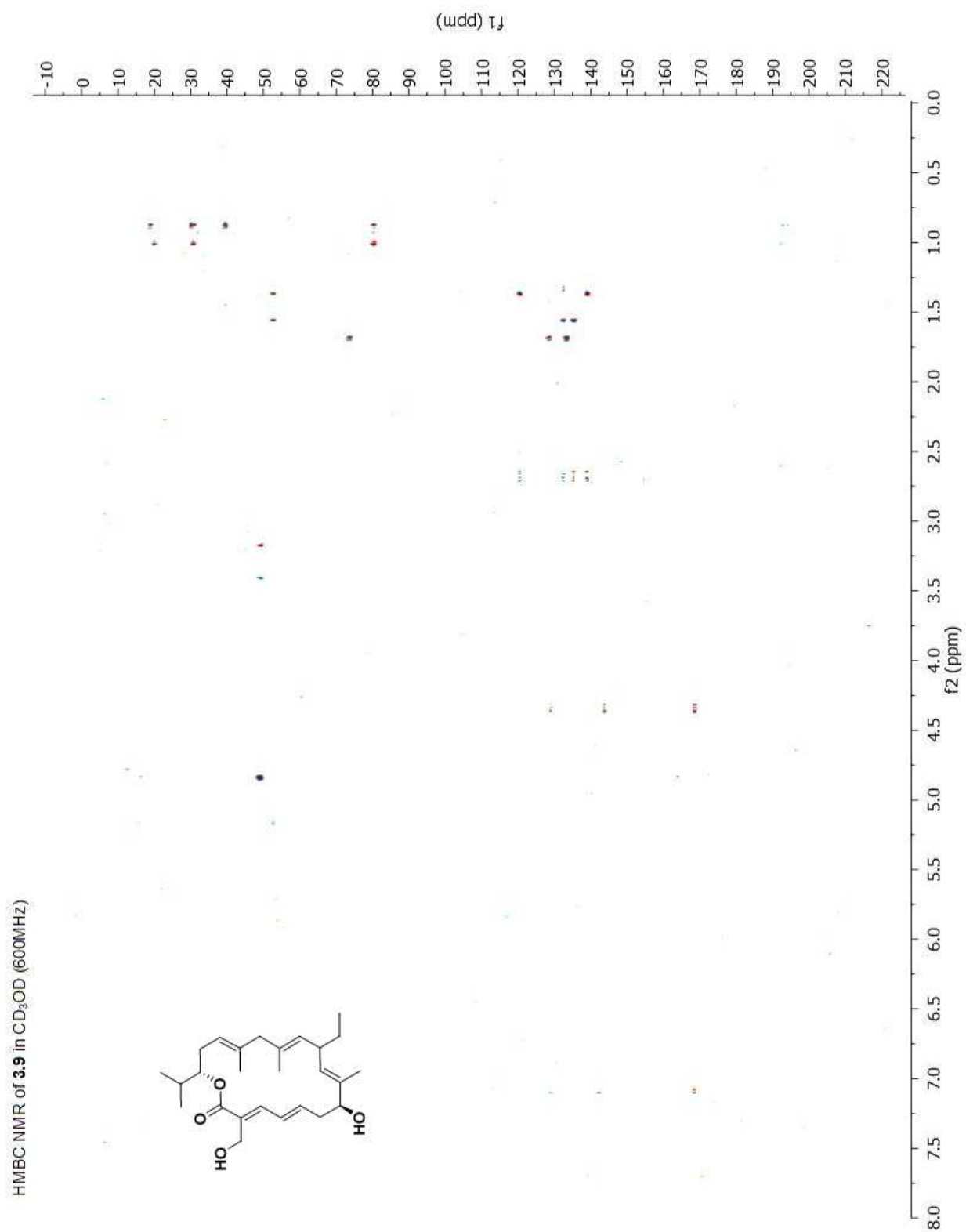


NMR data for **3.9**

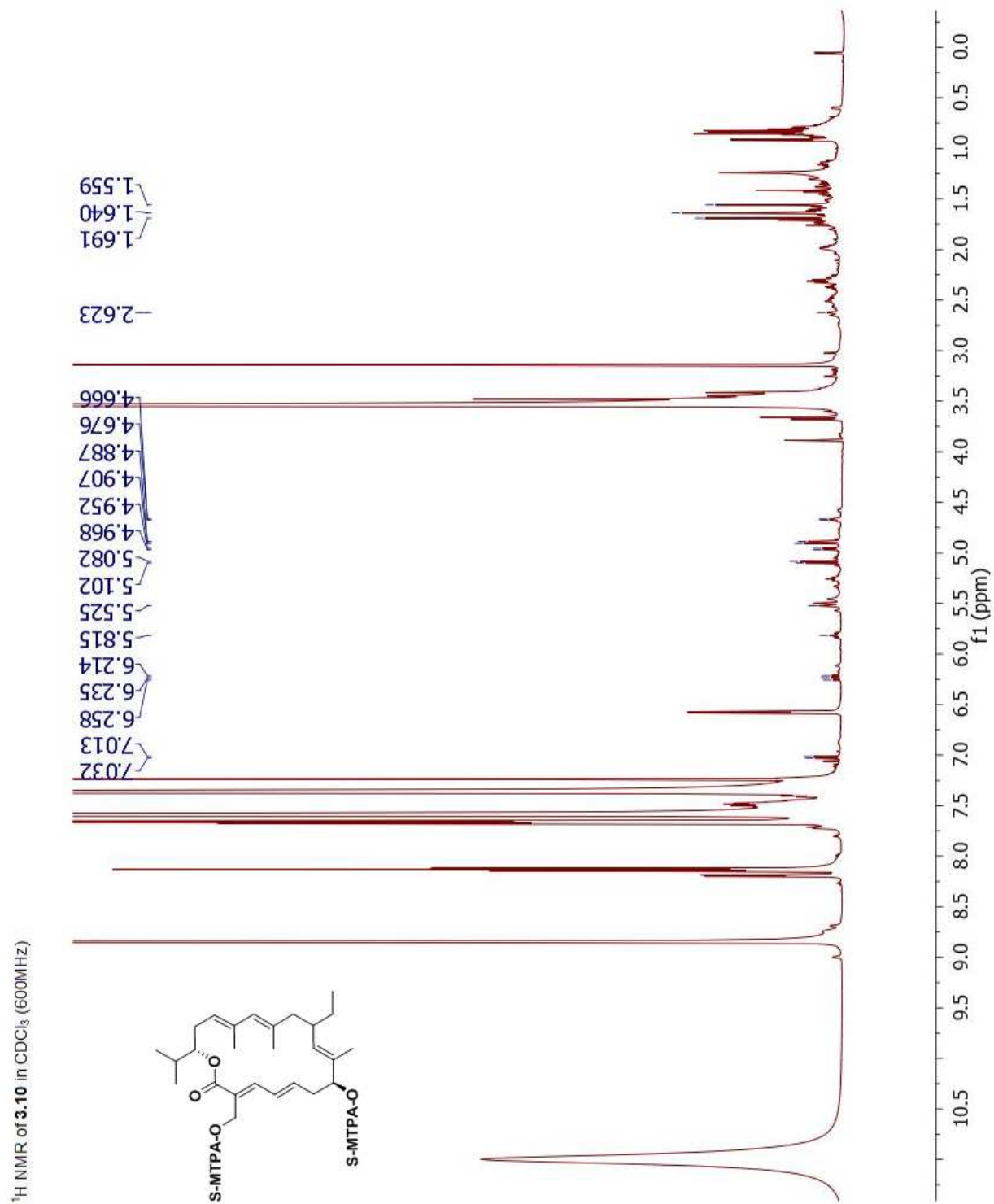
$^1\text{H}$ - $^1\text{H}$  COSY NMR **3.9** in  $\text{CD}_3\text{OD}$  (600MHz)



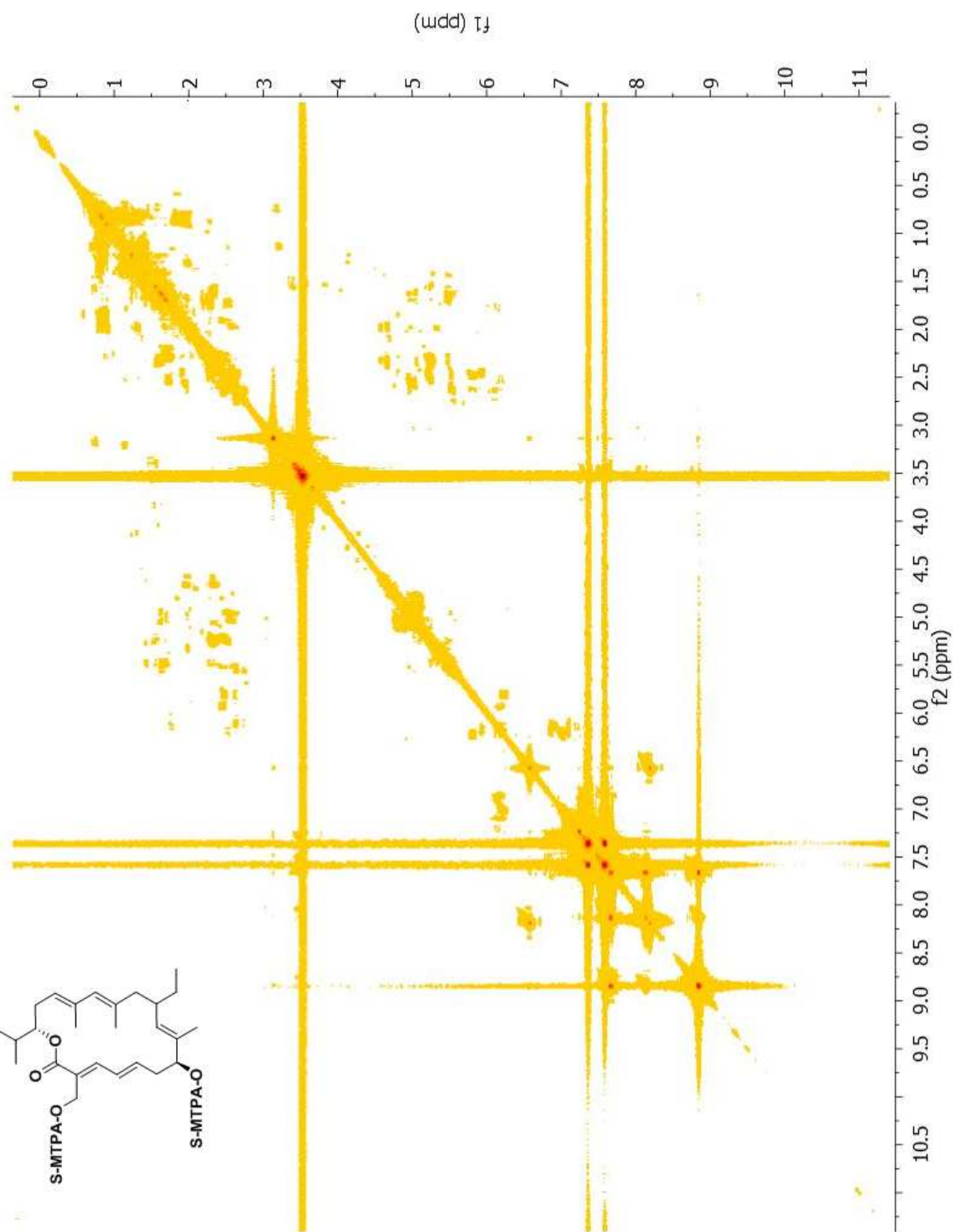
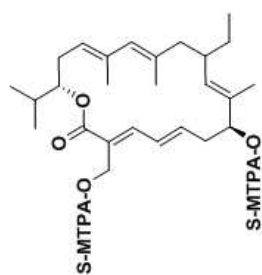


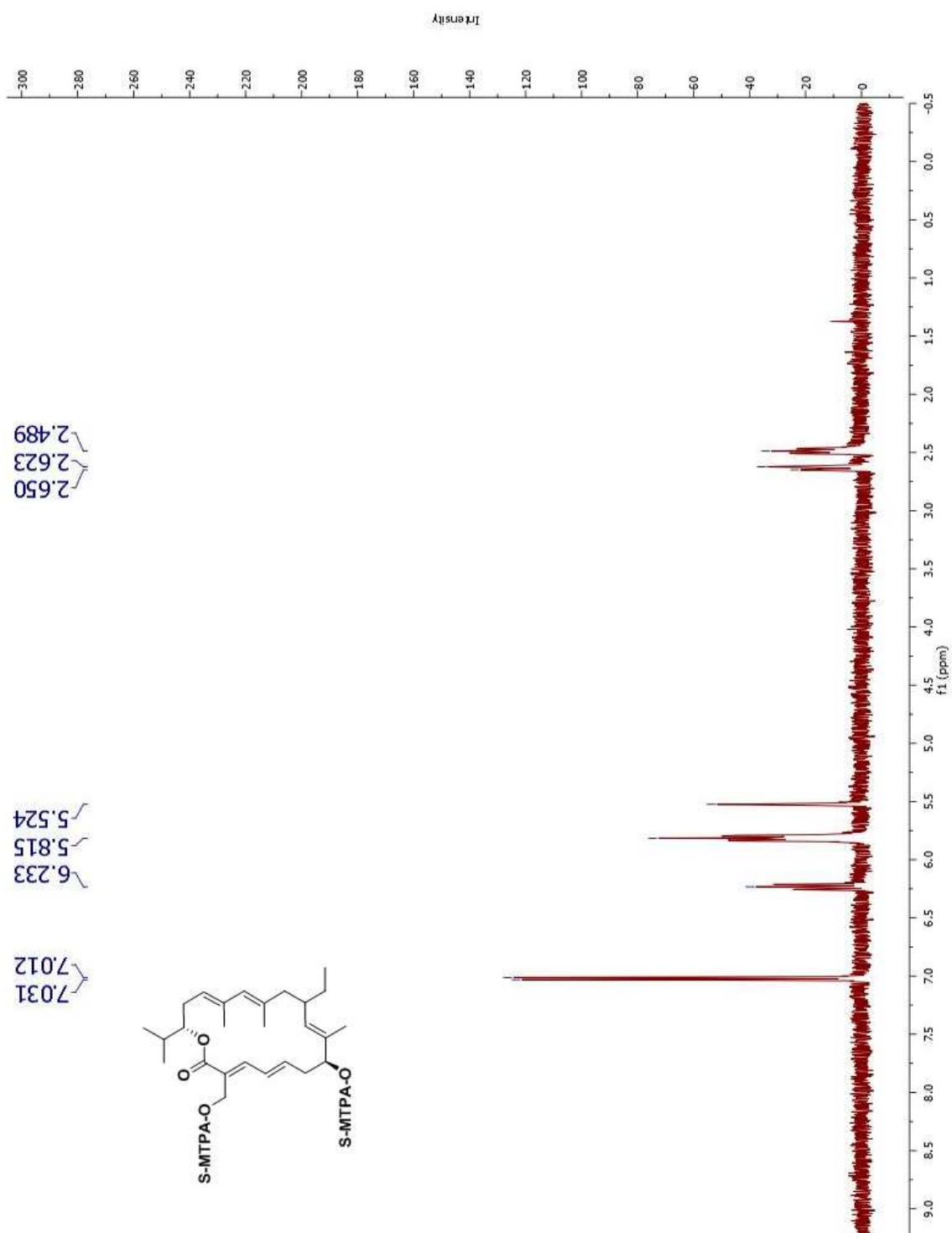


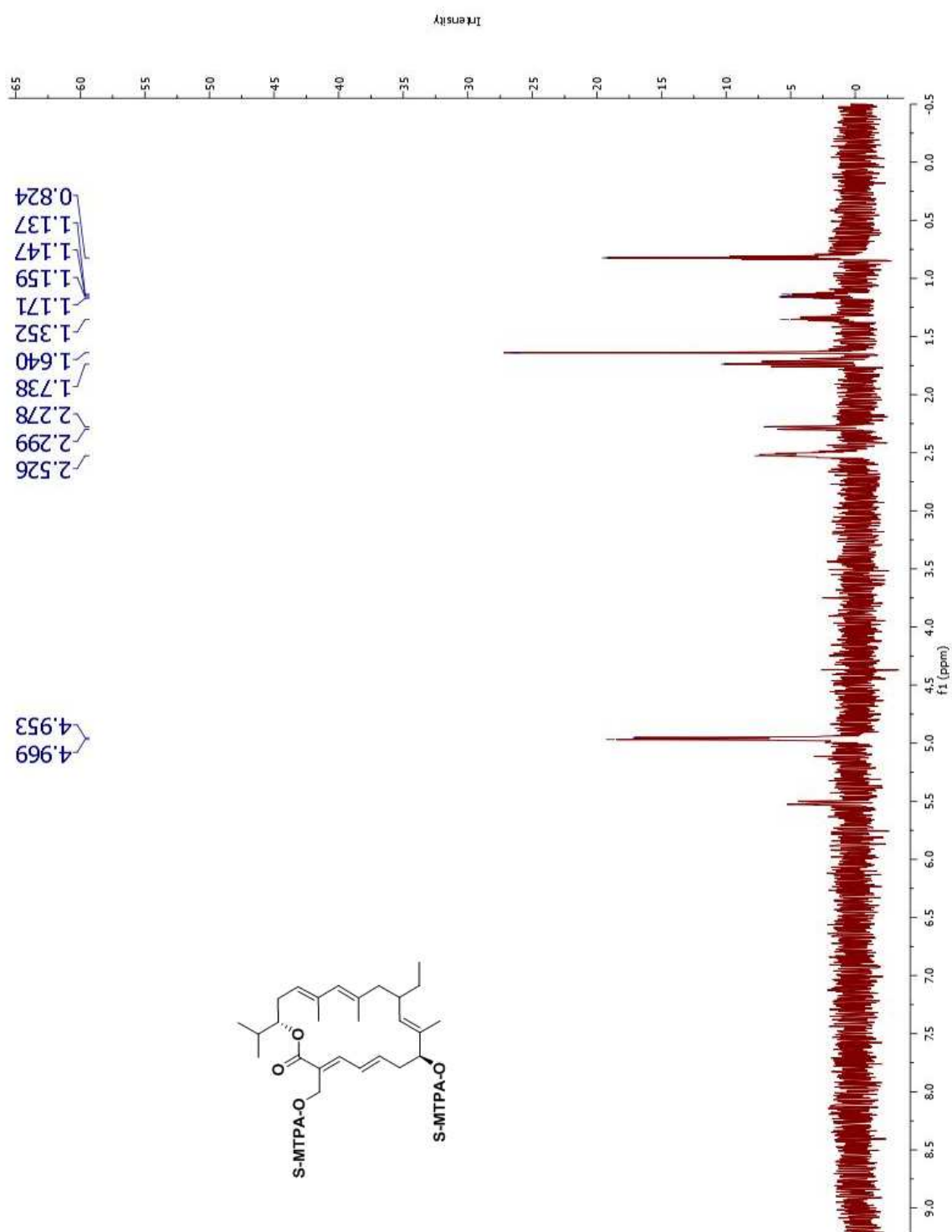
NMR data for **3.10**



$^1\text{H}$ - $^1\text{H}$  COSY NMR **3.10** in  $\text{CDCl}_3$  (600MHz)

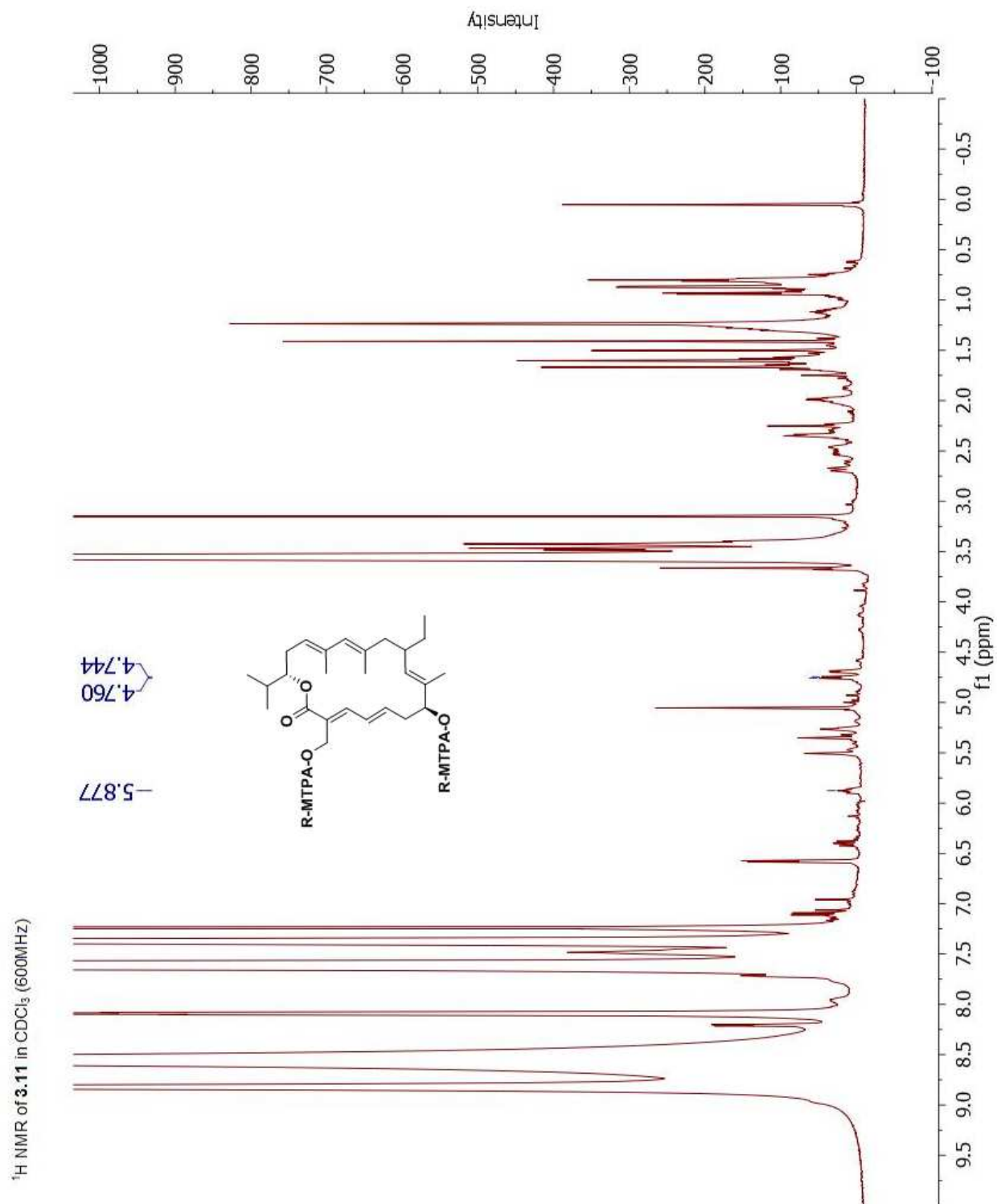


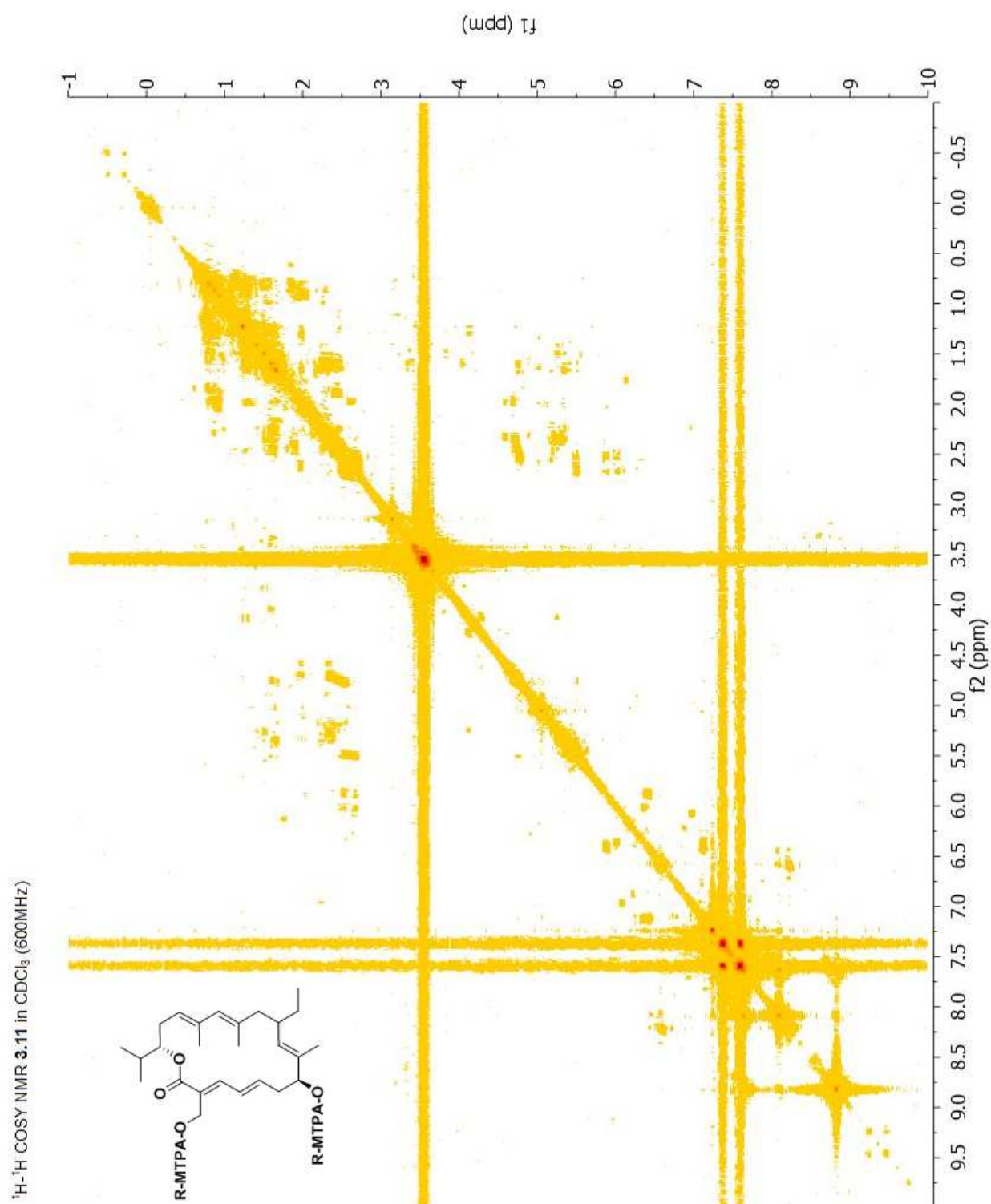


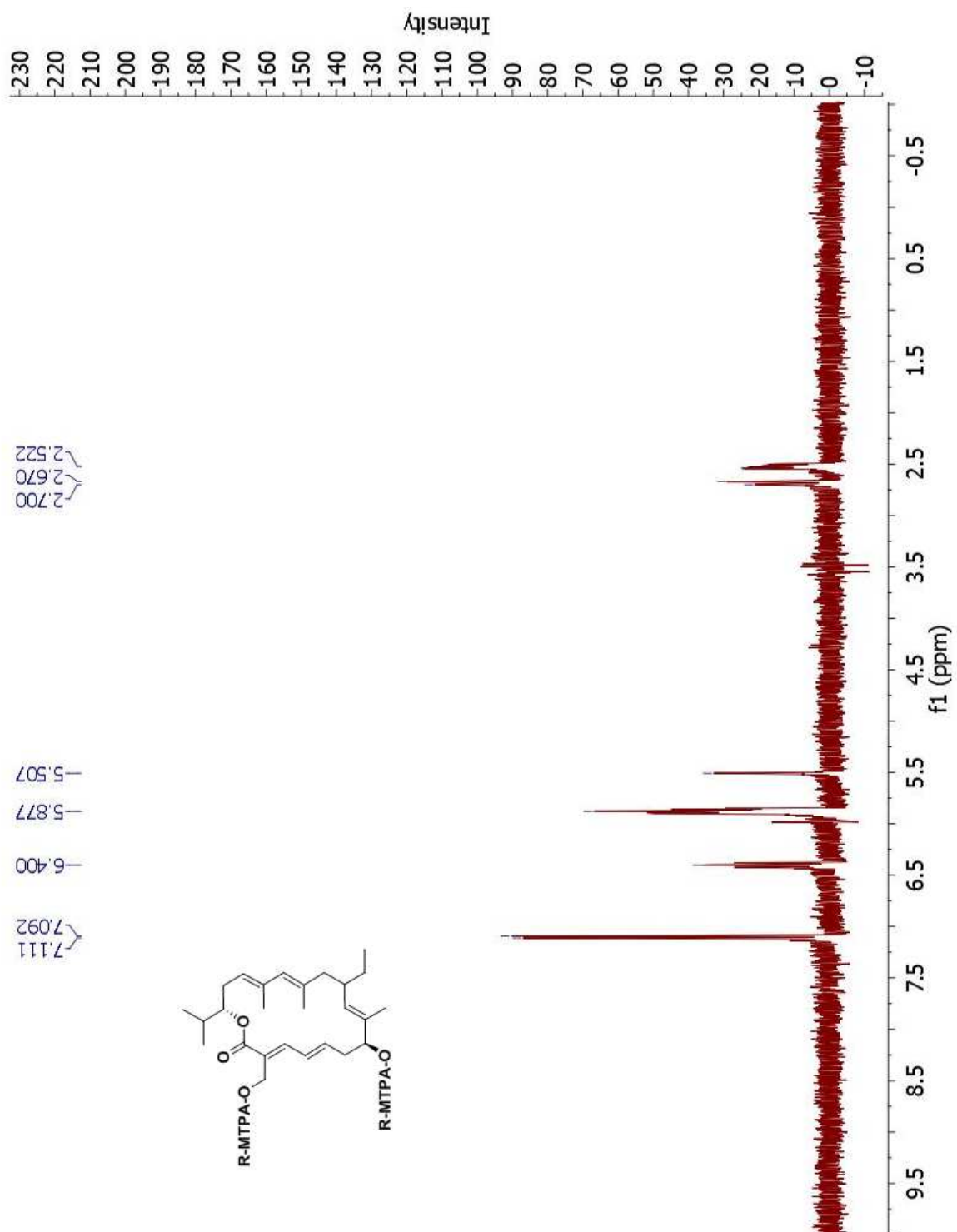


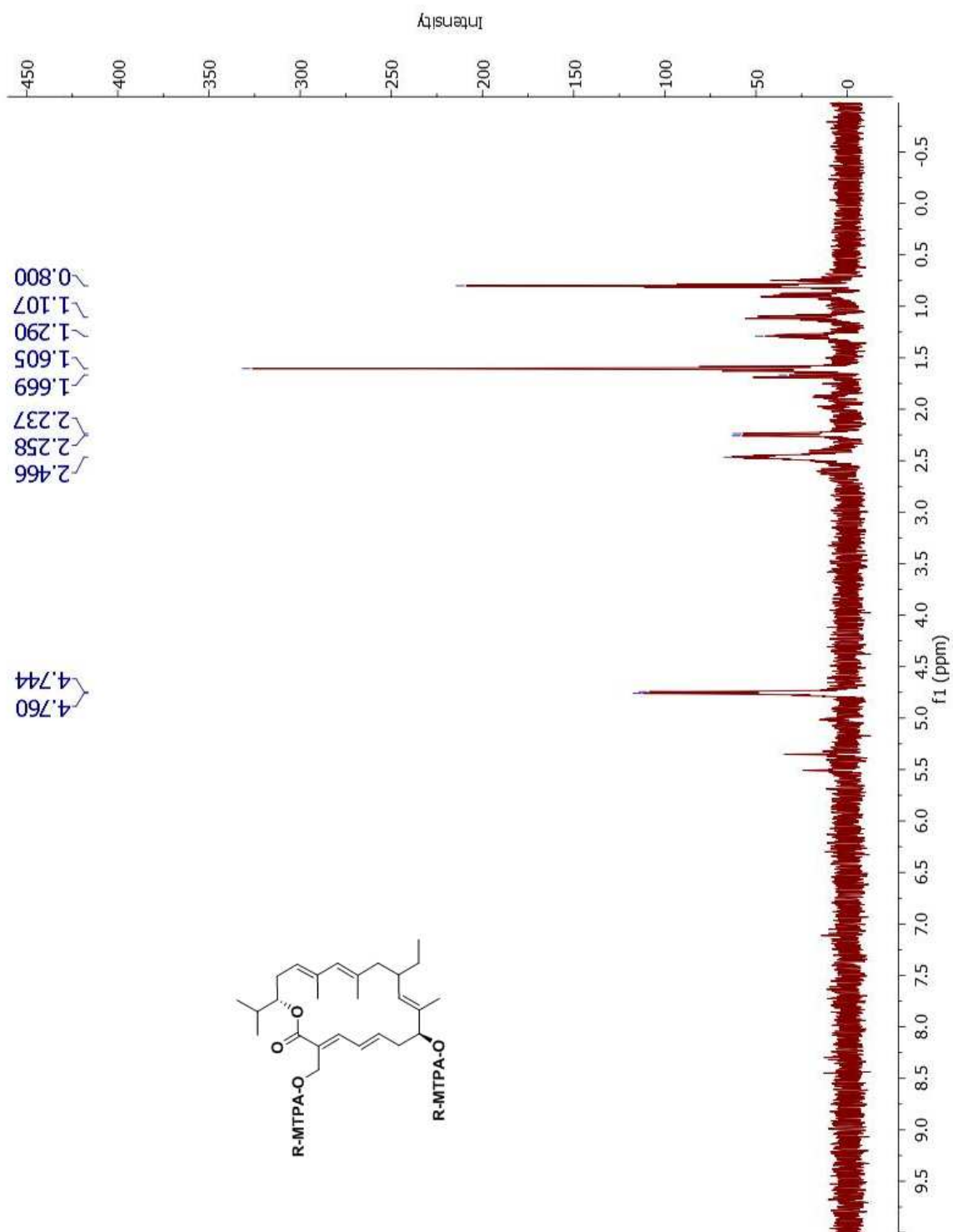


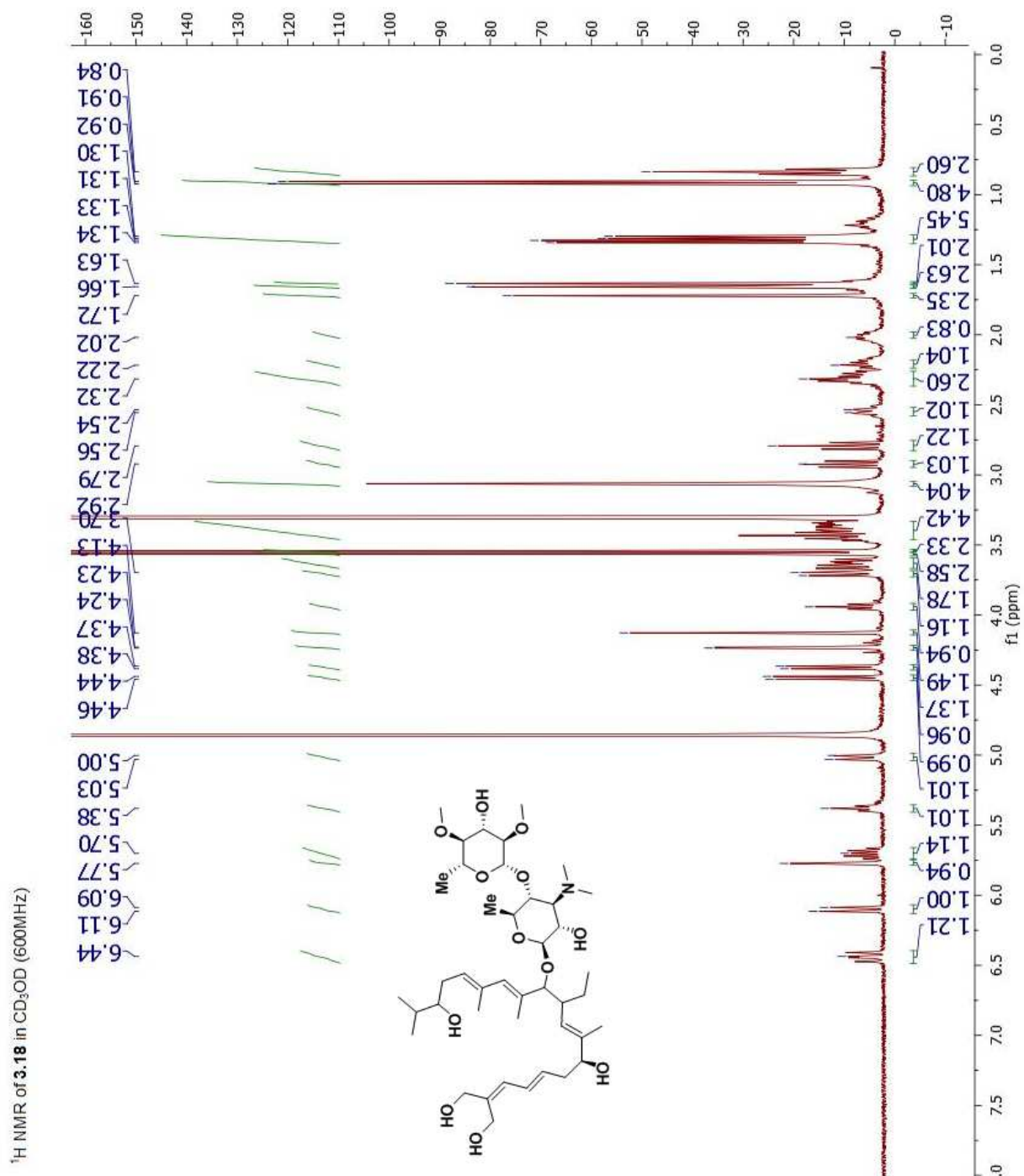
NMR data for **3.11**

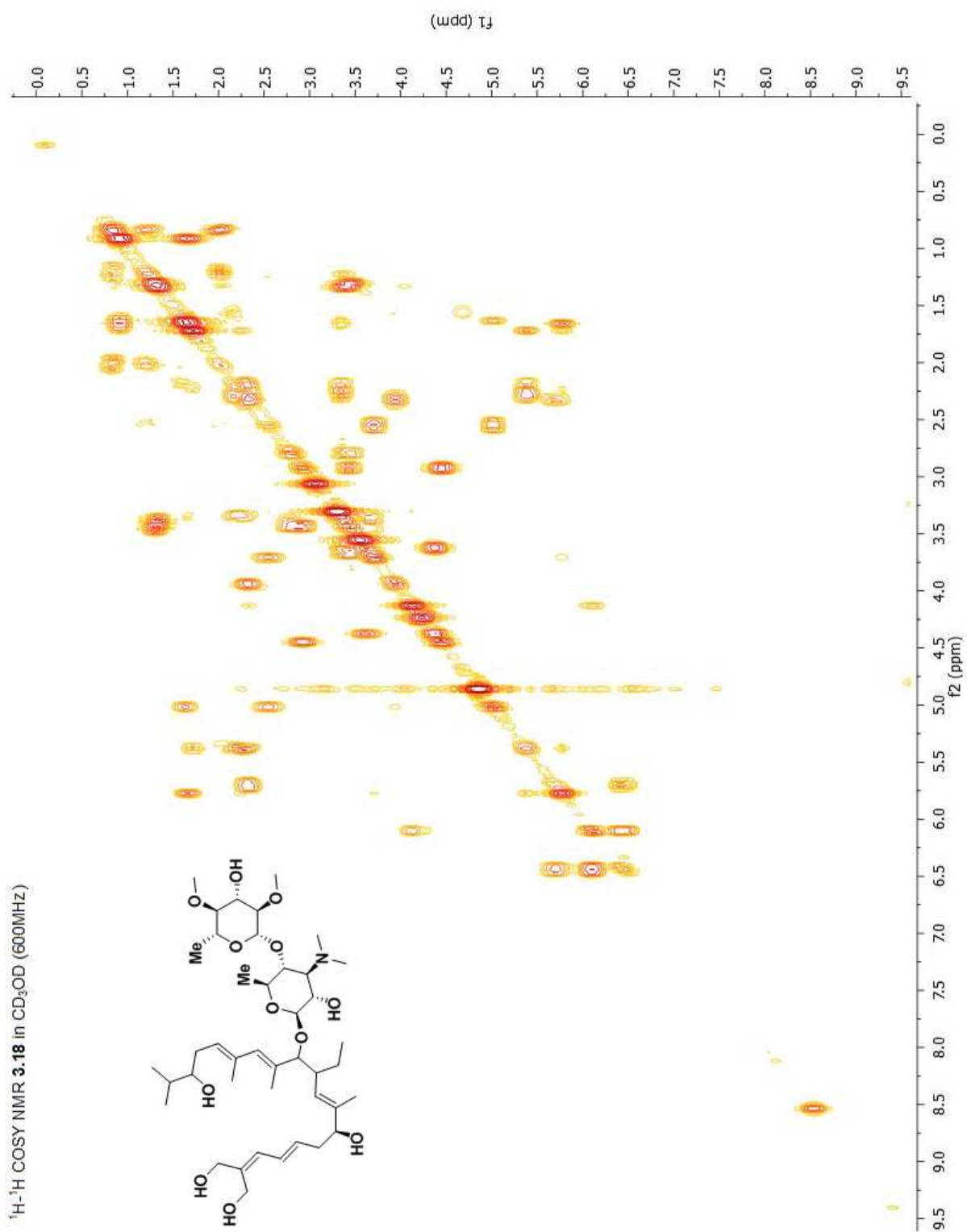


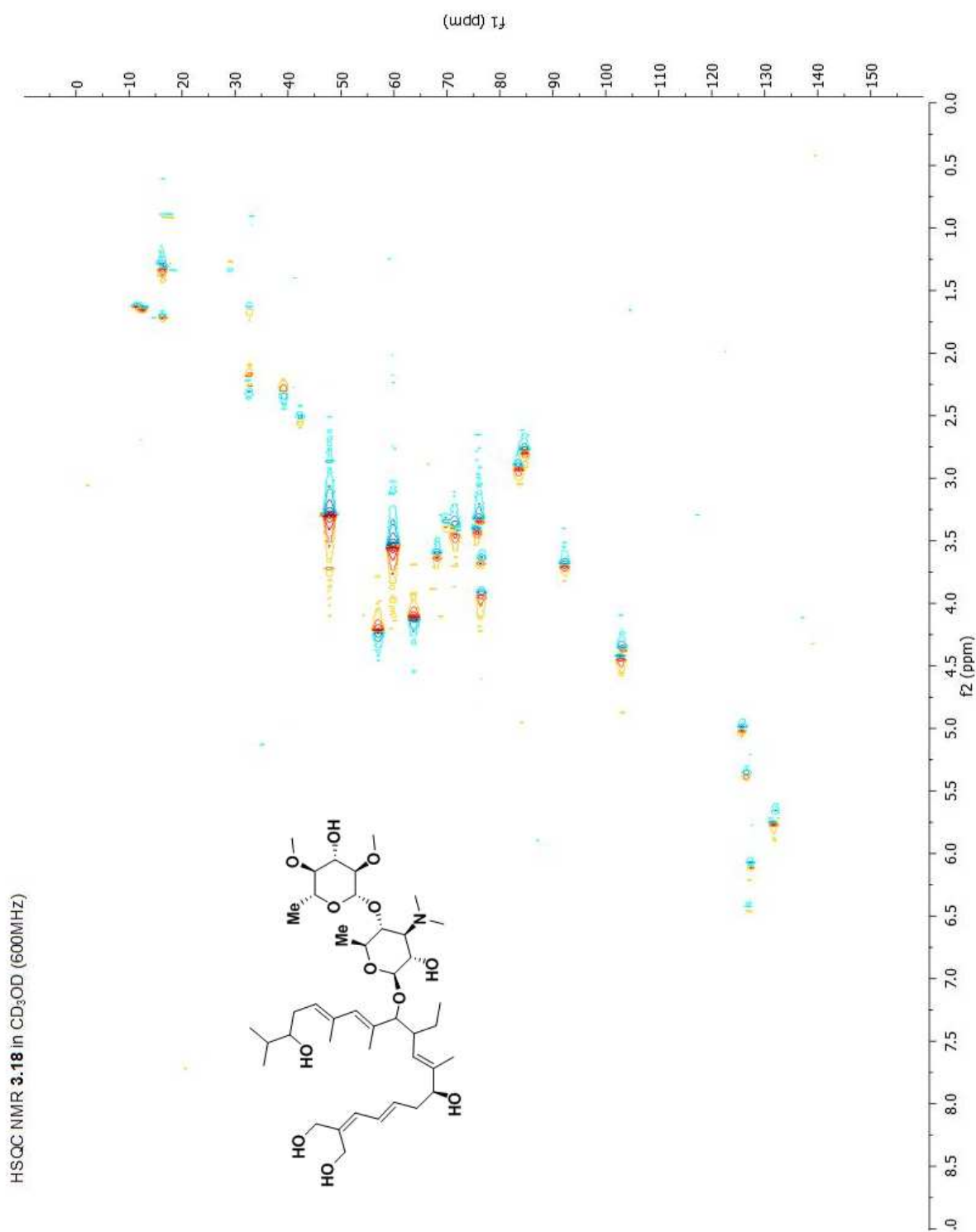




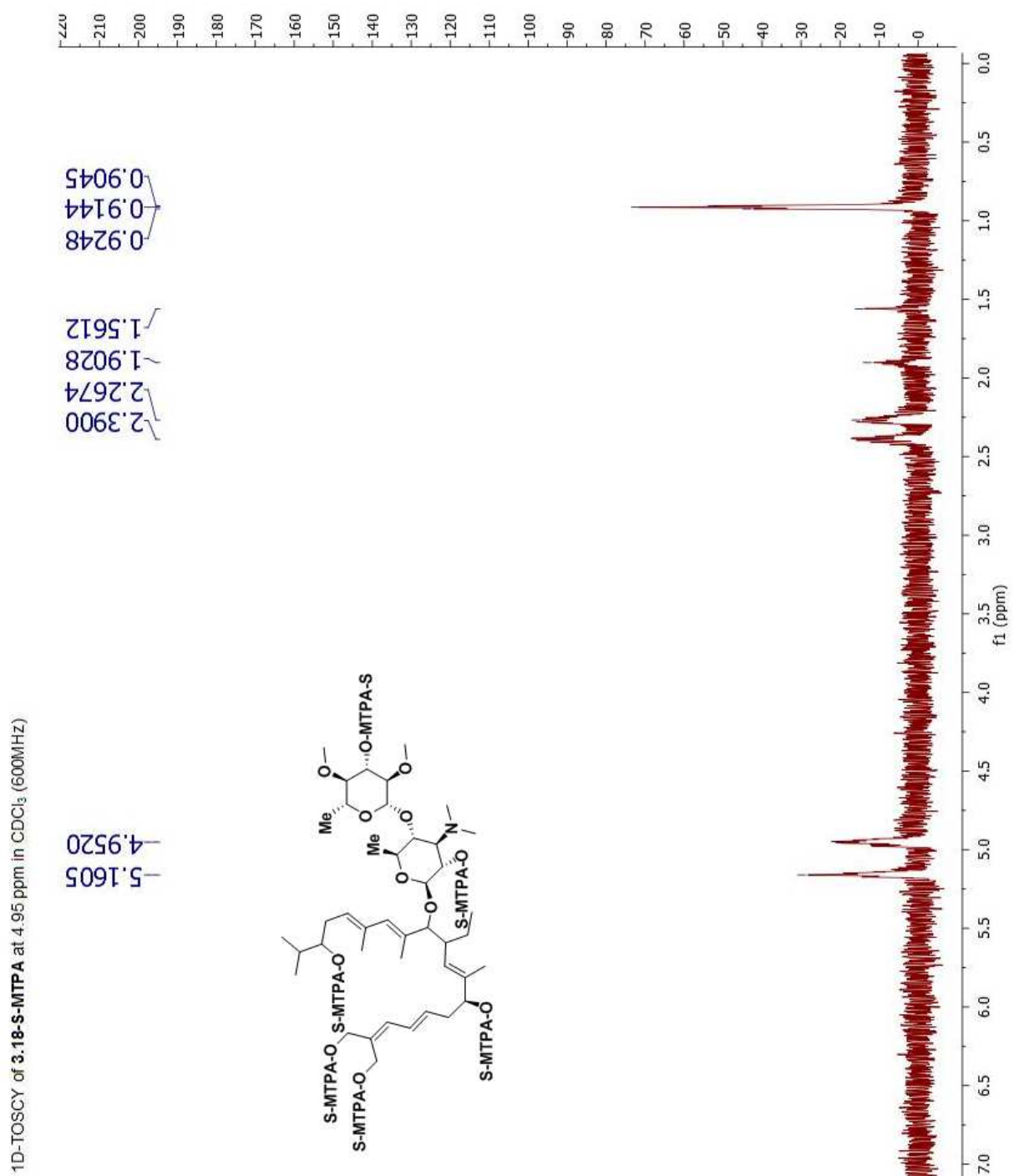
1D-TOSY of **3.11** at 4.75 ppm in CDCl<sub>3</sub> (600MHz)

NMR data for **3.18**



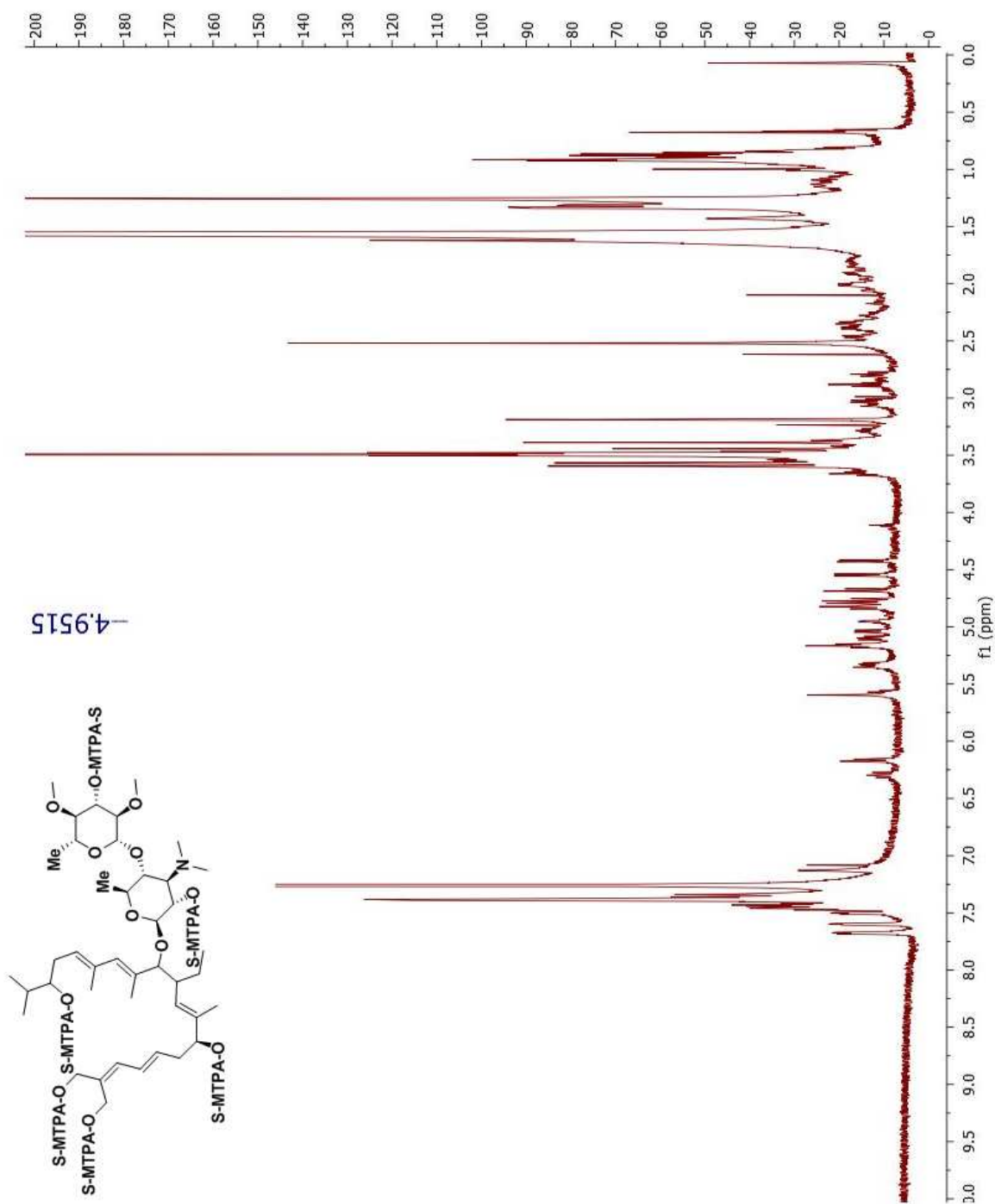


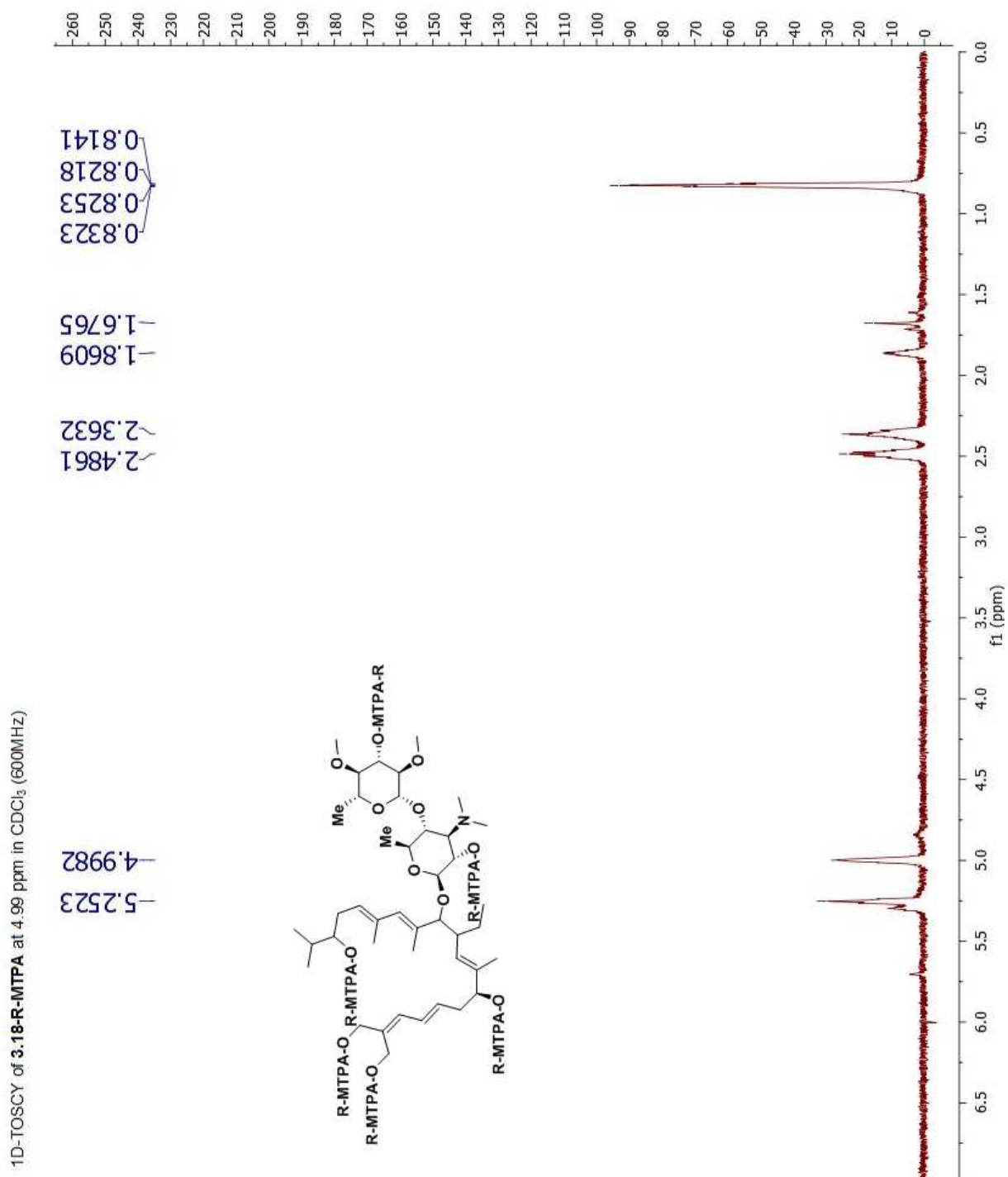


NMR data for **3.18 S-MTPA**

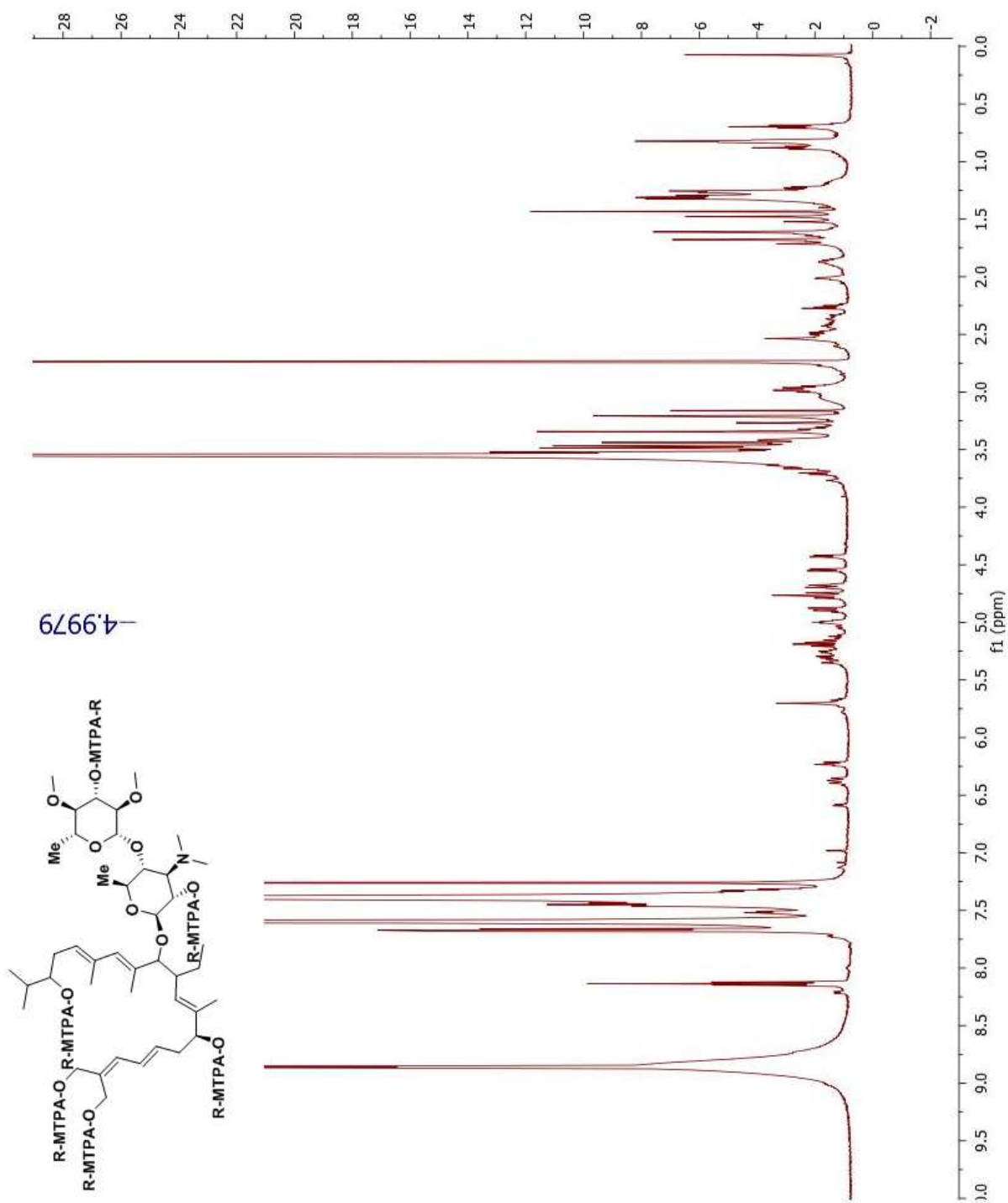


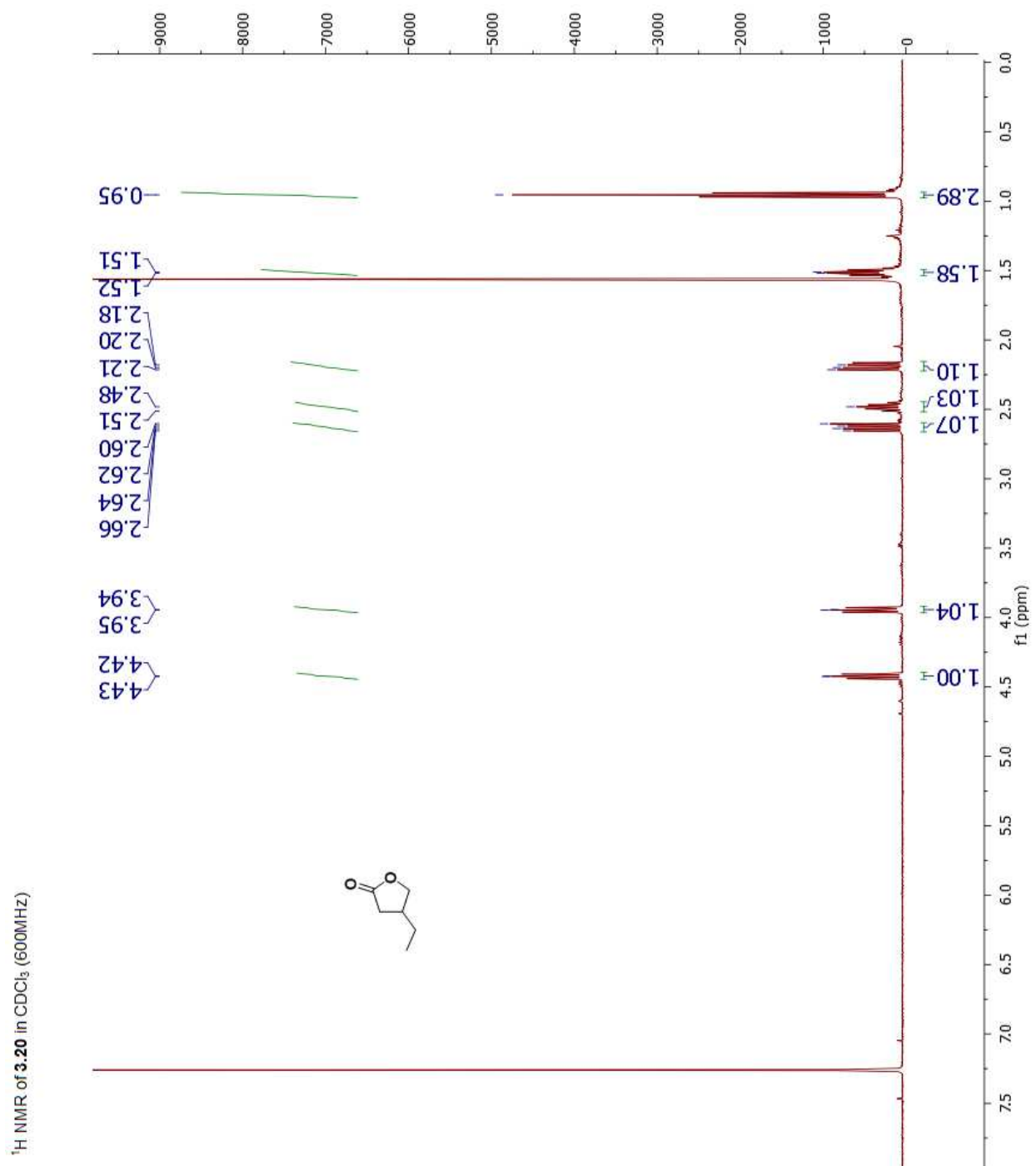
$^1\text{H}$  NMR of **3.18-S-MTPA** in  $\text{CDCl}_3$  (600MHz)

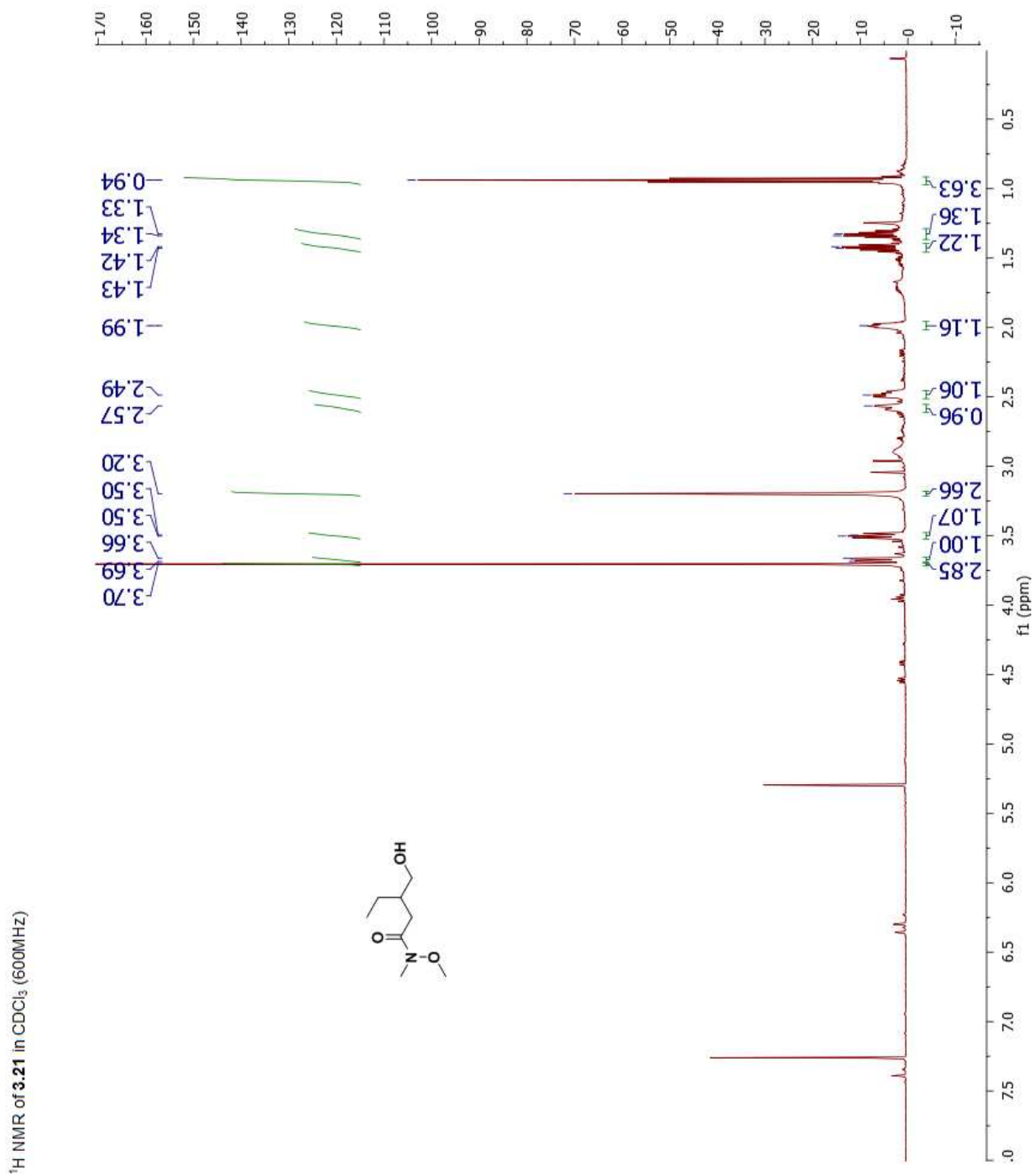


NMR data for **3.18 R-MTPA**

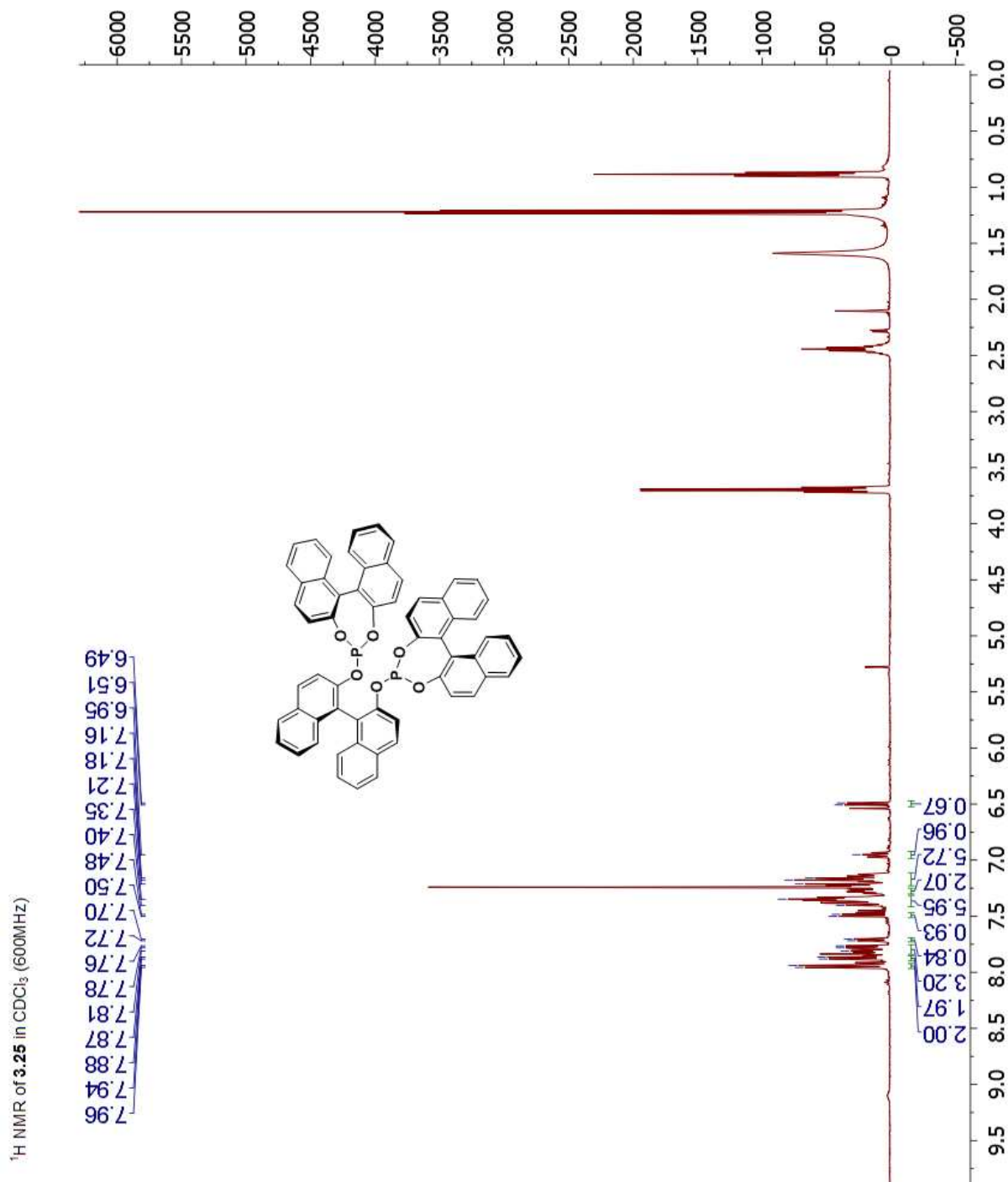
$^1\text{H}$  NMR of **3.18-R-MTPA** in  $\text{CDCl}_3$  (600MHz)



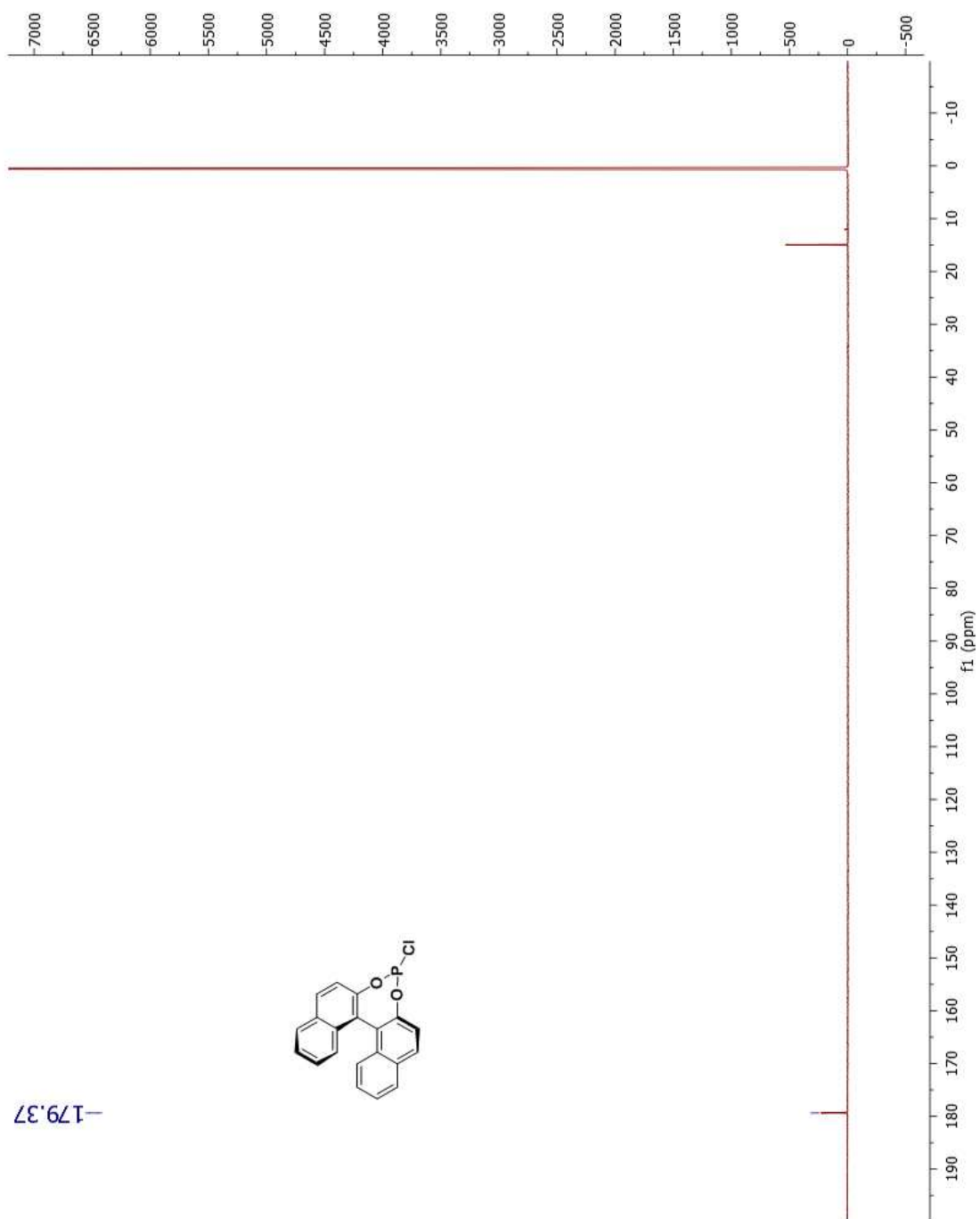
NMR data for **3.20**

NMR data for **3.21**

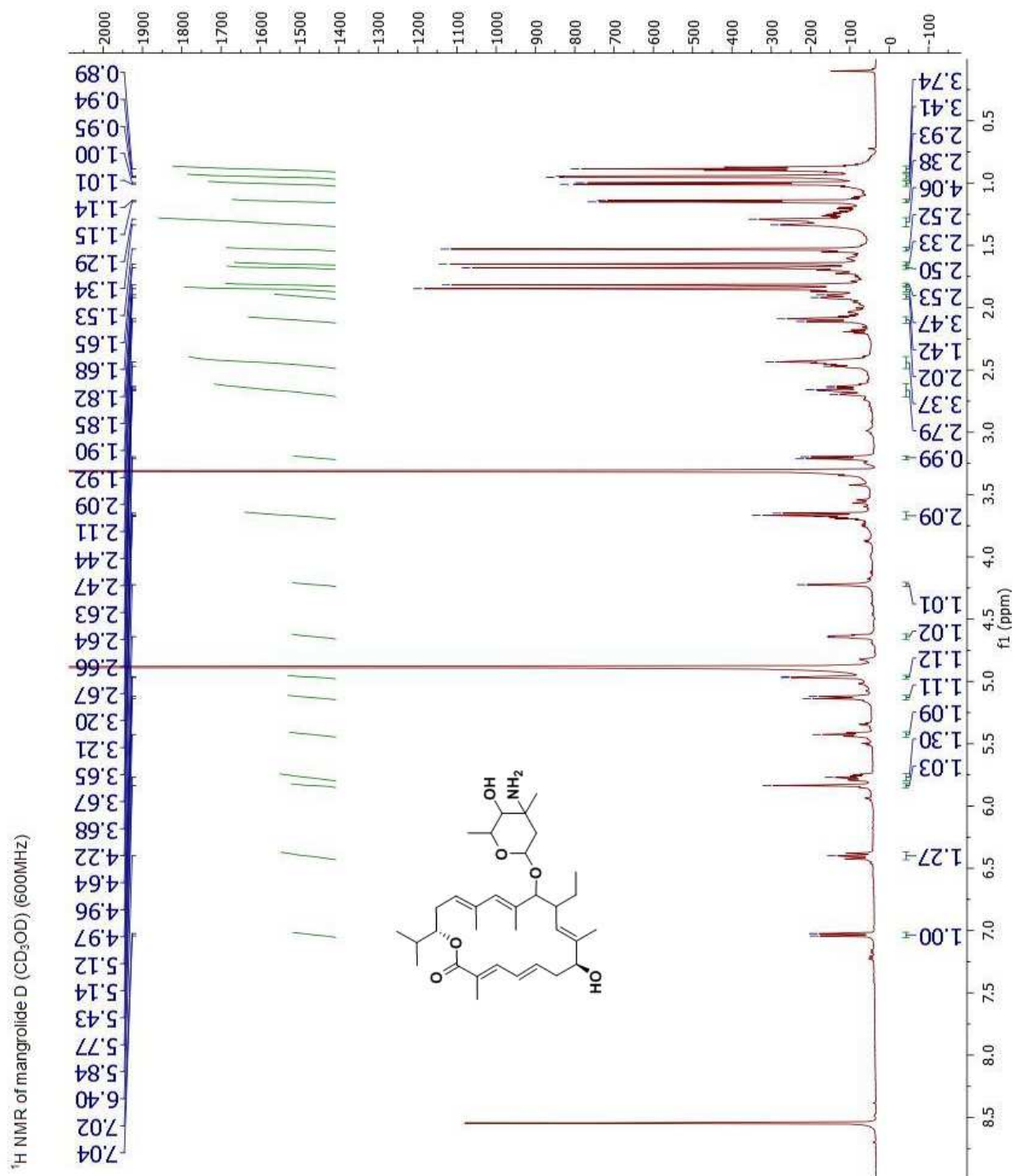
NMR data for **3.25**



$^{31}\text{P}$  NMR of S-BINAP-PCl ( $\text{CDCl}_3$ ) (500MHz)

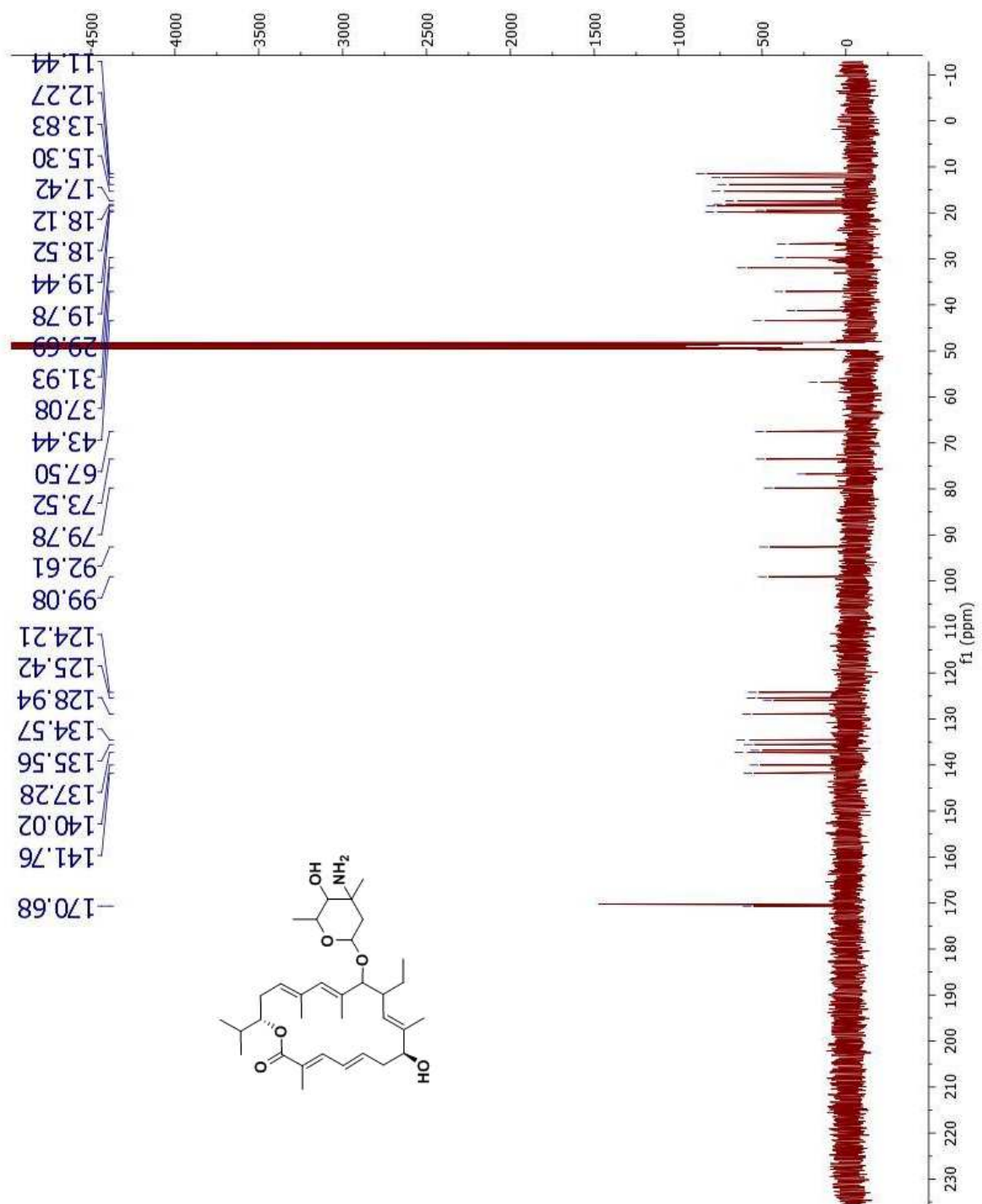


## NMR data for Mangrolide D

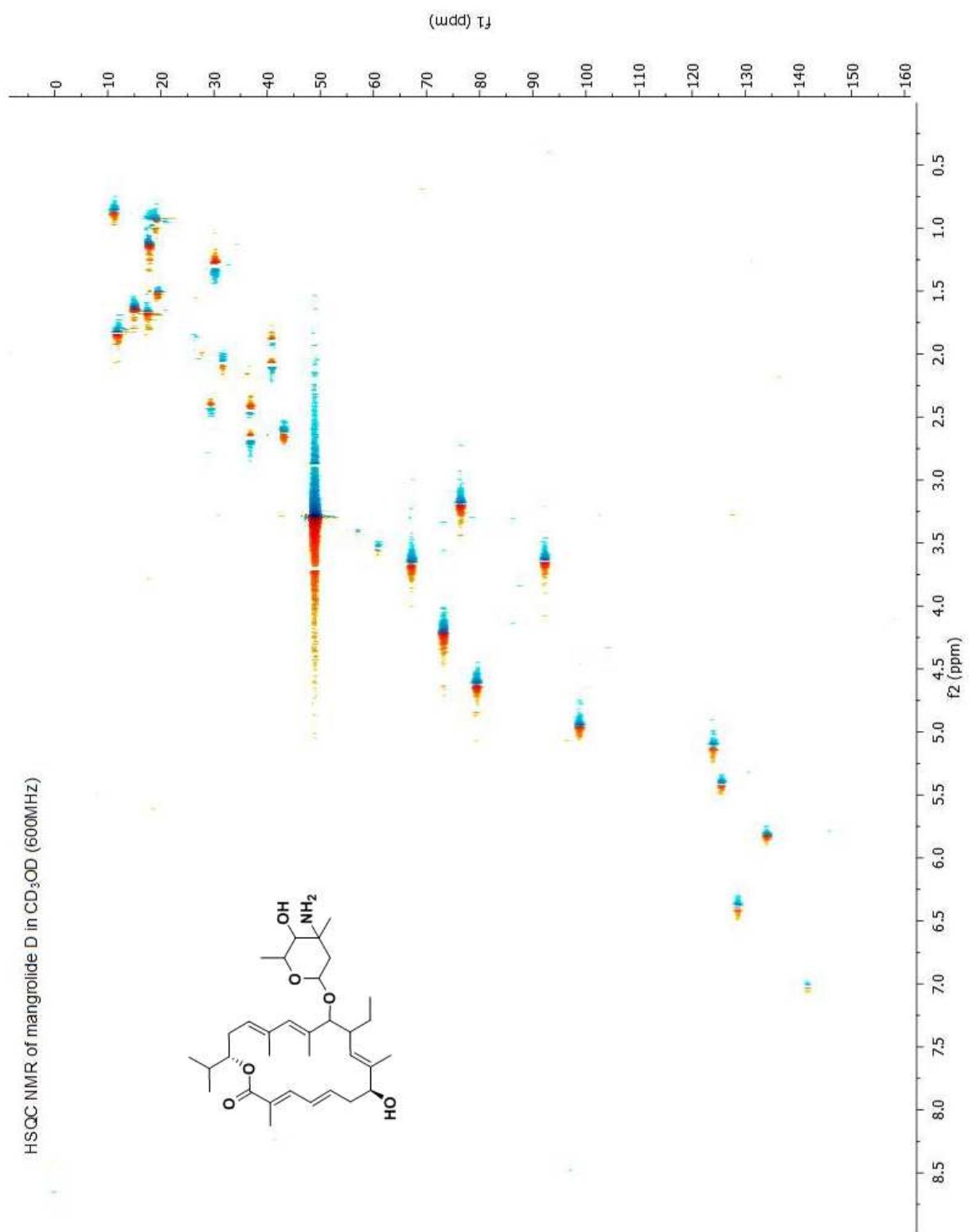


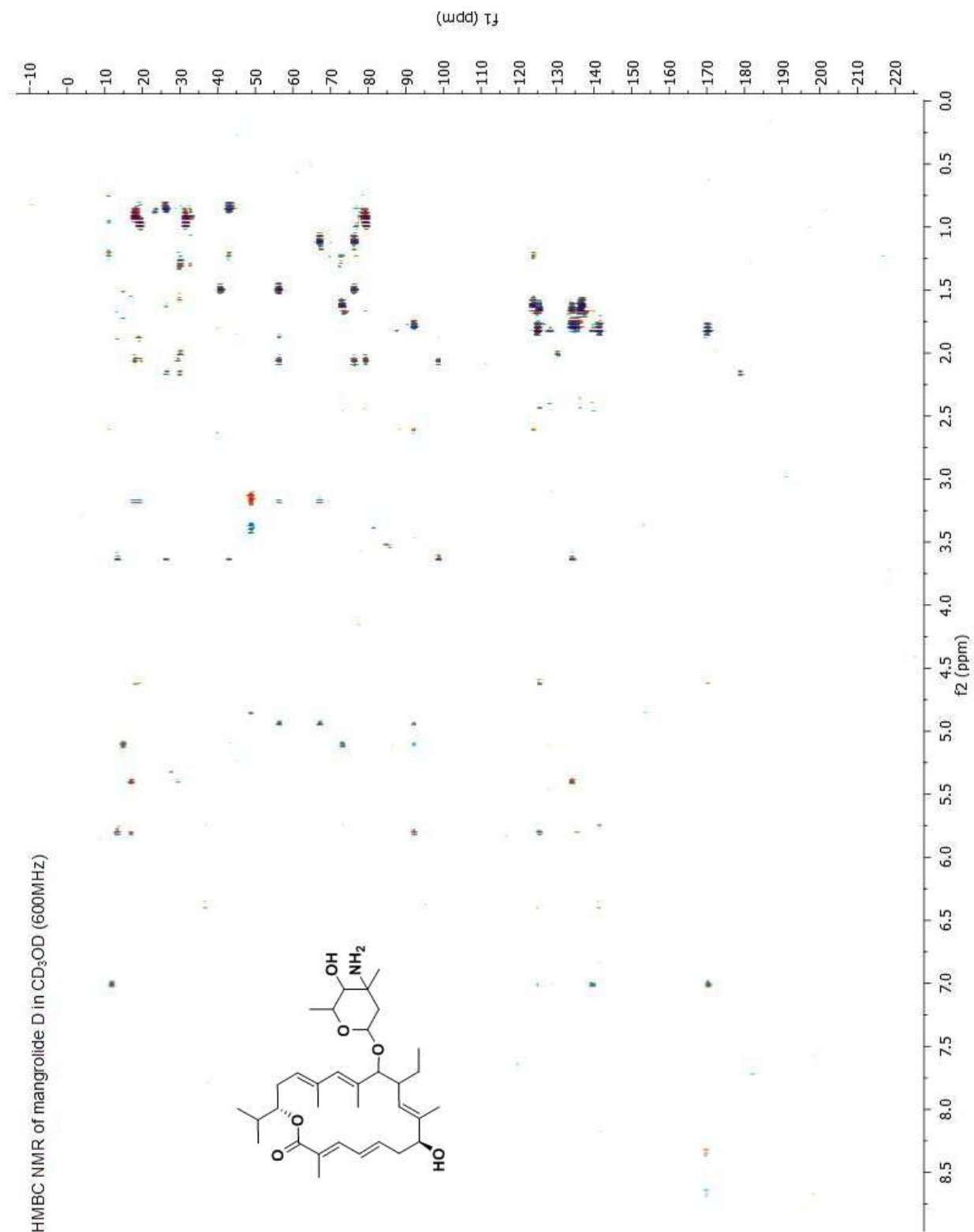


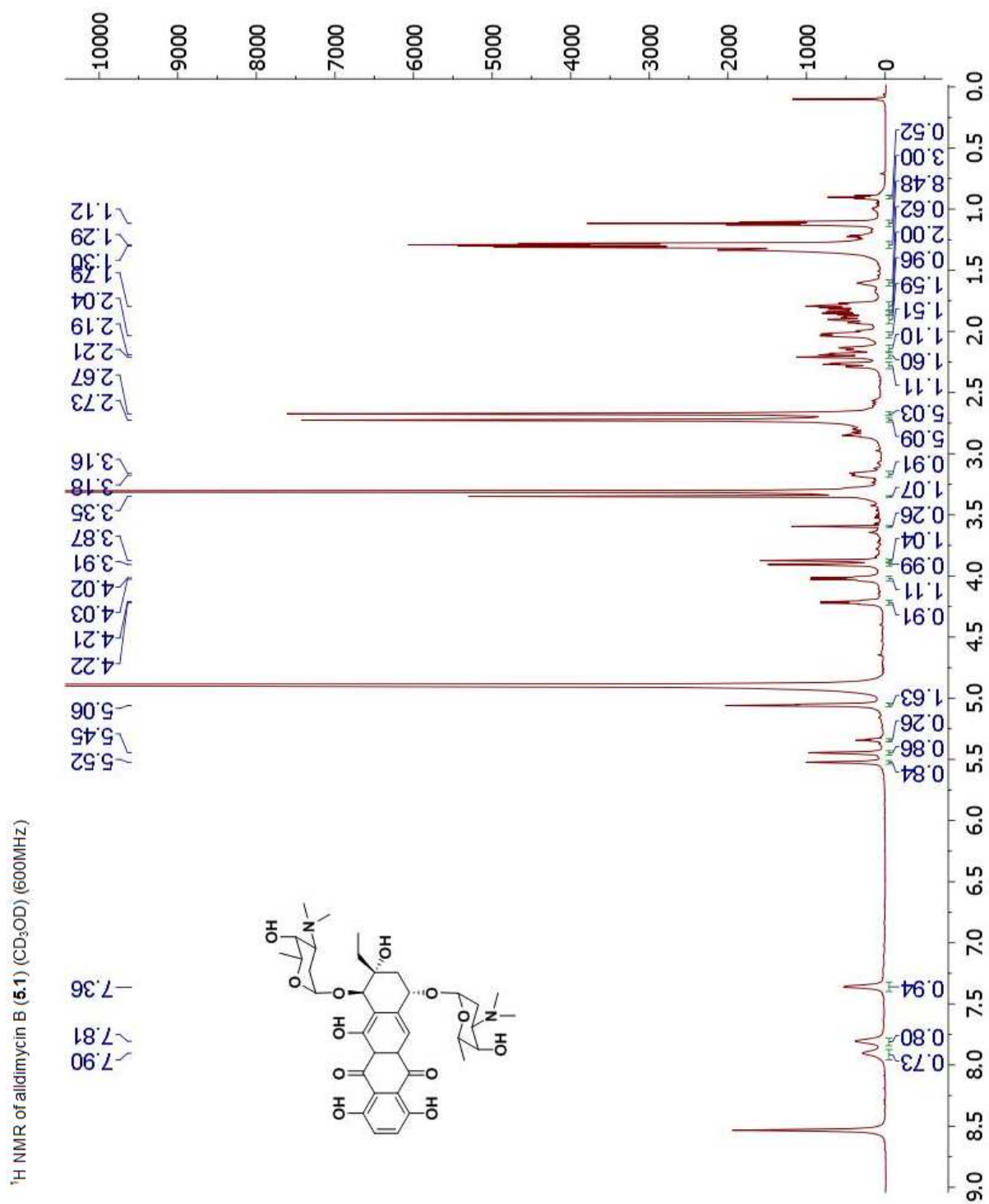
<sup>13</sup>C NMR of mangrolide D in CD<sub>3</sub>OD (125 MHz)

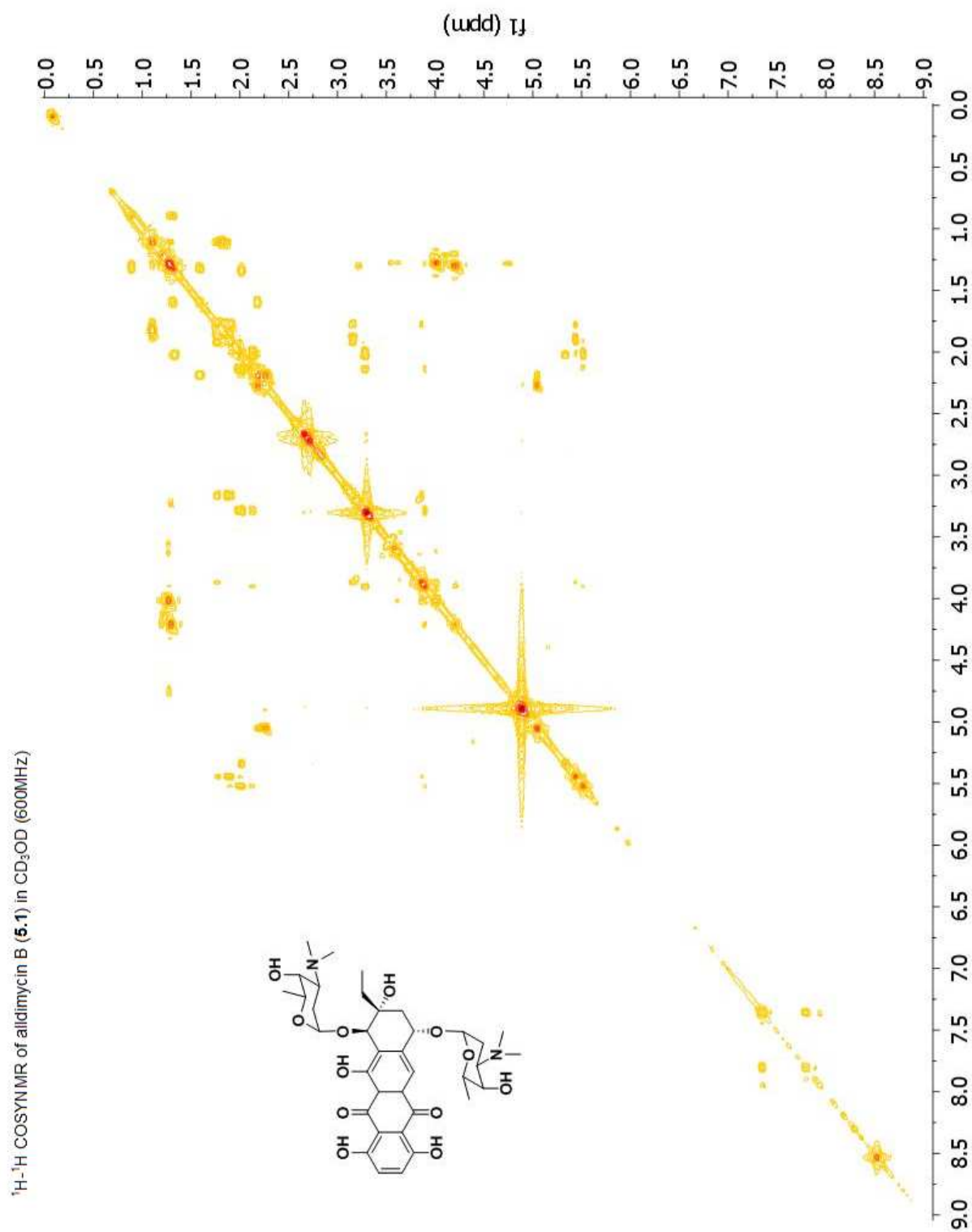


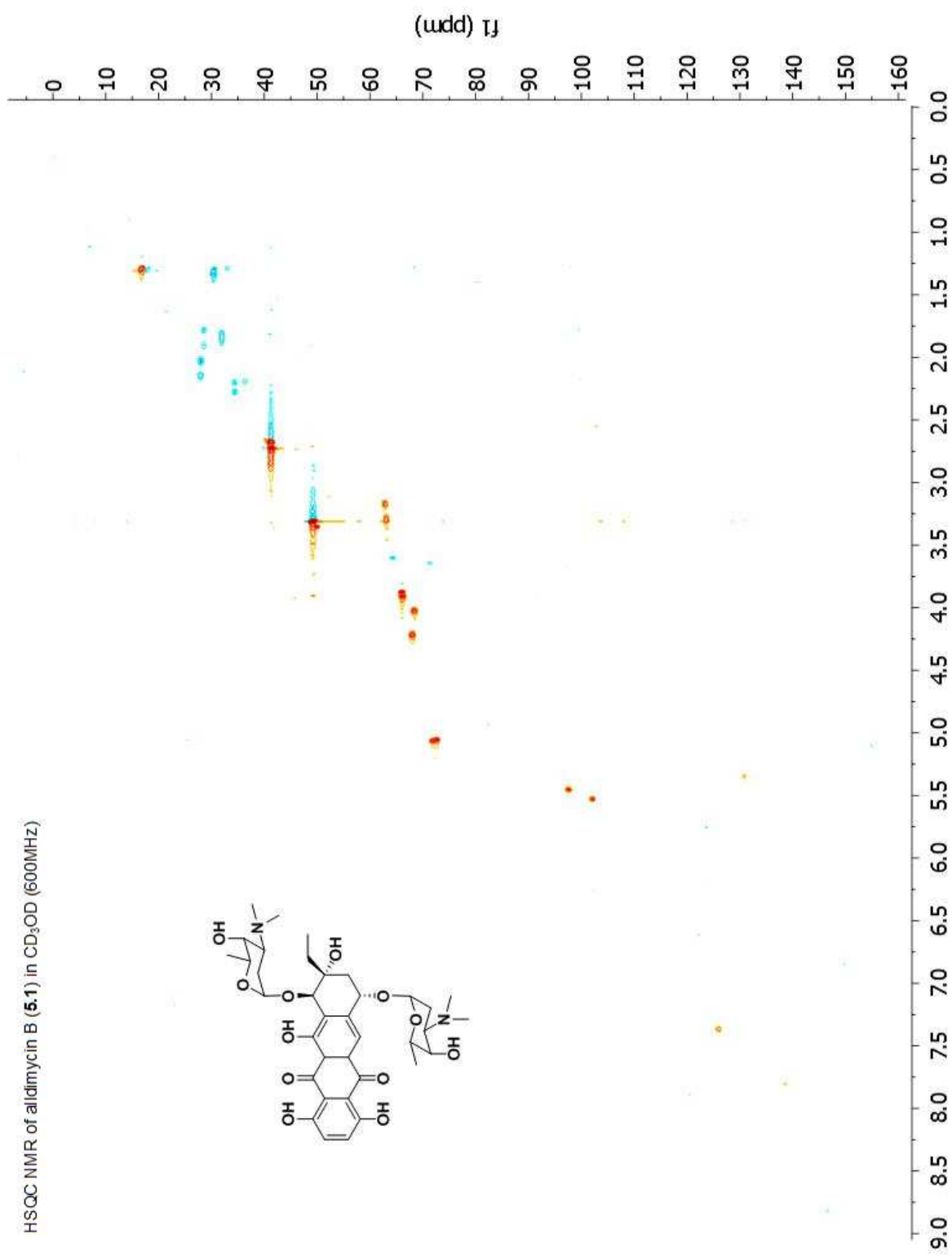


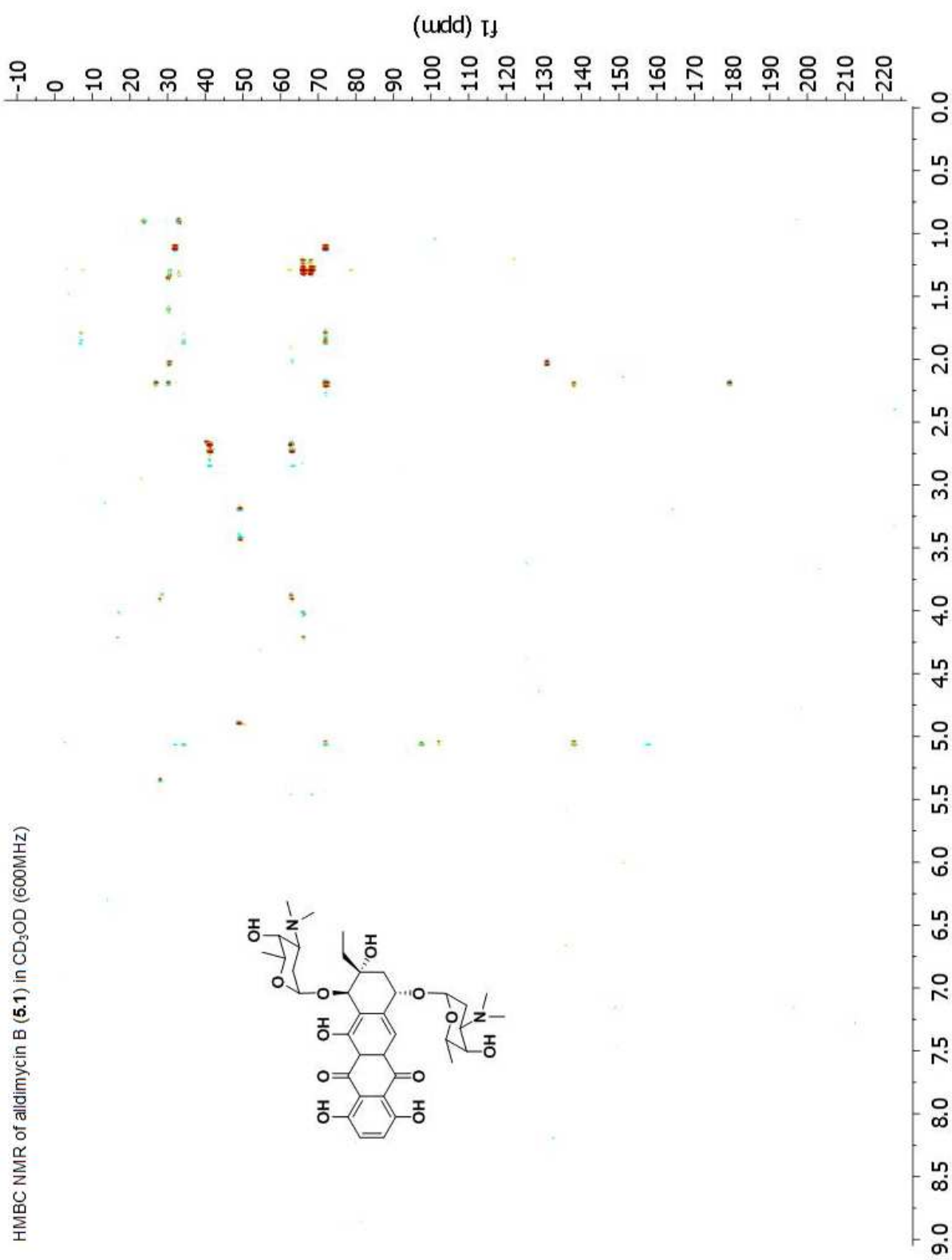




NMR data for alldimycin B (**5.1**)

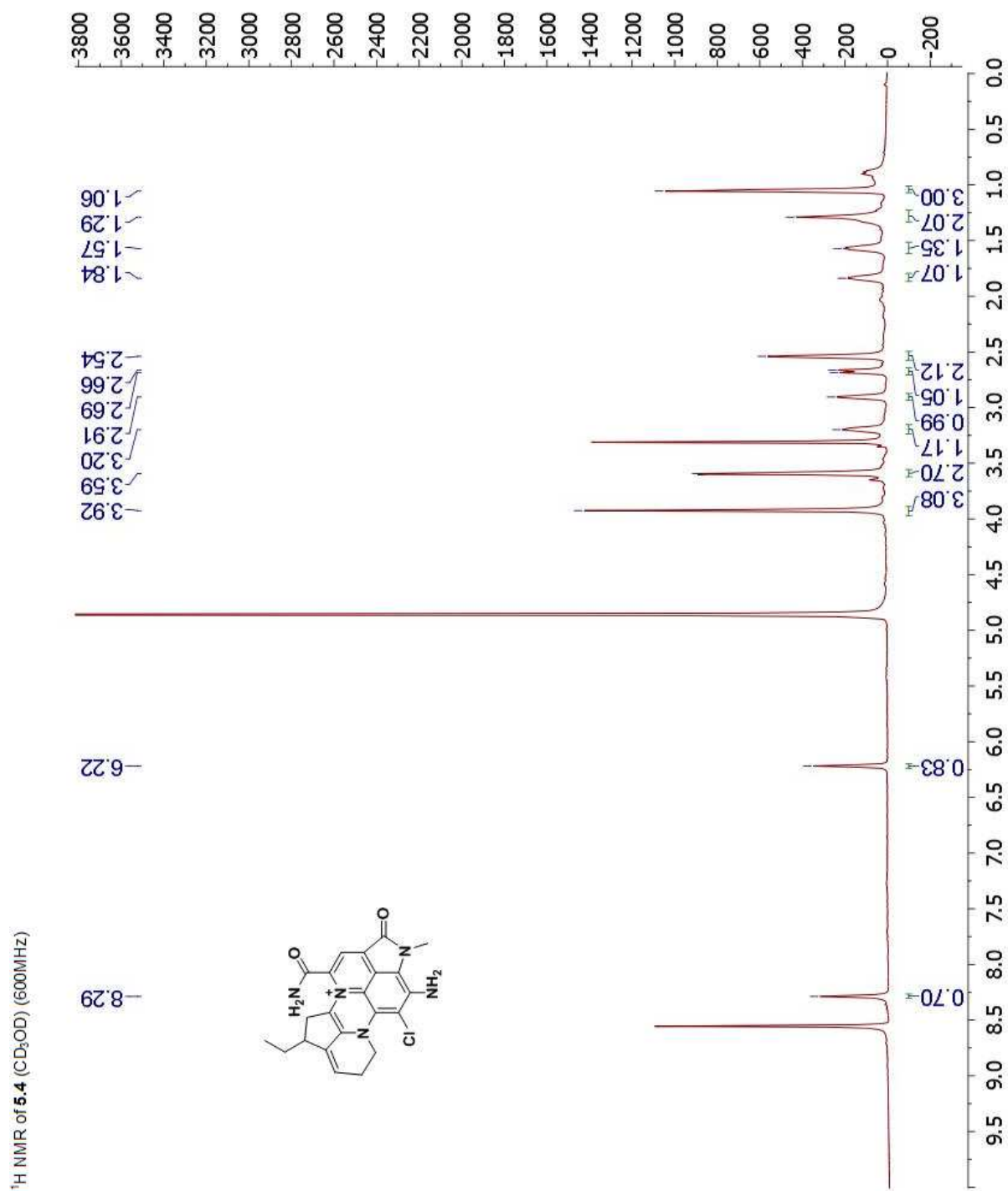


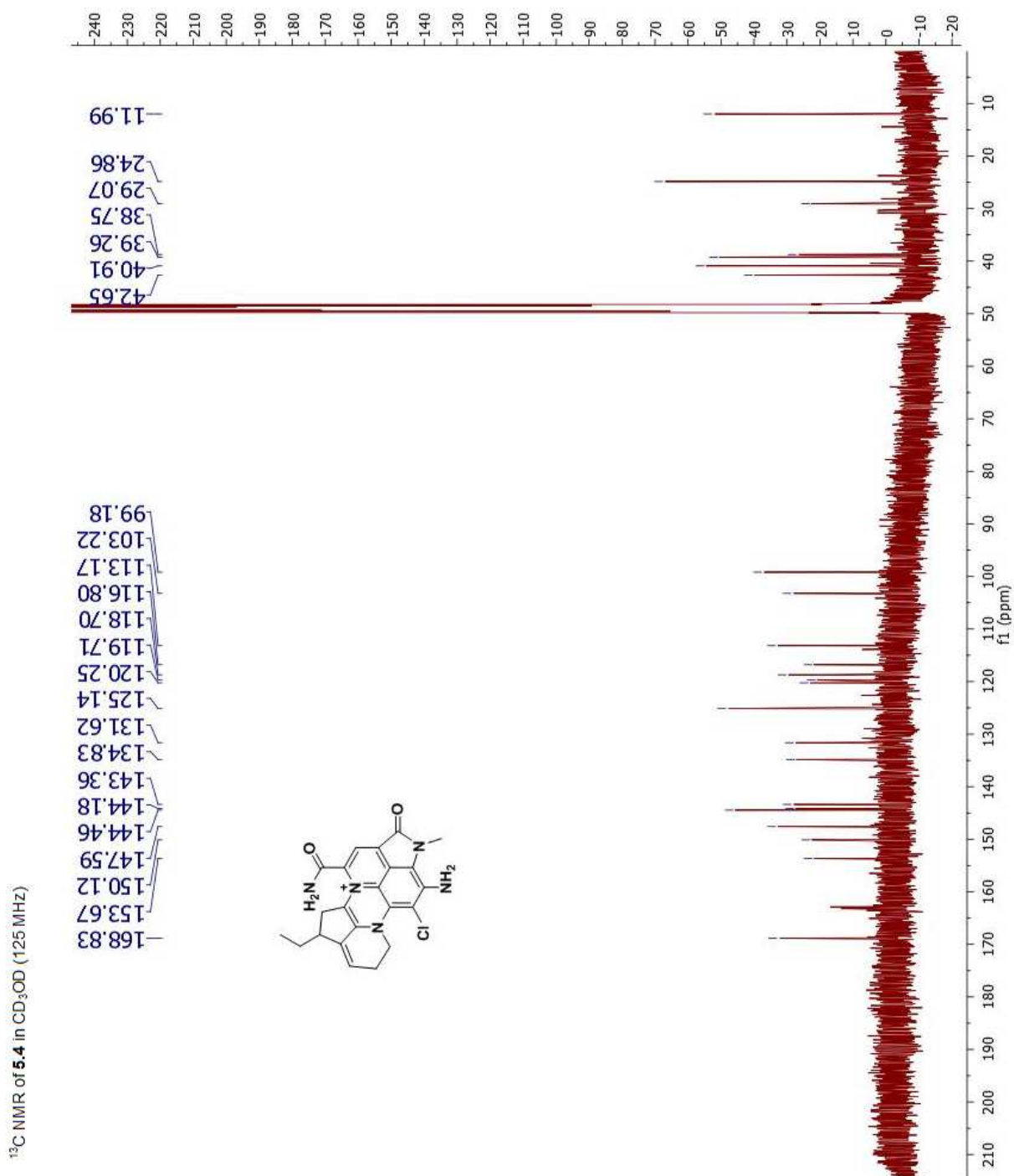


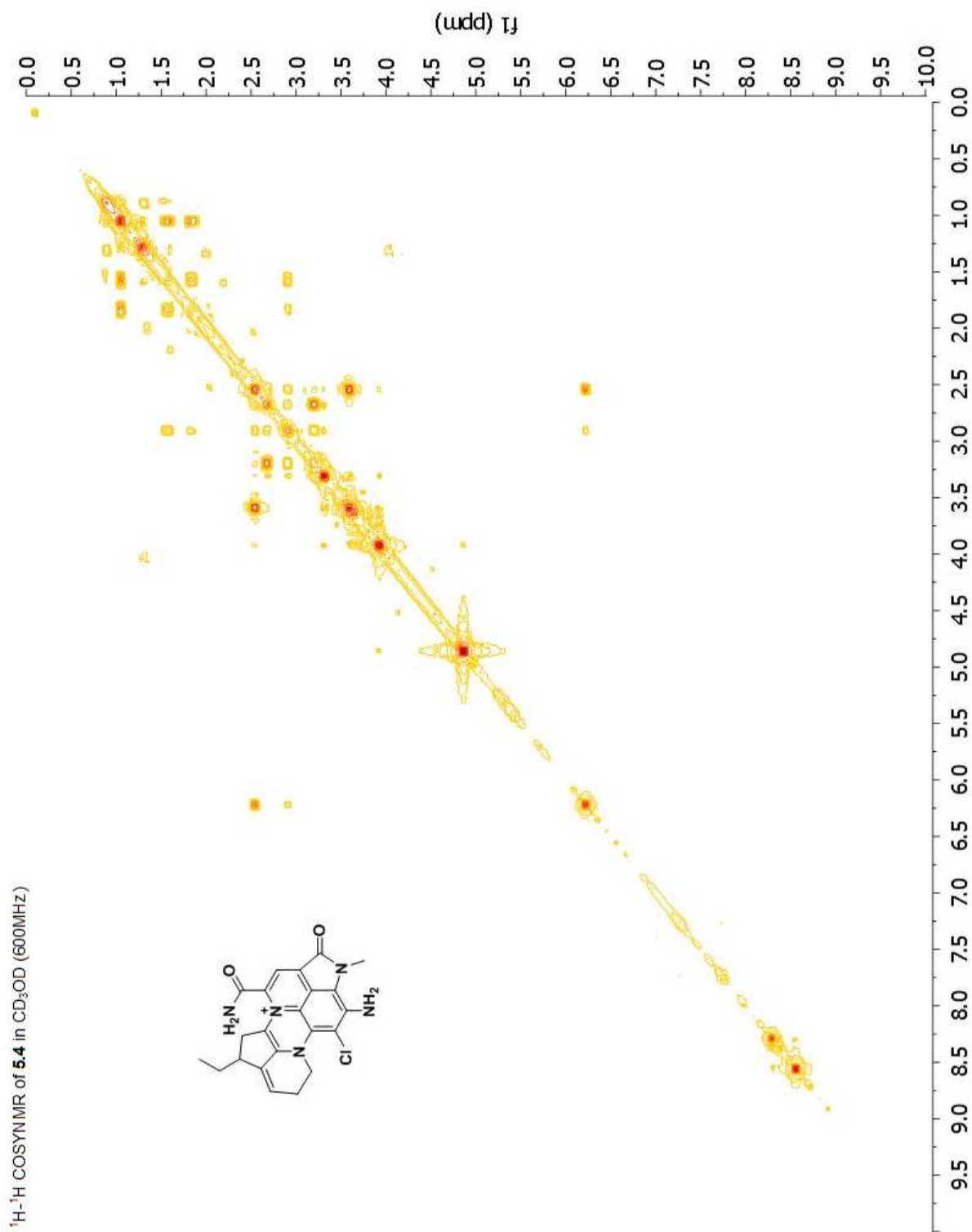


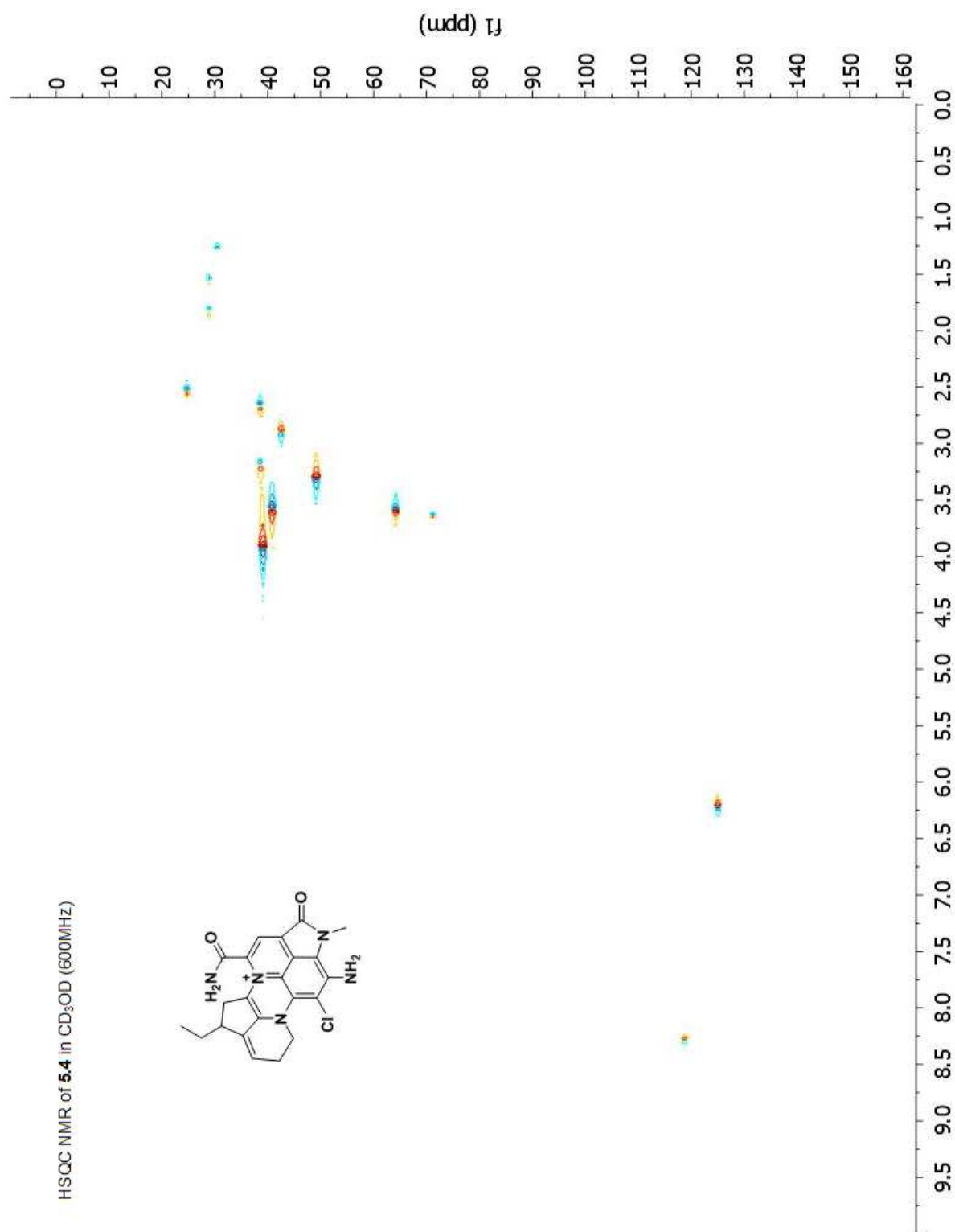


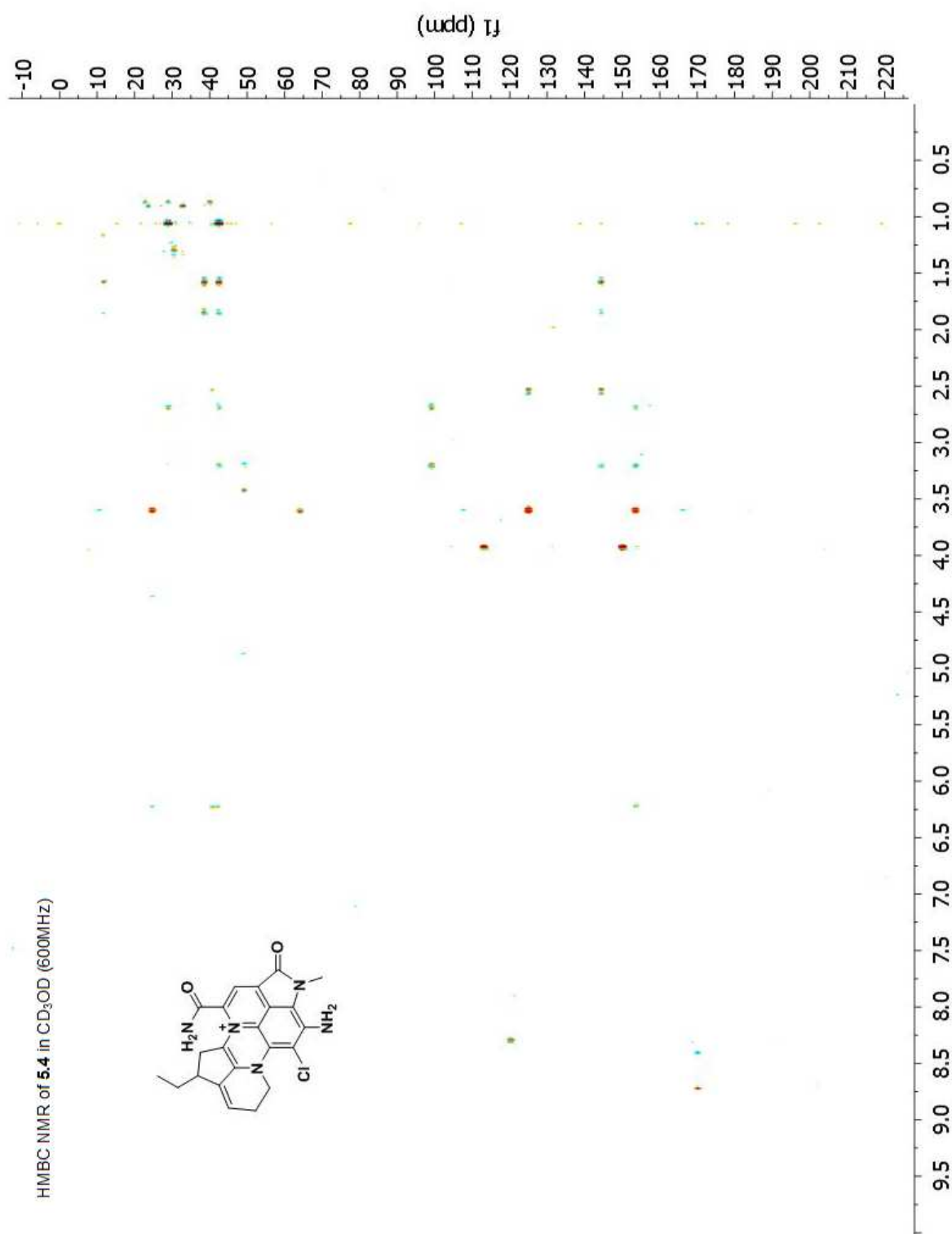
NMR data for **5.4**

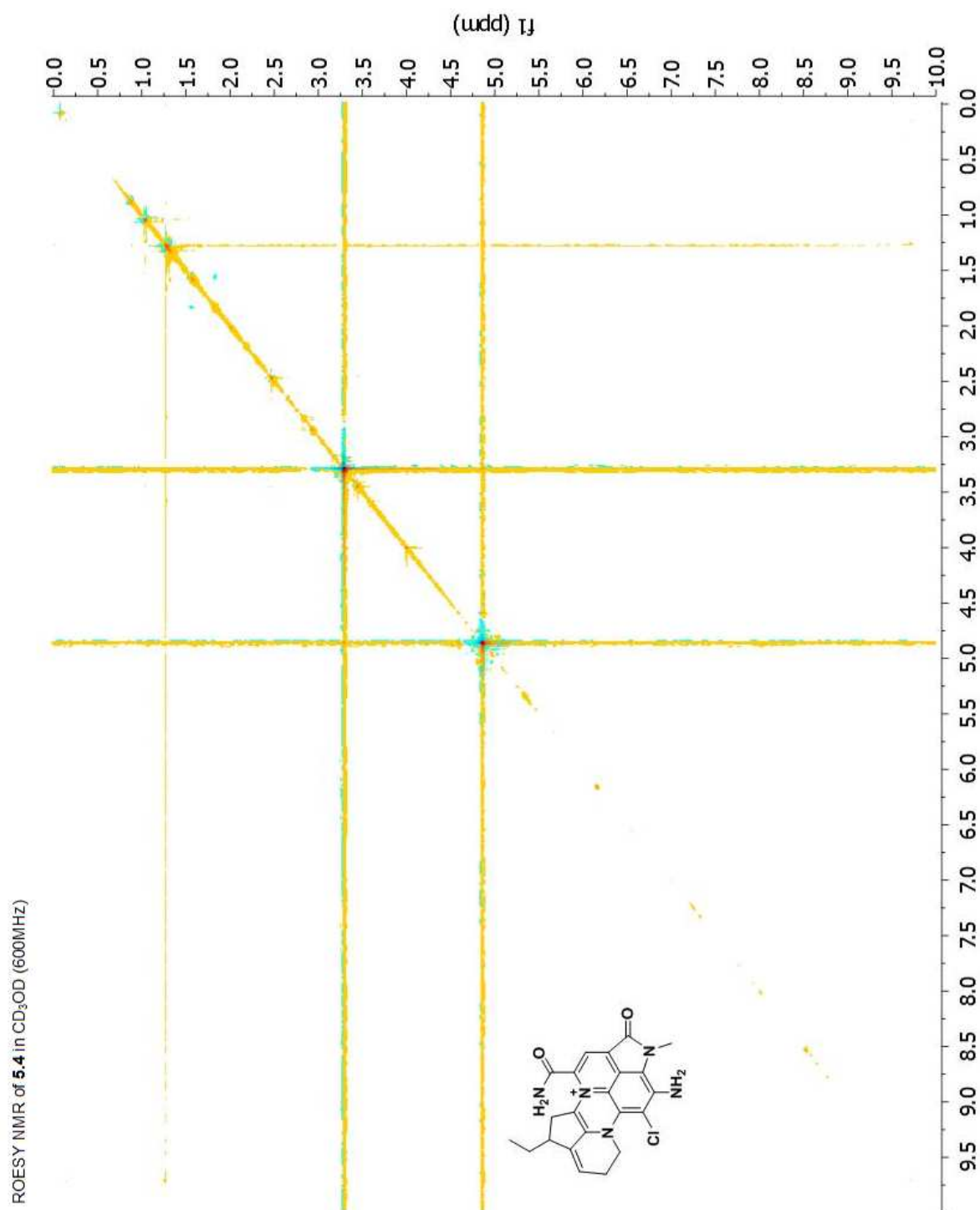












## BIBLIOGRAPHY

1. Dias, D. A.; Urban, S.; Roessner, U., A Historical Overview of Natural Products in Drug Discovery. *Metabolites* **2012**, 2 (2), 303-336.
2. Newman, D. J.; Cragg, G. M., Natural Products As Sources of New Drugs over the 30 Years from 1981 to 2010. *Journal of Natural Products* **2012**, 75 (3), 311-335.
3. Walsh, C. T.; Fischbach, M. A., Natural products version 2.0: connecting genes to molecules. *J Am Chem Soc* **2010**, 132 (8), 2469-93.
4. Powers, J. H., Antimicrobial drug development--the past, the present, and the future. *Clin Microbiol Infect* **2004**, 10 Suppl 4, 23-31.
5. (a) Feher, M.; Schmidt, J. M., Property Distributions: Differences between Drugs, Natural Products, and Molecules from Combinatorial Chemistry. *Journal of Chemical Information and Computer Sciences* **2002**, 43 (1), 218-227; (b) Ganesan, A., The impact of natural products upon modern drug discovery. *Current Opinion in Chemical Biology* **2008**, 12 (3), 306-317.
6. Kong, D. X.; Jiang, Y. Y.; Zhang, H. Y., Marine natural products as sources of novel scaffolds: achievement and concern. *Drug Discov Today* **2010**, 15 (21-22), 884-886.
7. Allsopp, M.; Pambuccian, S. E.; Johnston, P.; Santillo, D., *State of the World's Oceans*. Springer: 2009; Vol. XIV, p 256.
8. Baltz, R. H., Renaissance in antibacterial discovery from actinomycetes. *Curr Opin Pharmacol* **2008**, 8 (5), 557-63.
9. Whitman, W. B.; Coleman, D. C.; Wiebe, W. J., Prokaryotes: the unseen majority. *Proc Natl Acad Sci U S A* **1998**, 95 (12), 6578-83.
10. Mincer, T. J.; Jensen, P. R.; Kauffman, C. A.; Fenical, W., Widespread and persistent populations of a major new marine actinomycete taxon in ocean sediments. *Appl Environ Microbiol* **2002**, 68 (10), 5005-11.

11. Goodfellow, M.; Stach, J. E.; Brown, R.; Bonda, A. N.; Jones, A. L.; Mexson, J.; Fiedler, H. P.; Zucchi, T. D.; Bull, A. T., *Verrucosipora maris* sp. nov., a novel deep-sea actinomycete isolated from a marine sediment which produces abyssomicins. *Antonie Van Leeuwenhoek* **2012**, *101* (1), 185-93.
12. Bister, B.; Bischoff, D.; Strobele, M.; Riedlinger, J.; Reicke, A.; Wolter, F.; Bull, A. T.; Zahner, H.; Fiedler, H. P.; Sussmuth, R. D., Abyssomicin C-A polycyclic antibiotic from a marine *Verrucosipora* strain as an inhibitor of the p-aminobenzoic acid/tetrahydrofolate biosynthesis pathway. *Angew Chem Int Ed Engl* **2004**, *43* (19), 2574-6.
13. Imhoff, J. F.; Stohr, R., Sponge-associated bacteria: general overview and special aspects of bacteria associated with *Halichondria panicea*. *Prog Mol Subcell Biol* **2003**, *37*, 35-57.
14. Gerwick, W. H.; Moore, B. S., Lessons from the past and charting the future of marine natural products drug discovery and chemical biology. *Chem Biol* **2012**, *19* (1), 85-98.
15. Hughes, C. C.; Fenical, W., Antibacterials from the sea. *Chemistry* **2010**, *16* (42), 12512-25.
16. Montaser, R.; Luesch, H., Marine natural products: a new wave of drugs? *Future Med Chem* **2011**, *3* (12), 1475-89.
17. Blunt, J. W.; Copp, B. R.; Keyzers, R. A.; Munro, M. H. G.; Prinsep, M. R., Marine natural products. *Natural Product Reports* **2012**, *29* (2), 144-222.
18. (a) Mayer, A. M.; Glaser, K. B.; Cuevas, C.; Jacobs, R. S.; Kem, W.; Little, R. D.; McIntosh, J. M.; Newman, D. J.; Potts, B. C.; Shuster, D. E., The odyssey of marine pharmaceuticals: a current pipeline perspective. *Trends Pharmacol Sci* **2010**, *31* (6), 255-65; (b) Molinski, T. F.; Dalisay, D. S.; Lievens, S. L.; Saludes, J. P., Drug development from marine natural products. *Nat Rev Drug Discov* **2009**, *8* (1), 69-85.
19. Imhoff, J. F.; Labes, A.; Wiese, J., Bio-mining the microbial treasures of the ocean: new natural products. *Biotechnol Adv* **2011**, *29* (5), 468-82.



20. Olivera, B. M.; Gray, W. R.; Zeikus, R.; McIntosh, J. M.; Varga, J.; Rivier, J.; de Santos, V.; Cruz, L. J., Peptide neurotoxins from fish-hunting cone snails. *Science* **1985**, 230 (4732), 1338-43.
21. Wang, Y. X.; Gao, D.; Pettus, M.; Phillips, C.; Bowersox, S. S., Interactions of intrathecally administered ziconotide, a selective blocker of neuronal N-type voltage-sensitive calcium channels, with morphine on nociception in rats. *Pain* **2000**, 84 (2-3), 271-81.
22. (a) Rinehart, K. L.; Holt, T. G.; Fregeau, N. L.; Stroh, J. G.; Keifer, P. A.; Sun, F.; Li, L. H.; Martin, D. G., Ecteinascidin-729, Ecteinascidin-743, Ecteinascidin-745, Ecteinascidin-759a, Ecteinascidin-759b, and Ecteinascidin-770 - Potent Antitumor Agents from the Caribbean Tunicate Ecteinascidia-Turbinata. *J Org Chem* **1990**, 55 (15), 4512-4515; (b) Wright, A. E.; Forleo, D. A.; Gunawardana, G. P.; Gunasekera, S. P.; Koehn, F. E.; McConnell, O. J., Antitumor Tetrahydroisoquinoline Alkaloids from the Colonial Ascidian Ecteinascidia-Turbinata. *J Org Chem* **1990**, 55 (15), 4508-4512.
23. Hirata, Y.; Uemura, D., Halichondrins - Antitumor Polyether Macrolides from a Marine Sponge. *Pure Appl Chem* **1986**, 58 (5), 701-710.
24. Kuznetsov, G.; Towle, M. J.; Cheng, H. S.; Kawamura, T.; TenDyke, K.; Liu, D.; Kishi, Y.; Yu, M. J.; Littlefield, B. A., Induction of morphological and biochemical apoptosis following prolonged mitotic blockage by halichondrin B macrocyclic ketone analog E7389. *Cancer Res* **2004**, 64 (16), 5760-5766.
25. Towle, M. J.; Salvato, K. A.; Wels, B. F.; Aalfs, K. K.; Zheng, W. J.; Seletsky, B. M.; Zhu, X. J.; Lewis, B. M.; Kishi, Y.; Yu, M. J.; Littlefield, B. A., Eribulin Induces Irreversible Mitotic Blockade: Implications of Cell-Based Pharmacodynamics for In vivo Efficacy under Intermittent Dosing Conditions. *Cancer Res* **2011**, 71 (2), 496-505.
26. Pettit, G. R.; Kamano, Y.; Herald, C. L.; Tuinman, A. A.; Boettner, F. E.; Kizu, H.; Schmidt, J. M.; Baczynskyj, L.; Tomer, K. B.; Bontems, R. J., Antineoplastic Agents .136. The Isolation and Structure of a Remarkable Marine Animal Antineoplastic Constituent - Dolastatin 10. *Journal of the American Chemical Society* **1987**, 109 (22), 6883-6885.

27. Butler, M. S.; Cooper, M. A., Antibiotics in the clinical pipeline in 2011. *J Antibiot (Tokyo)* **2011**, *64* (6), 413-25.
28. The 10 × '20 Initiative: Pursuing a Global Commitment to Develop 10 New Antibacterial Drugs by 2020. *Clinical Infectious Diseases* **2010**, *50* (8), 1081-1083.
29. Mayer, A. M.; Rodriguez, A. D.; Berlinck, R. G.; Fusetani, N., Marine pharmacology in 2007-8: Marine compounds with antibacterial, anticoagulant, antifungal, anti-inflammatory, antimalarial, antiprotozoal, antituberculosis, and antiviral activities; affecting the immune and nervous system, and other miscellaneous mechanisms of action. *Comp Biochem Physiol C Toxicol Pharmacol* **2011**, *153* (2), 191-222.
30. Xu, M.; Davis, R. A.; Feng, Y.; Sykes, M. L.; Shelper, T.; Avery, V. M.; Camp, D.; Quinn, R. J., Ianthelliformisamines A-C, antibacterial bromotyrosine-derived metabolites from the marine sponge *Suberea ianthelliformis*. *J Nat Prod* **2012**, *75* (5), 1001-5.
31. Camp, D.; Davis, R. A.; Campitelli, M.; Ebdon, J.; Quinn, R. J., Drug-like properties: guiding principles for the design of natural product libraries. *J Nat Prod* **2012**, *75* (1), 72-81.
32. (a) Driscoll, J. A.; Brody, S. L.; Kollef, M. H., The epidemiology, pathogenesis and treatment of *Pseudomonas aeruginosa* infections. *Drugs* **2007**, *67* (3), 351-68; (b) Hsieh, P. C.; Siegel, S. A.; Rogers, B.; Davis, D.; Lewis, K., Bacteria lacking a multidrug pump: a sensitive tool for drug discovery. *Proc Natl Acad Sci U S A* **1998**, *95* (12), 6602-6.
33. Hughes, C. C.; Prieto-Davo, A.; Jensen, P. R.; Fenical, W., The marinopyrroles, antibiotics of an unprecedented structure class from a marine *Streptomyces* sp. *Org Lett* **2008**, *10* (4), 629-31.
34. Doi, K.; Li, R.; Sung, S. S.; Wu, H.; Liu, Y.; Manieri, W.; Krishnegowda, G.; Awwad, A.; Dewey, A.; Liu, X.; Amin, S.; Cheng, C.; Qin, Y.; Schonbrunn, E.; Daughdrill, G.; Loughran, T. P., Jr.; Sebt, S.; Wang, H. G., Discovery of marinopyrrole A (maritoclax) as a selective Mcl-1 antagonist that overcomes ABT-737 resistance by binding to and targeting Mcl-1 for proteasomal degradation. *J Biol Chem* **2012**, *287* (13), 10224-35.

35. Sanchez, L. M.; Wong, W. R.; Riener, R. M.; Schulze, C. J.; Linington, R. G., Examining the fish microbiome: vertebrate-derived bacteria as an environmental niche for the discovery of unique marine natural products. *PLoS One* **2012**, *7* (5), e35398.
36. Butler, M. S.; Buss, A. D., Natural products — The future scaffolds for novel antibiotics? *Biochemical Pharmacology* **2006**, *71* (7), 919-929.
37. Stone, M. J.; Williams, D. H., On the evolution of functional secondary metabolites (natural products). *Mol Microbiol* **1992**, *6* (1), 29-34.
38. Donadio, S.; Monciardini, P.; Sosio, M., Polyketide synthases and nonribosomal peptide synthetases: the emerging view from bacterial genomics. *Nat Prod Rep* **2007**, *24* (5), 1073-109.
39. Berdy, J., Bioactive microbial metabolites. *J Antibiot (Tokyo)* **2005**, *58* (1), 1-26.
40. Staley, J. T.; Konopka, A., Measurement of in Situ Activities of Nonphotosynthetic Microorganisms in Aquatic and Terrestrial Habitats. *Annual Review of Microbiology* **1985**, *39* (1), 321-346.
41. Tally, F. P.; DeBruin, M. F., Development of daptomycin for Gram-positive infections. *Journal of Antimicrobial Chemotherapy* **2000**, *46* (4), 523-526.
42. Stewart, E. J., Growing unculturable bacteria. *J Bacteriol* **2012**, *194* (16), 4151-60.
43. Rappe, M. S.; Connon, S. A.; Vergin, K. L.; Giovannoni, S. J., Cultivation of the ubiquitous SAR11 marine bacterioplankton clade. *Nature* **2002**, *418* (6898), 630-3.
44. Kaeberlein, T.; Lewis, K.; Epstein, S. S., Isolating "uncultivable" microorganisms in pure culture in a simulated natural environment. *Science* **2002**, *296* (5570), 1127-9.
45. Bollmann, A.; Lewis, K.; Epstein, S. S., Incubation of environmental samples in a diffusion chamber increases the diversity of recovered isolates. *Appl Environ Microbiol* **2007**, *73* (20), 6386-90.

46. Gavrish, E.; Bollmann, A.; Epstein, S.; Lewis, K., A trap for in situ cultivation of filamentous actinobacteria. *J Microbiol Methods* **2008**, 72 (3), 257-62.
47. D'Onofrio, A.; Crawford, J. M.; Stewart, E. J.; Witt, K.; Gavrish, E.; Epstein, S.; Clardy, J.; Lewis, K., Siderophores from neighboring organisms promote the growth of uncultured bacteria. *Chem Biol* **2010**, 17 (3), 254-64.
48. Pettit, R. K., Small-molecule elicitation of microbial secondary metabolites. *Microbial Biotechnology* **2011**, 4 (4), 471-478.
49. Bode, H. B.; Bethe, B.; Höfs, R.; Zeeck, A., Big Effects from Small Changes: Possible Ways to Explore Nature's Chemical Diversity. *ChemBioChem* **2002**, 3 (7), 619-627.
50. Doull, J. L.; Ayer, S. W.; Singh, A. K.; Thibault, P., Production of a novel polyketide antibiotic, jadomycin B, by *Streptomyces venezuelae* following heat shock. *J Antibiot (Tokyo)* **1993**, 46 (5), 869-71.
51. Berrue, F.; Withers, S. T.; Haltli, B.; Withers, J.; Kerr, R. G., Chemical screening method for the rapid identification of microbial sources of marine invertebrate-associated metabolites. *Mar Drugs* **2011**, 9 (3), 369-81.
52. Brady, S. F.; Simmons, L.; Kim, J. H.; Schmidt, E. W., Metagenomic approaches to natural products from free-living and symbiotic organisms. *Nat Prod Rep* **2009**, 26 (11), 1488-503.
53. Wang, G.-Y.-S.; Graziani, E.; Waters, B.; Pan, W.; Li, X.; McDermott, J.; Meurer, G.; Saxena, G.; Andersen, R. J.; Davies, J., Novel Natural Products from Soil DNA Libraries in a Streptomycete Host. *Organic Letters* **2000**, 2 (16), 2401-2404.
54. Banik, J. J.; Brady, S. F., Cloning and characterization of new glycopeptide gene clusters found in an environmental DNA megalibrary. *Proc Natl Acad Sci U S A* **2008**, 105 (45), 17273-7.
55. King, R. W.; Bauer, J. D.; Brady, S. F., An environmental DNA-derived type II polyketide biosynthetic pathway encodes the biosynthesis of the pentacyclic polyketide erdacin. *Angew Chem Int Ed Engl* **2009**, 48 (34), 6257-61.

56. Feng, Z.; Kallifidas, D.; Brady, S. F., Functional analysis of environmental DNA-derived type II polyketide synthases reveals structurally diverse secondary metabolites. *Proc Natl Acad Sci U S A* **2011**, *108* (31), 12629-34.
57. Feng, Z.; Chakraborty, D.; Dewell, S. B.; Reddy, B. V.; Brady, S. F., Environmental DNA-encoded antibiotics fasamycins A and B inhibit FabF in type II fatty acid biosynthesis. *J Am Chem Soc* **2012**, *134* (6), 2981-7.
58. Kim, J. H.; Feng, Z.; Bauer, J. D.; Kallifidas, D.; Calle, P. Y.; Brady, S. F., Cloning large natural product gene clusters from the environment: piecing environmental DNA gene clusters back together with TAR. *Biopolymers* **2010**, *93* (9), 833-44.
59. Flinspach, K.; Westrich, L.; Kaysser, L.; Siebenberg, S.; Gomez-Escribano, J. P.; Bibb, M.; Gust, B.; Heide, L., Heterologous expression of the biosynthetic gene clusters of coumermycin A(1), clorobiocin and caprazamycins in genetically modified *Streptomyces coelicolor* strains. *Biopolymers* **2010**, *93* (9), 823-32.
60. Feng, Z.; Kim, J. H.; Brady, S. F., Fluostatins Produced by the Heterologous Expression of a TAR Reassembled Environmental DNA Derived Type II PKS Gene Cluster. *Journal of the American Chemical Society* **2010**, *132* (34), 11902-11903.
61. Cichewicz, R. H.; Valeriote, F. A.; Crews, P., Psymberin, a potent sponge-derived cytotoxin from *Psammocinia* distantly related to the pederin family. *Org Lett* **2004**, *6* (12), 1951-4.
62. Fisch, K. M.; Gurgui, C.; Heycke, N.; van der Sar, S. A.; Anderson, S. A.; Webb, V. L.; Taudien, S.; Platzer, M.; Rubio, B. K.; Robinson, S. J.; Crews, P.; Piel, J., Polyketide assembly lines of uncultivated sponge symbionts from structure-based gene targeting. *Nat Chem Biol* **2009**, *5* (7), 494-501.
63. (a) Levy, S. B.; Marshall, B., Antibacterial resistance worldwide: causes, challenges and responses. *Nat Med* **2004**, *10* (12 Suppl), S122-9; (b) Coates, A. R.; Halls, G.; Hu, Y., Novel classes of antibiotics or more of the same? *Br J Pharmacol* **2011**, *163* (1), 184-94.
64. Rice, L. B., Progress and challenges in implementing the research on ESKAPE pathogens. *Infect Control Hosp Epidemiol* **2010**, *31* Suppl 1, S7-10.

65. Wright, G. D., Antibiotics: a new hope. *Chem Biol* **2012**, *19* (1), 3-10.
66. Bugg, T. D.; Wright, G. D.; Dutka-Malen, S.; Arthur, M.; Courvalin, P.; Walsh, C. T., Molecular basis for vancomycin resistance in *Enterococcus faecium* BM4147: biosynthesis of a depsipeptide peptidoglycan precursor by vancomycin resistance proteins VanH and VanA. *Biochemistry* **1991**, *30* (43), 10408-15.
67. McComas, C. C.; Crowley, B. M.; Boger, D. L., Partitioning the Loss in Vancomycin Binding Affinity for d-Ala-d-Lac into Lost H-Bond and Repulsive Lone Pair Contributions. *Journal of the American Chemical Society* **2003**, *125* (31), 9314-9315.
68. Xie, J.; Pierce, J. G.; James, R. C.; Okano, A.; Boger, D. L., A redesigned vancomycin engineered for dual D-Ala-D-ala And D-Ala-D-Lac binding exhibits potent antimicrobial activity against vancomycin-resistant bacteria. *J Am Chem Soc* **2011**, *133* (35), 13946-9.
69. Monaghan, R. L.; Barrett, J. F., Antibacterial drug discovery - Then, now and the genomics future. *Biochemical Pharmacology* **2006**, *71* (7), 901-909.
70. Kellner, R. L. L.; Dettner, K., Differential efficacy of toxic pederin in deterring potential arthropod predators of *Paederus* (Coleoptera: Staphylinidae) offspring. *Oecologia* **1996**, *107* (3), 293-300.
71. Parenti, F.; Pagani, H.; Beretta, G., Lipiarmycin, a new antibiotic from *Actinoplanes*. I. Description of the producer strain and fermentation studies. *J Antibiot (Tokyo)* **1975**, *28* (4), 247-52.
72. (a) Theriault, R. J.; Karwowski, J. P.; Jackson, M.; Girolami, R. L.; Sunga, G. N.; Vojtko, C. M.; Coen, L. J., Tiacumicins, a novel complex of 18-membered macrolide antibiotics. I. Taxonomy, fermentation and antibacterial activity. *J Antibiot (Tokyo)* **1987**, *40* (5), 567-74; (b) Omura, S.; Imamura, N.; Oiwa, R.; Kuga, H.; Iwata, R.; Masuma, R.; Iwai, Y., Clostomicins, new antibiotics produced by *Micromonospora echinospora* subsp. *armeniaca* subsp. nov. I. Production, isolation, and physico-chemical and biological properties. *J Antibiot (Tokyo)* **1986**, *39* (10), 1407-12; (c) Kurabachew, M.; Lu, S. H. J.; Krastel, P.; Schmitt, E. K.; Suresh, B. L.; Goh, A.; Knox, J. E.; Ma, N. L.; Jiricek, J.; Beer, D.; Cynamon, M.; Petersen, F.; Dartois, V.; Keller, T.; Dick, T.; Sambandamurthy, V. K., Lipiarmycin targets RNA polymerase and has good activity against multidrug-

- resistant strains of *Mycobacterium tuberculosis*. *Journal of Antimicrobial Chemotherapy* **2008**, 62 (4), 713-719.
73. Swanson, R. N.; Hardy, D. J.; Shipkowitz, N. L.; Hanson, C. W.; Ramer, N. C.; Fernandes, P. B.; Clement, J. J., In vitro and in vivo evaluation of tiacumicins B and C against *Clostridium difficile*. *Antimicrob Agents Chemother* **1991**, 35 (6), 1108-11.
  74. Xiao, Y.; Li, S.; Niu, S.; Ma, L.; Zhang, G.; Zhang, H.; Ju, J.; Zhang, C., Characterization of tiacumicin B biosynthetic gene cluster affording diversified tiacumicin analogues and revealing a tailoring dihalogenase. *J Am Chem Soc* **2011**, 133 (4), 1092-105.
  75. Tupin, A.; Gualtieri, M.; Leonetti, J. P.; Brodolin, K., The transcription inhibitor lipiarmycin blocks DNA fitting into the RNA polymerase catalytic site. *EMBO J* **2010**, 29 (15), 2527-37.
  76. (a) Rawlings, B. J., Type I polyketide biosynthesis in bacteria (Part A--erythromycin biosynthesis). *Nat Prod Rep* **2001**, 18 (2), 190-227; (b) Rawlings, B. J., Type I polyketide biosynthesis in bacteria (part B). *Nat Prod Rep* **2001**, 18 (3), 231-81.
  77. Moore, B. S.; Hertweck, C., Biosynthesis and attachment of novel bacterial polyketide synthase starter units. *Nat Prod Rep* **2002**, 19 (1), 70-99.
  78. Morris, J. G., Bacterial shock responses. *Endeavour* **1993**, 17 (1), 2-6.
  79. Friedman, L.; Miller, J. G., Odor incongruity and chirality. *Science* **1971**, 172 (3987), 1044-6.
  80. Stephens, T. D.; Brynner, R., *Dark Remedy: The Impact of Thalidomide and Its Revival as a Vital Medicine*. Nature Publishing Group: 2001.
  81. Silverstein R. M., W. F. X., *Spectrometric Identification of Organic Compounds*. 6th ed.; Wiley: 1997; p 482.
  82. Matsumori, N.; Kaneno, D.; Murata, M.; Nakamura, H.; Tachibana, K., Stereochemical Determination of Acyclic Structures Based on Carbon-Proton Spin-Coupling Constants.

- A Method of Configuration Analysis for Natural Products. *J Org Chem* **1999**, 64 (3), 866-876.
83. Qin, H. L.; Lowe, J. T.; Panek, J. S., Mild reductive opening of aryl pyranosides promoted by scandium(III) triflate. *J Am Chem Soc* **2007**, 129 (1), 38-9.
84. Hoye, T. R.; Jeffrey, C. S.; Shao, F., Mosher ester analysis for the determination of absolute configuration of stereogenic (chiral) carbinol carbons. *Nat. Protocols* **2007**, 2 (10), 2451-2458.
85. Wender, P. A.; Dechristopher, B. A.; Schrier, A. J., Efficient synthetic access to a new family of highly potent bryostatin analogues via a Prins-driven macrocyclization strategy. *J Am Chem Soc* **2008**, 130 (21), 6658-9.
86. Liang, L.; Yan, M.; Li, Y. M.; Chan, A. S. C., Highly enantioselective copper-catalyzed 1,4-conjugate addition of diethylzinc to cyclic enones and  $\alpha,\beta$ -unsaturated lactones. *Tetrahedron-Asymmetr* **2004**, 15 (16), 2575-2578.
87. Williams, J. M.; Jobson, R. B.; Yasuda, N.; Marchesini, G.; Dolling, U. H.; Grabowski, E. J. J., A New General-Method for Preparation of N-Methoxy-N-Methylamides - Application in Direct Conversion of an Ester to a Ketone. *Tetrahedron Lett* **1995**, 36 (31), 5461-5464.
88. Yang, S.-B.; Gan, F.-F.; Chen, G.-J.; Xu, P.-F., An Efficient One-Pot Synthesis of  $\omega$ -Hydroxy Ketones from Lactones. *Synlett* **2008**, 2008 (16), 2532-2534.
89. Hasserodt, J.; Janda, K. D.; Lerner, R. A., A class of 4-aza-lithocholic acid-derived haptens for the generation of catalytic antibodies with steroid synthase capabilities. *Bioorg Med Chem* **2000**, 8 (5), 995-1003.
90. Gao, Y.; Hanson, R. M.; Klunder, J. M.; Ko, S. Y.; Masamune, H.; Sharpless, K. B., Catalytic Asymmetric Epoxidation and Kinetic Resolution - Modified Procedures Including Insitu Derivatization. *Journal of the American Chemical Society* **1987**, 109 (19), 5765-5780.



91. Hosaka, T.; Ohnishi-Kameyama, M.; Muramatsu, H.; Murakami, K.; Tsurumi, Y.; Kodani, S.; Yoshida, M.; Fujie, A.; Ochi, K., Antibacterial discovery in actinomycetes strains with mutations in RNA polymerase or ribosomal protein S12. *Nat Biotechnol* **2009**, 27 (5), 462-4.
92. Chakraborty, R.; Bibb, M., The ppGpp synthetase gene (relA) of *Streptomyces coelicolor* A3(2) plays a conditional role in antibiotic production and morphological differentiation. *J Bacteriol* **1997**, 179 (18), 5854-61.
93. Cashel, M.; Gallant, J., Two compounds implicated in the function of the RC gene of *Escherichia coli*. *Nature* **1969**, 221 (5183), 838-41.
94. Potrykus, K.; Cashel, M., (p)ppGpp: still magical? *Annu Rev Microbiol* **2008**, 62, 35-51.
95. Artsimovitch, I.; Patlan, V.; Sekine, S.; Vassilyeva, M. N.; Hosaka, T.; Ochi, K.; Yokoyama, S.; Vassilyev, D. G., Structural basis for transcription regulation by alarmone ppGpp. *Cell* **2004**, 117 (3), 299-310.
96. Dalebroux, Z. D.; Svensson, S. L.; Gaynor, E. C.; Swanson, M. S., ppGpp conjures bacterial virulence. *Microbiol Mol Biol Rev* **2010**, 74 (2), 171-99.
97. Wexselblatt, E.; Oppenheimer-Shaanan, Y.; Kaspy, I.; London, N.; Schueler-Furman, O.; Yavin, E.; Glaser, G.; Katzhendler, J.; Ben-Yehuda, S., Relacin, a novel antibacterial agent targeting the stringent response. *PLoS Pathog* **2012**, 8 (9), e1002925.
98. Shima, J.; Hesketh, A.; Okamoto, S.; Kawamoto, S.; Ochi, K., Induction of actinorhodin production by rpsL (encoding ribosomal protein S12) mutations that confer streptomycin resistance in *Streptomyces lividans* and *Streptomyces coelicolor* A3(2). *J Bacteriol* **1996**, 178 (24), 7276-84.
99. Wang, G.; Hosaka, T.; Ochi, K., Dramatic activation of antibiotic production in *Streptomyces coelicolor* by cumulative drug resistance mutations. *Appl Environ Microbiol* **2008**, 74 (9), 2834-40.
100. Ochi, K., From microbial differentiation to ribosome engineering. *Biosci Biotechnol Biochem* **2007**, 71 (6), 1373-86.

101. Ochi, K., From microbial differentiation to ribosome engineering. *Biosci Biotech Bioch* **2007**, *71* (6), 1373-1386.
102. Mingeot-Leclercq, M. P.; Glupczynski, Y.; Tulkens, P. M., Aminoglycosides: activity and resistance. *Antimicrob Agents Chemother* **1999**, *43* (4), 727-37.
103. Li, J.; Xin, J.; Zhang, L.; Jiang, L.; Cao, H.; Li, L., Rapid detection of rpoB mutations in rifampin resistant M. tuberculosis from sputum samples by denaturing gradient gel electrophoresis. *Int J Med Sci* **2012**, *9* (2), 148-56.
104. Manteca, A.; Sanchez, J., Streptomyces development in colonies and soils. *Appl Environ Microbiol* **2009**, *75* (9), 2920-4.
105. Livermore, D. M., Current epidemiology and growing resistance of gram-negative pathogens. *Korean J Intern Med* **2012**, *27* (2), 128-42.
106. Kerr, K. G.; Snelling, A. M., Pseudomonas aeruginosa: a formidable and ever-present adversary. *J Hosp Infect* **2009**, *73* (4), 338-44.
107. Stover, C. K.; Pham, X. Q.; Erwin, A. L.; Mizoguchi, S. D.; Warrenner, P.; Hickey, M. J.; Brinkman, F. S.; Hufnagle, W. O.; Kowalik, D. J.; Lagrou, M.; Garber, R. L.; Goltry, L.; Tolentino, E.; Westbrook-Wadman, S.; Yuan, Y.; Brody, L. L.; Coulter, S. N.; Folger, K. R.; Kas, A.; Larbig, K.; Lim, R.; Smith, K.; Spencer, D.; Wong, G. K.; Wu, Z.; Paulsen, I. T.; Reizer, J.; Saier, M. H.; Hancock, R. E.; Lory, S.; Olson, M. V., Complete genome sequence of Pseudomonas aeruginosa PAO1, an opportunistic pathogen. *Nature* **2000**, *406* (6799), 959-64.
108. Hauser, A. R., The type III secretion system of Pseudomonas aeruginosa: infection by injection. *Nat Rev Microbiol* **2009**, *7* (9), 654-65.
109. Haussler, S., Multicellular signalling and growth of Pseudomonas aeruginosa. *Int J Med Microbiol* **2010**, *300* (8), 544-8.
110. Strausbaugh, S. D.; Davis, P. B., Cystic fibrosis: a review of epidemiology and pathobiology. *Clin Chest Med* **2007**, *28* (2), 279-88.

111. Lipuma, J. J., The changing microbial epidemiology in cystic fibrosis. *Clin Microbiol Rev* **2010**, 23 (2), 299-323.
112. Smith, E. E.; Buckley, D. G.; Wu, Z.; Saenphimmachak, C.; Hoffman, L. R.; D'Argenio, D. A.; Miller, S. I.; Ramsey, B. W.; Speert, D. P.; Moskowitz, S. M.; Burns, J. L.; Kaul, R.; Olson, M. V., Genetic adaptation by *Pseudomonas aeruginosa* to the airways of cystic fibrosis patients. *Proc Natl Acad Sci U S A* **2006**, 103 (22), 8487-92.
113. Mesaros, N.; Nordmann, P.; Plesiat, P.; Roussel-Delvallez, M.; Van Eldere, J.; Glupczynski, Y.; Van Laethem, Y.; Jacobs, F.; Lebecque, P.; Malfroot, A.; Tulkens, P. M.; Van Bambeke, F., *Pseudomonas aeruginosa*: resistance and therapeutic options at the turn of the new millennium. *Clin Microbiol Infect* **2007**, 13 (6), 560-578.
114. Giske, C. G.; Monnet, D. L.; Cars, O.; Carmeli, Y., Clinical and economic impact of common multidrug-resistant gram-negative bacilli. *Antimicrob Agents Chemother* **2008**, 52 (3), 813-21.
115. Beno, P.; Krcmery, V.; Demitrovicova, A., Bacteraemia in cancer patients caused by colistin-resistant Gram-negative bacilli after previous exposure to ciprofloxacin and/or colistin. *Clin Microbiol Infect* **2006**, 12 (5), 497-8.
116. Hughes, C. C.; MacMillan, J. B.; Gaudencio, S. P.; Jensen, P. R.; Fenical, W., The ammosamides: structures of cell cycle modulators from a marine-derived *Streptomyces* species. *Angew Chem Int Ed Engl* **2009**, 48 (4), 725-7.
117. Johdo, O.; Tone, H.; Okamoto, R.; Yoshimoto, A.; Naganawa, H.; Sawa, T.; Takeuchi, T., Anthracycline metabolites from *Streptomyces violaceus* A262. V. New anthracycline alldimycin A: a minor component isolated from obelmycin beer. *J Antibiot (Tokyo)* **1991**, 44 (10), 1160-4.
118. Rabbani, A.; Finn, R. M.; Ausio, J., The anthracycline antibiotics: antitumor drugs that alter chromatin structure. *Bioessays* **2005**, 27 (1), 50-56.
119. Gewirtz, D. A., A critical evaluation of the mechanisms of action proposed for the antitumor effects of the anthracycline antibiotics adriamycin and daunorubicin. *Biochem Pharmacol* **1999**, 57 (7), 727-41.

120. Sawyer, D. B.; Peng, X. Y.; Chen, B.; Pentassuglia, L.; Lim, C. C., Mechanisms of Anthracycline Cardiac Injury: Can We Identify Strategies for Cardioprotection? *Prog Cardiovasc Dis* **2010**, *53* (2), 105-113.
121. Pan, E.; Oswald, N. W.; Legako, A. G.; Life, J. M.; Posner, B. A.; Macmillan, J. B., Precursor-Directed Generation of Amidine Containing Ammosamide Analogs: Ammosamides E-P. *Chem Sci* **2013**, *4* (1), 482-488.
122. Pan, E.; Jamison, M.; Yousufuddin, M.; MacMillan, J. B., Ammosamide D, an oxidatively ring opened ammosamide analog from a marine-derived *Streptomyces variabilis*. *Org Lett* **2012**, *14* (9), 2390-3.